Department of Oceanography
School of Science
Oregon State University
Corvallis, Oregon 97331

John V. Byrne
Chairman

Progress Report

PHYSICAL FACTORS AFFECTING OREGON COASTAL POLLUTION

by

Victor T. Neal, Donald F. Keene,
and John Detweiler

Federal Water Pollution Control Administration Grant 16-070 EMO

(Reference)69-28

October 1969

TABLE OF CONTENTS

LIST OF TABLES

REPORT ON RESEARCH DONE UNDER THE RESEARCH GRANT WP01380-01 (16-070 EMO)

TITLE OF RESEARCH: Physical factors affecting Oregon coastal pollution.

The nearshore zones of the Pacific Northwest are those most likely to be affected by pollution. In fact we already have paper mill effluents being discharged in the nearshore region at Newport and Reedsport. Demands for more ocean outfalls can be expected in the future. Furthermore, pollutants brought into the ocean by rivers may seriously damage the water quality in coastal areas. Important factors in effective utilization of the ocean for natural purification of sewage effluent are currents and density distribution.

Norman H. Brooks (1968), civil engineer from the California Institute of Technology, stated:

"Initial planning for an ocean outfall should include oceanographic surveys in the vicinity of possible discharge sites to determine:

1. Currents (direction, magnitude, frequency, variation with depth, relation to tides, water displacements)
2. Densities (variation with depth determined from salinity and temperature data and standard tables)
3. Submarine topography, geology, and bottom materials
4. Marine biology
5. Turbidity
6. Dissolved oxygen, etc.

The final site selection for an ocean outfall is usually based on general characteristics of the coastal waters and on topography of the drainage area. Details of diffuser design are developed after the general site is chosen."

The ocean outfall at Newport, Oregon was built before any oceanographic survey was made. Even so, the data obtained from an oceanographic survey can still be used to evaluate the effectiveness of the outfall and therefore be useful in future site selections.

The biggest difficulty confronting those who must select or regulate ocean outfall sites in the Pacific Northwest is an almost complete lack of oceanographic information in the nearshore region. An exhaustive search has revealed that no useful current data had been collected before 1968 anywhere along the coast of the United States from Cape Mendocino to Cape Flattery. The many difficulties associated with collecting data in the nearshore areas of the Pacific Northwest are mostly caused by adverse weather and sea conditions. Therefore no nearshore salinity, temperature, or dissolved oxygen data has been available except that taken directly on a few beaches and in estuaries of the Pacific Northwest.

Our research program has been the first of its kind in this region. Therefore, no precedents had been established for this type of work. Some trial and error in selecting the best techniques and devices was necessary in order to carry out the research in the most effective manner. Our research plan was based on the use of charter aircraft to make current measurements and the use of the Department of Oceanography's 33 foot R/V PAIUTE to obtain water samples and water temperatures.

The research program was designed to give information on all factors that would be expected to influence the distribution of pollutants in the area. These factors are: currents in the outfall area, longshore currents, tides, winds, waves, water temperature and salinity, water density, and dissolved oxygen concentration. The details and results of the research are given in the remainder of this report.

TEMPERATURE, SALINITY, AND DISSOLVED OXYGEN MEASUREMENTS

One of the factors affecting pollution distribution is the density of the water. If the effluent is less dense than the bottom water, it will rise to the surface layers. Whereas if it is more dense than the surface waters, it will remain below the pycnocline. It is not feasible to measure the density directly in situ. Temperature and salinity measurements are normally used to calculate density of ocean water. Standard tables are readily available for determining density of seawater once temperature and salinity are known.

Temperature is also important if thermal wastes are to be discharged into the marine environment. Undue changes in temperature could be detrimental to the biota of the region. Before decisions can be made in this regard it is necessary to know what natural temperature variations occur in the area throughout the year.

We measured temperature with a shallow water (100 ft.) mechanical bathythermograph and with a thermistor probe. As is typical of equipment purchased from oceanographic suppliers, the bathythermograph was not properly set at the factory. We therefore tested it in fresh water environments at known depths and temperatures in an attempt to calibrate it properly. The BT still is not as accurate as the thermistor probe. However, the BT does give a continuous trace of temperature vs depth and is therefore useful because the tendency toward stratification is readily shown. We used both methods through most of the project period.

We took temperature readings directly over the outfall (surface and bottom) as well as in the outfall plume and outside the outfall plume. In addition, we took readings well away from the outfall in oceanic water generally just outside the reef directly west of the outfall (see Fig. 1). All temperature readings were taken at the surface and either at the bottom or at the depth measured at the outfall, generally 35 to 40 feet. When using the BT we

measured to either 100 feet or the bottom whichever came first.

We used the R/V PAIUTE to obtain temperature measurements, salinity and dissolved oxygen water samples. The PAIUTE was generally not permitted to go into the area when small craft warnings were displayed or when waves were breaking over the reef. Therefore it was not possible to get measurements and samples every time we went to Newport (56 miles from the Corvallis campus). Frequently conditions were so severe that we could not cross the bar at Newport. In spite of the bad sea and weather conditions (particularly throughout the fall, winter and spring months) we were able to obtain reliable data throughout the year. Whenever the PAIUTE was used the currents were also measured by aircraft, and waves and longshore currents were measured from the beach.

Water samples obtained at the surface and bottom (or surface and 40 feet down)were taken simultaneously with temperature measurements over the outfall, inside the plume, outside the plume and just outside the reef. Salinity samples were analyzed by a standard laboratory inductive salinometer at the Marine Science Center at Newport, Oregon.

Dissolved oxygen samples were preserved immediately upon being taken. They were later analyzed in the Marine Science Center at Newport.

The cooking liquor from the paper mill consists of Na_2S, CH_3SH, and $(CH_3)_2S$. Some of the waste is diluted liquor. NaOH, Na_2SO_4, and $Na_2S_2O_3$ are also present in the plume as well as trace organics cooked from the wood (O'Neal, 1966). These organics probably give the plume its characteristic color, while the sulfides and mercaptans give it the odor which is noticeable in the outfall area. The cooking liquor is 10-20% solids, of which 40-45% is NaOH, 22% is Na_2S, 7% is Na_2SO_4 and Na_2CO_3 makes up most of the remainder.

In view of all the materials found in the effluent, it is worthwhile to consider whether the Winkler method of dissolved oxygen analysis is suitable for waters taken from the outfall area. Of all the compounds listed, Na_2S is the one most likely to disturb oxygen analysis. The sulfide ion can directly consume oxygen according to the equation:

$$S^{--} + 2O_2 \longrightarrow SO_4^{--}$$

It can also take up iodine that is liberated and titrated during the analysis, yielding free sulfur

$$I_2 + S^{--} \longrightarrow 2I^- + S\downarrow .$$

Thiosulfate is also present, and it can also react with a portion of the iodine. The result of such interference should be low values for oxygen concentration.

In spite of the presence of interfering chemicals, no large oxygen depression occurs over the outfall. This is not explained by a rough calculation of the sulfide concentration. If the waste diluted liquor can contain as much as 20% solids, and Na_2S is about 20% of the solids, and S^{--} is about 40% of Na_2S, then the pure effluent can contain about 1 1/2% sulfide. The dilution ratio for the effluent is given as 100:1. Thus sulfide can be around 0.02% by weight, or about 6×10^{-3} moles/liter. Oxygen at 6 ml/l is about 3×10^{-4} moles/liter. Thus, a noticeable drop from saturation concentration could be expected. However, the possibility of sulfide oxidation can probably be eliminated by prompt pickling of the sample since the sulfide reaction is slow. The iodine uptake, on the other hand, is sufficiently rapid to disturb any titration if the sulfide is present in significant amounts. The mixing of the effluent with adjacent waters may be sufficient

to disperse the sulfide and dilute it to an insignificant concentration. In spite of the possibility of interference in the oxygen analysis, the dissolved oxygen concentrations measured remained quite high.

WAVE MEASUREMENTS

Waves were measured on the same days that currents were measured. Waves were measured by visual means since no wave gage was available to us. We measured the significant breaker heights by lining up the crests of the breakers with the horizon. We determined the elevation of the observer's eye by using two poles marked in one-foot sections. The first pole was stuck in the sand midway between the uprush and backwash of the water. We placed the second pole further back up the beach. The observer then stood by the second pole and lined up the six foot marker on the first pole with the horizon. The observer's eye was then known to be 6 feet above still water level and this point (or other more convenient level) was marked on the second pole. The observer then stood by the second pole and lined up the crests of the breakers with the horizon by moving his eye level up or down as required. The eye level which was also the height of the wave crest above still water level was then read off by referring to the previously chosen reference point on the second pole. The average height of the breakers above still water was computed then multiplied by 4/3 to get the true average height of the significant breakers. The factor of 4/3 was used because the wave troughs are depressed below the still water level.

Significant breaker periods were measured with a stop watch. When the first wave of a group of large waves broke at a given point, the stop watch was started and it was stopped when the last wave reached approximately the same point. The wave period was then determined by dividing the number of

intervals between breakers into the elapsed time.

The direction from which the waves were coming was determined from aerial observations while over deep water.

Wave data were needed to determine the contribution waves make toward circulation in the outfall area. Also, waves are generally considered as the main cause of littoral currents. Furthermore, waves are one of the prime agents for mixing the upper layers of water and in shallow water can produce mixing to the bottom.

LONGSHORE CURRENTS MEASUREMENT

The water movement along the beach, inside the surf zone, is called the littoral or longshore current. It has proven impractical to place current meters within the surf zone since there is so much sand in suspension that the meter bearings will not last. Furthermore, the force of breaking waves make it impractical to moor any meters there. The wave forces would also damage meters so that they either would not function or at best would not function properly.

The method we used to measure the longshore currents was a drift bottle method. We used plastic bottles (8 oz. size) which we sprayed with orange fluorescent paint. They were readily visible in the air and on the beach. We numbered the bottles so we would know when and where each bottle entered the water. We filled the bottles with fresh water, which is about 2.5% lighter than seawater so the bottles would drift with very little exposure above the water surface. We deployed the drift bottles in either of two ways. When we were taking current measurements in deeper water by means of aircraft, we would drop four bottles at a time in selected areas of the surf zone. One of our men on the beach (who also measured wave heights) would

then measure the rate of movement of these bottles along the beach. At times tourists and beachcombers would pick up some of our bottles before the man on the beach could measure the distance of travel. On days when the weather was not suitable for flying, we simply threw the bottles into the surf zone and measured the rate of drift along the beach. The rate of drift was determined by measuring the distance along the beach from the point where the bottles hit the water to where they grounded. The time required for this drift was measured by the observer on the beach.

Some investigators have used dye for measuring longshore currents. However, it is difficult to differentiate between the diffusion and advection by this means. It is also difficult to eliminate wind effects on the dye. Therefore we, as have many others, stayed with a floating device.

TIDAL MEASUREMENT

The tide gauge closest to our area of work is installed on the dock at the Oregon State University Marine Science Center, Newport, Oregon. The gauge is inside the Yaquina Estuary and therefore does not record the tides exactly as they occur in the outfall area. The gauge is the standard type used by the U. S. Coast and Geodetic Survey. We also have used the tide predictions of the U. S. Coast and Geodetic Survey for some of our studies.

WIND MEASUREMENT

In spite of the fact that man has been measuring winds for many tens of years, the methods have never been completely satisfactory for detailed studies. The main problems associated with most wind measuring devices are threshhold velocities of the anemometer and the inertia of the rotating

parts (mechanical types). The winds produce further problems by their very nature. For example, they are not steady but commonly blow in gusts. Winds vary in speed from one place to another even within small areas. Furthermore, they vary with distance above the surface. Topographic features of the earth also produce variations in winds. The same difficulties pertain to measuring wind direction as apply to measuring wind speed.

When the project first began, we used wind data from a continuously recording anemometer that was operated by the Pacific Northwest Water Laboratory personnel. This anemometer was installed on the jetty at Newport. This operation was discontinued in December and we had to rely on field measurements taken with the hand-held type (the same as used by the U. S. Navy) which we purchased for our work. We used the hand anemometer at various places, depending upon the number of personnel available in the field. We used it aboard the PAIUTE, on the beach, and even tested it on Yaquina Head. We preferred to take wind data from approximately the same location each time. On 3 March 1969 the Weather Facility at the Marine Science Center in Newport installed a recording anemometer on the south jetty. The device records the direction from which the wind comes as well as the speed.

The anemometer operated by the Marine Science Center Weather Facility, records the direction in components. If the wind blows within 65 1/2° of a cardinal point for a minute it will record a component from this point for that minute. For example, if the wind blows from 045° for one minute, it will be recorded as having a component from north and another from east for that minute. If it blows from 075°, it will be recorded as having a component from east.

We have set up a computer program to resolve the wind data into usable form (see appendix). The direction and speed of the wind for the previous hour is calculated in the program. The direction is accurate to within 22 1/2° and the speed is computed to the nearest knot. Unfortunately, we had no choice in the anemometer which was installed at the Marine Science Center by ESSA. The accuracy of the wind measurements from March 3rd through August is not as good as required since the deviation of the current from the wind is expected to be on the order of 22°. We would naturally prefer greater accuracy in wind data, but we do not feel justified in spending the necessary funds to install an accurate wind recorder of our own choosing. Furthermore, those who will wish to predict the wind driven currents will probably not have weather data of any better accuracy.

CURRENT MEASUREMENT

The rate of change in concentration of pollutants due to physical factors may be expressed by the equation:

$$\frac{\partial C}{\partial t} = u\frac{\partial C}{\partial x} + v\frac{\partial C}{\partial y} + w\frac{\partial C}{\partial z} + \frac{\partial}{\partial x}\left(D_x\frac{\partial C}{\partial x}\right) + \frac{\partial}{\partial y}\left(D_y\frac{\partial C}{\partial y}\right) + \frac{\partial}{\partial z}\left(D_z\frac{\partial C}{\partial z}\right)$$

where C is the concentration, t is the time, and u, v, and w are the water movement rates in the horizontal (x and y) and vertical (z) directions. The first three terms on the right hand side of the equation are the advective terms (i.e., they depend upon advection of water) while the past three terms are the changes in concentration due to turbulence and other motions. One of the main goals of this research was to determine u, and v in the outfall area.

The water movements (currents) in any area may be described by two methods, the Eulerian and Lagrangian methods. The Eulerian method describes

the velocity field, the pressure and the density at every point within the fluid. The usual method of measuring the velocity field is to install current meters at fixed points within the fluid system.

The other method of representing fluid flow, the Lagrangian method, has led to several very useful results (Neumann and Pierson, 1968). It is ideally measured by marking or "tagging" each fluid element as to its position at some particular time, t_o, and then noting its position at some later time, t_1. When the future positions of all fluid elements with reference to their positions at time zero, usually along with the temperature, salinity, pressure and density of those fluid elements, have been described, we have a Lagrangian representation of fluid flow.

In our study we have used the Lagrangian system to describe the fluid movement in the Newport area by using a dye float system. It is costly to attempt a thorough Eulerian method of fluid measurement since it would require several current meter installations. However, this method needs to be carried out for a thorough analysis.

The area of specific interest in the Newport area is the area bounded on the north by Yaquina Head and on the south by the jetties at the entrance to Yaquina Bay. This area lies inside a reef (Fig. 1) and is in generally shoaling waters. Therefore it is too dangerous to use surface craft for measurements throughout the area as well as throughout the season. Frequently, especially during the winter months, when waves break over the reef we cannot use surface craft in the area. The currents that run along the south side of Yaquina Head cannot be measured safely from a surface craft because the water depths there are poorly charted and there are stacks, cliffs and many partially submerged rocks near the water's edge. It is also dangerous to operate too near the jetty due to the reef and the danger to the surface craft should

power be lost. Therefore we used chartered aircraft to get most of our current data. The system we used consisted of dropping dye floats from the air and also measuring their displacements from the air.

We used a "tin" can weighted with about 1 1/2 pounds of lead to make it sink and act as an anchor. We used lead because it is easily melted and poured at a temperature that does not distort the shape of the cans. Sixty feet of nylon or fish line was wound on a used film spool and mounted inside the can above the lead by using a metal shaft as an axle. One end of the line was fastened to the spool and the other to a round styrofoam float. A doughnut-shaped cake of fluorescein dye (enclosed in water soluble plastic) was attached to the float. A second float with a 30 x 13 cm cloth drogue and a doughnut-shaped cake of rhodamine B dye attached to it was taped with masking tape to the first float system. When the water soluble plastic dissolved the two floats came free from each other. The drogue on the second float would deploy six feet below it so the float would move with the current while discharging red dye. The first float remained anchored at the point of drop while releasing green dye. The dye marker system is shown in the photograph (Figure 2).

The "tin" can dual release dye marker system was dropped from an aircraft at low altitude (200 to 400 feet) at the desired location. Our final system was designed so the floats pulled line from the spool on the way down to the water. When they hit the water, the anchor can immediately sank to the bottom. The two floats stayed together for less than one minute while the water soluble plastic dissolved. The rhodamine dye float then was free to drift with the current with its drogue extended beneath it while the fluorescein dye float remained anchored to the can (Fig. 3). After the

markers had been in the water approximately 15 to 20 minutes we flew back over them to measure the displacement. We measured the displacement by two methods. We used a 35mm camera with Kodachrome II daylight type film to photograph the dye markers from a known altitude (generally from 1,000 to 2,000 feet). We took the door off the aircraft to make it easier to get a good vertical photograph. We also measured the displacement by visually sighting both floats simultaneously over the points of a divider held at a fixed distance from the eye. At the time of measurement we logged the time and altitude as well as the direction of the aircraft heading. The pilot flew directly over the dye marker path so the aircraft heading was the same as the current direction.

The current speed can be calculated from visual sighting by the formula: $V = \frac{2H \tan \frac{1}{2}\theta + (3600 - h^2)^{\frac{1}{2}}}{\Delta t}$ where H is the altitude of the plane, h is the water depth, θ is the angle subtended at the plane and Δt is the elapsed time between launching and observation (see Fig. 3).

The two dye colors, red and green, usually show up quite well in the photographs. The white floats within the dye patches can be located and the distance between them measured when the pictures are projected on a screen. The distance between the dye markers is obtained by the following equations:

a) $L = 35 \frac{H}{f}$ b) $\frac{x}{L} = \frac{b}{c}$

where L is the width of the field of view on the water surface, H is the altitude, f is the focal length of the camera in millimeters and 35 is the width of the film in millimeters, x is the actual separation of the floats on the water, L is the width of the field of view on the water surface, b is the distance between floats as measured on the screen and c is the total width of the slide on the screen.

We have checked the method by taking photographs of the runway at the Newport airport from various heights. The largest error was 0.6 feet over a 150 foot runway width. This represents an error of less than 0.5%. Although the method of visual sighting is not as accurate as the photographic technique, it is probably more accurate than many current measurement methods. For example, an error of 50 feet in altitude or of one degree in angle would result in an error of only about 1 ft/min in current measurement.

Very windy weather (i.e., winds on the order of 20 knots or more) proved to be difficult for flying such small airplanes and maintaining proper headings. It was also difficult for the pilot to control the aircraft through the highly turbulent areas on approaching and leaving the runway. It was particularly uncomfortable to fly under windy conditions with the door off. Below freezing temperatures during the winter season also make flights with the door off very uncomfortable but not impossible. Heavy rainfall also made operations difficult since the dye markers would not hold together until they hit the water. Rainfall combined with near freezing temperatures at times caused icing problems on the aircraft. When the wind was very strong, the surface condition of the ocean was very frothy and it became very difficult to see the dye markers even though they were readily visible in calmer weather.

For the benefit of others who may wish to use this technique, we will discuss problems associated with the handling of dyes. We initially used dye in powdered form. Rhodamine B is particularly difficult to handle in this form. We found it necessary to have an exhaust fan system to help keep the fine powder from infiltrating everything in the room when we placed the dye in cloth bags (originally used for the project). The process of measuring out the correct amount of dye, placing it in the

cloth bag, tying the bag and attaching the bag to the float was very disagreeable. Furthermore, we found that the wind effects within the aircraft (especially while flying with the door off) caused some of the rhodamine dye to emerge from the system and circulate throughout the cabin of the aircraft, staining the aircraft and the clothing of persons inside. It also was very irritating to breathe under such conditions.

In view of the problems associated with the handling of powdered dyes, we were especially pleased to learn after much investigation that Carl Fisher & Co., Inc., Oxford, Michigan produces dye cakes (both fluorescein and rhodamine) that eliminate the problems associated with powdered dye. The dye cakes are enclosed in water soluble plastic and have a metal ring within the doughnut-shaped dye cake. The metal ring gives the cake sufficient strength to withstand the impact of the dye with the water. The water soluble plastic enabled us to tape the two dye cakes together for the descent from the aircraft to the water. However, we found that on days when the wind speed was 15 knots or more the two dye cakes would sometimes come apart in the air, therefore rendering the drop almost useless because the two floats usually hit the water too far from each other. However, even under these conditions the current direction could be measured by photographing the floats immediately after the drop and again a few minutes later. We sometimes were able to obtain a current speed even under these conditions.

We also tried another technique for measuring currents that was intended to overcome some of the handicaps mentioned above. It consisted of a buoy system like the one shown in Fig. 4. It consisted of a buoy that was tethered to an anchored buoy system. The tether supported a known weight

and the tethered buoy had a vane drogue beneath it so the water flow would exert a definite pull on it. The amount of space between the two buoys B & C would give a measure of the current speed while the orientation of the three buoys (A, B, C) would give the current direction. The distance between the floats A and B served as a reference distance for aerial observation. This system also served as a reference point for sampling from the R/V PAIUTE as well as for air drops. Unfortunately, several days after the system was installed, the vane was broken loose, probably by wave action, rendering the system useless.

The system is worth using again because of its simplicity. We have calibration curves that can be used to determine the current speed from the separation of the buoys. Once this system has been perfected, it could be used to measure currents from a high point on shore if the required surveying instruments are available.

During the late stages of the research program we received the loan of three Geodyne current meters from the Pacific Northwest Water Laboratory. These current meters had been used elsewhere and were in such need of repair that out of the three we were only able to produce one working meter. This meant that we had to take parts from the other two to make the third one usable. We modified the one usable Geodyne current meter by attaching a large vane to it (see photograph in Fig. 5). The large vane makes the meter more stable and tends to filter out the direction changes caused by the oscillatory motions set up in the water by surface waves. The current meter still remains quite sensitive to the low current speeds observed.

The horizontal water motion u_o, due to waves in deep water is given by:

$$u_o = A_o \sigma e^{-kz} \cos (kx-\sigma t).$$

Where A_o is the wave amplitude in deep water, σ is the angular frequency (i.e. $2\pi/T$ where T is the wave period), K is the wave number ($2\pi/L_o$ where L_o is the deep water wave length, x is the distance along the surface in the direction of wave travel, z is the distance beneath the surface and t is the time from a given reference time.

In order to avoid this wave motion, most current meter installations are made in such a manner that the meter is below the surface at a depth greater than one-half the average wave length of waves expected in the area.

In the area with which we are concerned, the waves may be either deep water waves or shallow water waves. In contrast to deep water waves, whose horizontal disturbances decay exponentially with depth, shallow water waves produce uniform horizontal velocities from surface to bottom, as indicated in the equation: $u_s = \frac{A_s \sigma}{hk_s} \cos (k_s x - \sigma t)$

Where the symbols are the same as in the deep water wave equation. The subscript s denotes shallow water wave values. The letter h represents water depth.

The maximum magnitude of horizontal water movement due to the waves is a function of wave amplitude, wave length and wave period. Knowing the average wave conditions that occur during the recording period of the current meter, one should be able to interpret the current record.

Our initial test mooring of the Geodyne current meter proved successful although we had some anxious moments as we had to make the retrieval when winds were increasing to the point that the small craft warnings were up. Once we knew that our mooring technique was satisfactory (Fig. 6) we installed the meter again and obtained a record over a 7-day interval.

Unfortunately, the Geodyne current meter that we had records only on film. The only way to learn whether the record is good or bad is to send the film to the manufacturer for decoding. This procedure takes a considerable amount of time (several weeks). In the meantime, one does not know whether the meter is functioning properly or not. Our records were returned from the factory on October 2, 1969, with the statement that the recording camera was out of focus and the records were therefore not decoded. However, closer inspection of the record reveals that the film drive mechanism was binding so that the film would not advance the proper amount. Transferring the camera system from one meter to another possibly caused this. That is the risk one takes when trying to produce one good current meter out of three.

Now that we know our mooring technique is suitable, at least for summer sea conditions, we would not hesitate to use it again. Very few oceanographers have been successful at obtaining current meter records in an environment such as the one in which we have operated.

DATA, DATA PROCESSING AND RESULTS

Temperature. The results of the temperature measurements at the outfall are shown in Fig. 7. The deviations from the outfall temperatures at three locations: 1) downstream from the outfall but inside the effluent plume, 2) upstream and out of the effluent and, 3) outside the reef, are also shown in Fig. 7. Maximum temperatures occurred in June and early July when the northerly winds were either weak or non-existent. The minimum temperatures were recorded in early February (about 8°C) and in late July (about 8°C). During early February an unusually cold mass of air had penetrated the coastal region which brought snow and ice to the Newport area (Table I& Fig. 8). The water temperature dipped in mid-May but then

TABLE I. Weather averages for Newport, Oregon (August 1968-April 1969)

Month	Observed Temp. (°F)	Average Temp. (°F)	Deviation	Observed Precip. (Inches)	Average Precip. (Inches)	Deviation	Averaged Observed Wind Speed (ft/min)	Averaged Observed Wind Direction (from)
Aug.	58.5	57.9	+ .6	7.60	1.06	+ 6.54		
Sept.	57.2	57.0	+ .2	3.24	2.10	+ 1.14	853	178°
Oct.	51.9	53.9	-2.0	10.22	5.76	+ 4.46	1004	277°
Nov.	49.1	49.1	0.0	17.22	9.26	+ 7.96	924	334°
Dec.	41.7	45.6	-3.9	22.68	10.48	+12.20	724	280°
1969								
Jan.	38.8	43.9	-5.1	15.66	9.75	+ 5.91	1291	311°
Feb.	42.6	45.3	-2.7	9.15	8.35	+ .80	637	336°
March		46.4		4.03	7.74	- 3.71	1114	29°
April		49.1		5.91	4.51	+ 1.40	1312	348°

began a warming trend until the maximum for the year was reached in mid-June (over 14°C). From mid-June the bottom waters continued to cool until late July. The cooling of the bottom waters before the surface waters indicates that water was beginning to well upward from deeper offshore waters (Fig. 9). The surface waters were usually warmer than the bottom waters, although the difference in temperature was normally less than 1.0°C. Out of 174 BT traces obtained, the only ones showing any significant thermal stratification are those taken on June 30th (Figures 10a, b, c, d). Outside the reef (Figure 10a) the surface temperature was at least 4°C warmer than the water at 40 feet. The mixed layer outside the reef extended at least 15 feet beneath the surface. The temperature differences between surface and 40 feet were less pronounced inside the reef although there still was a significant difference (about 3°C). Greater mixing of water inside the reef due to waves and tides could account for the smaller temperature difference between surface and bottom.

Within 24 hours (June 30 - July 1) the stratification had definitely weakened (Figures 11a, b, c, d). The mixed layer outside the reef had decreased to less than 10 feet in thickness. The mixed layer had disappeared in most areas inside the reef. Over the outfall, the temperature profile was nearly isothermal on July 1 and the surface temperature was about 2°C colder than at the other areas outside the plume.

The temperature profiles shown on all other BT traces were very much like those obtained on March 4 (Figures 12a, b, c, d). The temperature profiles were generally nearly isothermal from surface to bottom throughout most of the year. The BT traces of June 30th and July 1st clearly indicate colder waters were beginning to well upward toward the surface.

The conditions that lead to upwelling of colder waters have been treated mathematically by Ekman. He assumed a steady state homogeneous deep ocean system. He solved the equations of motion and equation of continuity to obtain the following equations where V_o is the velocity at the surface and u and v the velocity components in the x and y directions at depth z.

$$u = v_o \exp\left(-\frac{\pi z}{D}\right) \cos\left(45° - \frac{\pi}{D} z\right)$$

$$v = v_o \exp\left(-\frac{\pi z}{D}\right) \sin\left(45° - \frac{\pi}{D} z\right)$$

$$V_o = \frac{T}{(\sqrt{\rho A 2\sigma \sin 0})} = \frac{\pi T}{(D\rho\sigma \sin 0)\sqrt{2}}$$

T is the wind stress directed along the y-axis, ρ is the water density, σ is the angular frequency of the earth's rotation, 0 is the latitude and $D = \pi\sqrt{\frac{A}{\rho\sigma \sin 0}}$ where A is the eddy viscosity coefficient.

As can be seen from these equations, the wind surface current is directed 45° to the right from the direction of the wind. The angle of deflection increases linearly with depth until at a depth z = D the current is opposite to the surface current. The velocity decreases exponentially with depth. The net result of the Ekman theory is that there is a net mass transport of water 90° to the right of the wind in the northern hemisphere. Therefore, when the winds circulating around the Pacific High in the summer blow from the north along the Oregon coast, the surface waters are driven offshore and must be replaced near the coast by colder and denser subsurface water. This process is commonly referred to as upwelling. The rate of vertical movement of water in upwelling is not known but is generally assumed to be very slow. The upwelled water apparently came from depths between 200 to 300 feet.

The temperature at the other locations (in the plume, out of the plume and outside the reef) followed very closely the temperatures at the outfall. The maximum deviation of temperatures at these locations from the outfall temperatures was only 2.2°C which occurred outside the reef on June 30th, the day before upwelling began to show its effects. On that date the surface temperatures both out of the plume and outside the reef were warmer than the waters over the outfall and in the effluent plume. A similar situation was found on other dates in July and August, indicating the vertical motion of the effluent over the outfall carries colder water from the bottom upward. The diffusers produce enough vigorous upward motion to show a "boil" on the surface. Average deviations calculated are given in Table II.

The average deviations clearly show the effect of the diffusers on the temperature. At the outfall the surface temperatures average cooler than the surface temperatures at all other locations while at the bottom the temperatures average warmer at the outfall than at comparable depths at all other stations although the differences are small. Another factor that could cause the differences between water outside the reef and water inside the reef is the degree of turbulent mixing caused by the shoaling of waves and tidal action.

For those stations inside the reef but not over the outfall, there seems to be very little difference in temperature whether the station was taken inside the plume or outside the plume.

TABLE II. Average standard deviations of temperature in the plume, out of the plume, and outside the reef compared to the temperatures at the sewer outfall.

	In Plume	Out of Plume	Outside Reef
Surface	+0.23°C	+0.26°C	+0.35°C
Bottom	-0.07°C	-0.18°C	-0.14°C

TABLE III. Average standard deviations of salinities in the plume, outside the plume and outside the reef compared to salinities at the sewer outfall.

	In Plume	Out of Plume	Outside Reef
Surface	+0.13‰	+0.13‰	+0.07‰
Bottom	-0.05‰	-0.05‰	-0.11‰

Air Temperature. The Newport weather summary is listed in Table I. The air temperature (°C) trends are shown in Figure 8. The upper line connects maximum temperatures on selected days while the lower line connects the minimum temperatures. Both the maximum and minimum air temperatures indicate a warming trend from late January into mid-July. A slight decrease shows up in late July. The maximum air temperature was always warmer than the water except in December, January and February with the maximum difference being during July and August during the upwelling season. The water temperatures also indicate a warming trend from early February into mid-June when upwelling caused them to drop sharply. If the northerly winds should fail to develop (that is, if the Pacific High would not move northward) it is likely that the water temperatures would continue to rise and produce unusually high temperatures in late July and August. However, such an event would probably also produce more cloudy and rainy weather as the Aleutian Low would remain active during the summer season. Even so, the sea surface temperature would be warmer in July and August than it is when upwelling occurs.

Salinity. Salinity trends are shown in Fig. 13. The same style of representation is used for salinity as for temperatures. More saline water moved into the area at the time upwelling began. A similar salinity ($\sim$33 o/oo) was found at a depth of about 200 feet in the off-shore waters. The water remained more saline during the months of July and August than during any other period. As with temperatures, the greatest difference between surface and bottom salinities occurred in June before upwelling began. The lowest salinity values recorded were during December, January and February. These three months span the normally heavy rainfall season (Figure 1). Local

runoff, precipitation and flow from Big Creek and the Yaquina estuary combine to produce the lower salinities inside the reef.

There was little variation of salinity between stations, the only exception being in mid-May, when the salinity outside the plume and outside the reef was more than 1.0 o/oo higher than at the surface in the plume and over the outfall. (At that particular time the effluent plume was going south.) The average deviations of salinity are given in Table III.

On the average the surface waters away from the outfall are more saline than the water directly over the outfall. The bottom (40 feet) waters are more saline at the outfall than at the other stations. The occurrence of fresher water at the surface over the outfall might be attributed to the fresh water which carries the waste materials from the diffuser into the marine environment, although the pumping rates stated by the paper mill operators would not support such a large deviation. Closer study will be required to determine why the bottom water over the outfall is more saline than the surrounding bottom water. However, it could be flowing in from the deeper and slightly more saline water just west of the outfall. The average difference between the outfall and surrounding station bottom salinities is not considered significant.

On the average the water outside the reef is more saline at surface and bottom than the water inside the reef. From a study of the current data, it appears that the reason for this phenomenon is that some water from Yaquina Bay frequently enters the area inside the reef. Also, Big Creek empties into the area continuously although its flow rate is very small. This is also an indication that there is not a free and rapid exchange between the waters in the outfall area and the open ocean waters. The danger

exists that the effluent materials are "pooled" behind the reef and these waters may be involved in a fractional exchange with the waters of Yaquina Bay. The actual flushing time of the outfall area may be worthwhile studying.

Oxygen. Dissolved oxygen content is classified as a non-conservative property while salinity and temperature are considered conservative properties. The reason for this differentiation is that oxygen is subject to variations caused by non-physical inputs such as biological consumption and release and chemical reactions. Since it is non-conservative, it could vary widely from day to day in the same place as well as from place to place on the same day. In addition, the concentration of dissolved oxygen is generally increased by wind and wave activity. Oxygen saturation concentrations are determined by temperature and salinity. Cold water can hold more oxygen than warm water and salt water can hold less oxygen than fresh water. Nevertheless, dissolved oxygen can be useful in tracing water mass movements and exchanges.

There was very little difference between the oxygen concentration at the surface and at the bottom over the outfall, although the surface values were generally slightly higher. Likewise there is generally little variation from bottom to surface at each station. The variations are indicated in Table IV. The values at the bottom show very little variation from one station to another (Fig. 14). The dissolved oxygen concentrations were mostly near and above the saturation values with two notable exceptions. The first substantial difference between saturation values and observed occurred in mid-May, while another large difference occurred in July-August.

TABLE IV. Average standard deviations of dissolved oxygen concentrations in the plume, outside the plume and outside the reef compared to concentrations at the sewer outfall

	In Plume	Out of Plume	Outside Reef
Surface	+0.3ml/l	+0.5ml/l	+0.4ml/l
Bottom	0.0ml/l	0.0ml/l	-0.4ml/l

All stations had surface values of dissolved oxygen that were significantly higher than was found over the outfall. Those values out of the plume averaged 0.5 ml/l higher than the surface values over the outfall. These figures indicate that the effluent does affect the surrounding waters for some distance because the "in plume" stations were generally taken from 2,000 to 3,000 feet from the outfall. More detailed studies of dissolved oxygen concentrations in the entire area should produce useful information concerning the mixing of the effluent and its effect on the surrounding environment.

An oxygen sag is notable about mid-May which also coincides with a drop in temperature and an increase in salinity. It would appear that upwelling may have existed for a short time during this period. In early July, the oxygen concentrations dropped to less than 4 ml/l and remained low throughout July and August. The oxygen sag is undoubtedly caused by upwelling of deeper waters from offshore which do not contain as much oxygen as the surface waters

Density. The density variations in the area of study are shown in the graph of Figure 15. In this graph σ_t values are plotted vs time. [$\sigma_t = (\rho - 1)\ 10^3$]. The anomalous increase in density in mid-May coincides with the changes in temperature, salinity and oxygen of that period. This is further evidence that upwelling occurred at that time, however it did not continue. Stratification was greatest during the two months (May and June) before upwelling definitely set in. The increase in density occurring in July and August is typical of that caused by upwelling in nearshore waters. There was a tendency for a greater difference between surface and bottom (40 feet) density outside the reef than inside the reef indicating greater

mixing inside the reef, although the difference was not of significant proportions.

Upwelling. Upwelling initially started in May when a temperature of less than 9.5°C and a salinity of over 33.0 o/oo produced a sigma-t value of almost 26.0 at the outfall. This fact is borne out by the offshore sections of temperature, salinity and sigma-t shown in Figures 16, 17 and 18 in which the isopleths of temperature, salinity and sigma-t all slope upward toward the shore. However, this situation was apparently short-lived. In late June, while the local coastal winds were generally from the south, the surface water was much warmer than the bottom water (about 3°C). During this time a noticeable thermocline developed (see BT traces Figures 10a, b, c and d) with the mixed layer being about 15 feet deep. It was not until about July 1 that upwelled waters were clearly noticeable at the surface again. That date clearly marked the beginning of the upwelling season. During July and August the conditions in the vicinity of the outfall indicated that upwelling was continuous with temperatures remaining low (generally less than 10°C), salinities high (generally in excess of 33 o/oo) and densities high (sigma-t, generally in excess of 25.5). Examination of Figures 19, 20 and 21 shows that upwelling was apparently temporarily cut off farther offshore during the period July 27-August 1.

As can be seen from the graph of sigma-t values versus distance offshore and depth for August 9-11 (Fig. 24), the upwelled water apparently would have come from a depth of nearly 300 feet assuming no mixing with other waters had occurred. Salinity values of water in the outfall area also correspond to the salinity values offshore at depths of about 200-300 feet. The general slope of the isohalines, isotherms, and isopycnal lines

(Figs. 22, 23, and 24) is upward toward the shore which is typical during periods of upwelling.

Upwelling may be rather localized along the Oregon Coast. The Oregon State University Albacore Central organization, which has used infra-red sensors from NASA aircraft, reported on July 6th, 1969 that coastal upwelling was observed from Brookings to Lincoln City. They reported no upwelling from Lincoln City to Astoria. The width of the zone affected by upwelling varied at that time from 25 miles off Gold Beach, Oregon to five miles off Coos Bay and Newport.

Longshore currents. Longshore currents, if sustained, could spread pollutants along a beach. Therefore, longshore currents were measured in the Newport area. It is well known that when waves approach a straight coastline at an oblique angle, a mean current tends to be set up along the beach. This current is frequently called the longshore current. Many hypotheses have been advanced by a variety of authors to explain this phenomenon. Furthermore, many prediction schemes have been tried. However, according to Galvin (1957): "A proven prediction of current velocity is not available, and reliable data on longshore currents are lacking over a significant range of possible flows."

Putman, Munk and Traylor (1949) have considered the relationship between the energy of the incoming waves and the longshore current. They also considered the relationship between the momentum of the incoming waves and the longshore current. Of these two approaches, it seems that the momentum approach is better since momentum is conserved whereas energy may be dissipated. The difficulty with the momentum theory is that the value of the friction coefficient must vary over a wide range of 3 1/2 orders of magnitude. The equations developed by Putman, Munk and Traylor follow:

$$V = \left[\left(\frac{1}{4x^2} + y \right)^{\frac{1}{2}} - \frac{1}{2x} \right]^2$$

where $x = \frac{108.8 H_b m}{T} \cos \theta_b$

and $y = C_b \sin \theta_b$.

The speed, V, of the longshore current is dependent upon the height of the breaking wave, H_b, the speed of the breaking wave, C_b, the wave period, T, the beach slope m, and the angle the breakers make with the bottom contours, θ_b. The most critical factors of this or any other equation for predicting the longshore current is that the value of θ must be known more precisely than it is commonly possible to measure; the beach must be a straight sand beach with straight and parallel contours; and there must be no wave reflections from heads, jetties, or other structures. Applications of this equation to the observed data have indicated the accuracy of prediction is anywhere from 25% to 300%. More recently M. S. Longuet-Higgins (1969) has generated simpler prediction equations based principally on Airy wave theory.

$$\overline{V} = \frac{5\pi}{8} \frac{s}{c} u_{max} \sin \theta$$

In this equation the mean longshore component of velocity is dependent upon a constant coefficient of bottom friction, c, the maximum orbital velocity in the waves, u_{max}, the angle of incidence, θ, and the beach slope, s. As in Putnam, Munk and Traylor's theory the critical factor is the angle of approach.

A glance at the data on longshore currents (Tables V & VI) will indicate the difficulty of trying to predict the longshore currents in the Newport area.

TABLE V Longshore current & wave data for Newport Oregon; Sept '68 - Aug '69

STATE PARK BIG CREEK

Date	Min. Speed (ft/min)	Flowing to	Min. Speed (ft/min)	Flowing to	Wave Direction (from)	T_s	H_b	H_o
9-17				N	235°	13.0	11.3	7.8
9-18		S		S	280	11.0	6.6	4.1
9-27		S		S	300	10.0	10.0	8.5
10-3	32	N			295	9.2	5.6	3.9
10-4		N	0		290	9.1	9.1	8.1
10-10		N		S	280	9.6	11.3	10.6
10-23				S	280	9.5	9.3	8.0
10-28	133	N	30	N	250	10.3	9.6	7.8
10-31				S	265	10.7	8.7	6.4
11-5				S	260	12.0	11.3	8.5
11-7				N	230	11.2	11.0	8.8
11-12		N			170	13.3	10.0	6.4
11-14	27	S	24	N	285	12.4	9.3	6.2
11-19		N		N	270	12.5	8.0	4.9
11-26		N		N	285	12.8	8.0	4.8
11-29		S		S	270	13.6	13.0	9.3
12-5		S		S	297	13.0	15.3	12.4
12-12			18	N	270	11.9	13.0	10.6
12-17	25	N			290	9.0	9.3	8.5
12-24			21	N	255	14.7	15.0	10.6
12-26		S		S	270	9.2	10.4	9.8
1-2		N			270	8.7	13.3	---
1-9	0			N	280	11.8	16.0	14.6
1-14			34	N	280	12.7	11.7	8.5
1-16		N		N	290	9.1	9.0	8.0
1-21		S		S	270	9.2	8.6	7.4
1-23	11	S	15	S	290	11.8	9.3	6.5

TABLE V (Continued)

2-4	50	N	55	N	280/230	10.3	7.8	5.7
2-6			48	N	260/210		10.7	
2-11		N	30	N	240	17.8	10.0	4.8
2-13	8	S	54	N	290	14.2	13.3	9.2
2-18	30	N&S	11	N&S	280	13.7	14.7	11.1
2-20	43	S	44	S	282	15.5	16.1	11.2
2-25		N	16	N	290	11.8	10.7	8.0
2-27			57	N	245	10.7	14.6	----
3-4	0				280	10.7	11.1	9.3
3-6			43	S	295	13.5	16.0	12.8
3-11		N			290	14.4	8.0	4.2
3-13	0			N	280	9.8	9.3	7.8
3-18	50	N	50	N	265	13.5	11.3	7.6
4-1			0		270	11.4	12.3	10.2
4-3				N	280	11.3	14.0	12.5
4-7	8	S	64	S	295	10.9	8.6	6.2
4-8			0		287	14.7	10.5	6.2
4-10			14	S	280	10.6	12.0	10.5
4-22	16	S		S	255	11.4	9.3	6.7
4-24		N	21	N	290	10.6	8.7	6.5
4-29	86	S	37	S	305	9.4	9.3	8.1
5-1		N	33	S	285	14.5	14.7	10.4
5-5		S			292	12.1	8.7	5.7
5-8		N	18	S	290	11.6	6.0	3.4
5-13	6	S			315	12.9	9.3	5.9
5-16	18	S	5	S	315	9.6	9.3	7.9
5-21		S	161	S	285	12.0	5.3	2.7
5-27	80	N	49	N	260	8.6	14.6	----
6-3		S		N	270	7.6	5.3	4.3
6-5	3	N	18	S	315	9.8	6.7	4.6

6-10			46	N	275	11.6	9.3	6.6
6-13	17	S	48	N	320	9.3	5.3	3.5
6-14	41	S			270	11.7	4.0	1.8
6-18			13	N	280	7.1	7.0	----
6-19		N			320	7.8	4.0	2.8
6-25		S	0		280	11.6	8.7	5.9
6-30			10	S	335	7.0	8.7	----
7-1			11	S	340	6.4	7.3	----
7-7	32	S			320	5.8	9.0	
7-8	54	S			310	5.7	5.4	----
7-14	28	S			300	11.3	4.7	2.4
7-16			28	S	315	7.8	7.3	6.8
7-18	20	S		S	320	8.1	4.3	3.0
7-21		S			330	5.2	9.3	----
7-28	23	S			315	11.4	5.3	2.9
7-29		S			330	6.6	4.4	3.8
8-1			29	S	335	7.2	4.4	3.4
8-11		S		N	320	9.0	4.4	2.8
8-18	13/35	S			320	6.3	8.7	7.4
8-19	15/127	S			325	6.1	8.7	----

TABLE VI. Direction frequency of longshore currents for angles of deep water wave approach. (Angles of wave approach are rounded off to the nearest whole multiple of ten degrees).

Longshore movement	240° or less	250°	260°	270°	280°	290°	300°	310°	320°	330°	340°
STATE PARK											
North	2	1	1	3	2	9	1		2		
South			1	5	2	5	5	2	7	3	
None					4						
BIG CREEK											
North	3	2	3	4	7	6			2		
South			2	4	4	5	4	1	4		3
None				1	2	2					

The wave direction (a critical factor) may be out of the northwest but the longshore current may still be travelling to the north! We have observed in the Newport area that the waves are sometimes reflected from the north jetty of Yaquina Bay entrance, thus producing waves travelling parallel to the beach in a northerly direction while the incoming waves are approaching from the northwest. Furthermore, on many occasions a dual system of substantial waves were observed. For example, a swell from the northwest would be arriving at the same time a swell (of a different period and height) from the southwest was arriving.

The beaches between Newport and Yaquina Head have several reefs nearly parallel to the shore that are lower in some places than others. The reefs will direct the longshore current (depending on the tide) to a low spot in the reef where a rip current temporarily develops to take the water back through the breakers. When drift bottles got into these rips they seldom returned to the beach. There were three general areas where rips seemed to arise, one was along the south side of Yaquina Head, another was in the vicinity of Big Creek and another was along the south side of the rubble mound opposite the sewer outfall. Since none of these rips were sustained over a very long period of time (with the exception of the one south of Yaquina Head), they would not be useful for dispersing sewer effluents.

The longshore currents were measured at generally two locations in the study area, between Big Creek and Little Creek and at the beach north of Yaquina Bay State Park. The data in Table V summarizes the longshore current as well as the wave data obtained throughout the year. Blank spaces in the current columns indicate that no bottles were recovered on the beach, an event that occasionally happened on ebb tide, especially when the bottles

got into a rip current. Sometimes the bottles were picked up by people walking along the beach so no distance measurement could be made. The longshore currents are definitely not sustained since at times they are in opposite directions at different portions of the beach. During the fall, winter and spring months (through May) the currents are about evenly divided between northerly flow and southerly flow. During the summer months (June, July and August) the flow is predominantly south. However, the direction of wave approach was predominantly out of the northwest (270°-340°) for the entire year. The longshore current velocities measured ranged from zero to over 100 ft/min.

Waves. The wave data obtained is also given in Table V. Some days there were significant waves coming from two or more directions. In these cases the larger waves were measured. Since the wave heights were measured as the waves were breaking, it was necessary to calculate the deep water wave height. The deep water wave height was obtained from a combination of Airy wave theory (deep water waves) and solitary wave theory. Waves change to an approximation of solitary waves just before breaking. The following equation was used:

$$H_o = \left(\frac{H_b^3 \, dl_s}{0.027 L_o dl_o} \right)^{\frac{1}{2}}$$

where H_b is the height at breaking, L_o is the deep water wave length and dl_s/dl_o is the refraction coefficient which was assumed close to unity, and neglected.

The significant wave periods ranged from as low as 5.2 seconds (July 21) to as long as 17.8 seconds (Feb. 11) with some waves of periods up to 21 seconds being observed in the winter months. The average wave period measured for

the entire year was 10.5 seconds. The breaker heights ranged from a low of 4 ft. (June 19) to a high of 16.1 ft. (Feb. 20). The average significant breaker height measured was 9.5 ft. The deep water wave heights ranged from 2.8 ft. (August 11) to 14.6 ft. (Jan. 9). The average deep water wave height was 7.2 ft. As one would expect, the longer period waves are affected more in the shoaling process than are the short period waves since they "feel" bottom sooner and undergo a greater reduction in celerity.

The average monthly wave statistics measured are listed in Table VII. The average direction of wave approach for each month was always greater than 270°. The average wave periods were somewhat shorter in the summer months, a rather surprising result since the "textbook" examples indicate shorter periods in the winter or storm season and longer periods during calmer weather when swell from distance storms arrive at the beach. The average deep water wave height, however, does indicate higher values in the winter season, which is generally expected.

Currents. Several driving forces can contribute to the water movement or currents in coastal areas. The more important forces are winds, main ocean currents on the continental shelf, wave transport, tides and pressure gradients. The topography of the coastal area under investigation (Newport area) sets it apart from the straight and sandy beach areas that have a direct connection with the open sea at all depths that have been studied in other areas. Yaquina Head forms a northern boundary and the north jetty at Yaquina Bay entrance forms a southern boundary for the area we have studied. Both of these structures can be expected to influence the flow of water. The eastern boundary of the area is the beach. The western boundary is a partial one; a submerged reef that extends northward

TABLE VII.

Monthly wave averages, Newport, Oregon, September 1968 - August 1969

Month	Sept. '68	Oct.	Nov.	Dec.	Jan. '69	Feb.	March	April	May	June	July	Aug.
Direction from	272°	276°	268°	277°	280°	271°	282°	283°	292°	297°	320°	324°
Period (sec)	11.4	9.7	12.5	11.5	10.5	11.8	12.3	11.3	11.6	9.3	9.8	7.4
H_o (feet)	6.8	7.5	7.0	10.4	9.0	8.3	8.3	8.4	6.1	5.2	6.6	4.5

from the jetty. The beach has some reefs in the offshore section and part of the foreshore section which are generally submerged except at lower low water on spring tides. Above the reefs there is a sand beach which is backed by cliffs.

Local topography is important for several reasons. The water in this area does not have a completely free connection with ocean waters; it is set off from other coastal waters both to the north and to the south. The presence of the jetty, Yaquina Head and the reef cause nearly all waves that reach the area to undergo some modification. Winds are strongly influenced by the presence of Yaquina Head (356 ft. elevation) to the north. Yaquina Bay may act as a channel for winds coming over the Coast Range of mountains to the east.

Pressure gradient forces set up by unequal heating and evaporation, as considered in geostrophic flow, are generally not important in the circulation within small areas especially when compared to the other driving forces. Therefore, they will not be considered further at this time.

The main ocean circulation on the Oregon continental shelf is not known in detail even at the present time. In general the California Current flows southward particularly in the summer season. The California Current (as listed by the USC & GS Coast Pilot 7, 1951, Pacific Coast) is about 300 miles wide with an average speed of 0.2 knots. When compared with other surface currents of the world it may be characterized as a broad, slow and shallow current.

During the winter season the Davidson Current flows northerly along the coast. According to Schwarzlose (1964) "The Davidson Current develops along the Washington-Oregon coasts in September first close to shore and

later widening. It appears as far south as Point Conception by October. It appears to be at least 50 miles wide with speeds of at least 0.5 to 0.9 knots for distances of several hundred miles. In the spring the process is reversed, it disappears in April off central California and in May off Oregon and Washington." Schwarzlose based his conclusions on the returns of drift bottle measurements.

Collins (1967) reported that northerly currents were common, dominating the September and October flow. However, in July the flow at 10, 20m and 60m was usually southward. Stevenson, et al., (1969) reported on the basis of drogue studies made about 40 miles offshore from Newport: "Drogue trajectories showed that the annual mean flow of ocean water off Oregon was southward from the surface to 500m. The most rapid meridional transport was found between the surface and 50 m." The trajectories of the drogues were notably erratic. Average values were used for calculating current flow. Drogues at all depths tended to move in the same direction during a single observation period. Since their data represent only 15 cruises between January 1962 and September 1965 considerable variation can be expected between cruises and for other years and seasons. Stevenson's group did make transport calculations which revealed a zonal transport in the surface layer which was toward the coast while below 200 m the zonal transport was to the west. The general direction of flow was southward in the summer and northward during the fall and winter. During spring and some fall periods, the currents tended to be transitional and variable.

The role of waves in producing longshore currents has already been discussed. Although waves in the ocean may be approximated by Airy theory they actually do have some net forward transport associated with them. The

net forward transport is sometimes referred to as a wave drift current. Kinsman (1965) states that wave currents may reach 1% of the wave speed while wind currents generally reach 3% of the wind speed. Therefore, Stoke's wave equations are called upon to give an indication of the net forward transport:

$$F = H^2_o \quad \exp\ (-\ 2k_o \not{z}) \quad \left(\frac{g\pi^3}{2L^3_o} \right)^{\frac{1}{2}}$$

where the subscript,o,indicates deep water conditions. As before H is the wave height, k is the wave number, $\not{z}$ is the depth below the surface, L is the wave length and g is the acceleration due to gravity. The equation above is applicable only to deep water. Longuet-Higgins (1953) reported that experiments show the equation to be unsatisfactory for shallow water.

Very little work has been attempted in shallow water wave transport studies due to the complex environment. We have included wave data in our study to see if waves do have a noticeable effect on shallow water currents exclusive of the breaker zone.

The effect of tides on currents in waters of the continental shelf has been discussed by several authors. A study of observed tidal currents in shelf waters reveals that each area has a unique rotating tidal current system. The ellipses found by Collins in his study of currents 20 m and greater beneath the surface at about 5 miles off Depoe Bay are shown in Figure 25. Some of these ellipses are of diurnal periods (24 hours) and semi-diurnal periods (12.4 hours) both of which are tidal components. Tidal currents in semi-enclosed basins and estuaries may have a much different configuration due to the confines of the basin. The tidal currents in the outfall area are unknown. Had the Geodyne current meter worked properly

(or had we been able to see the results immediately) we believe we would have been able to measure the tidal components. Future work should include current meter measurements and analysis of the records so that tidal components will be determined as well as inertial currents.

According to Fleming (1938) the maximum tidal current velocity at a location is given by the equation: $V_{max} = \frac{H\pi x}{T h}$ where x is the distance from shore, T is the tidal period, H is the tidal range and h is the water depth. An eight foot tide having a period of 6 hours should then produce a maximum current of about 5 ft/min. at the sewer outfall. This speed would account for 20% of the average currents (25 ft/min) measured at the outfall. The tidal contribution to the currents would increase for larger tidal ranges. The tidal contribution would also be cyclic and reach a maximum only about twice a day.

The time of maximum currents is not generally in close agreement with the mid-flood and mid-ebb stages of the tides as predicted at Newport. There is a slightly greater tendency for more time variation with increasing tidal range. Although there is considerable scatter, the time difference is generally less than one hour. If the tides on the open coast are similar to those inside the bay, the maximum current should come at mid-tide. The tides in Yaquina Bay have been shown to be of the standing wave type (Neal, 1966) which have the maximum current midway between high and low tide.

If the tides off Newport do produce an eliptically rotating system, it is not known at this time what the orientation of the major axis is. The direction of the major axis for tidal ellipses along the Pacific coast of North America generally lie roughly in the northwest-southeast direction.

many exceptions are known, especially in restricted waters. Little work has been done on the direction of tidal currents in nearshore areas. Therefore, our use of tidal data has had to be largely exploratory.

Collins (1967) also observed inertial currents which are nearly circular. Inertial flow is that in which the deflecting force of the earth's rotation is the only acting force. In this case the equations of motion are reduced to:

$$\frac{du}{dt} = 2v\sigma \sin \theta \qquad \frac{dv}{dt} = -2\sigma u \sin \theta$$

where u = velocity along x-axis, v = velocity along y axis, t = time, θ = angle of latitude and σ = angular rotation of earth.

These equations describe the motion in an inertial circle. In this case, the centripetal acceleration must be supplied by the Coriolis acceleration, hence: $F = \frac{V^2}{r} = 2V\sigma \sin \theta$ and the period is given by $T = \frac{2\pi}{2\sigma \sin \theta}$. At 45°N the inertial period is about 17 hours.

The inertial periods observed by Collins were associated with the passage of storms. Thereby suggesting atmospheric coupling with the oceanic environment in the coastal area. It is not known how inertial currents on the shelf affect the nearshore circulation.

Probably the single most important driving force for the currents near Newport is the wind stress. Most empirical equations indicate that the wind stress is a function of the square of the wind speed and take a form similar to: $T = \rho_a C_D U^2$ where T is the wind stress, ρ_a is the air density, U is the wind speed at some given height above the water surface and C_D is the drag coefficient. The proper value

to be used for the drag coefficient is still under study by several investigators. Evidence indicates that the drag coefficient depends upon the "roughness" of the water surface which in turn depends upon the wind speed, at least within certain limits. Mooers et al., (1968) used $C = 2.4 \times 10^{-3}$ (dimensionless) when U is expressed in cm/sec. for wind values over the so-called critical wind speed of 7 to 8 m/sec. For wind speeds below 7-8 m/sec he used $C = 1.5 \times 10^{-3}$. Rossby (Sverdrup, et al., 1942) found that at moderate to high wind speeds the roughness is independent of wind velocity.

Bretschneider (1967) proposed that the steady state surface velocity in shallow water is related to the wind velocity by the equation: $V = 0.0173\ h^{1/6}\ U\ (\sin\theta)^{\frac{1}{2}}$ where U is the wind velocity, h is the depth and θ is the angle the wind blows as measured from the perpendicular to the coast line. Collins (1967) has indicated that on the continental shelf off Oregon (near Depoe Bay) shelf waters respond most directly and completely to changes in the longshore component of wind stress indicating general agreement with Bretschneider's proposal. However, the winds off Newport show evidence of the " land-sea breeze" system at times. Such winds frequently do not have a component alongshore and therefore cannot be used in Bretschneider's formula.

Since the area under investigation is known to undergo seasonal upwelling, it seems appropriate to look again at the equations of Ekman. The net movement of water to the right of the wind in the northern hemisphere as predicted by Ekman's work is considered the principle cause of upwelling. Ekman's equation for surface flow driven by wind is:

$$V_o = \frac{\pi T}{\sqrt{2}\, D\rho\sigma \sin\theta}$$

Where T is the wind stress, D is the depth of frictional resistance, ρ is the water density, σ is the angular velocity of the earth's rotation, and

$$D = \pi\sqrt{\frac{A}{\rho\sigma \sin\theta}}$$

Where A is the coefficient of eddy diffusion and θ is the angle of latitude. The above equation applies to infinitely deep water. For the deflection of the surface current from the wind direction in water of finite depth, Neumann and Pierson (1966) give the following equation:

$$\text{Tan } \gamma = \frac{\sinh 2Kh - \sin 2Kh}{\sinh 2Kh + \sin 2Kh}$$

where γ is the angle between the wind and the current direction, h is the water depth and $K = \pi/D$ where, as before, D is the depth of frictional resistance. A value for A that has frequently been used in calculating D is 100 which gives D = 50 meters in mid-latitudes. The eddy coefficient cannot be used as a constant since it varies with both wind speed and depth. The exact dependency of the coefficient on these two independent variables has not been determined. Since the value of the velocity V_o, even in the case of a known wind stress, depends on the effective eddy viscosity coefficient, theoretical determinations of the speed of pure drift currents are very difficult even in water of infinite depth.

Looking at the equation for the angle of deviation of current from wind, it can readily be seen that if h/D is small, the angle will be small and the surface current will flow nearly in the direction of the wind. The value of h/D in the outfall area at Newport is approximately 0.25

which would produce an angle of about 22°. This value appears to be satisfactory when light winds are blowing in the Newport area (i.e. 6-10 knots), but there are many exceptions. Several observations, for example, showed the current to be almost 180° from the wind! In addition to this paradox, photographs (Fig. 26a, b, c) taken of the dye markers frequently indicated a deviation of the surface dye trace from the actual movement of the markers (which have a drogue six feet beneath them). All of the color prints in Figures 26 (a,b,c and d) were produced from 35mm Kodachrom II slides. A discussion of the pertinent features of each photograph follow.

The photograph dated 28 October 1968 (taken off Big Creek) is an example of what dye markers look like from the air. The dye float that is anchored is shown at the top of the photo (it is giving off a plume of fluorescein dye) the free drifting dye float is at the lower end of the green plume (towards the bottom of the picture). The free drifting float was giving off rhodamine dye (red) which generally drifts with the float making it possible to locate the float from the air. (When slides are projected on a screen, the white floats can usually be seen clearly enough for accurate measurement.)

Frequently the photographs indicate the differences between water movement at the surface and at the drogue depth (6 feet). In the October 28th photo, the green on the surface spread to both sides of the red but more heavily to the left of the picture indicating the surface drift had a component to the left which was, however, much smaller than the component toward the bottom of the photo.

The photograph taken 8 May 1969 was taken just south of Yaquina Head from an altitude of 1000 feet. Some of the rocks at Yaquina Head are visible in the upper part of the picture. The red dye marker, in this case, eventually ran to within about 10 feet of the rocks then turned eastward toward the beach. This photograph illustrates a time when the current at drogue level was greater than the surface flow, although in the same direction, as illustrated by the red "plume" given off by the rhodamine dye cake.

Dye plumes sometimes indicated a highly irregular surface movement of water as illustrated in the photo listed as 21(a) January 1969. This photo was taken in the vicinity of the outfall (note the turbid boundary just to the right of the dye markers which is caused by the effluent) taken from an altitude of 1600 feet. In this photo the surface movement, although quite irregular, appears to be slightly faster than the flow at drogue depth since the red plume is preceding the rhodamine dye float.

The photo listed as 26(b) January 1969 shows the foam frequently produced by the outfall diffusers. The foam movement indicates a variety of surface water movements. The "boil" over the diffusers is at the extreme right in the lower part of the picture. The foam moves across the picture and slightly upward until it apparently strikes a current running out to sea. In the upper right hand part of the picture, the foam turns again and runs roughly northward (to the right of the picture).

The photograph taken 12 November 1968 (from 1500 feet altitude) shows how much the effluent discolors the water. The fluorescein dye is easily visible just to the left of the effluent plume. The green plume given off by the fluorescein dye cake runs parallel to the movement of the dark

effluent. The green dye plume is on the surface. The drifting dye float (red dot about 7 mm to the right of the green marker in the photo) in the effluent has moved to the right, more in the direction in which the "foam line" caused by the diffusers, is going. In this case the surface water where the green dye was found was apparently moving not only faster than the drogue but also in a different direction (roughly 60° away from the line of drogue movement). Since the foam, which was definitely at the surface, was moving in a different direction than the brown effluent as well as the green dye, there must have been divergence in that region on 12 November 1968. The divergence was probably caused by the upward movement of the effluent from the diffusers.

The photo taken on 14 November 1968 shows the well-defined foam line produced by the outfall. This photo was taken from 3000 feet. At this altitude, the dark color of the effluent is hardly noticeable in the photograph (although visible from the plane); it can be seen in the "boil" area. The fluorescein dye is readily seen in the photograph, however, the rhodamine dye is very difficult if not impossible to distinguish. The rhodamine dye was typically hard to see in the foam and in the brown effluent.

The photograph taken on 1 May 1969 (900 feet altitude) shows both dye floats releasing plumes. Both plumes were moving to the right while the net path of the drifting float was nearly in line with the axis of the wheel skirt of the airplane. In this case the surface water was moving faster than the water at drogue level but in a different direction. The research vessel, R/V PAIUTE, is visible in the photograph.

The photos taken on 23 October 1968 and 6 February 1969 show the plume from the sewer outfall heading directly for the beach at Newport.

The photograph taken on 4 March 1969 shows the effluent plume heading for the beach near Big Creek and Agate Beach. The foam line was deflected by the rip current activity which was indicated by discolored water coming from the beach. The darker discolaration of the water to the left of the foam line was caused by the effluent.

The results of our current observations for the project period are indicated in the series of figures included under Figure 27 (a through cc). The early observations were compared to average winds three hours and five hours before current measurement. In general the response to the winds is rapid so that wind history of much more than one hour before current measurement is not important. Stevenson (1964) also found that the current response to winds was rapid in Monterey Bay. Therefore, the wind values used on the charts are the hourly averages before and during the current measurement period. The short arrows on the charts indicate the current direction measured while the figures shown with the current vectors indicate the current speed in feet per minute (above the line) and the current heading (below the line). For example, the notation, $\frac{26}{240}$, at the outfall on February 11th, (Fig. 27k), indicates a current of 26 ft/min flowing toward 240° true. The wind vectors (the long arrows) also have wind speeds and direction annotations. For example on February 11th, the wind was 101 ft/min blowing towards 053° true. The letters, E and F, which appear in the lower right hand corners, indicate tidal stages (E for ebb, F for flood). A study of the entire series of charts shows the extreme variability of the currents and winds in the Newport coastal

area. Furthermore, there is a considerable variation in currents from one station to another. For example, on August 11, 1969 (Figure 27aa), the current at the outfall is flowing nearly opposite to the current off Big Creek. This indicates that fairly large eddies must be set up in the area. The frequent variation between the currents off Big Creek and south of Yaquina Head indicate eddy formation behind Yaquina Head. Perhaps the most puzzling currents occurred on February 27th (Figure 27L). The tide was at ebb, and the wind (13 knots) was blowing offshore yet all currents measured were moving onshore. A thorough check of data and methods has been made to determine if the current measurements were somehow recorded incorrectly, but no such errors were found! There were other occasions when the currents at the outfall or Big Creek were nearly out of phase with the wind.

The plot of points in Figure 28 indicates the deviation of current from wind at the outfall area vs wind speed. When the wind was 10 knots or less the currents deviated mostly to the left (negative values) of the wind (mostly less than 50°). However, when the wind was greater than 10 knots the current deviated almost entirely to the right of the wind. In Figure 29 the current speed at the outfall is plotted vs wind speed for the same period. Although there is considerable scatter, a difference in relationship between current speed and wind speed is noticeable for winds under 10 knots compared to wind speeds over 10 knots. (Two lines have been sketched in for comparison of trends only). This change in relationship seems to justify the change in drag coefficient for changing wind speeds. However, the change appears to come at about 10 knots rather than 14 to 16 knots (7 to 8 m/sec) as suggested by Mooers et al., (1968).

Further analysis of the relationship of current speed to wind speed for the outfall area (for the entire project period) shows that for winds less than or equal to 10 knots, the ratio u/U (current speed/wind speed) averages 0.0450 while for winds greater than 10 knots the average is 0.0194. The average ratio off Big Creek for winds less than or equal to 10 knots was 0.0487 while it was 0.0199 for winds greater than 10 knots. The results are summarized in Table VIII.

The standard deviation (positive square root of the variance) shows an extremely variable ratio, especially for winds less than 10 knots. This seems reasonable because if tides and waves are to have any effect on currents they should be most effective when the wind is weakest and least effective. At higher wind speeds the standard deviation is smaller indicating less variability. Therefore the current must be more dependent upon the wind. It is commonly accepted that the wind current is about 2 - 3% of the wind speed which seems to hold time in this area for winds in excess of 10 knots even though wave and tide effects have not been filtered out.

It is remarkable that the average ratios are so similar at Big Creek and the outfall, since currents in these two places frequently do not flow in the same direction. The influence of Yaquina Head on winds and wind effects would be expected to be greater at Big Creek.

The dissimilar nature of currents measured at the various stations is further illustrated in the histograms in Figures 30, 31, 32, 33, and 34. The directions of flow are also extremely variable.

There seems to be no predominant direction of flow south of Yaquina Head, although there were more times when the current flowed toward the beach

TABLE VIII. Average ratios of current speed, u, to wind speed, U.

	Average (u/U)	Standard Deviations
Outfall ($U \leq 10$ knots)	0.0450	0.0417
Big Creek ($U \leq 10$ knots)	0.0487	0.0434
Outfall ($U > 10$ knots)	0.0194	0.0096
Big Creek ($U > 10$ knots)	0.0199	0.0116

(090° and 130°) than toward any other direction. The currents measured off Big Creek flowed most frequently in northeasterly and southeasterly directions. At the sewer outfall the currents flowed most frequently towards either the northeast (towards Agate Beach) or towards the southwest. North of the jetty the currents flowed most frequently in a general westerly direction (between 200° and 300°). Currents near the end of the north jetty showed a fairly even distribution with a slight tendency for flow toward the northeast quadrant.

The wind did show some predominant flow patterns (Figure 35). The most frequent flow was toward the south. The second most frequently observed winds blew toward the north. The wind data are somewhat biased since we were able to make more measurements during the summer months when the winds are typically from the north. East winds probably were recorded more frequently than would normally be expected because we had to get to sea early in the morning before sea conditions became too severe for the R/V PAIUTE. The land-sea breeze system generally produces winds from the east in the early morning.

There is no readily apparent correlation between the wind histogram and any of the current histograms when considering the entire year of measurements. The degree of correlation will be discussed later.

Figures 36, 37, 38, 39, and 40 are velocity plots of currents measured south of Yaquina Head, off Big Creek, at the sewer outfall, north of the jetty and near the end of the north jetty respectively. The current vectors at Yaquina Head again show strength toward the beach (090°) and also toward 310°. Off Big Creek the currents showed the greatest strength flowing toward the region between 010° and 190°. There was considerable scatter, however,

with no single direction showing significant predominance. At the outfall the single direction showing greatest flow strength was toward Agate Beach. North of the jetty the currents were predominantly strongest toward the southwest quadrant. Near the end of the jetty there was more variability but flow towards the northeast quadrant seemed to be strongest.

Our first look at the data was by plotting the current values against the wind, wave, and tide values to determine any obvious relationships. Current speed appeared to be related to wind speed, but only during relatively strong winds (over 10 knots). During wind speeds of less than 10 knots considerable scatter resulted. Likewise, considerable scatter resulted when we plotted wind direction versus current direction. However, the relationship between current direction and wind direction was better for high wind velocity than for low wind velocity.

Tidal stages were plotted vs current speed and vs current direction for all values of wind as well as for light winds only. At low wind speeds the current appeared to run north and south during predicted maximum tidal flows. An interesting plot was obtained for current speed vs tidal stage for winds under 7 knots. Of the 19 current speed values used, 14 were between 11 and 20 ft/min. These speeds had no relationship to the stage of the tide, suggesting the wind as the dominant driving force at nearly all wind speeds, and that the tide and wave effects are overwhelmed by the wind. However, this is not borne out in wind speed and direction plots versus current speed and direction. Unfortunately when the data are separated according to tidal stage, wind speed, current direction, etc., the number of observations fitting any special set of circumstances is not sufficient for reaching "air tight" conclusions.

Plots of breaker heights, breaker periods, and deep water wave heights against currents were all tried. No relationships were even remotely suggested in those plots, therefore, we assumed that any contribution made by the waves was insignificant when compared to the effects of the other possible driving forces. We did, however, consider the waves in the regression analysis.

In view of the apparent lack of correlation between currents and the forcing functions we decided to test the actual importance of the various agents that could have an effect on the currents. The current data were collected mostly as random observations, that is, there was no control over the entire range of tidal stages and over as wide a variety of wind conditions as practical. Therefore, we assumed it would be possible to find a statistical regression equation that fits the data. Such an equation should allow one to determine not only which factors or conditions are most significant in relation to the currents observed but also the relative importance of all conditions considered.

The Oregon State University Department of Statistics maintains a library of computer programs, which are available to researchers at the university. We chose the computer program *STEP, a stepwise multiple linear regression analysis program discussed by M. A. Efroymsen (Ralston and Wilf, 1960). The rationale for trying to express the current in terms of the primary current producing forces is that measurements of the primary forces are generally more readily available than current measurements. Furthermore, prediction schemes already exist for the primary driving forces (winds, waves, and tides). When current conditions can be predicted at the outfall, decisions can be made regarding allowable or desirable changes in effluent pumping rates.

The regression equation we used is a mathematical statement relating one or more variables to one observed resultant value, the current. Using the method of least squares, the relative dependency between the observed current and the driving forces can be determined. In addition, a straight line "best fit" for the data is formulated. Since a straight line is generated, the variables wind, waves and tide must be linear expressions such that increasing values of the variables give proportionally increasing values of current velocity. It is this feature of the equation which requires "modeling" an expression for each of these variables such that the current-producing forces become linear expressions. Once the variables are in an acceptable linear form, the coefficients of each variable are determined. The coefficients indicate the relative importance of each term in the overall relationship. The general form of the equation is

$$V = A_o x_o + A_1 x_1 + \ldots\ldots\ldots + A_{n-1} x_{n-1} + E$$

where V is the predicted current vector, the A's are constants specifically determined from the program, the x's are the values of the variables at which the prediction is desired, and E is an error term. The values of A are chosen by the program so that the error term is a minimum after a large number of observations have been analyzed.

The computer program considers one variable at a time. The contribution of a variable in reducing the variance is considered for all variables in the equation and the simple correlation coefficients are calculated. If the contribution of a variable is insignificant, this particular variable is disregarded.

Various values are given as the program proceeds which indicate how well the equation generated actually fits the observations. Perhaps the

most useful of these is the multiple correlation coefficient, R^2, which is the ratio of the sum of the predicted current minus the simple average of the current, the quantity squared, to the sum of the observed current minus the simple average, the quantity squared, as in the equation:

$$R^2 = \frac{\Sigma (V_p - \bar{V})^2}{\Sigma (V_o - \bar{V})^2} .$$

The closer R^2 comes to unity the better the equation. Thus the value of R^2 may be used as an indication of the per cent of the variance explained by the individual variable. Large deviations between predicted and observed values are indicated by low values of R^2.

We put our data, obtained from field measurements, on IBM cards and ran them through a computer routine (see appendix). That routine calculates current speed, true direction, tidal values, wind speed in knots, and lists the data in usable computer format. The problem then was to linearize the effects of the various forces. Linearization of the driving forces is not only complex but largely unknown to the degree of accuracy desired.

There are many different methods of linearizing each variable which are, for the most part transformations of the original data. The methods we used have been used or suggested by various observers. Although the degree of success that others have had depended upon the special set of data selected for use, we felt that we should use the methods as a starting base.

We calculated the wind component according to Thorade (Neumann & Pierson, 1966), where the current velocity V is given by the equation

$$V = \frac{2.59\ W^{1/2}}{(\sin \phi)^{1/2}} \quad \text{(for winds equal to or less than 6 m/sec)}$$

and

$$V = \frac{1.26\ W}{(\sin \phi)^{1/2}} \quad \text{(for winds greater than 6 m/sec).}$$

In these equations V is current velocity in cm/sec, W is wind speed in cm/sec and $\emptyset$ is the angle of latitude. We calculated the vector component by subtracting the wind direction from the current direction and taking the cosine of the angle. We multiplied the cosine by the wind speed to give the wind vector component acting in the same direction as the current vector.

The wave component we used came from the Stoke's transport equations described earlier. The vector component was calculated from the cosine of the difference in direction multiplied by the wave induced speed.

The tidal component is the component least well known. It is impossible to accurately assign, a priori, a direction or shape to the tidal current system. (Continuous current meter records are required to determine the correct tidal components.) Observations taken in other areas indicate that tidal currents are rotary and seldom if ever equal to zero. We initially chose a direction of 315° for maximum ebb current and 135° for maximum flood current. We calculated a speed by the following equation (Fleming, 1938):

$$V = (\sin \frac{2\pi t}{T}) \quad \frac{2\pi Ax}{T\,h}$$

where V is the tidal current in ft/min, t is the time elapsed during either the ebb or flood, T is the duration of the tidal flow, h is the depth, A is the amplitude of the tide and x is the distance offshore. We obtained the tidal vector component by multiplying the tidal current calculated above by the cosine of the angle difference between the estimated tidal flow and the observed current flow.

We then had three independent variables with the current vector as the dependent variable. The regression equation obtained for currents in any direction was

$$V = 17.96 + 695.8\, x_1 + 0.0057\, x_2 - 1.28 x_3 + E$$

where x_1, x_2 and x_3 were the wave, wind and tidal components respectively. The R^2 value for the current predicting equation in this case was only 12%. The tidal component received a negative coefficient possibly because the tidal input is out of phase with the real tidal flow. The tidal component could be checked in steps until the correct orientation is obtained if the magnitude were known. When this data was put through the regression program, the variance explained by each variable was: wind, 4.4%; waves, 4.0%; and tide, 4.0%. The results were disappointing to say the least. Obviously these transformations, although used with some success in other situations, have little value when applied to the currents measured at the outfall off Newport, Oregon.

We used another approach. We separated the current and related variables into north-south components and east-west components, then ran them through the regression program. The sine or cosine as appropriate of the wind direction was multiplied by the wind speed to obtain the wind vector. We multiplied the sine or cosine of the wave direction by the breaker height to get a wave vector. The tidal vector was obtained by multiplying the fraction of tidal range at the observation time by the sine or cosine of the direction assigned to the tide. In this case we chose an easterly direction for mid-tide flood and west for mid-tide ebb. In addition, the three vector components obtained as described above were multiplied against themselves (e.g. wind component times tidal component) to effect a combination. Using the north-south components the current prediction equation obtained was

$$V = 3.87 - 0.72x_1 + 0.0196x_2 + 0.54x_3 - 0.17x_1x_3 + E$$

where all symbols are as indicated before. The product of the wave and tide components is given by x_1x_3. The R^2 value given was 48% in this case. Even though rough data were used, the variance explained by each variable was wind 40%, tide 6%, waves 1%, and all component products negligible.

For east-west components the equation became

$$V = -6.408 - 0.0087x_2 + 1.60x_3 + 0.0020x_1x_2 + 0.00065x_2x_3 + E$$

where again all symbols are as indicated above. The R^2 value obtained was 28%. The variance explained by each variable was: wind 1%; tide negligible; waves negligible; wind and waves product 23%; and wind and tide product 2%.

The approach using directional components was considerably better than the results obtained as outlined in the preceding paragraphs. Two important points are suggested by our results. First, the currents at the outfall do not appear to be predictable with a general equation which assumes forces have uniform effect regardless of direction. Equations generally in use for current predictions elsewhere do not seem to apply to the currents in the outfall area off Newport.

We have looked over our data carefully and searched for errors that could be eliminated in either data collection or data processing. Although we have found occasional errors which may have influenced the analysis slightly, we feel the data are in general very good and therefore usable. It is rather unique to have data of this type even though we feel we definitely need at least some current meter records to improve the tidal component determination.

MISCELLANEOUS OBSERVATIONS

Whenever conditions permitted we recovered the styrofoam floats and "tin cans" from the ocean. Those floats and strings used in the outfall very quickly (within a week) accumulated an ugly slimy covering of brown material which evidently came from the paper mill effluent. Floats and strings recovered from areas remote from the outfall (one mile away) did not have the accumulation of dark brown material on them. The accumulated brown material also seemed to "eat" into the styrofoam. Those floats recovered in the effluent always were dark and had the appearance of being nearly half "eaten".

FUTURE WORK

At the present time at least two master's degree theses are taking shape as a result of this research program. One of these will be an analysis of the winds along the Oregon coast. A definitive study of the coastal winds has never been made as far as we can ascertain. This study of the winds is already underway. The results of the wind study should provide valuable information for future current studies all along the Oregon coast.

Further work is being done on the data we now have concerning the currents at Newport. This work is expected to become the major part of another thesis. A large number of approaches to the prediction of currents can be imagined. Time is the factor limiting how many of them may be attempted. The proposed thesis work consists of grouping the data according to quadrants of the compass. With boundaries on three sides of the area it is possible that forces such as the wind and waves vary considerably in different quadrants (as indicated in the east-west regression). In addition, closer

examination of the wind components appears useful. Rather than using more specific transformations developed by others, a more general approach is suggested which applies to the Newport area.

RECOMMENDATIONS

On the basis of the data and results we have now obtained, we make the following recommendations:

1. Continuous records of currents should be obtained in the outfall area so that tidal and/or inertial components can be determined. Continuous records of currents should be taken simultaneously a few miles offshore so that the effect of shelf circulation on the outfall circulation can be determined.
2. A more efficient wind measuring device should be installed on the Newport jetty during any future work (i.e. one with better resolution of direction). Whatever anemometer is used should be such that the record does not have to be sent away for decoding. Such procedures are very wasteful of time since no meaningful data processing and analysis can take place until they are returned. An effective program requires "real time" data acquisition.
3. Continuous records of currents near the end of the north jetty should be obtained to determine what exchange of waters occur between Yaquina Bay and the outfall area.
4. Additional dye-float studies should be concentrated near the end of the north jetty (in the channel and out of the channel) to determine the path the water takes in that region.

5. Continuous records should be obtained of temperature and salinity both in the mouth of Yaquina Bay and in the outfall area so that the exchange of waters between the two areas can be better determined.
6. A calculation of flushing time for the outfall area should be made. Such a calculation would require installation of tide gages and current meters in the area.
7. The biota found in the plume area should be studied and compared to areas outside the plume to see if the plume has a deleterious effect.
8. Bottom samples should be taken all around the outfall area to see if the sludge that we detected on our floats is also being deposited on the bottom.

We are willing to carry out as many of these recommendations as are compatible with any future funding we obtain from FWPCA and with our own capabilities. We would especially like to carry out recommendations numbered 1, 3, 4, and 5.

REFERENCES

Bretschneider, C. L. 1967. Estimating wind-driven currents over the continental shelf. Ocean Industry, June 1962.

Brooks, Norman H. 1968. Ocean disposal, in: Stream and Estuarine Analysis. Manhattan College, New York.

Collins, Curtis A. 1967a. Currents on the Oregon continental shelf (Abstr). Trans Amer. Geophys. Union 48 (1): 130.

Collins, Curtis A. 1967b. Description of measurements of current velocity and temperature over the Oregon continental shelf, July 1965 - February 1966. Ph.D. Thesis Oregon State University, 1967.

Fleming, Richard H. 1938. Tides and tidal currents in the Gulf of Panama. Journal of Marine Research. Vol. 1. pp 192-206.

Galvin, C. J. 1967. Longshore current velocity: a review of theory and data. Rev. Geophys. 5: 287-304.

Kinsman, Blair. 1965. Wind Waves. Prentice-Hall, Englewood Cliffs, N. J.

Longuet-Higgins, M. S. 1953. Mass transport in water waves. Phil. Trans. Roy. Soc. of London. Ser H. Vol. 295 No. 903 pp 535-581.

Longuet-Higgins, M. S. 1969. On the long-shore currents generated by obliquely incident sea waves. J. Geophysical Res. (In Press).

Hooers, C. N. K., L. M. Bogert, R. L. Smith and J. G. Pattullo. 1968. A compilation of observations from moored current meters and thermographs (and of complimentary oceanographic and atmospheric data) Volume II: Oregon Continental Shelf, August-September 1966. Oregon State University, Dept. of Oceanography Data Report #30. Ref. 68-5.

Neal, Victor T. 1966. Tidal currents in Yaquina Bay. Northwest Science, Vol. 40 #2.

Neumann, Gerhard and Willard J. Pierson, Jr. 1968. Principles of Physical Oceanography. Prentice-Hall, Inc., Englewood Cliffs, N. J.

O'Neal, Gary. 1966. The degradation of Kraft pulping wastes in estuarine waters. Ph.D. Thesis, Oregon State University.

Putnam, J. A., W. H. Munk, and M. A. Traylor. 1949. The prediction of longshore currents. Trans. Amer. Geophys. Un. 30: 337-345.

Ralston, A. and H. Wilf (editors). 1960. Mathematical methods for digital computers. John Wiley & Sons.

Schwarzlose, R. A. 1964. Nearshore currents of the Western United States and Baja, California as measured by drift bottle. CALCOFI Report. June, 1962. Sacramento, California.

Stevenson, C. D., 1964. A study of currents in southern Monterey Bay. M.S. Thesis, U.S. Naval Postgraduate School.

Stevenson, Merritt R., June G. Pattullo and Bruce Wyatt. 1969. Subsurface currents off the Oregon coast as measured by parachute drogues. (In press).

Sverdrup, H. V., Martin W. Johnson and Richard H. Fleming, 1942. The Oceans, their physics, chemistry and General Biology. Prentice Hall Inc., Englewood Cliffs, N. J.

LIST OF FIGURES

12b. BT trace taken at the outfall at 1130 PDT, 4 March 1969.

12c. BT trace taken inside the outfall plume at 1140 PDT, 4 March 1969.

12d. BT trace taken outside the outfall plume at 1150 PDT, 4 March 1969.

13. Salinity at the outfall during the period October 1968-August 1969. The three lower lines show deviations from outfall salinities (b) in the plume (c) outside the plume and (d) outside the reef.

14. Dissolved oxygen concentrations at the outfall in ml/liter (October 1968 - August 1969). The dashed line in the upper plot indicates saturation values. The lower traces are deviations from outfall concentrations (b) inside the plume, (c) outside the plume and (d) outside the reef.

15. Sigma-t values (a) at the outfall, (b) outside the plume and (c) outside the reef (October 1968 - August 1969).

16. Temperature structure off Newport, May 13-15, 1969

17. Salinity structure off Newport, May 13-15, 1969.

18. Density structure off Newport, May 13-15, 1969

19. Temperature structure off Newport, July 27 - August 1, 1969.

20. Salinity structure off Newport, July 27 - August 1, 1969.

21. Density structure off Newport, July 27 - August 1, 1969.

22. Temperature structure off Newport, August 9 - 11. 1969.

23. Salinity structure off Newport, August 9 - 11, 1969.

24. Density structure off Newport, August 9 - 11 , 1969.

25. Current velocity ellipses. "H" corresponds to high tide and north is toward the top of the figure (Collins, 1967).

26a. Color photographs of dye markers and foam from the outfall.

26b. Color photographs of the outfall plume.

26c. Color photographs of dye markers near the outfall and the outfall plume.

26d. Color photographs of the outfall plume.

27.(a through cc). Current and wind vectors measured in the coastal waters near Newport. Tidal stages are indicated by E (ebb) and F (flood) in the lower right hand of each diagram. Dates are indicated in the upper portion of each diagram.

28. A sample plot showing the deviation of current direction from air movement vs wind speed. Positive values indicate current deviations to the right. The wind speed, U, is indicated in knots.

29. A sample plot of current speeds, u, in ft/min vs. wind speed, U, in knots.

30. Histogram of currents measured south of Yaquina Head. Arrows indicate direction toward which the currents were flowing.

31. Histogram of currents measured off Big Creek.

32. Histogram of currents measured at the sewer outfall.

33. Histogram of currents measured north of the jetty.

34. Histogram of currents measured near the tip of the north jetty.

35. Histogram of winds measured at Newport. Arrows indicate the direction toward which the winds were blowing.

36. Vector plot of currents south of Yaquina Head.

37. Vector plot of currents off Big Creek.

38. Vector plot of currents at the sewer outfall.

39. Vector plot of currents north of the jetty.

40. Vector plot of currents near the end of the jetty.

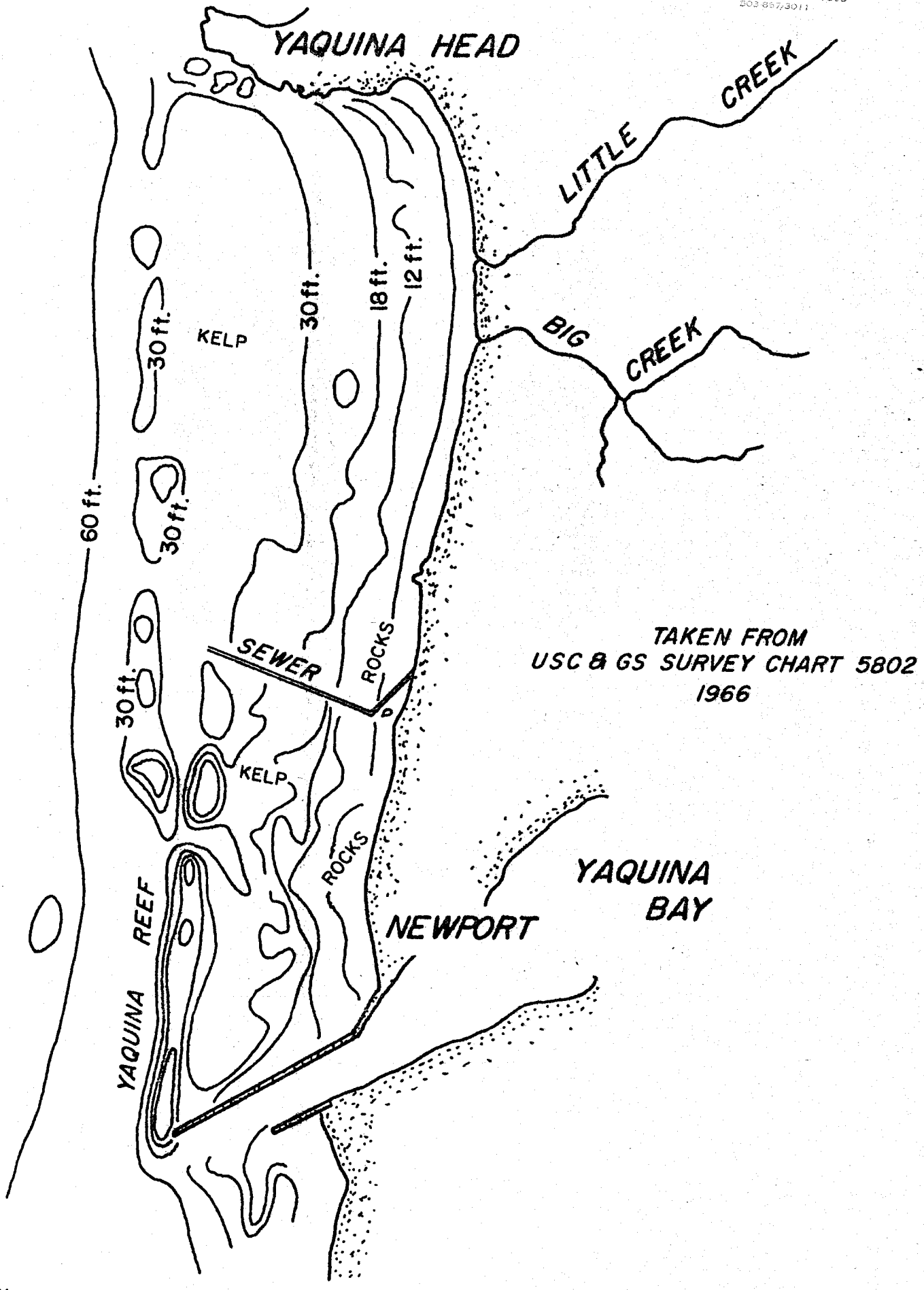

Figure 1 Chart of the nearshore region, Newport, Oregon

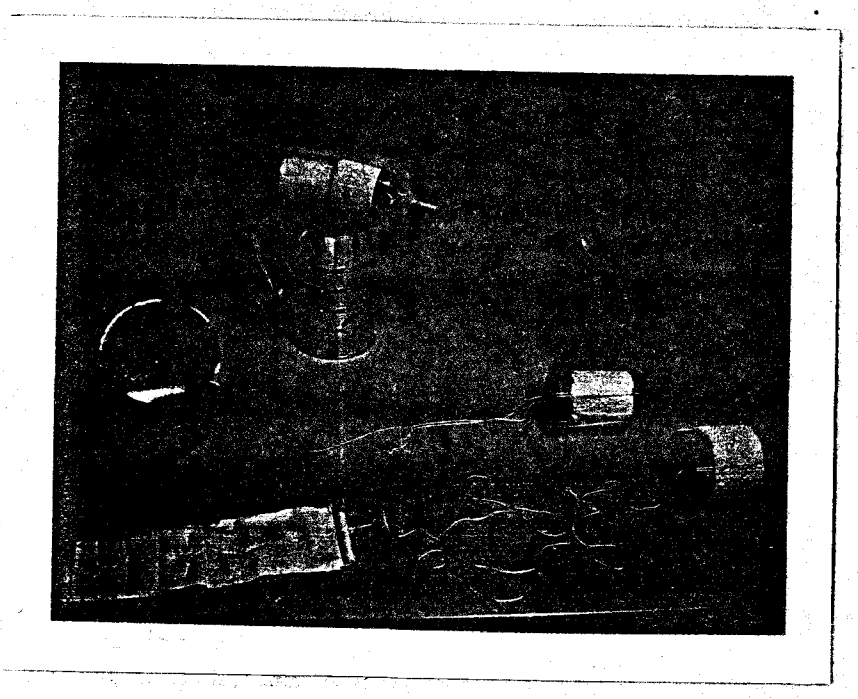

Figure 2. The dye-float system before final assembly (foreground) and in final assembled form (background).

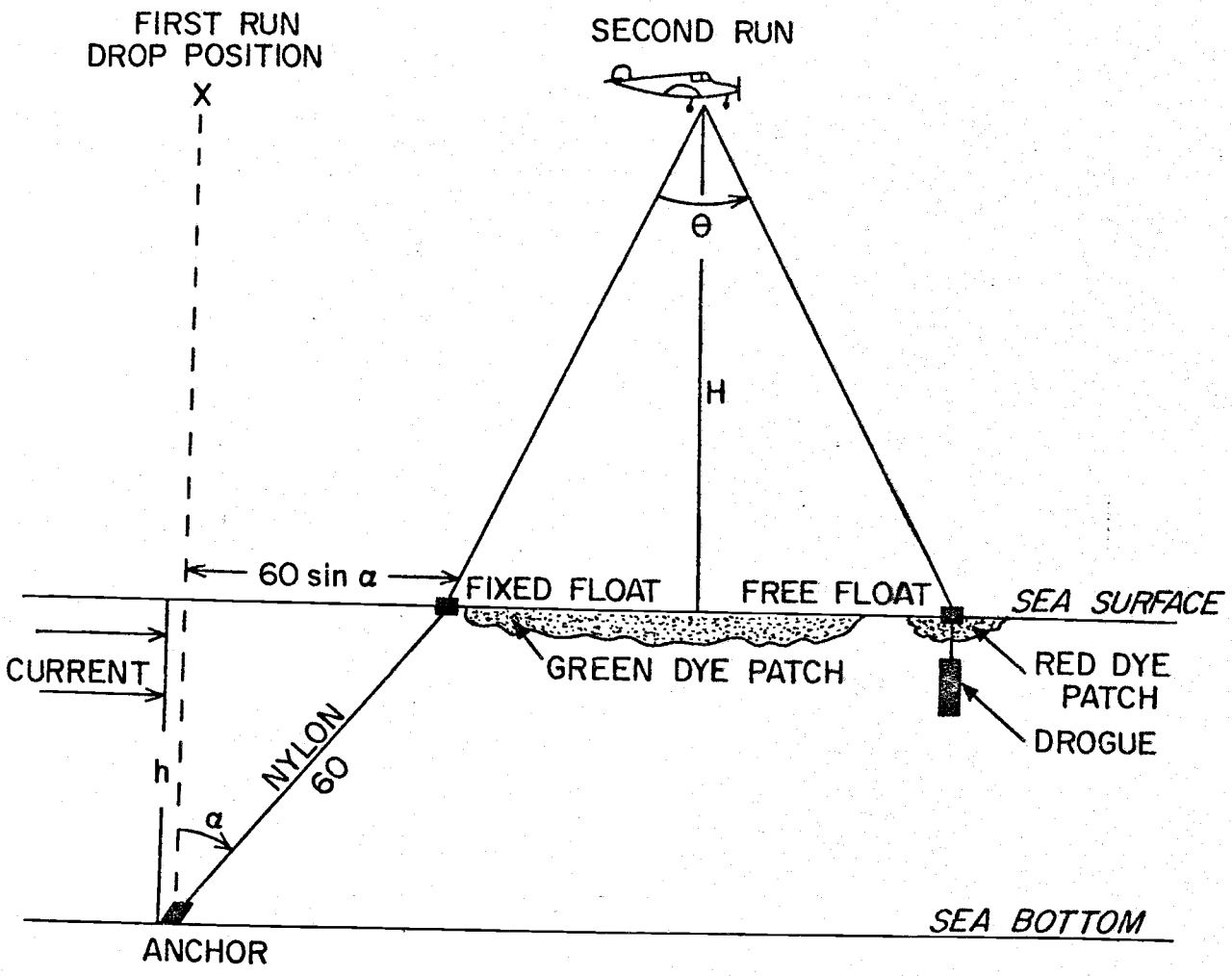

Figure 3. A schematic diagram of dye-float system as deployed for current measurement.

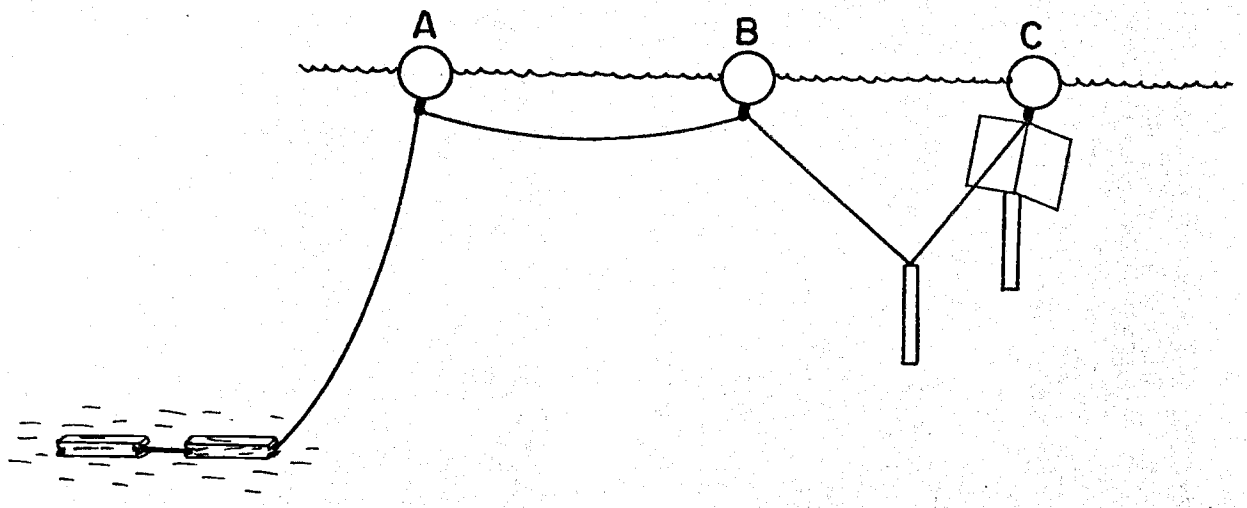

Figure 4. Tethered buoy system for measuring current speed and direction. The distance between floats A and B serves as a reference distance for aerial observation. Float C has a weighted drogue attached beneath it.

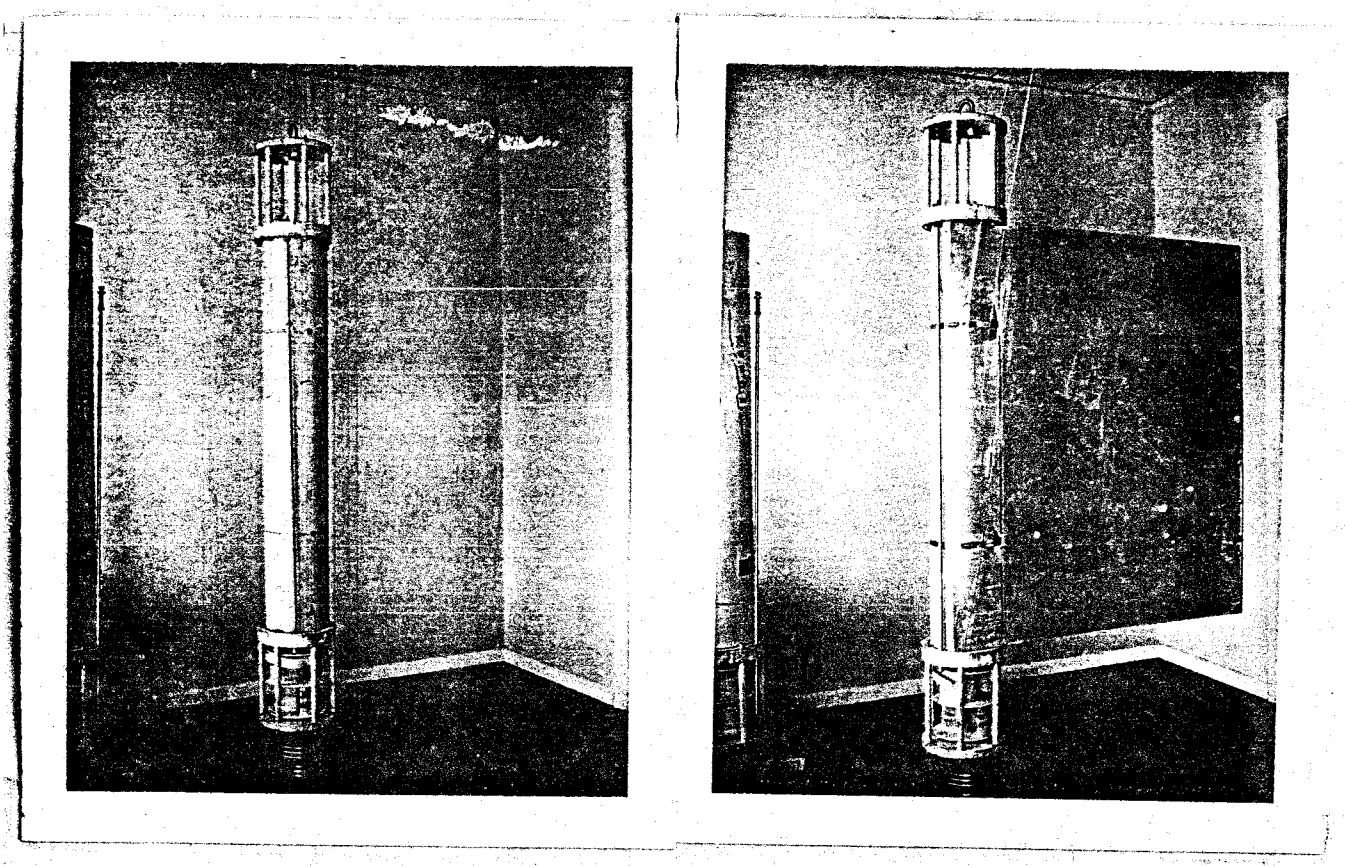

(a) (b)

Figure 5. The Geodyne current meter; without vane (a) and with vane attached (b).

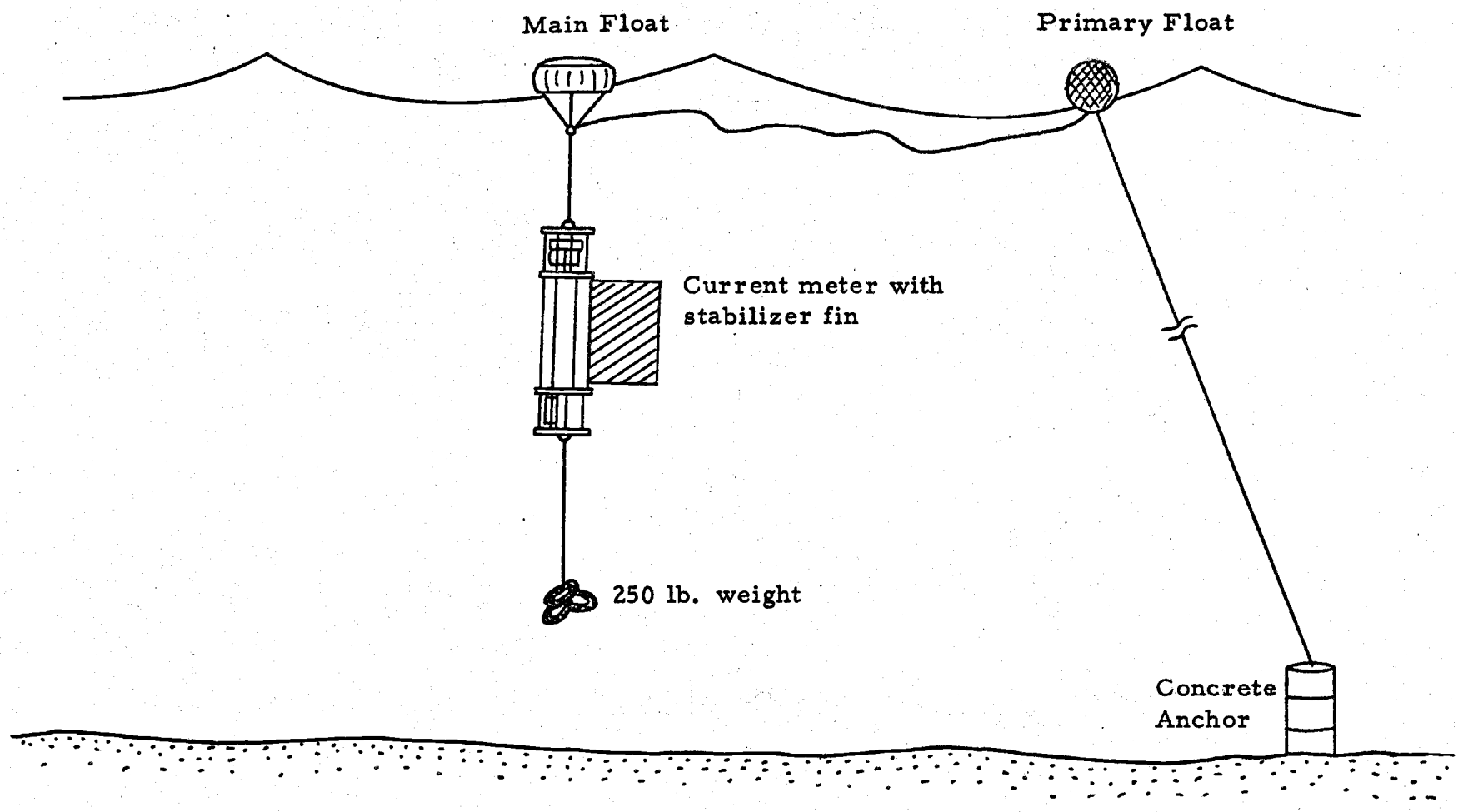

Figure 6 A system for mooring a current meter in shallow water. The primary float absorbs wave surge.

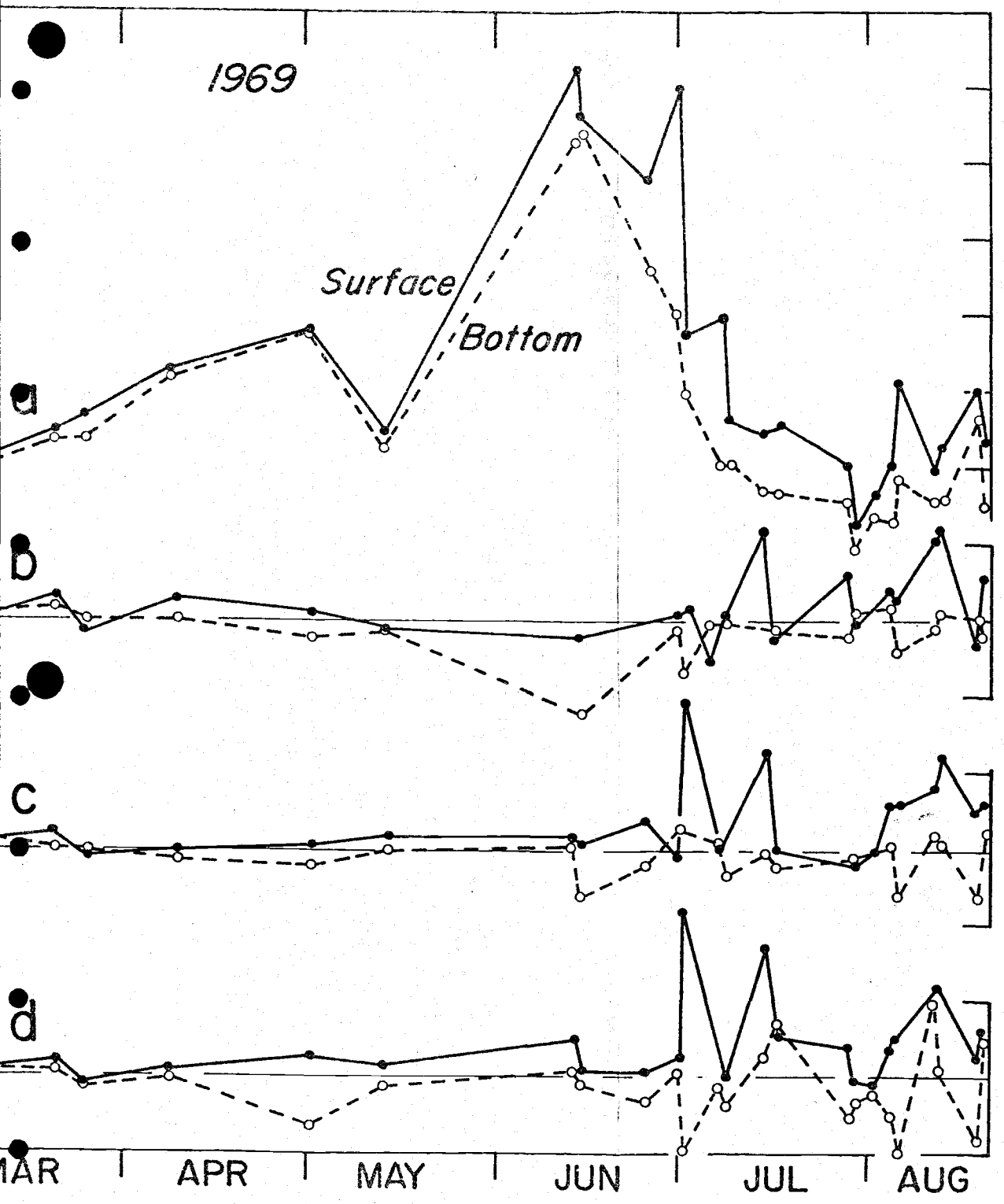
1969
Surface
Bottom
a
b
c
d
MAR
APR
MAY
JUN
JUL
AUG

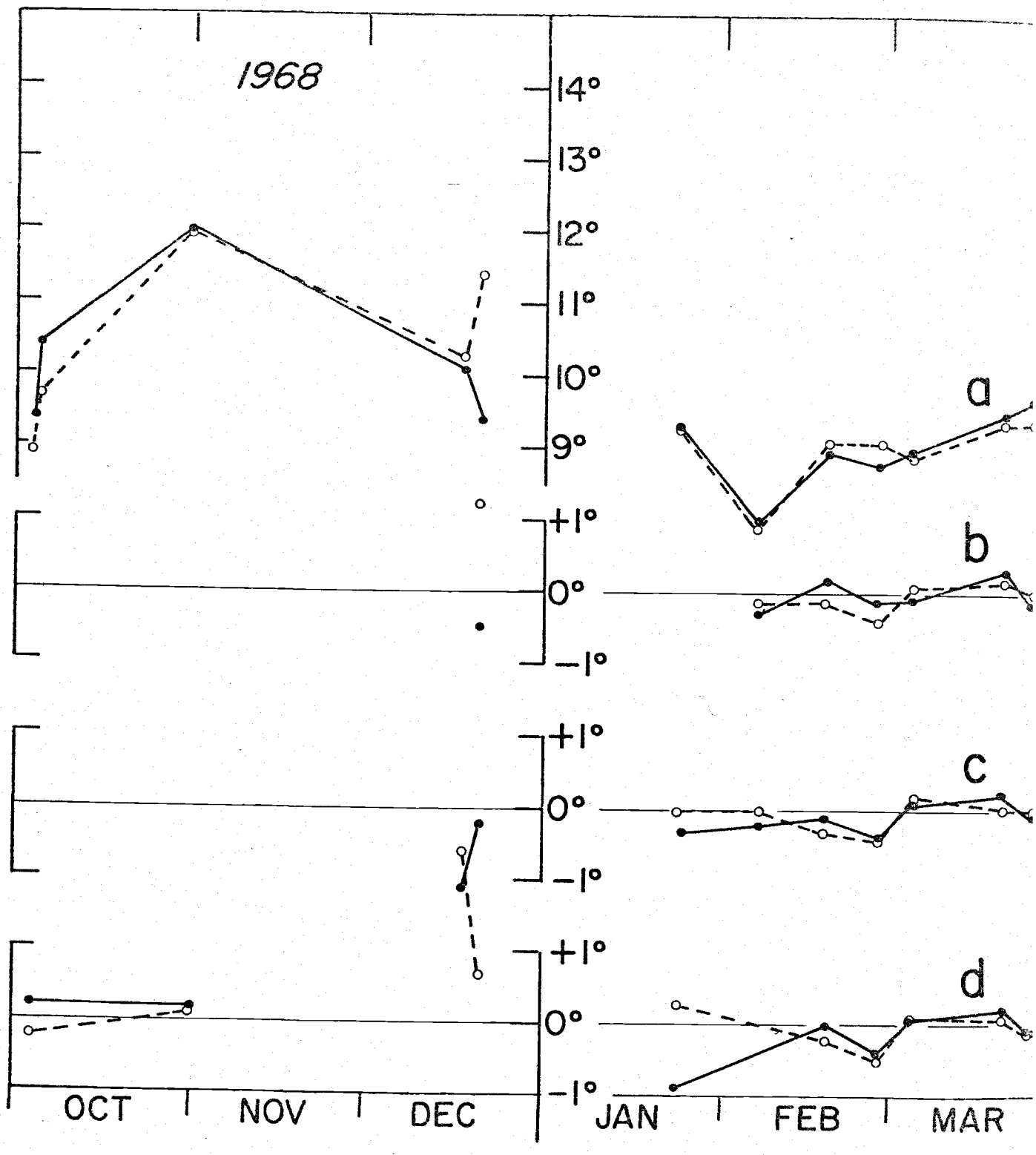

Figure 7 Water temperatures from October 1968 through August 1969. The upper traces (a) show surface and bottom temperatures at the sewer outfall. The lower traces show the deviations from temperatures at the outfall (b) in the plume (c) out of the plume, and (d) outside the reef.

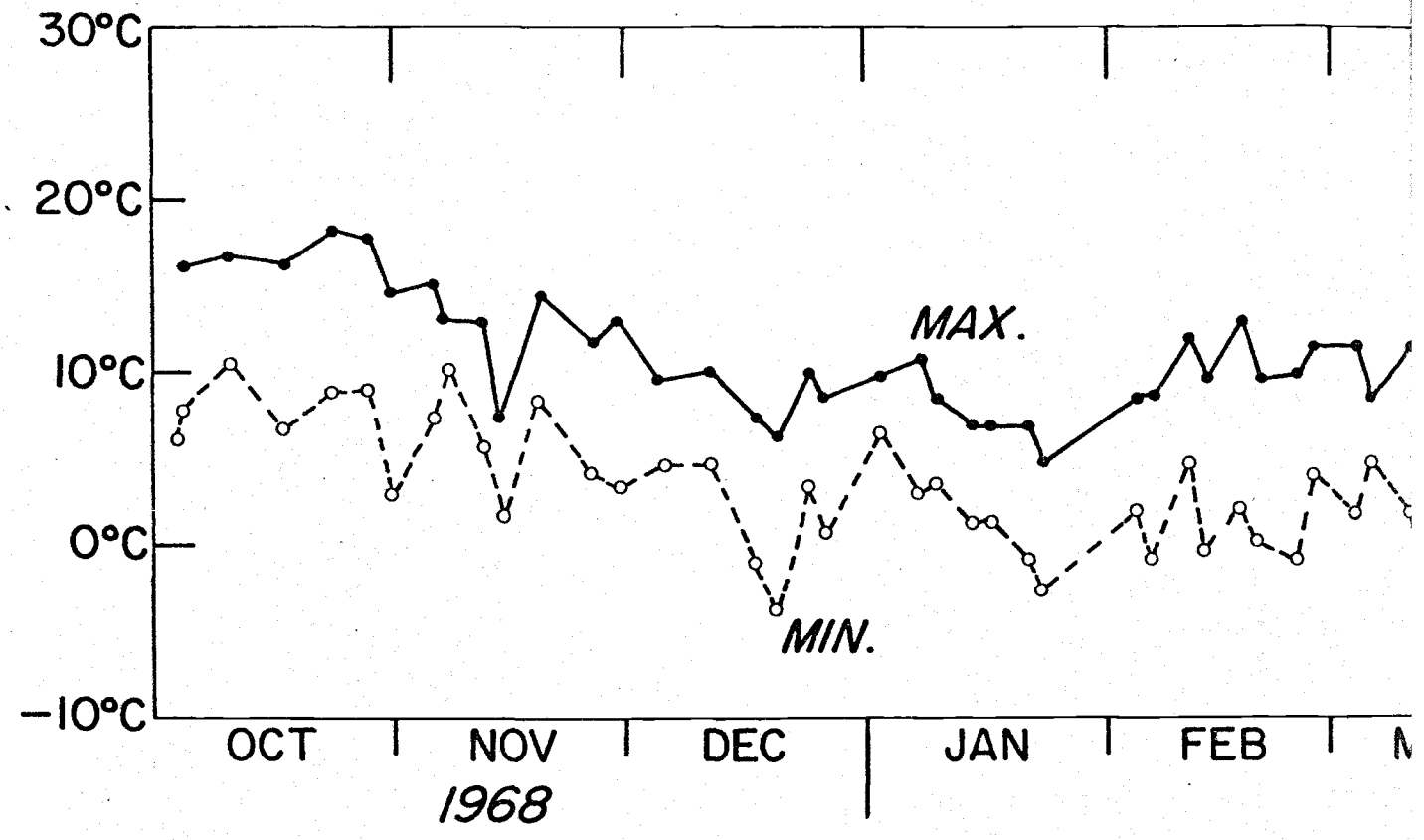

Figure 8 Maximum and minimum air temperatures at Newport (in °C). The upper line connects maximum temperature while the lower lone connects minimum temperatures on selected dates.

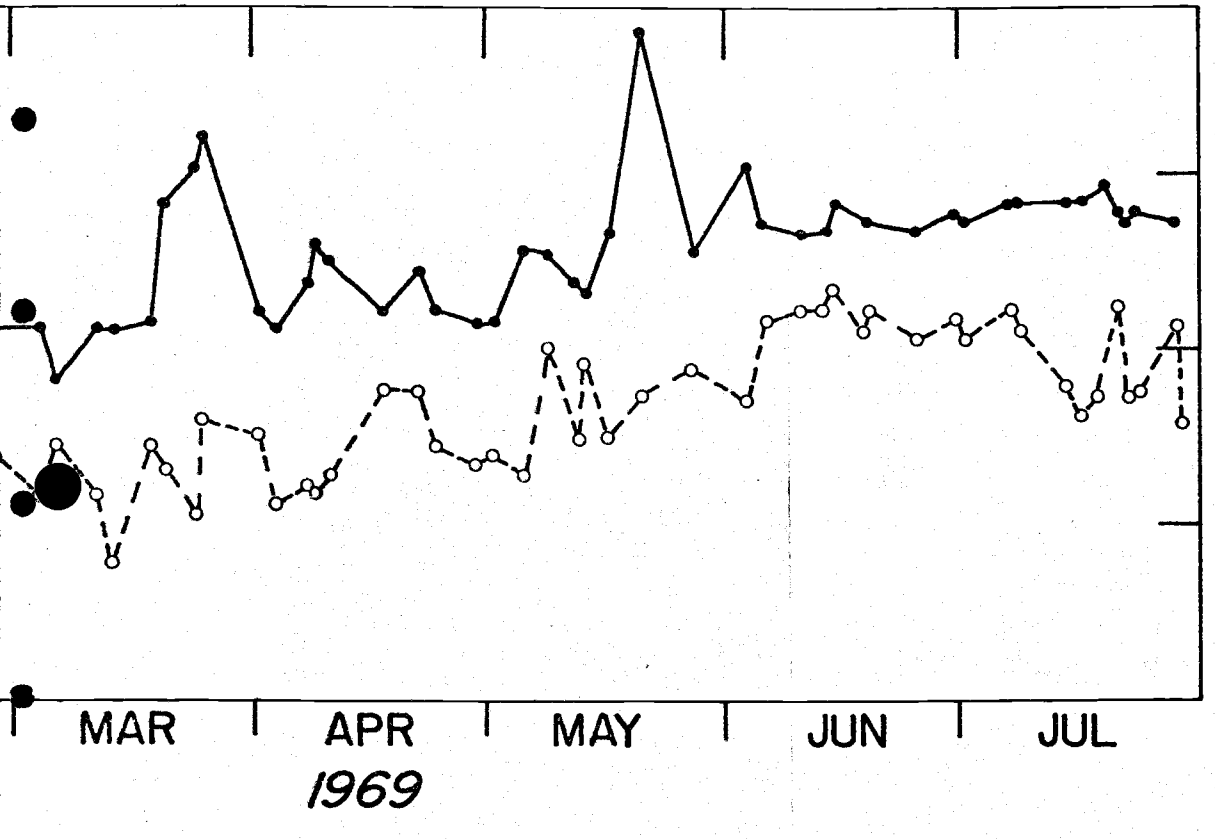
MAR
APR
MAY
JUN
JUL
1969

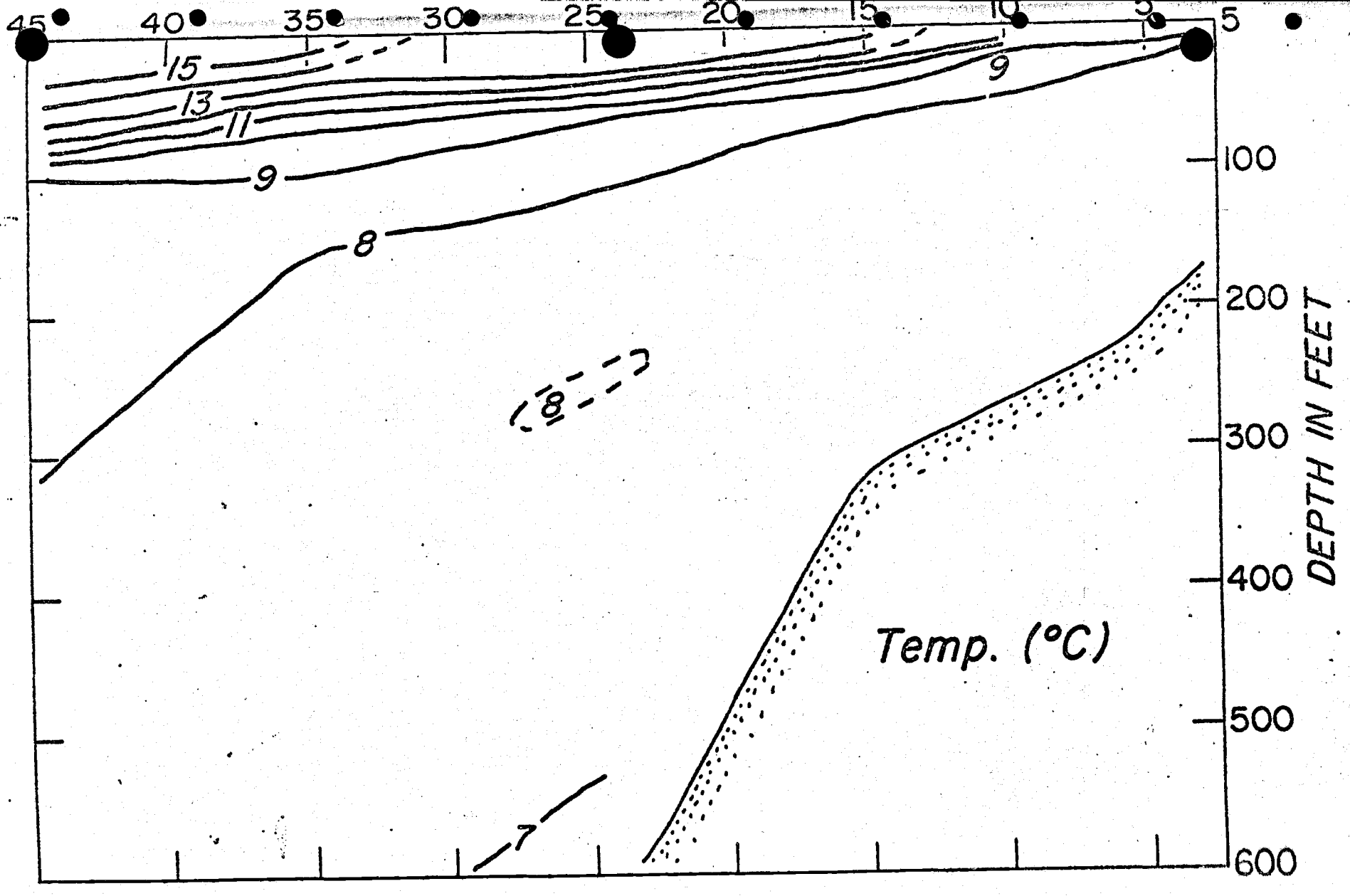

Figure 9. Temperature structure off Newport (August 9-11) showing the effects of upwelling.

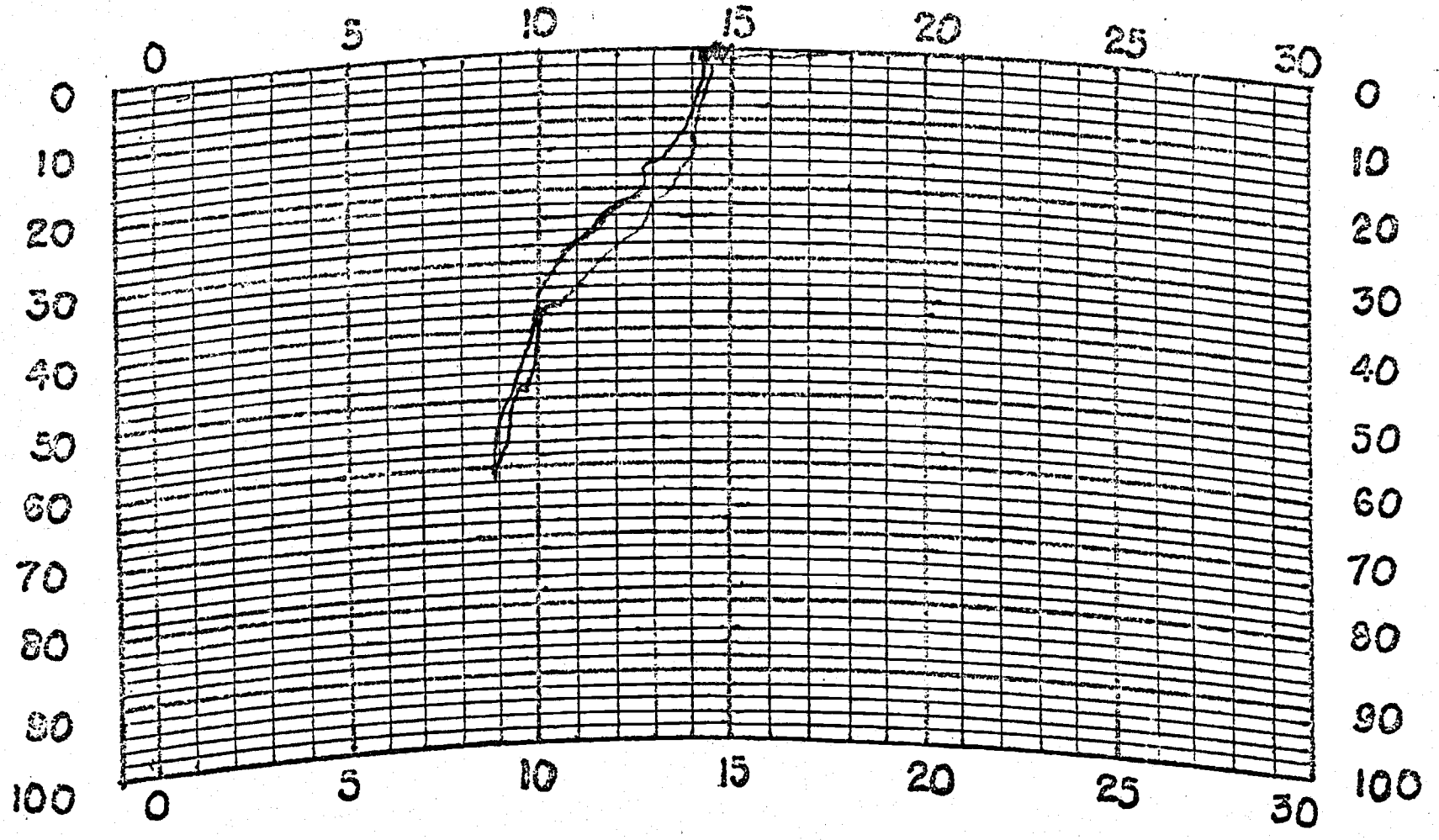

Figure 10a. BT trace taken outside Yaquina Reef at 1540 PDT, 30 June 1969.

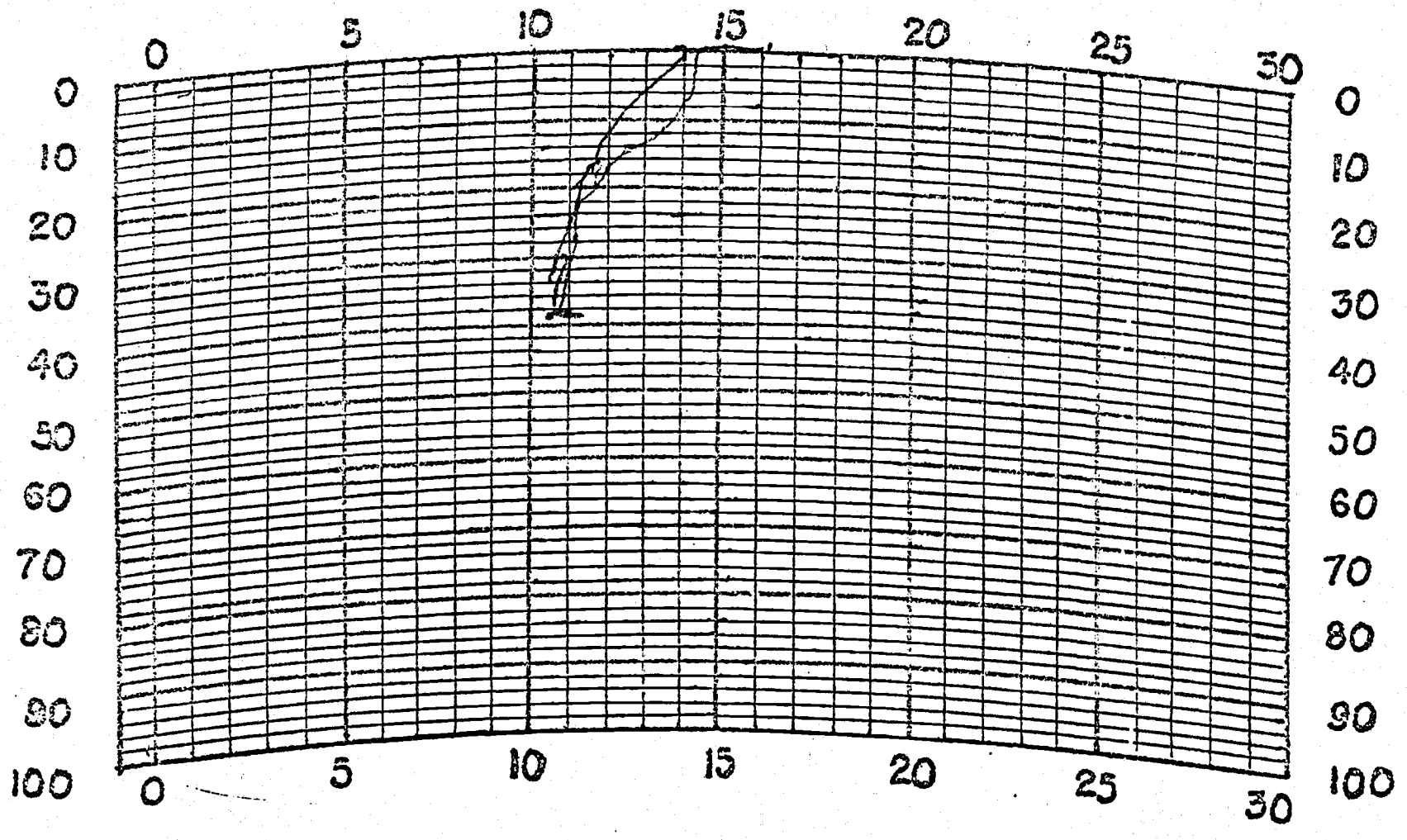

Figure 10b. BT trace taken in the outfall plume at 1300 PDT, 30 June 1969.

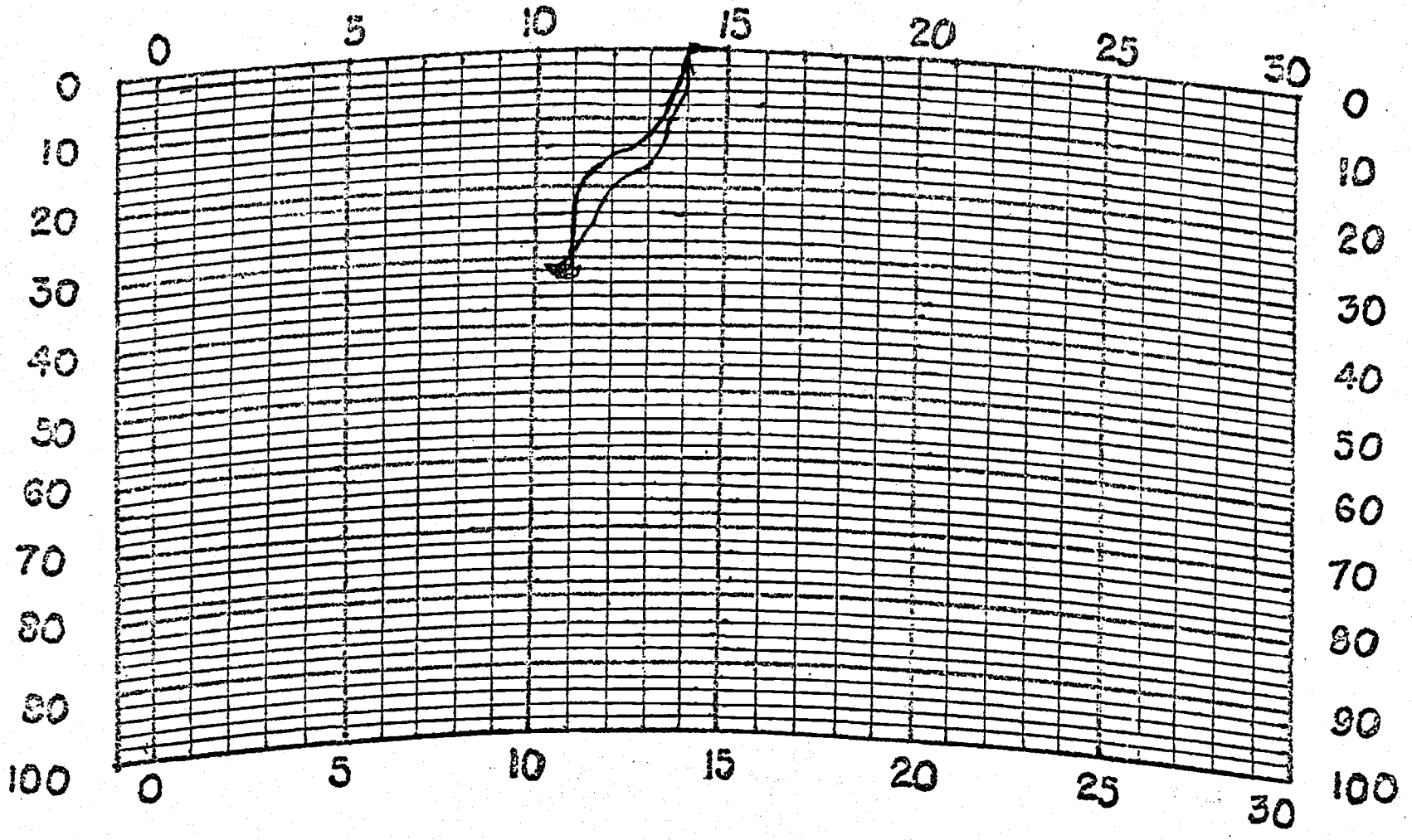

Figure 10c. BT trace taken over the outfall at 1230 PDT, 30 June 1969.

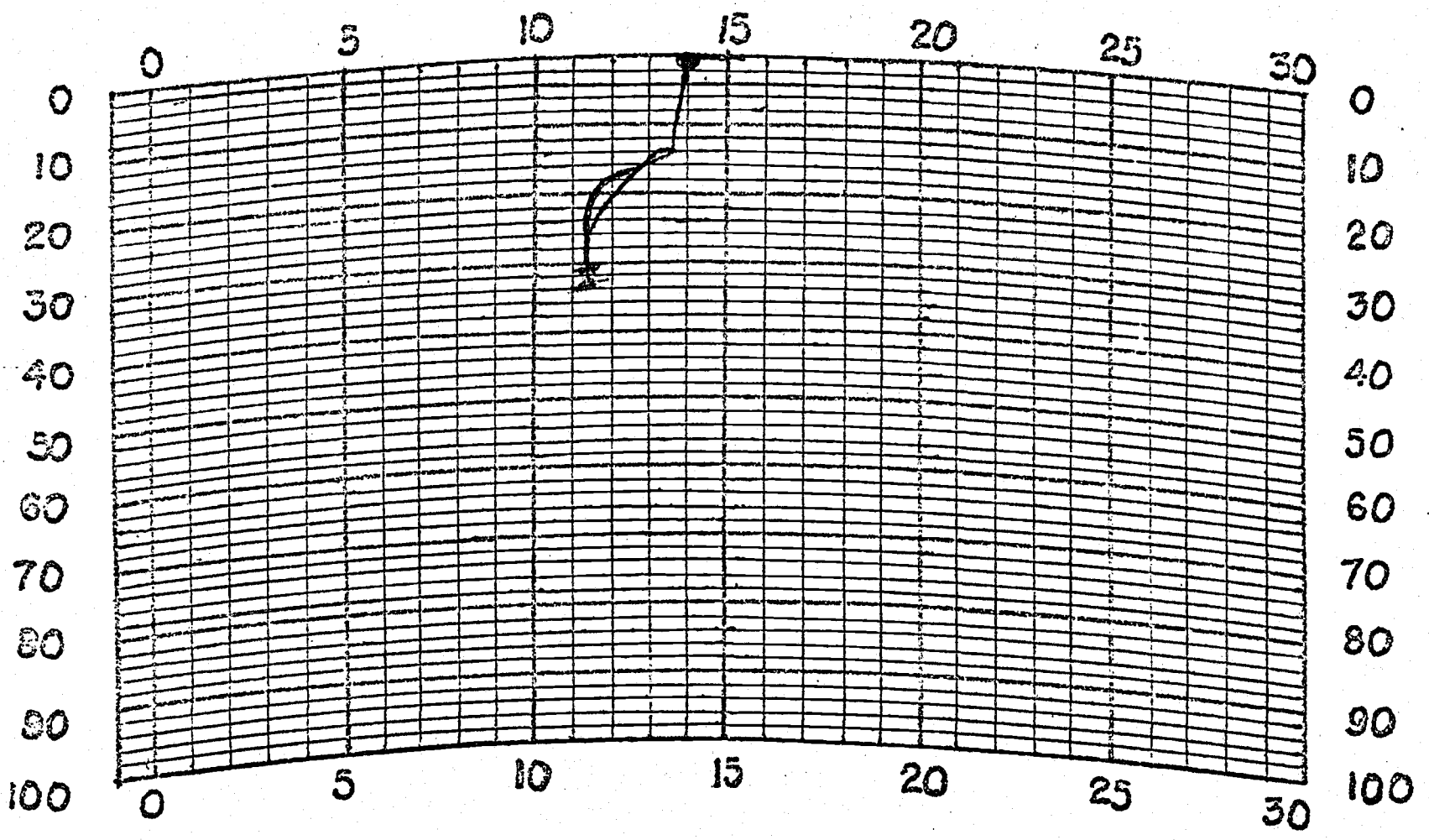

Figure 10d. BT trace taken outside the outfall plume at 1245 PDT, 30 June 1969.

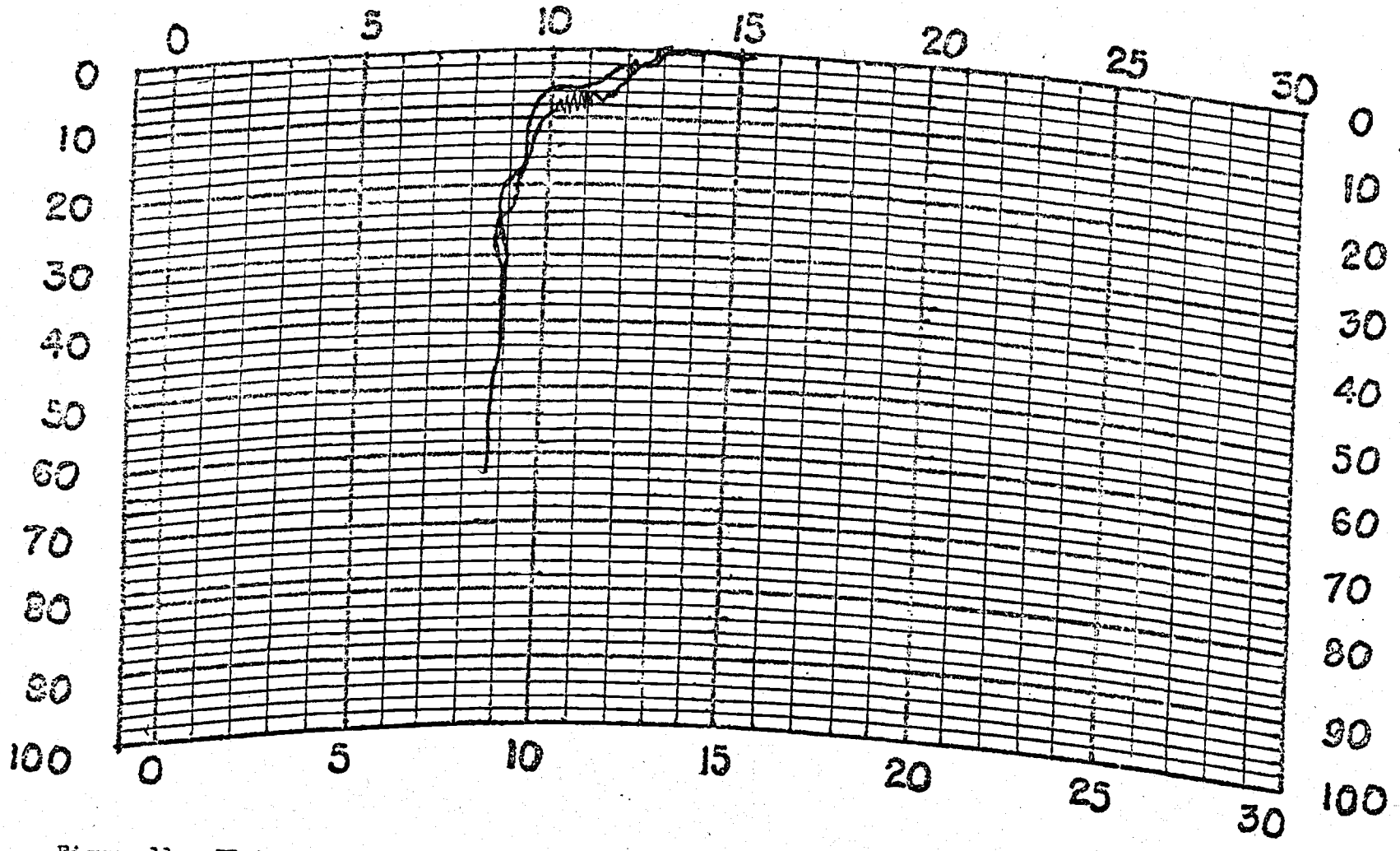

Figure 11a. BT trace taken outside Yaquina Reef at 1345 PDT, 1 July 1969.

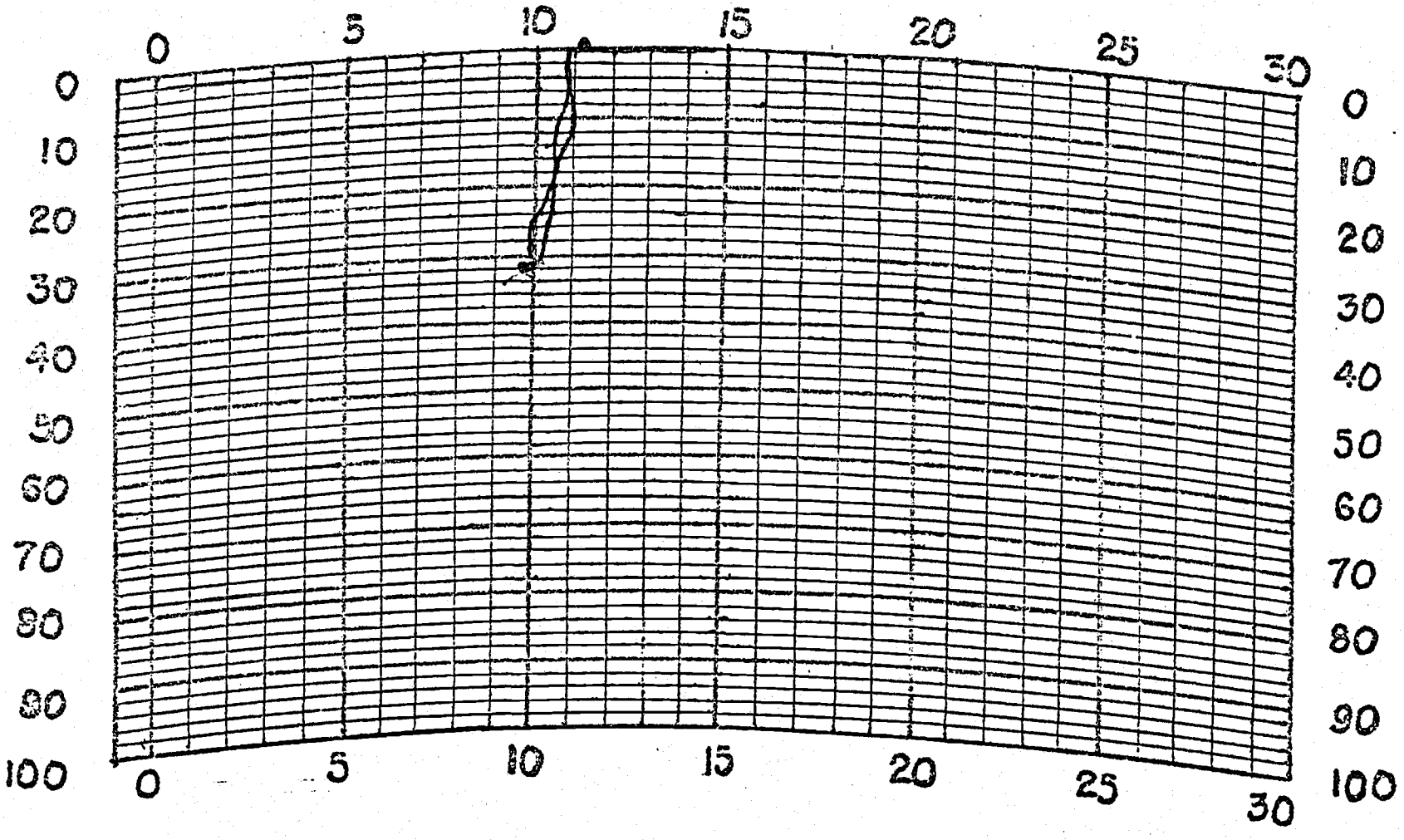

Figure 11b. BT trace taken over the outfall at 1050 PDT, 1 July 1969.

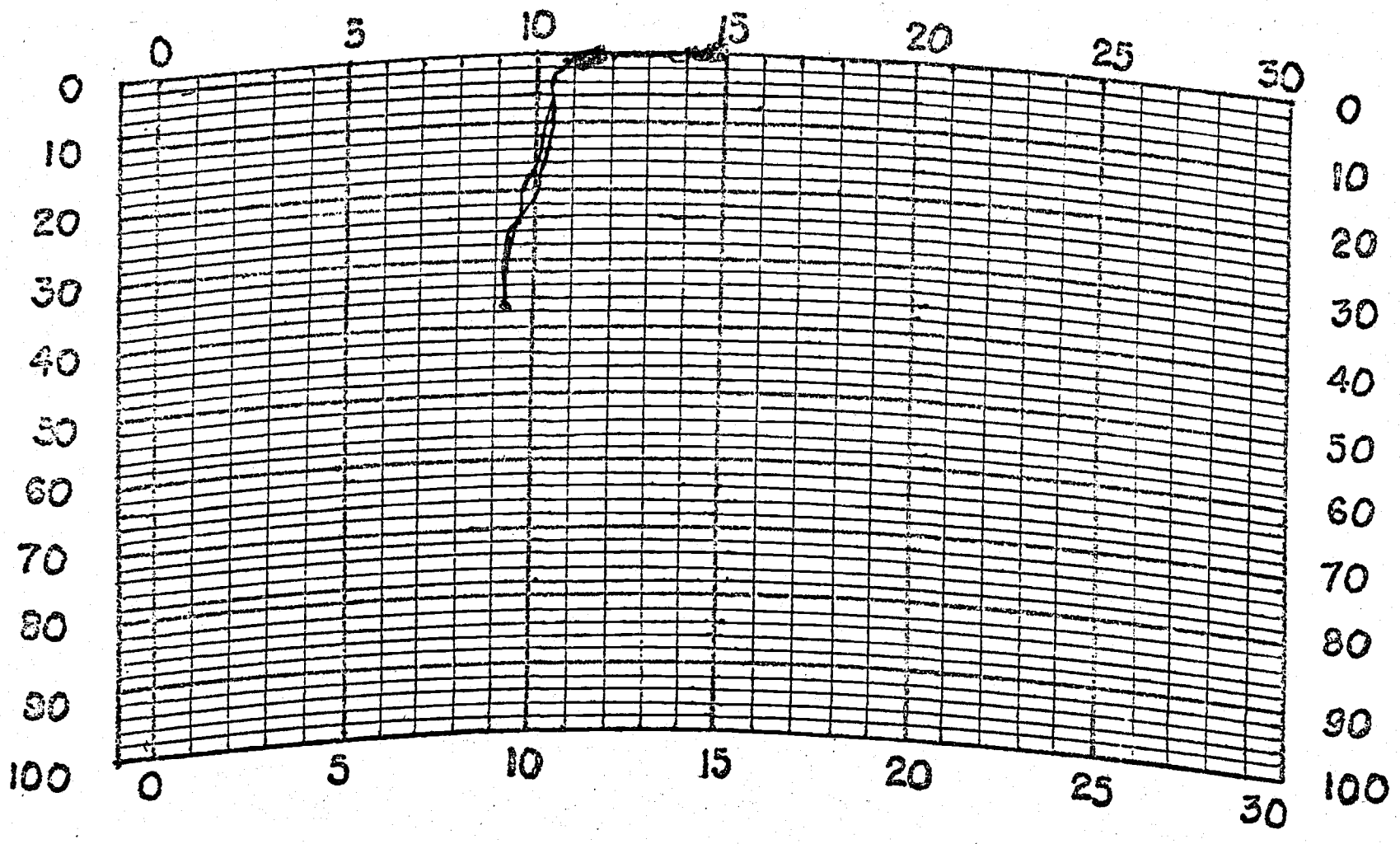

Figure 11c. BT trace taken in the outfall plume at 1315 PDT, 1 July 1969.

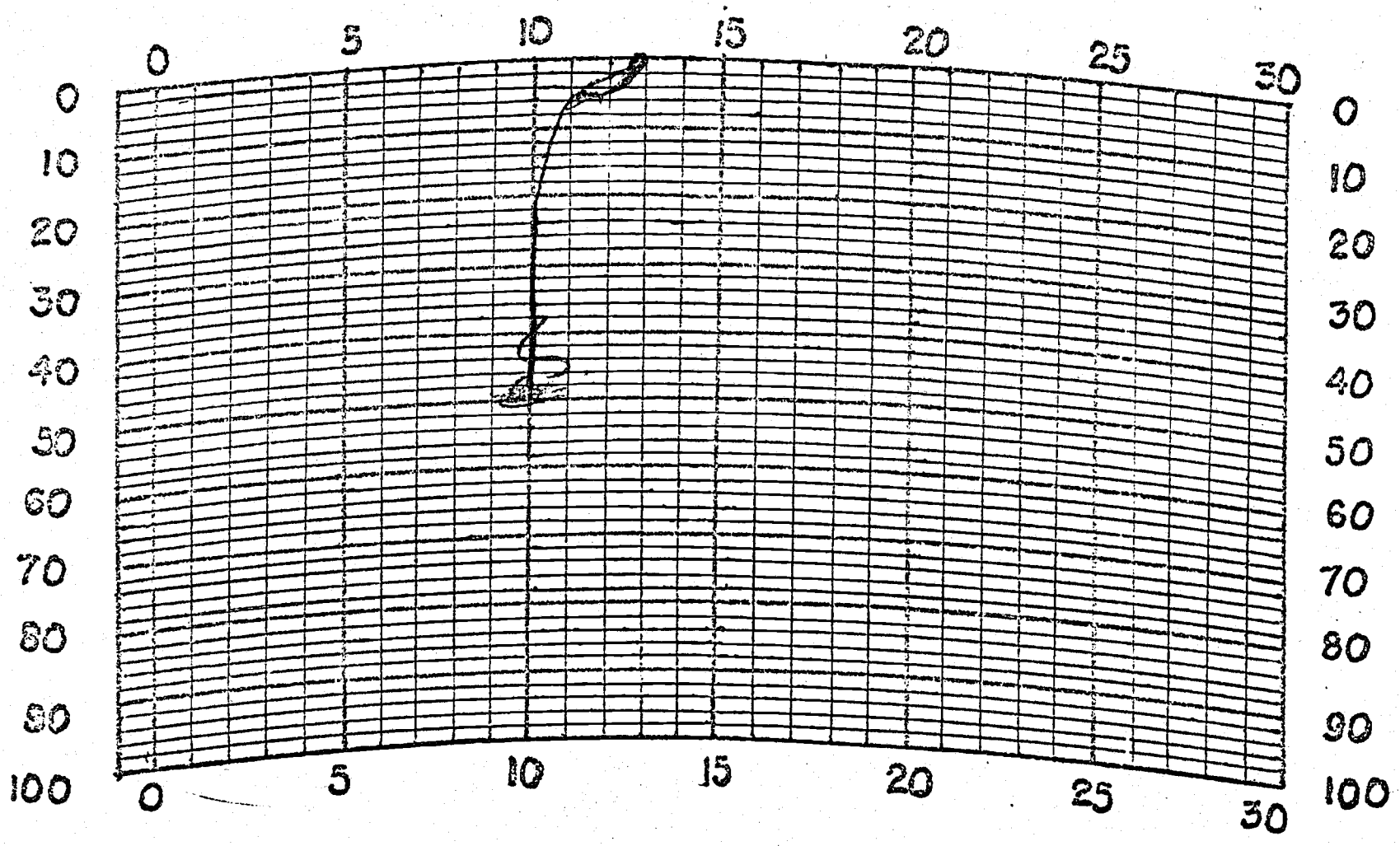

Figure 11d. BT trace taken out of the outfall plume at 1250 PDT, 1 July 1969.

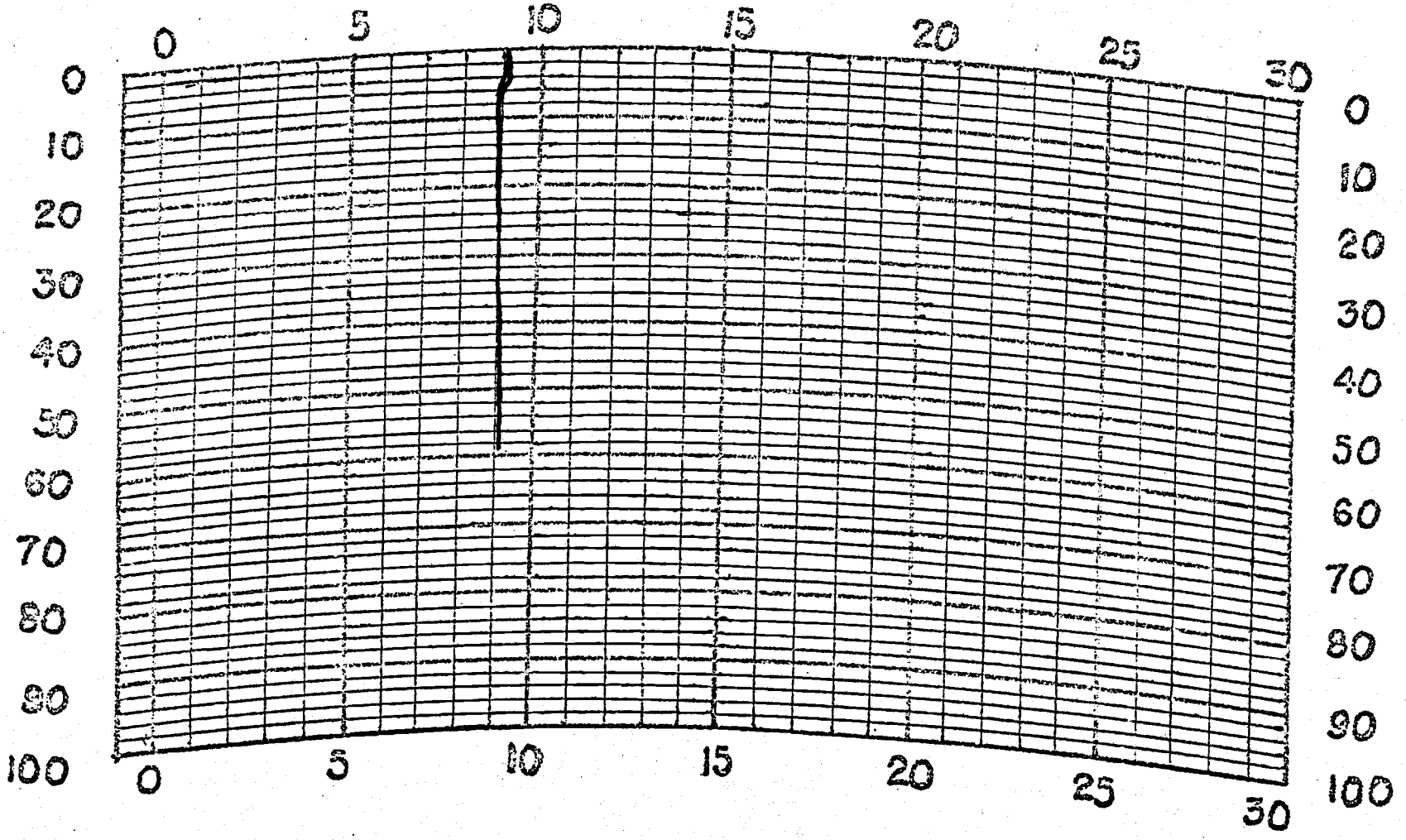

Figure 12a. BT trace taken outside Yaquina Reef at 1210 PDT, 4 March 1969.

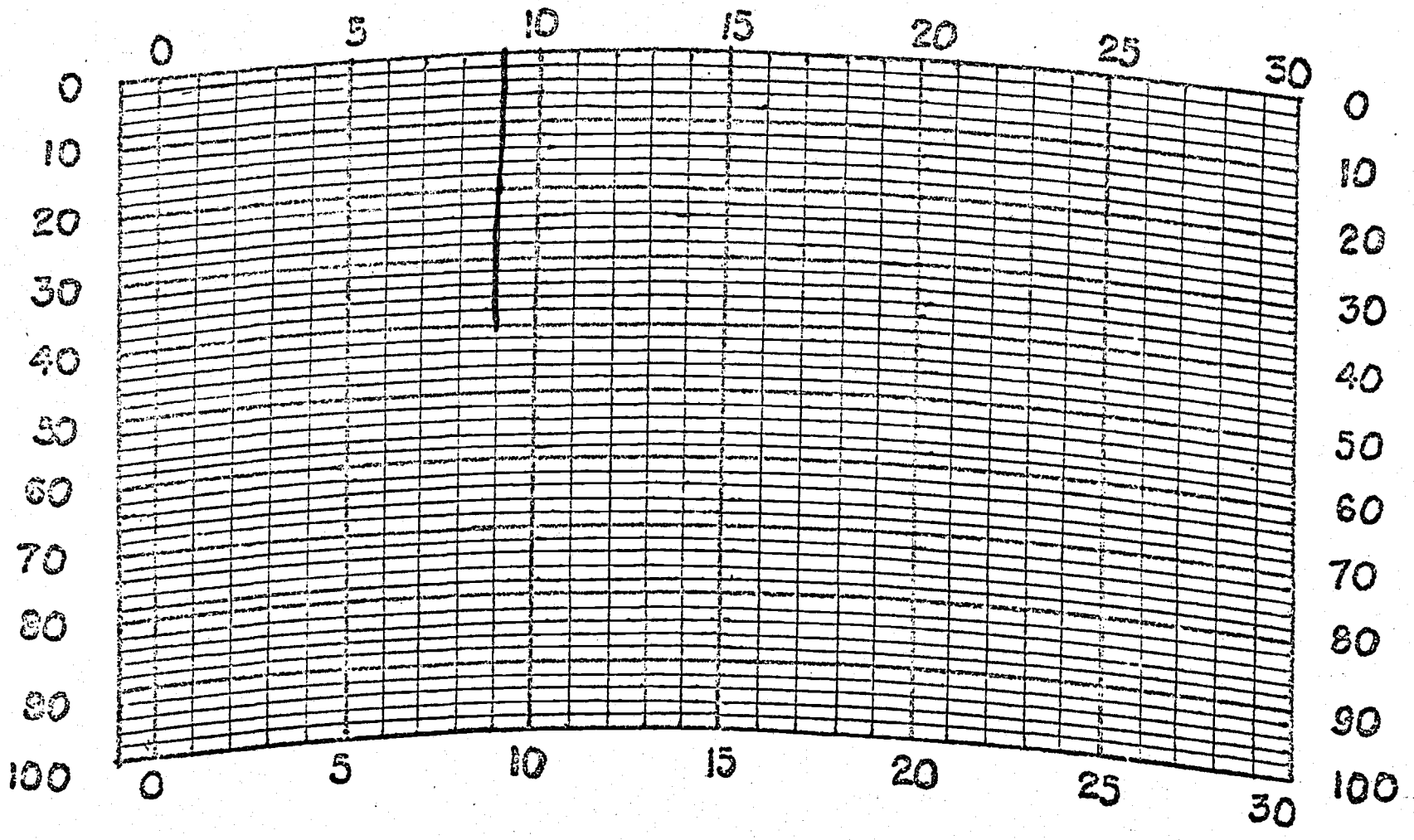

Figure 12b. BT trace taken at the outfall at 1130 PDT, 4 March 1969.

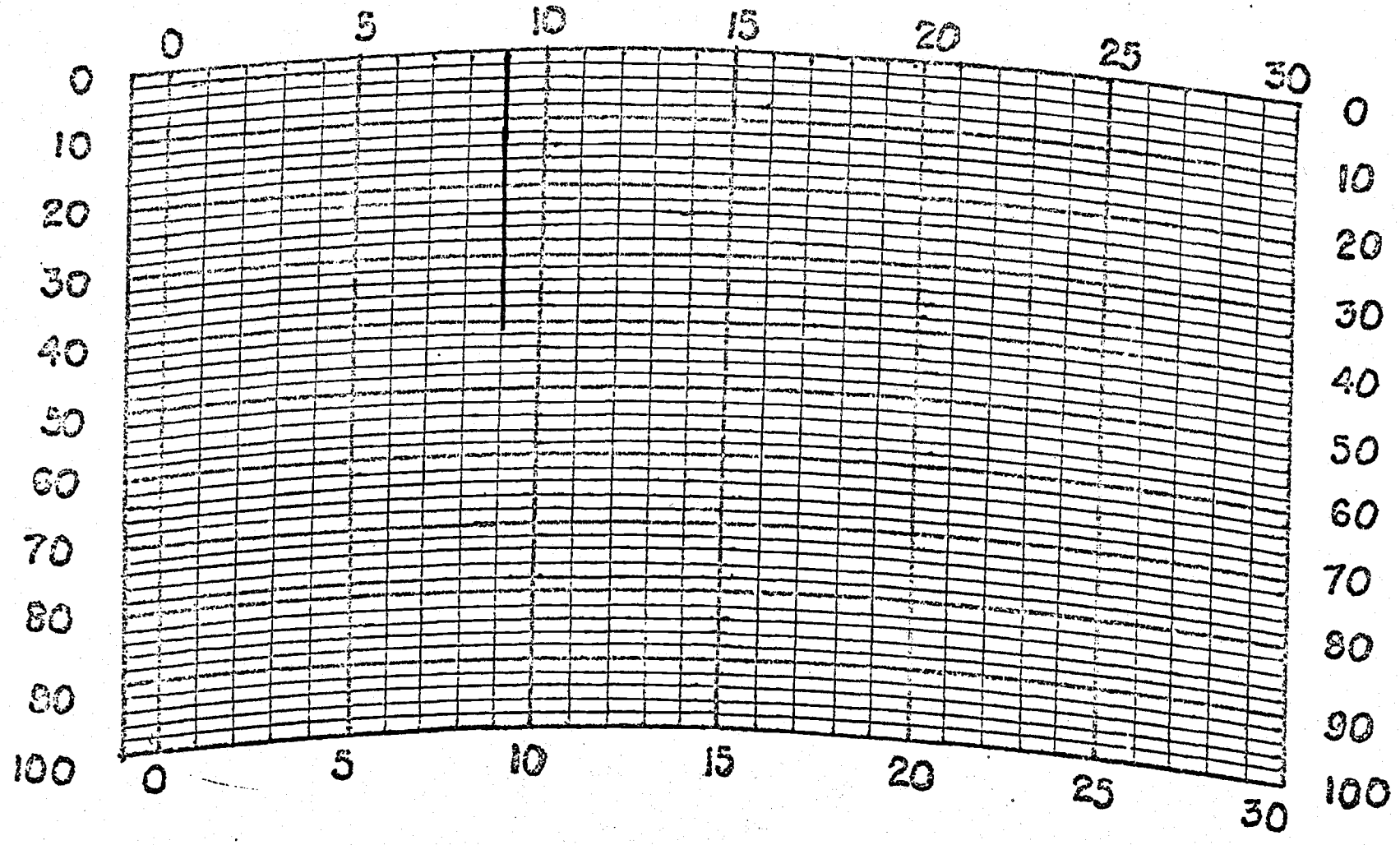

Figure 12c. BT trace taken inside the outfall plume at 1140 PDT, 4 March 1969.

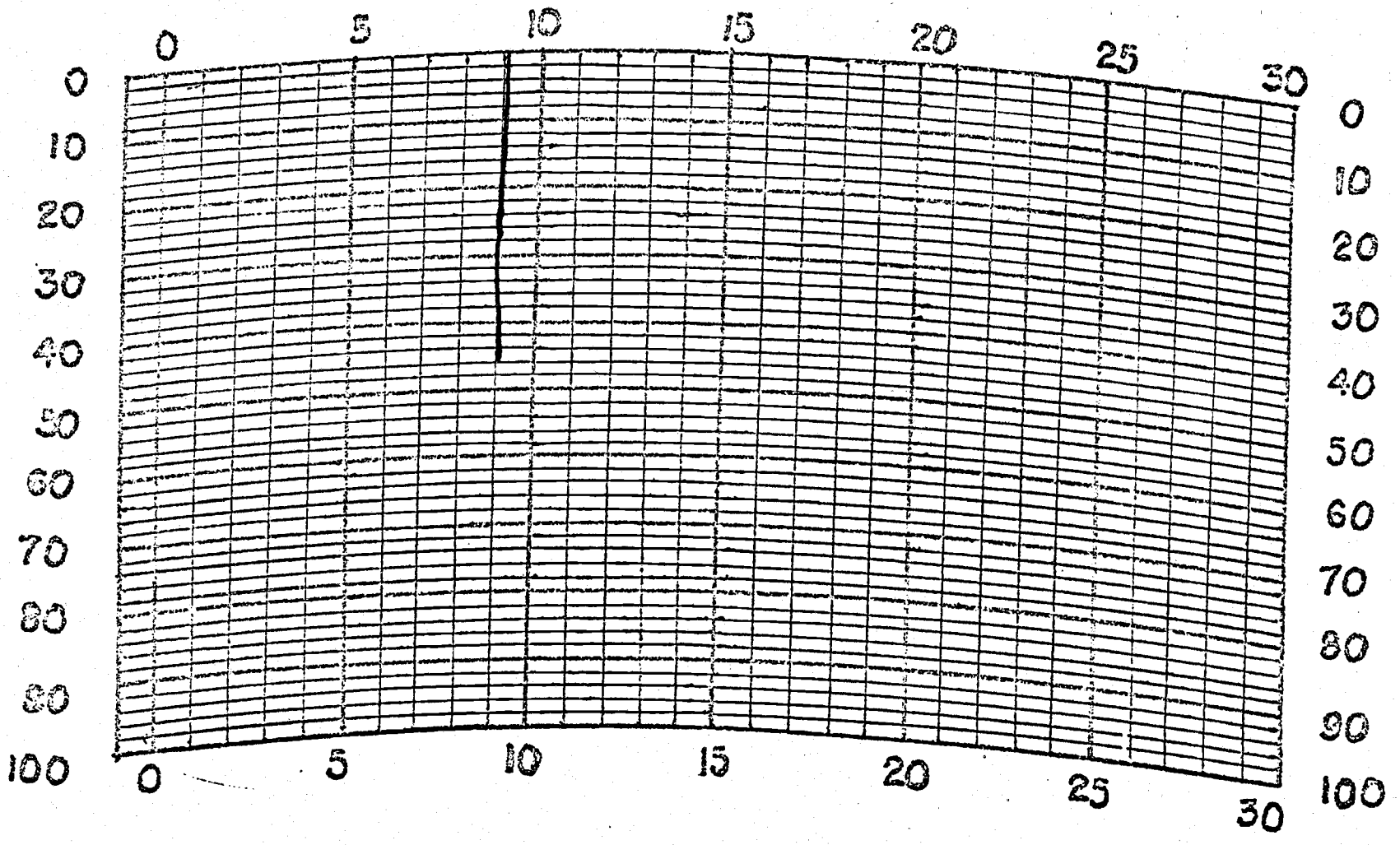

Figure 12d. BT trace taken outside the outfall plume at 1150 PDT, 4 March 1969.

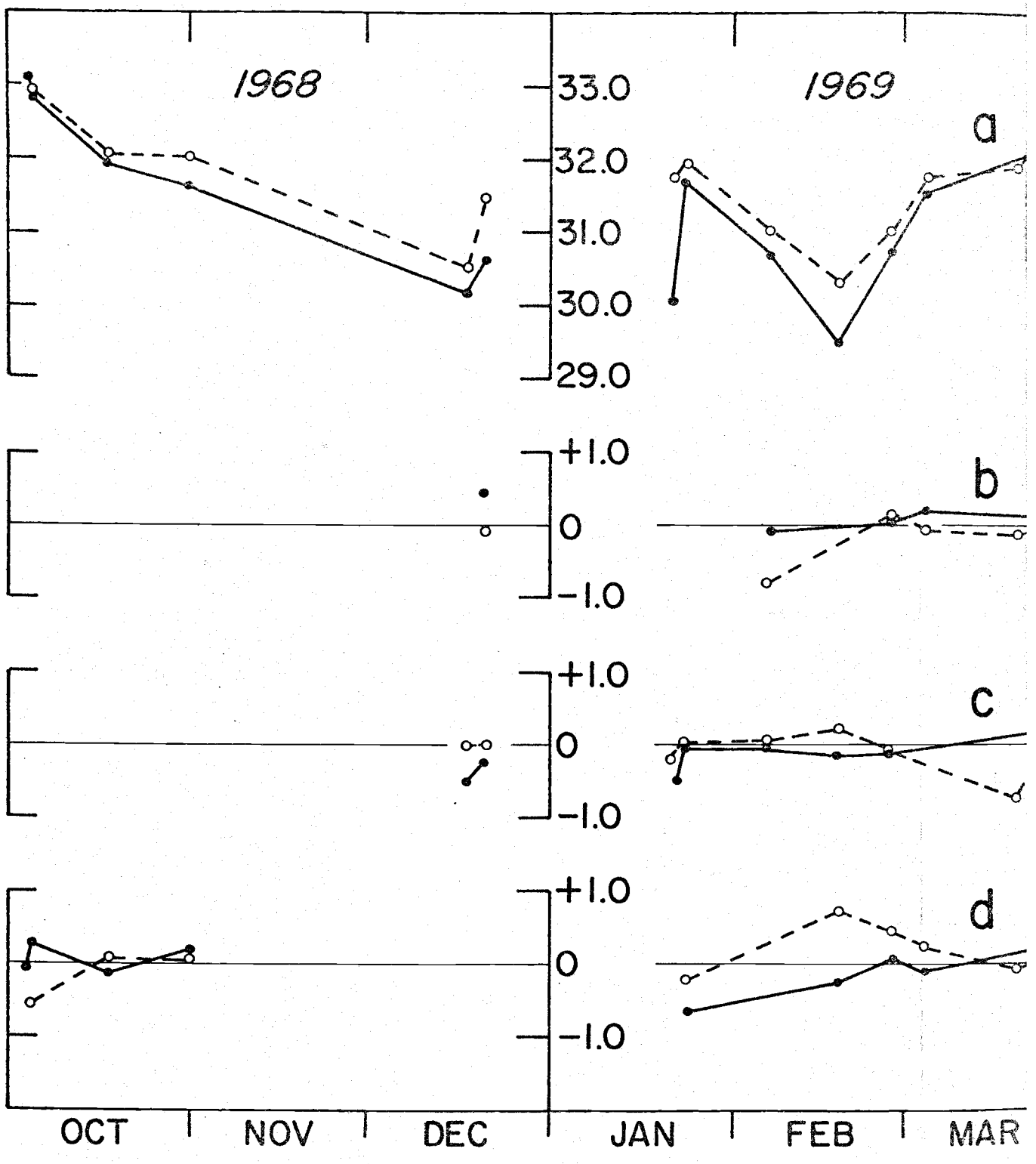

Figure 13 Salinity at the outfall during the period October 1968-August 1969. The three lower lines show deviations from outfall salinities (b) in the plume (c) outside the plume and (d) outside the reef.

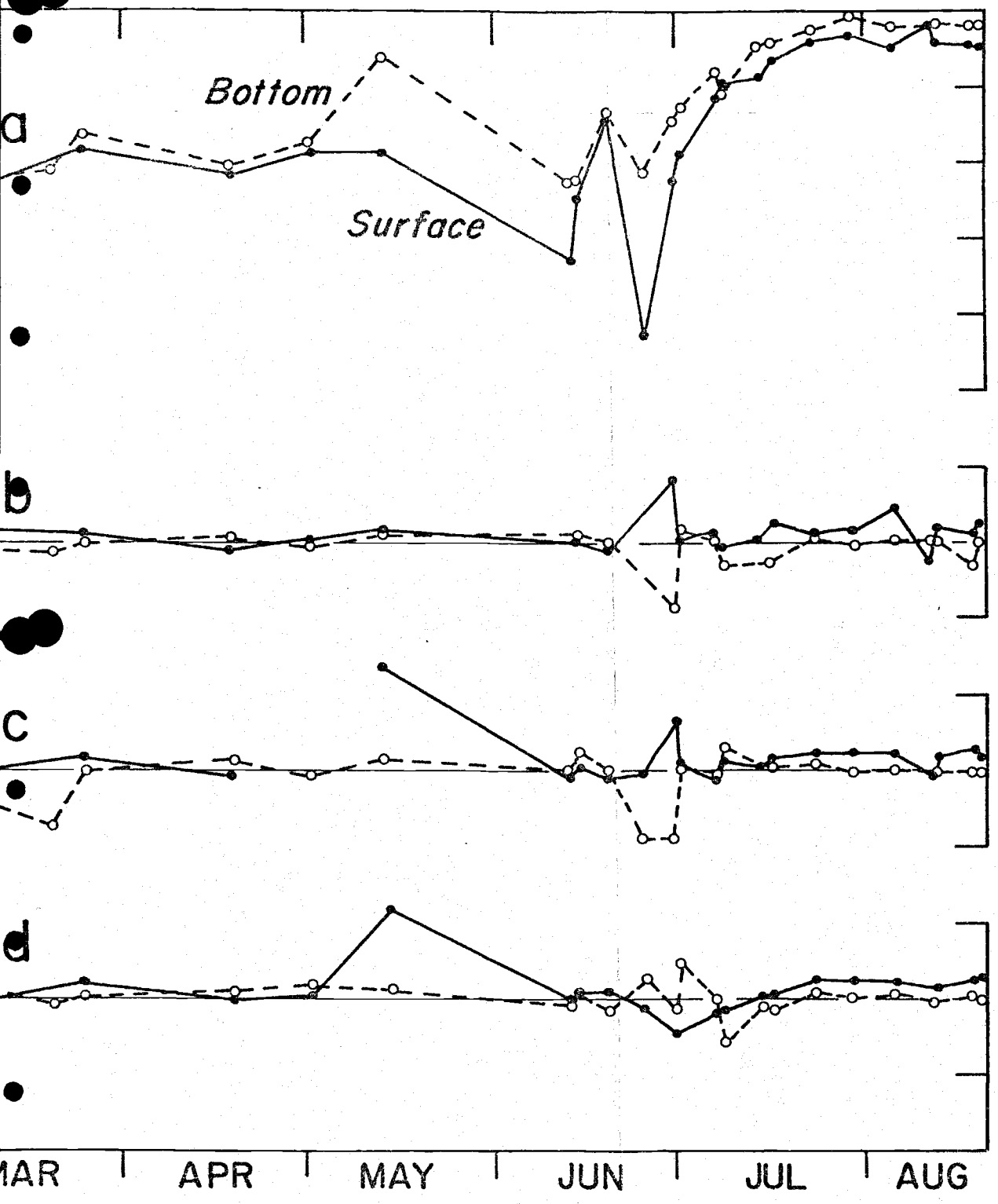
Bottom
Surface
a
b
c
d
MAR
APR
MAY
JUN
JUL
AUG

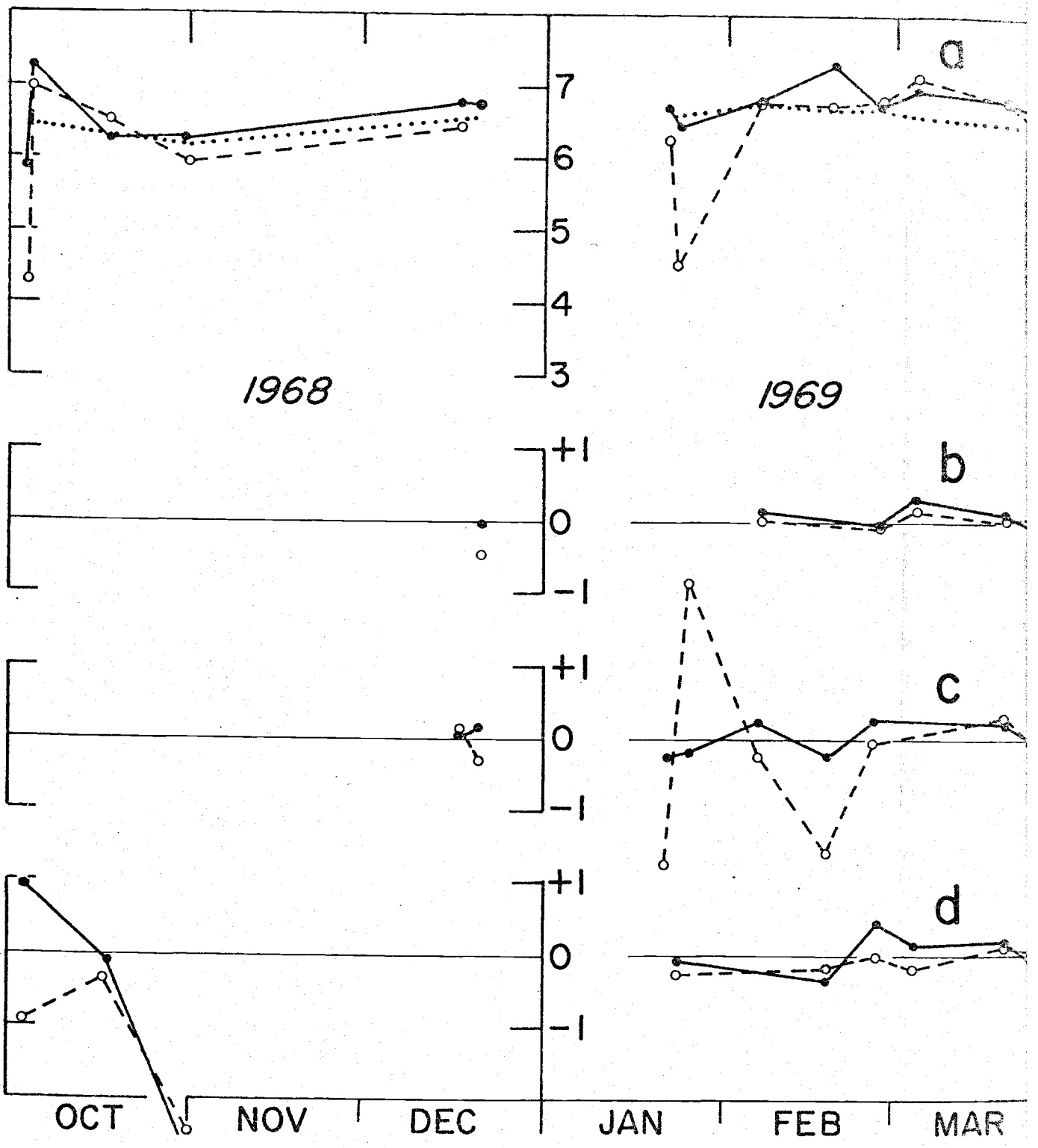

Figure 14 Dissolved oxygen concentrations at the outfall in ml/liter (October 1968-August 1969). The dashed line in the upper plot indicates saturation values. The lower traces are deviations from outfall concentrations (b) inside the plume, (c) outside the plume and (d) outside the reef.

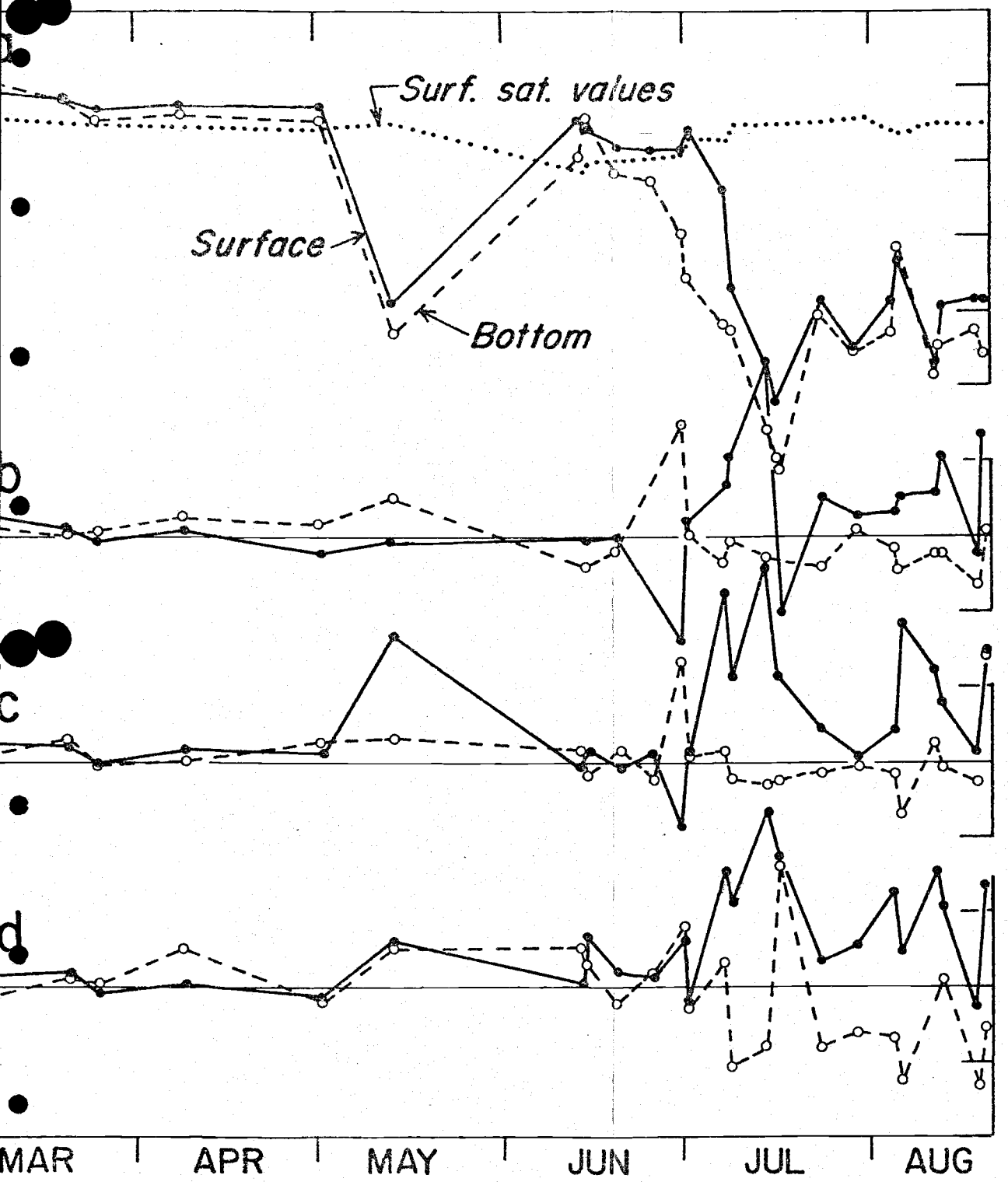
Surf. sat. values
Surface
Bottom
b
c
d
MAR
APR
MAY
JUN
JUL
AUG

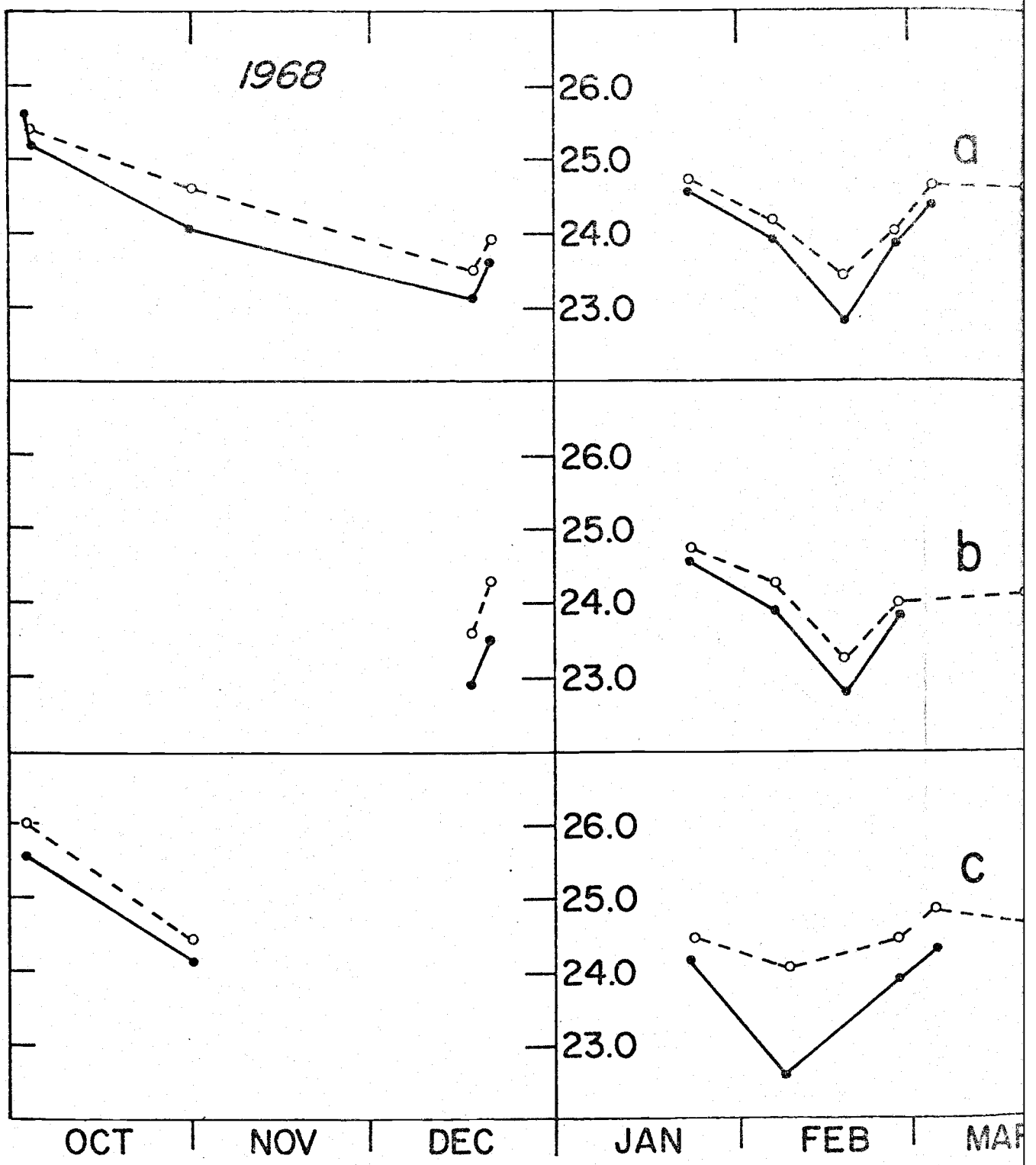

Figure 15. Sigma-t values (a) at the outfall, (b) outside the plume and (c) outside the reef (October 1968-August 1969).

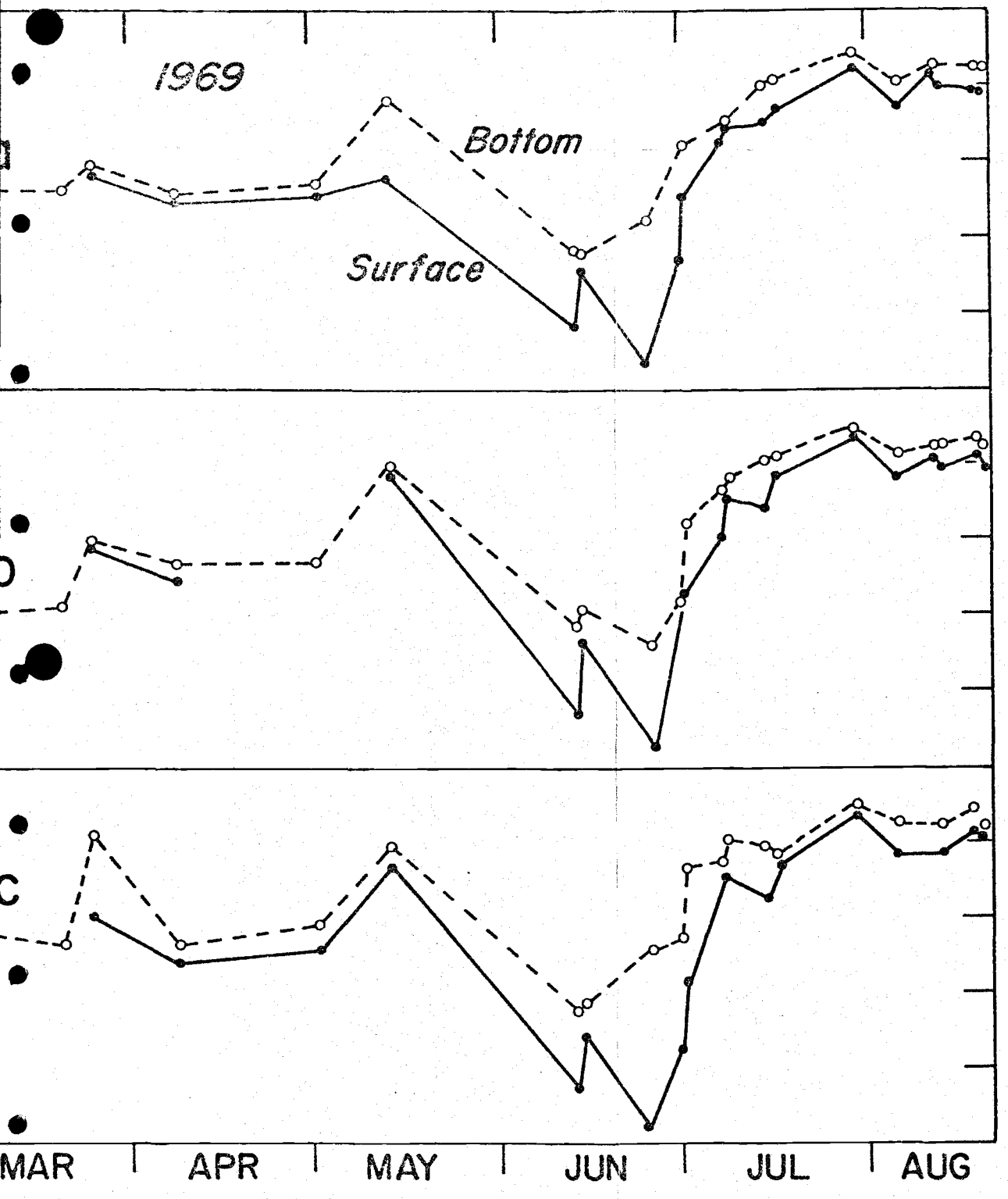
1969
Bottom
Surface
MAR
APR
MAY
JUN
JUL
AUG

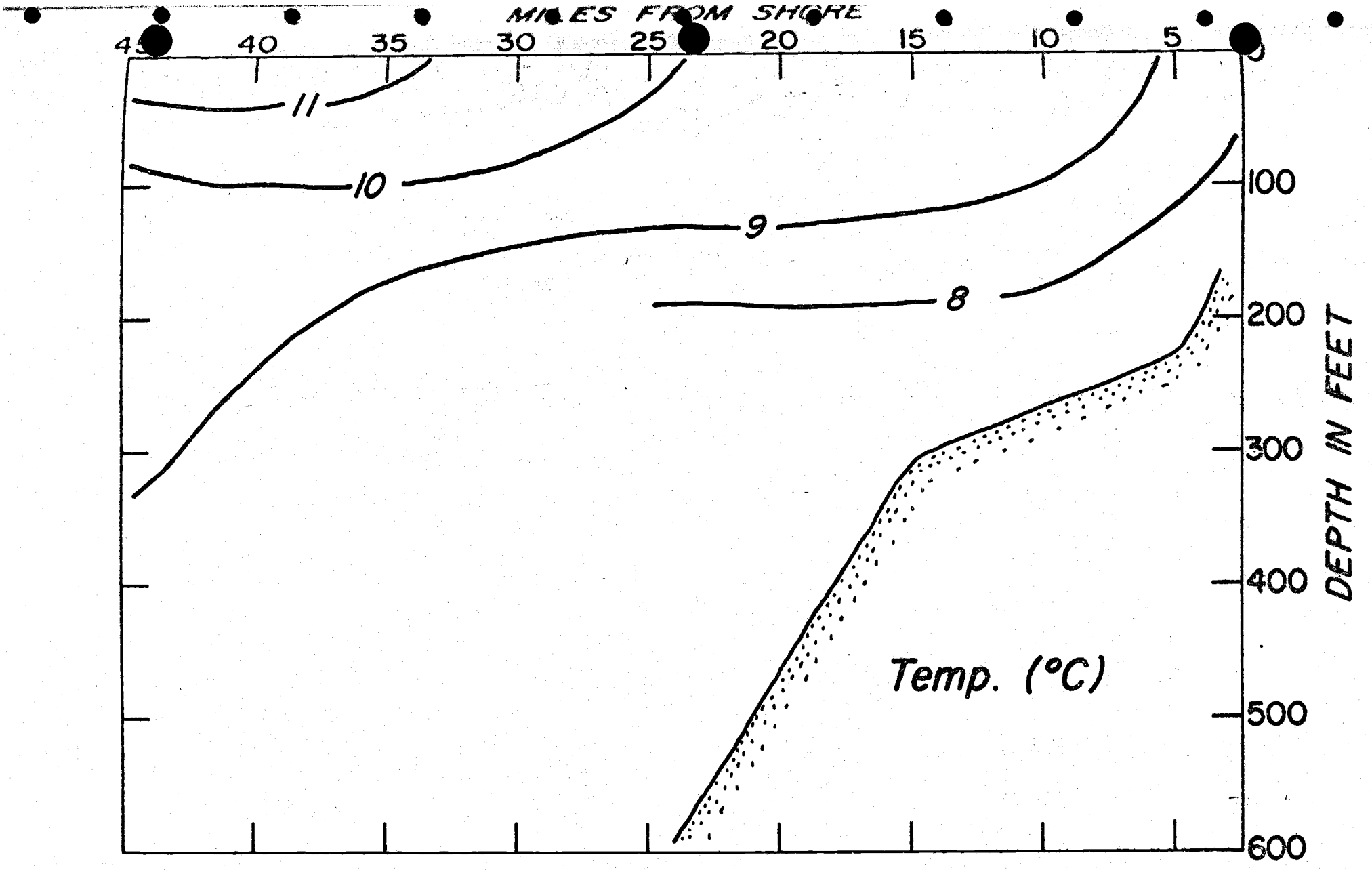

Figure 16. Temperature structure off Newport, May 13-15, 1969.

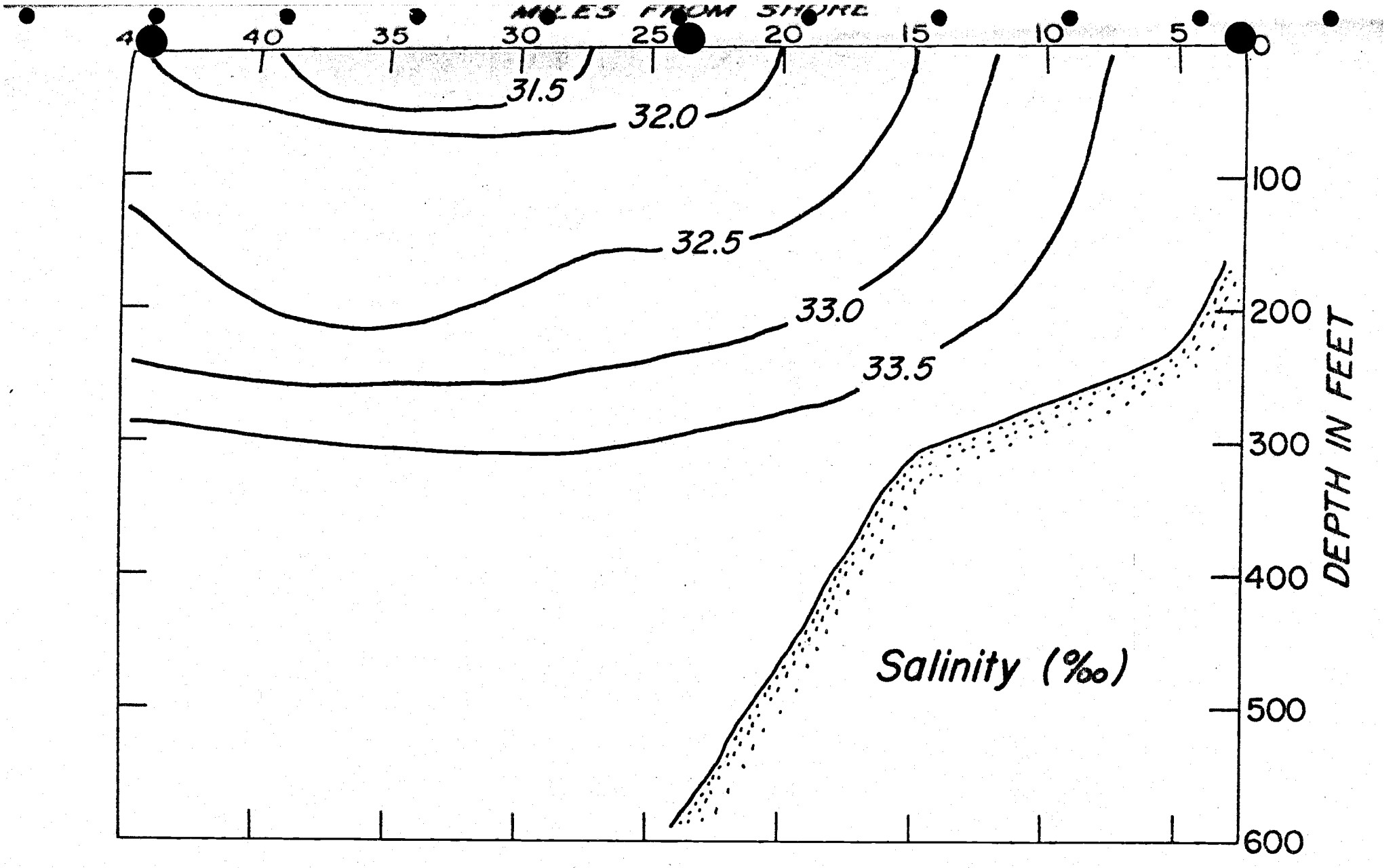

Figure 17. Salinity structure off Newport, May 13-15, 1969.

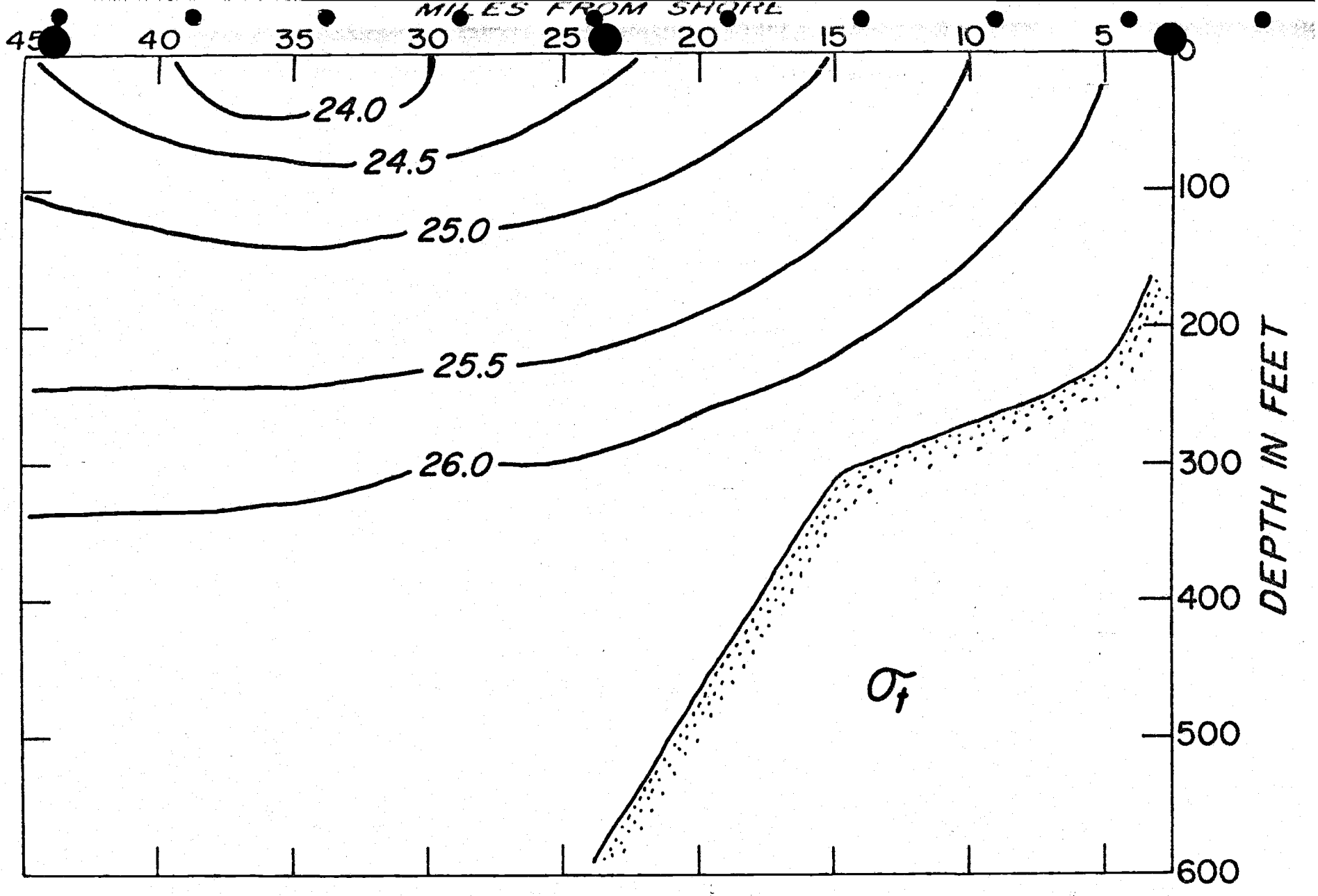

Figure 18. Density structure off Newport, May 13-15, 1969

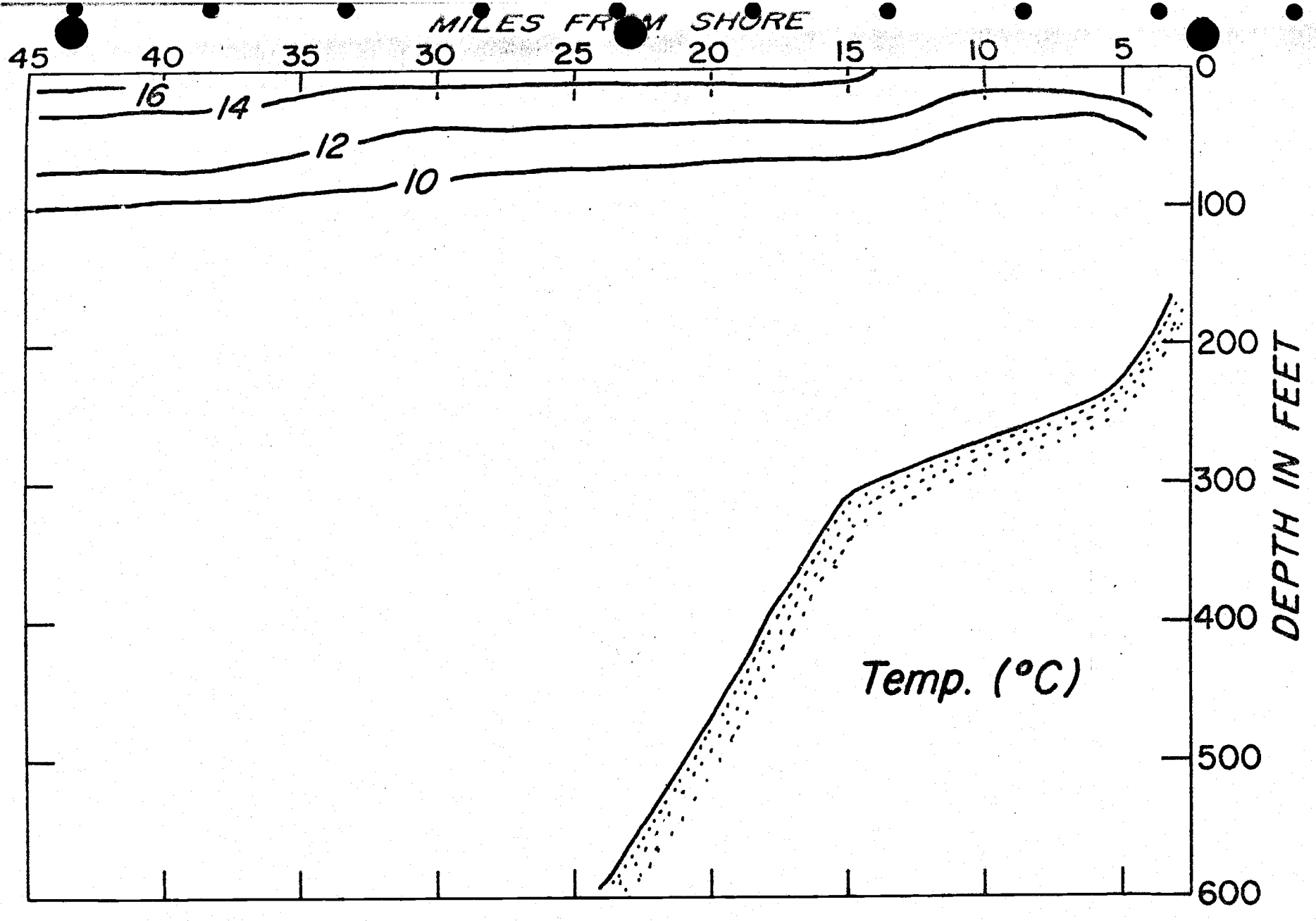

Figure 9. Temperature structure off Newport, July 27-August 1, 1969

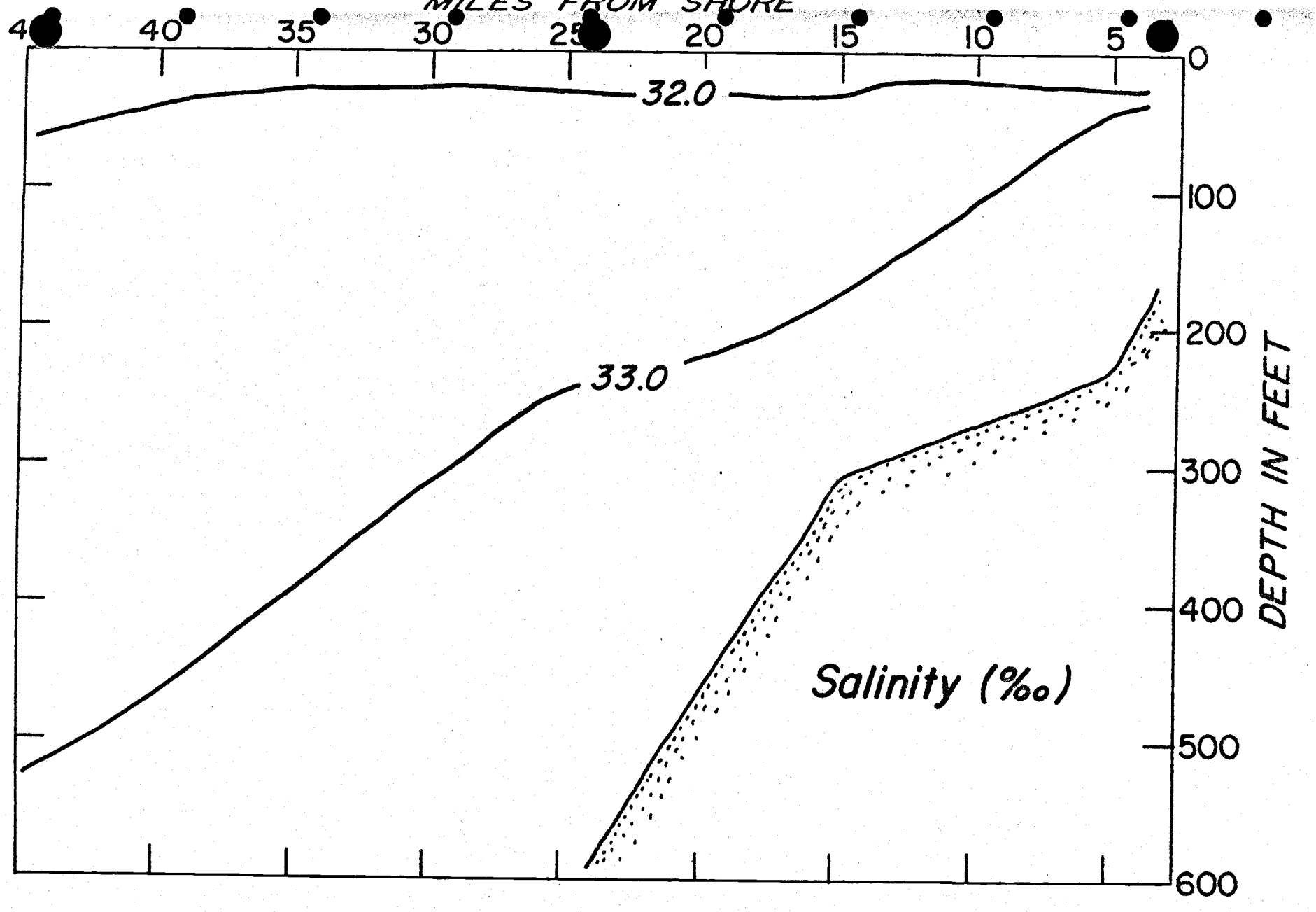

Figure 20. Salinity structure off Newport, July 27-August 1, 1969

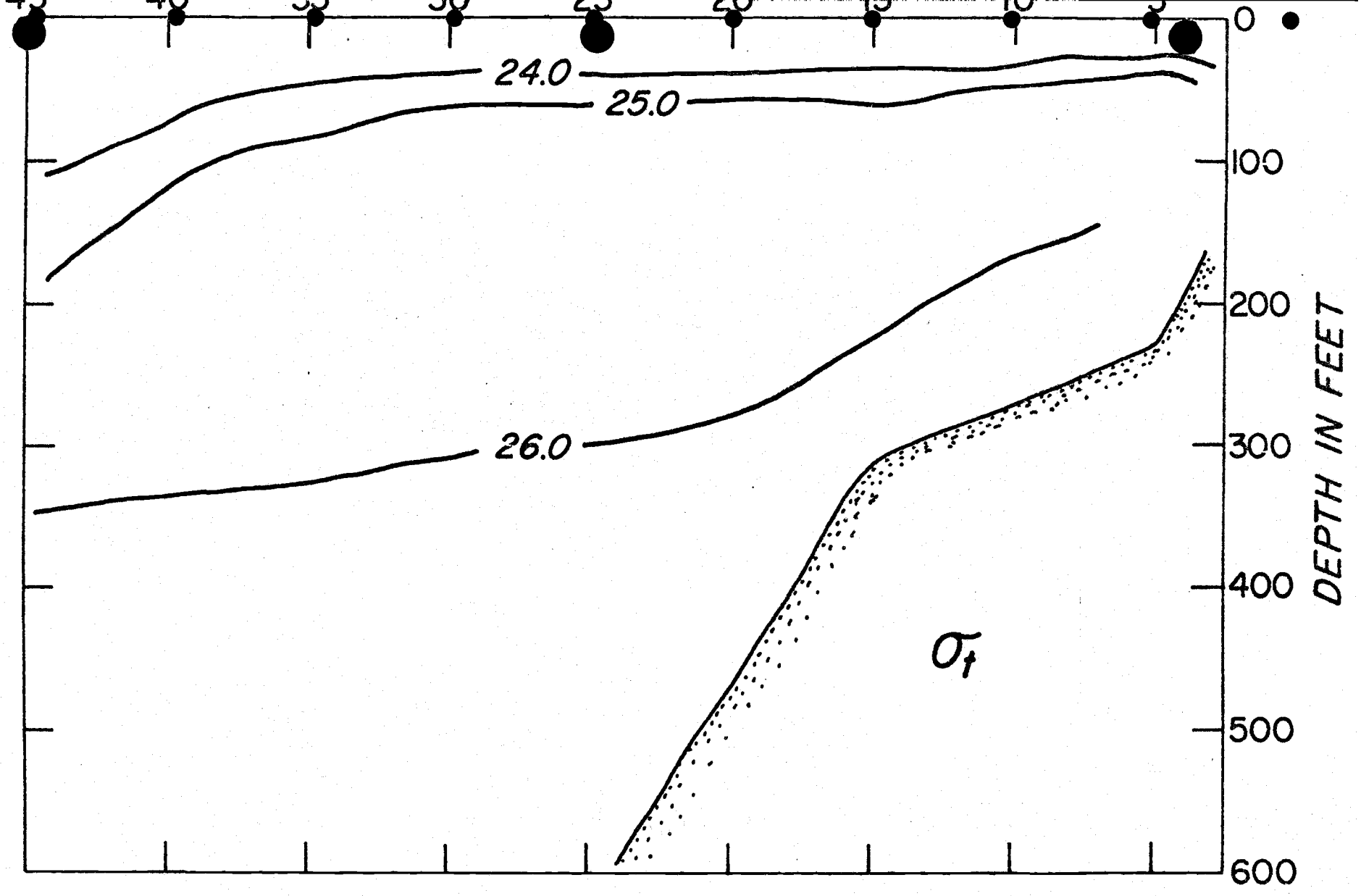

Figure 21. Density structure off Newport, July 27-August 1, 1969

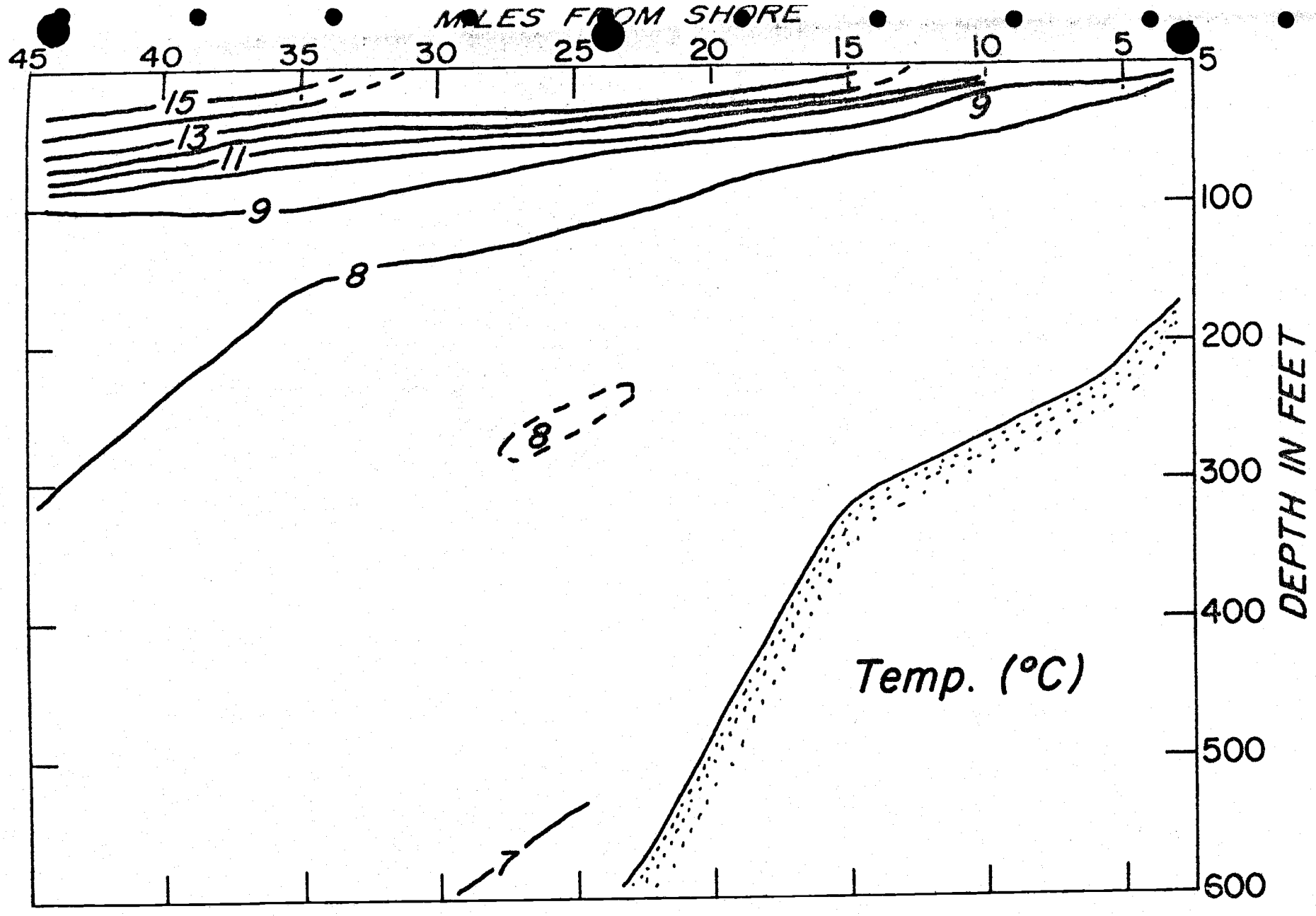

Figure 22. Temperature structure off Newport, August 9-11, 1969

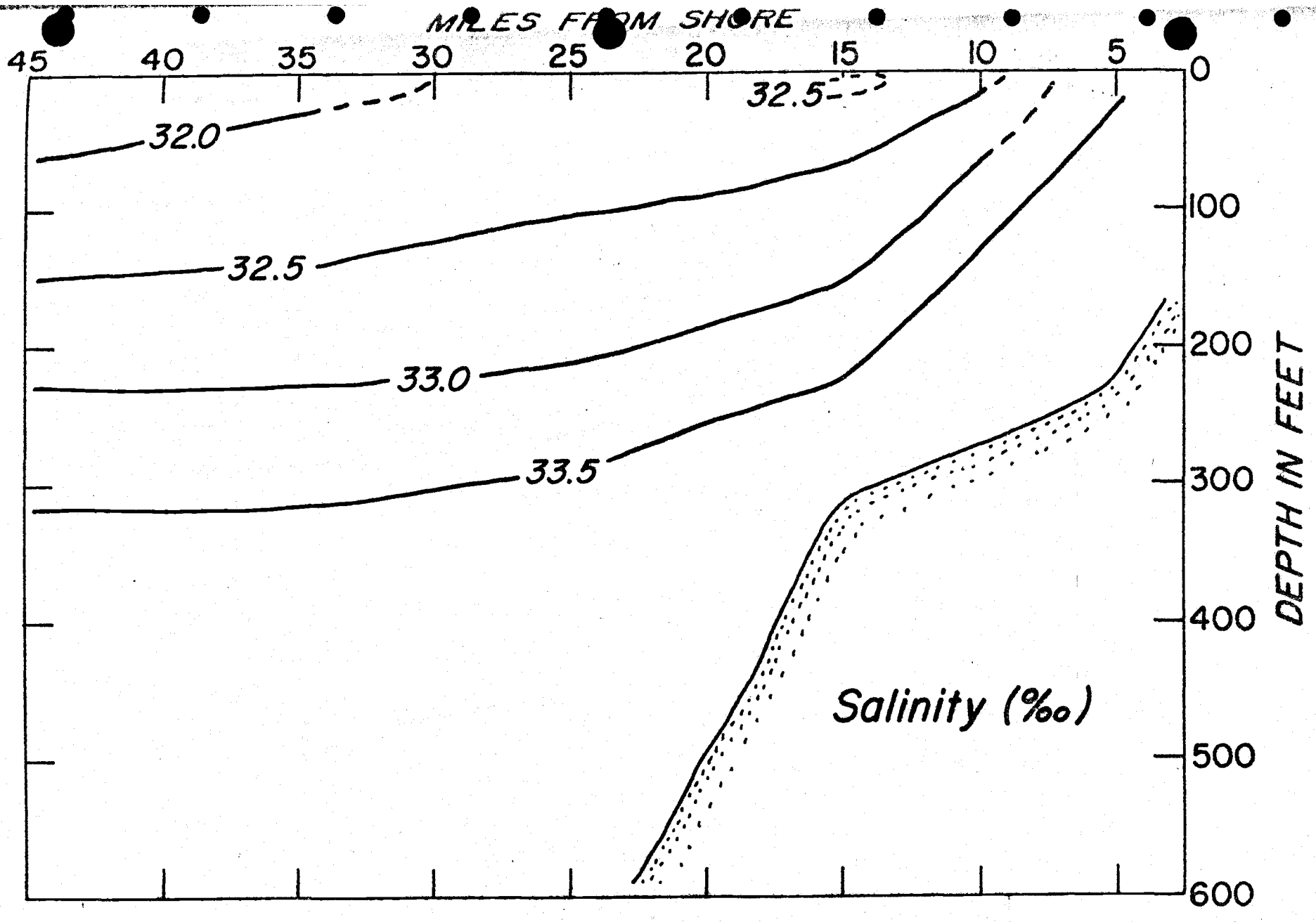

Figure 23. Salinity structure off Newport, August 9-11, 1969.

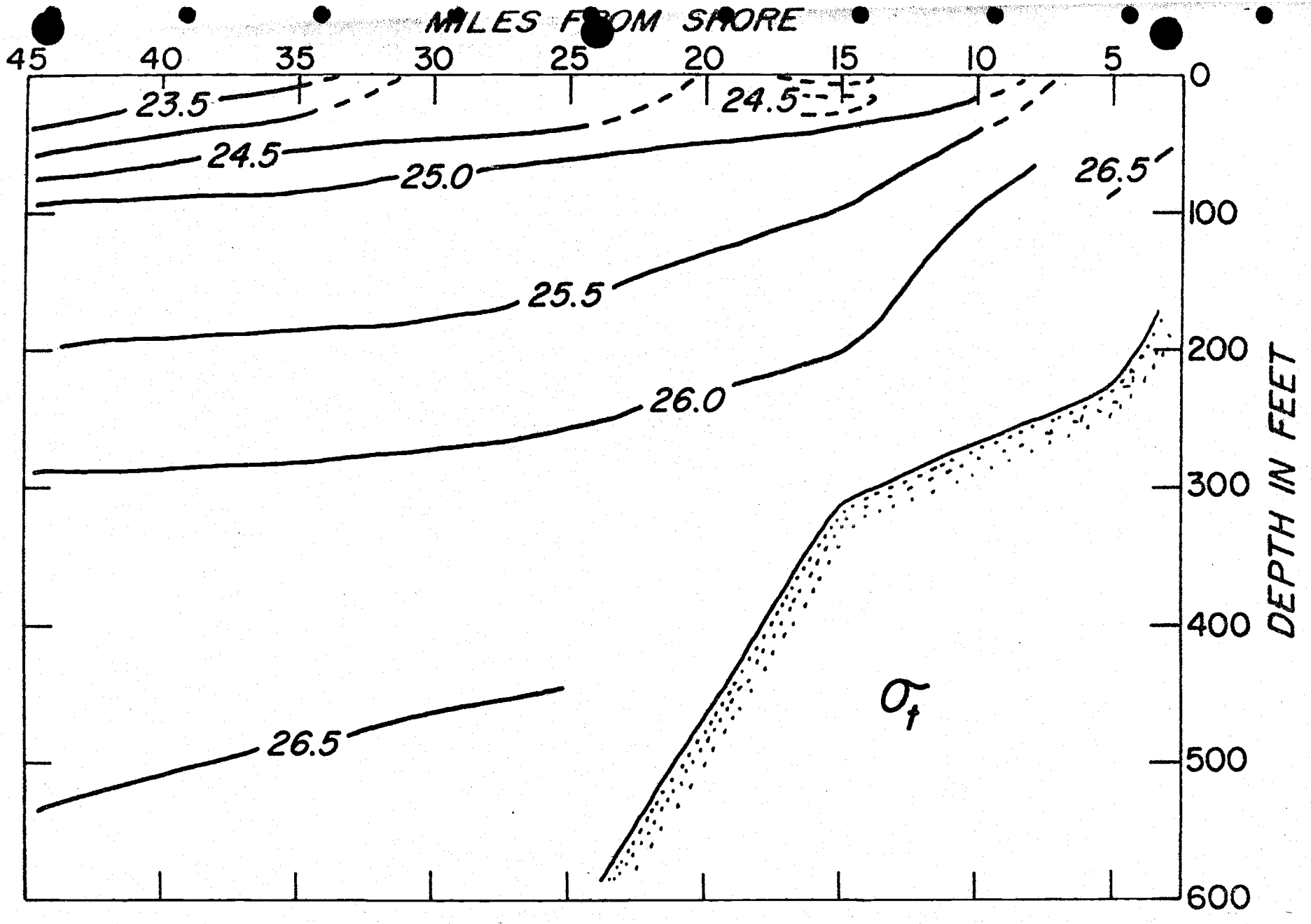

Figure 24. Density structure off Newport, August 9-11, 1969

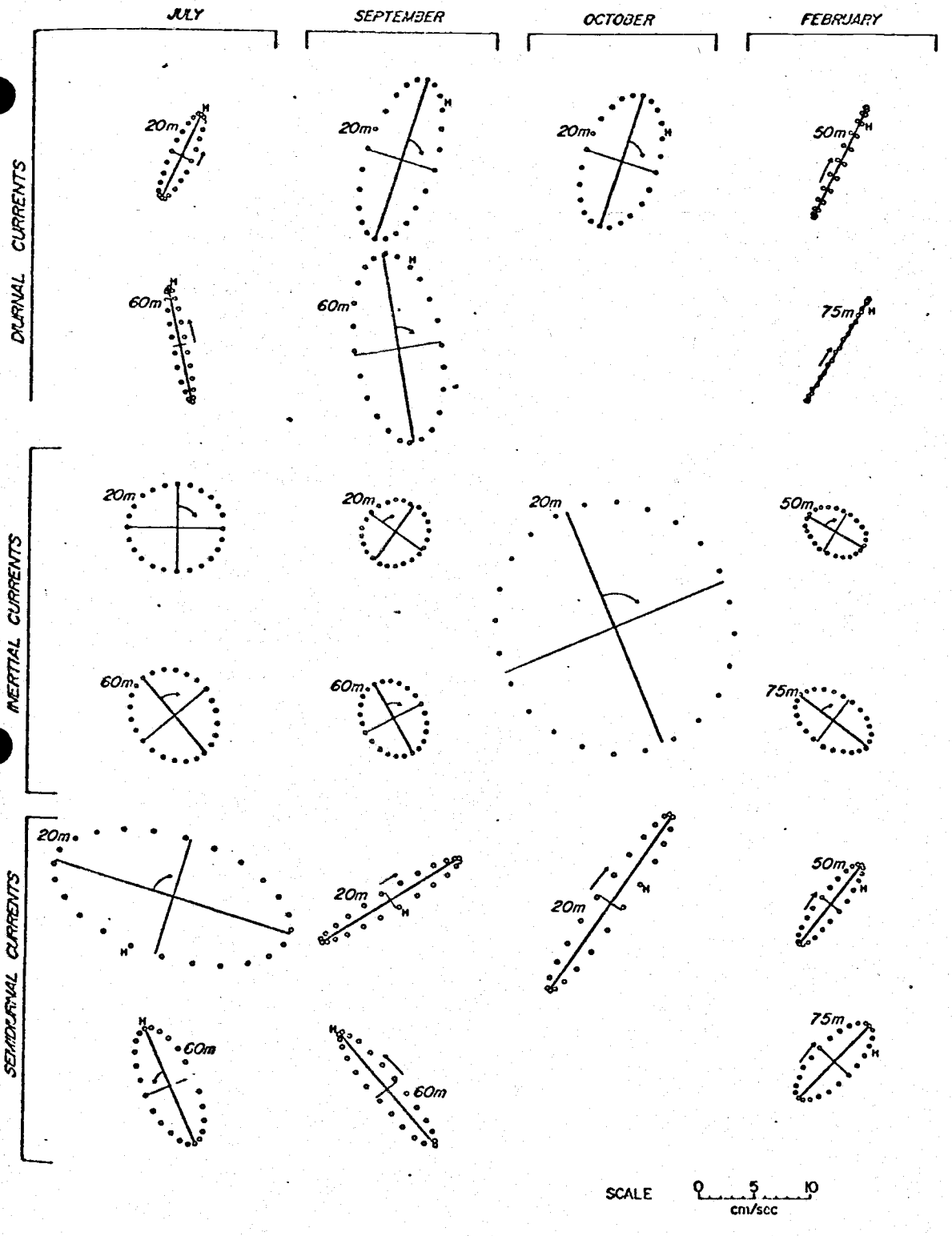

Figure 25. Current velocity ellipses. "H" corresponds to high tide and north is toward the top of the page (Collins, 1967).

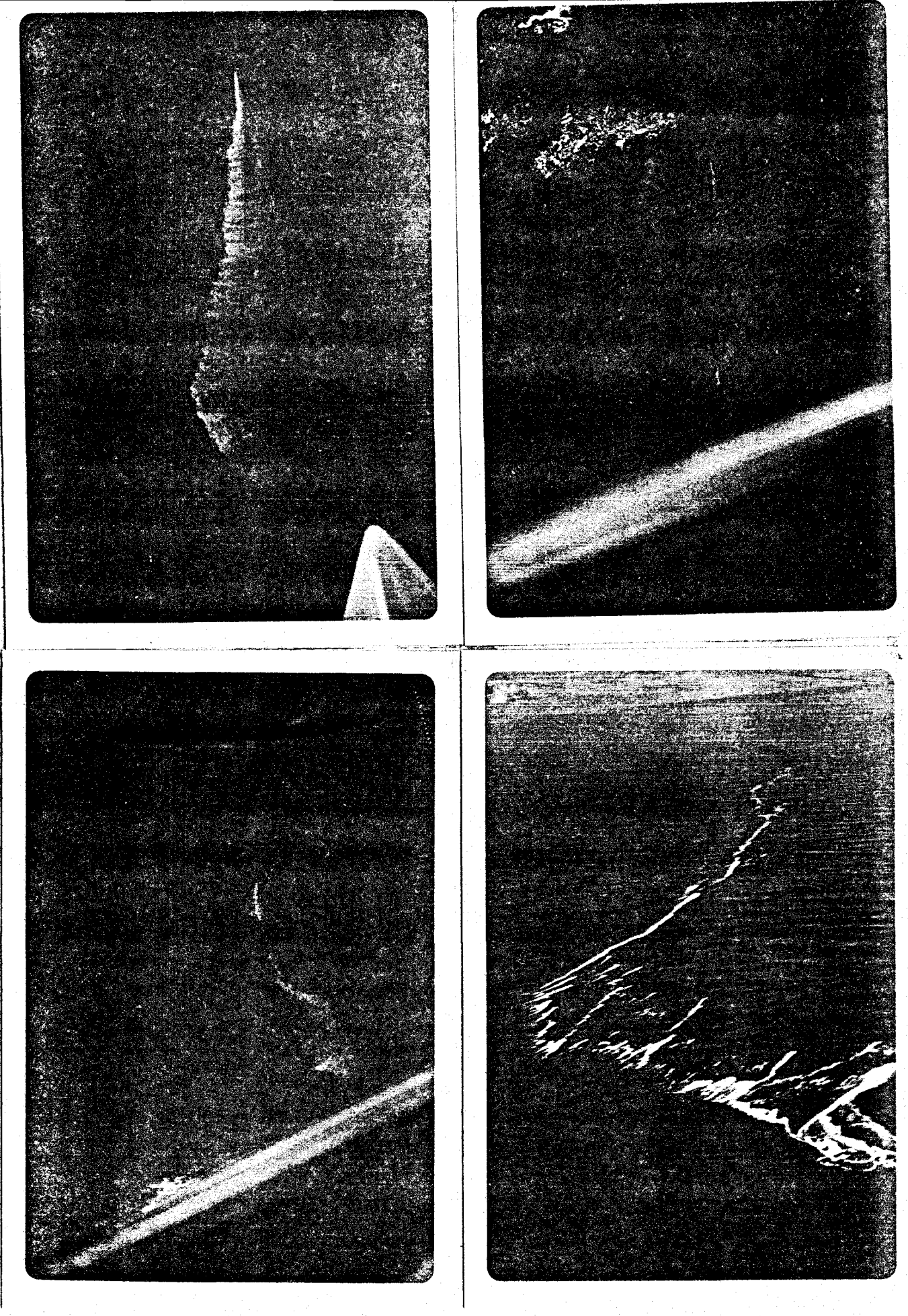

Figure 26a. Color photographs of dye markers and foam from the outfall.

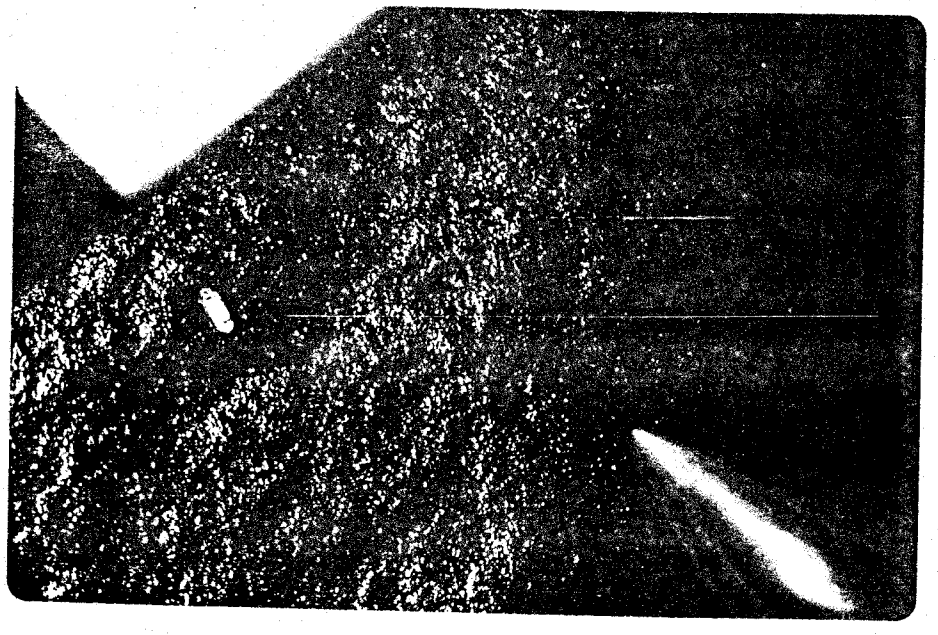

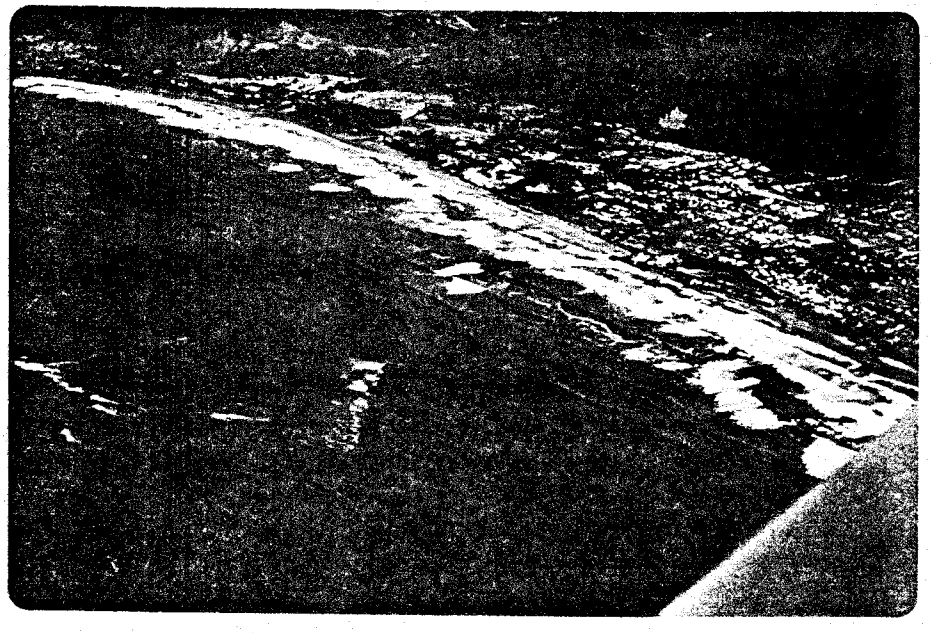

Figure 26c. Color photographs of dye markers near the outfall and the outfall plume.

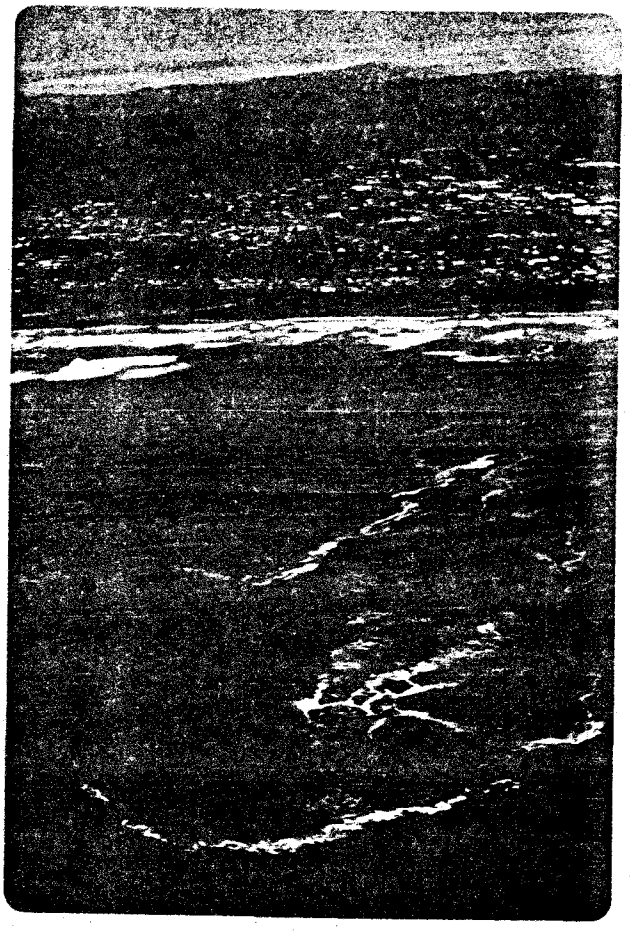

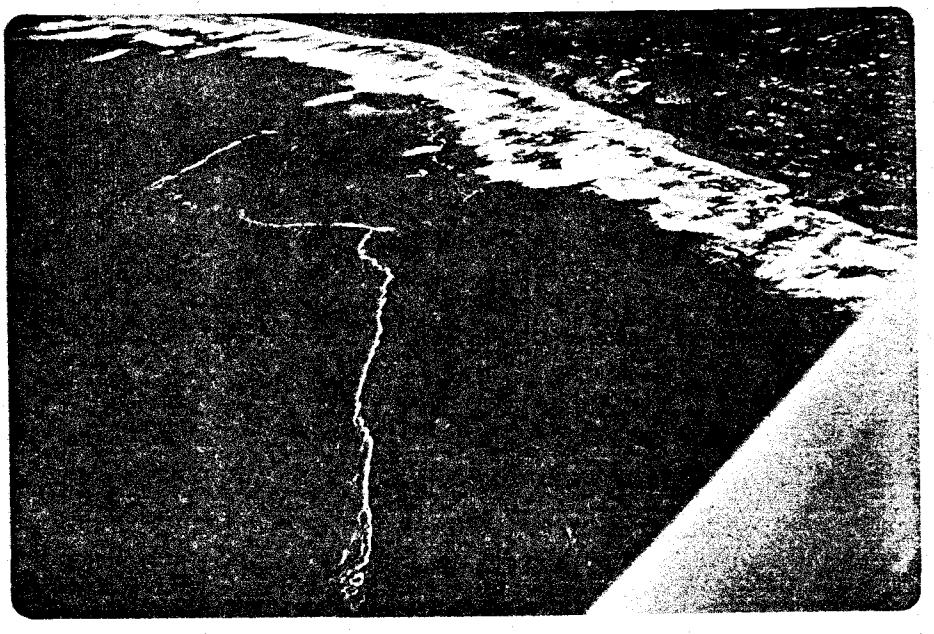

Figure 26d. Color photographs of the outfall plume.

Figures 27. (a through cc). Current and wind vectors measured in the coastal waters near Newport. Tidal stages are indicated by E (ebb) and F (flood) in the lower right hand of each diagram. Dates are indicated in the upper portion of each diagram.

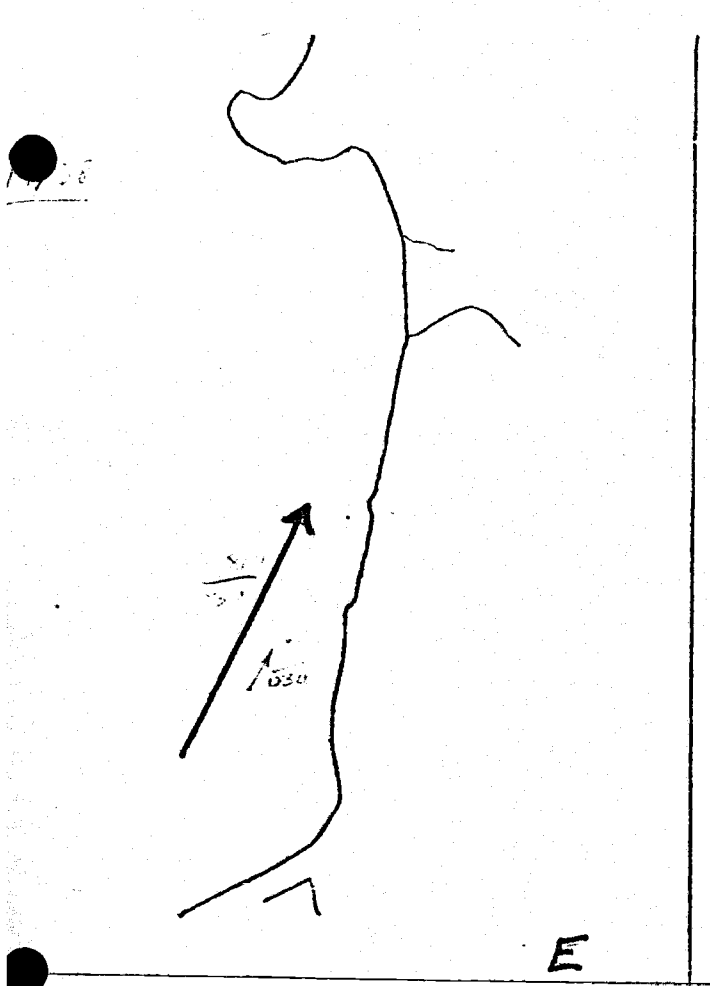
E

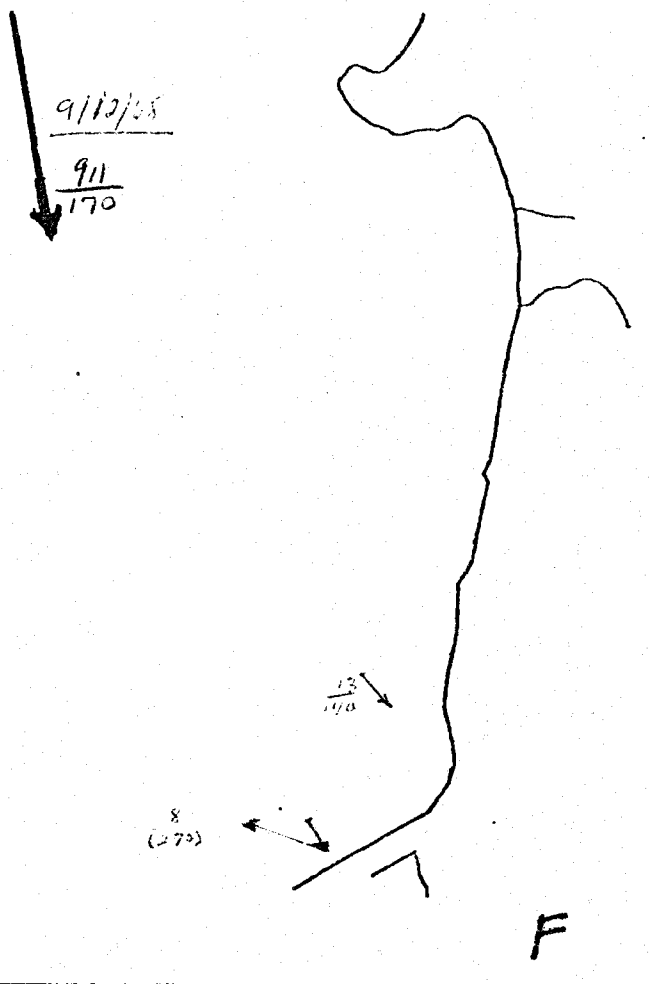
9/12/58
911
170
F

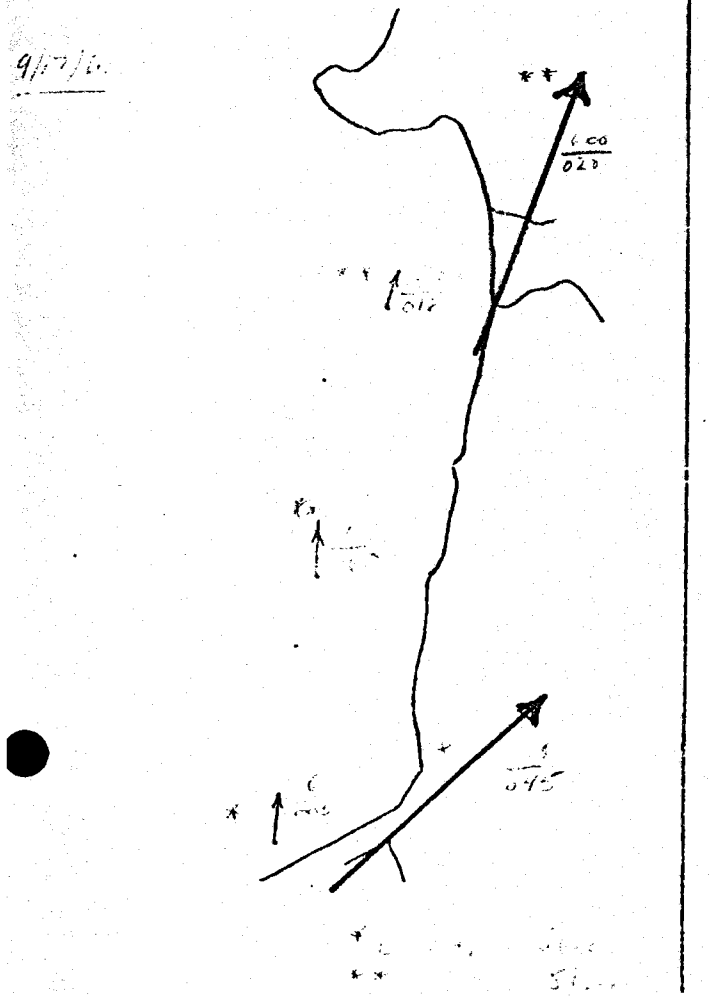
9/17/58

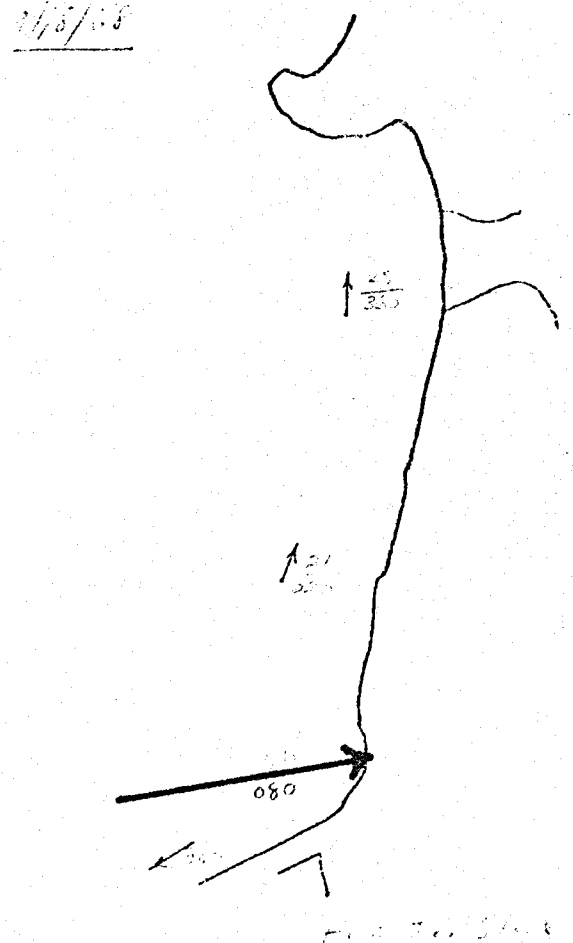
9/18/58
080

9/27/68

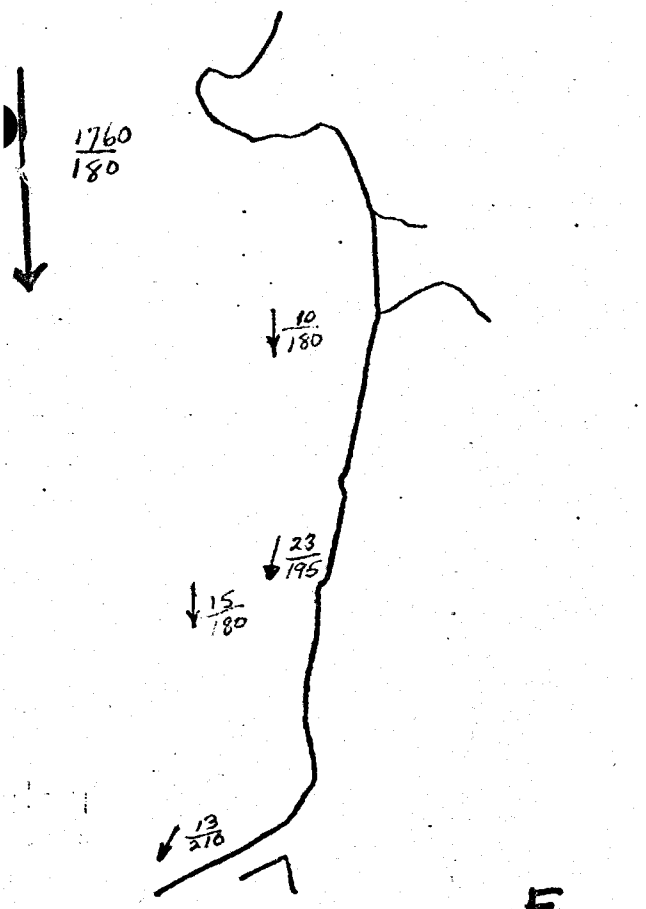

F

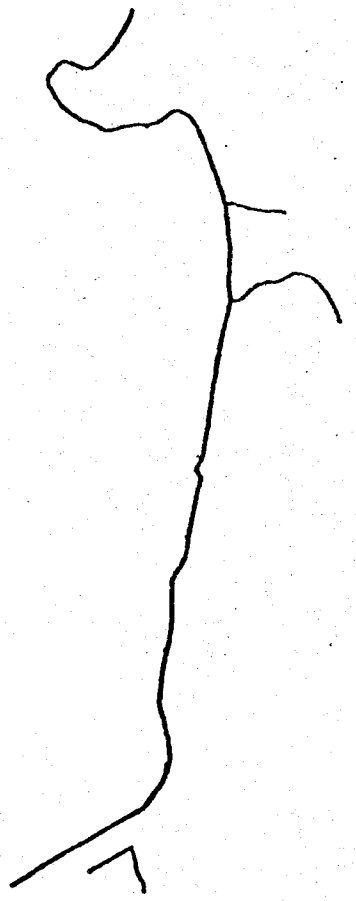

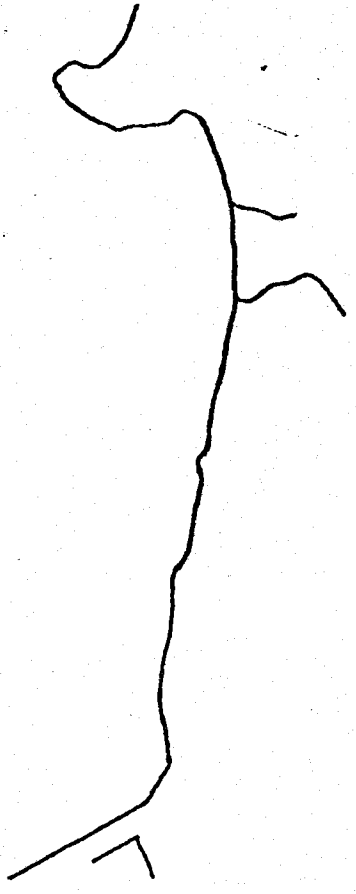

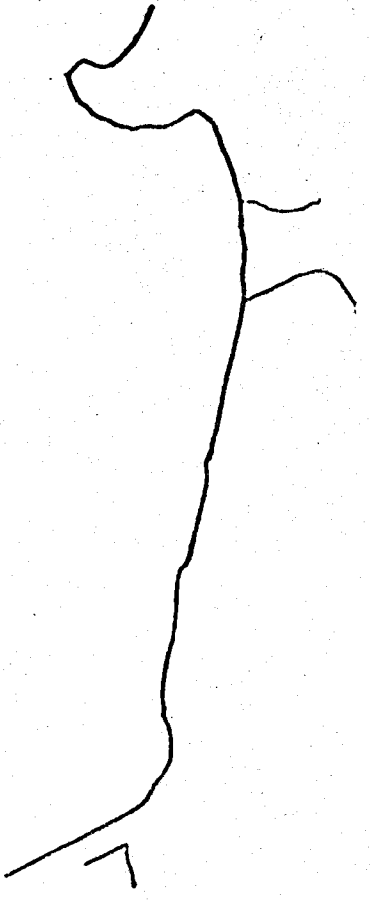

10/3/68

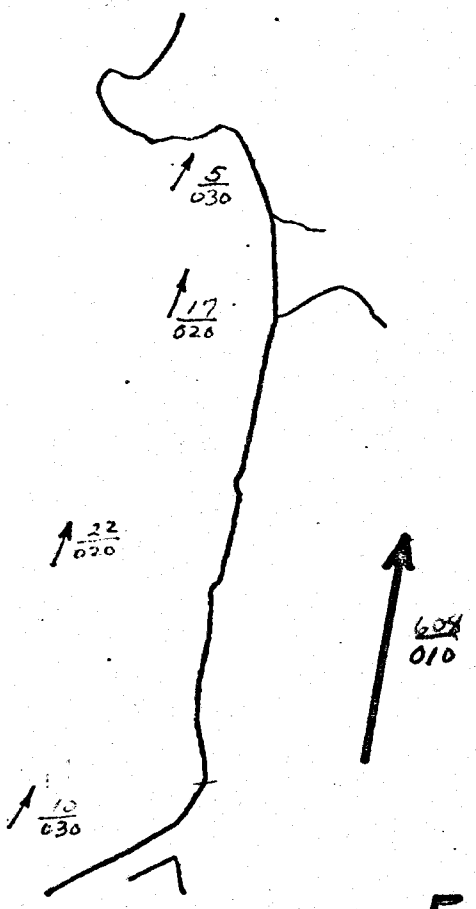

10/4/68

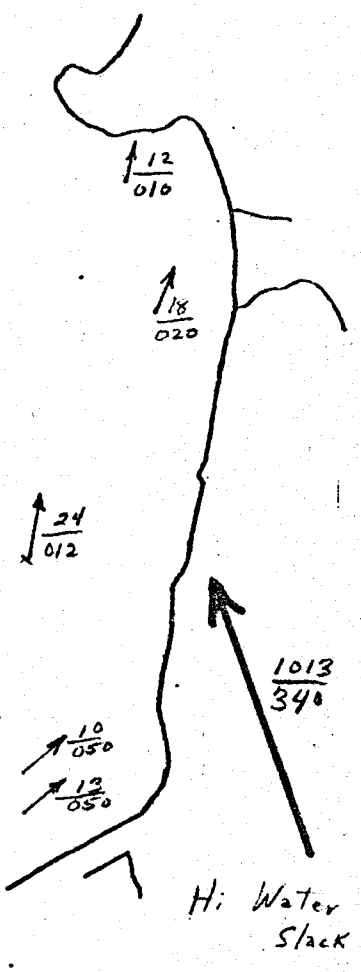

10/10/68

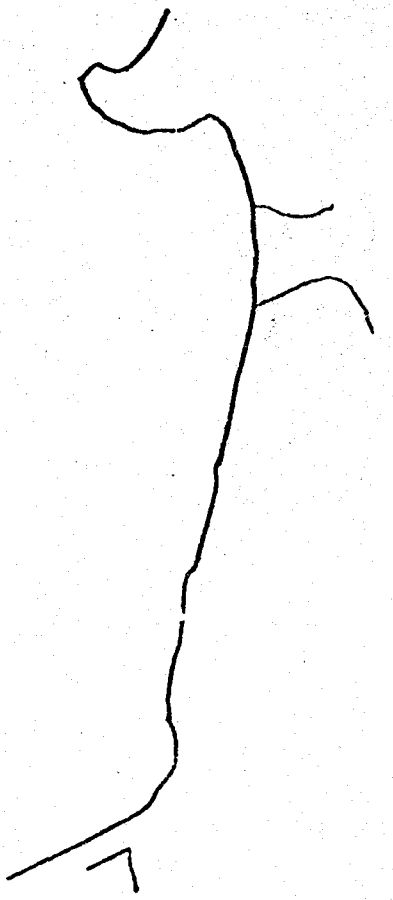

10/23/68

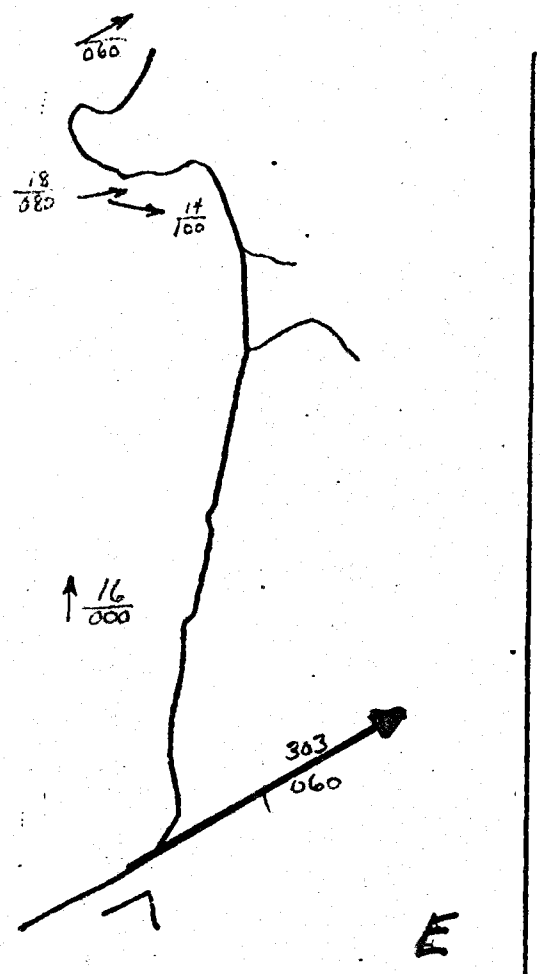

10/28/68

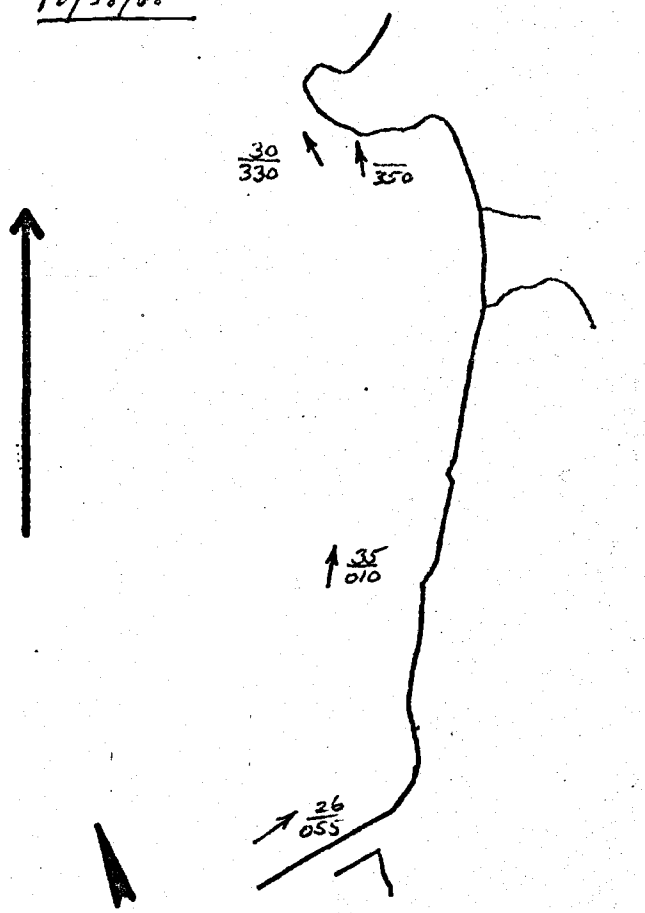

10/31/68

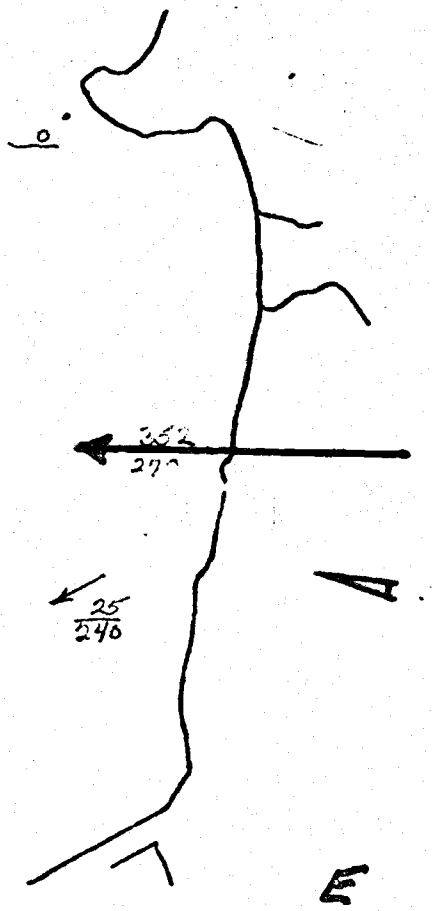

11/5/68

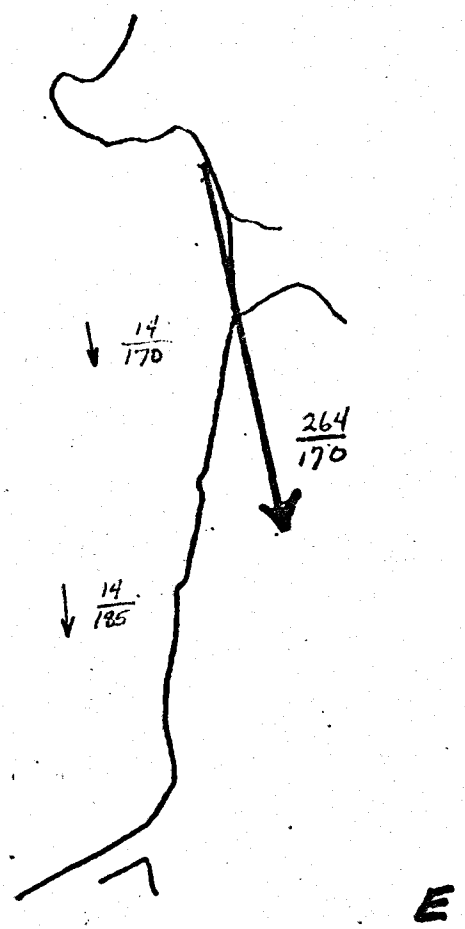

11/7/68

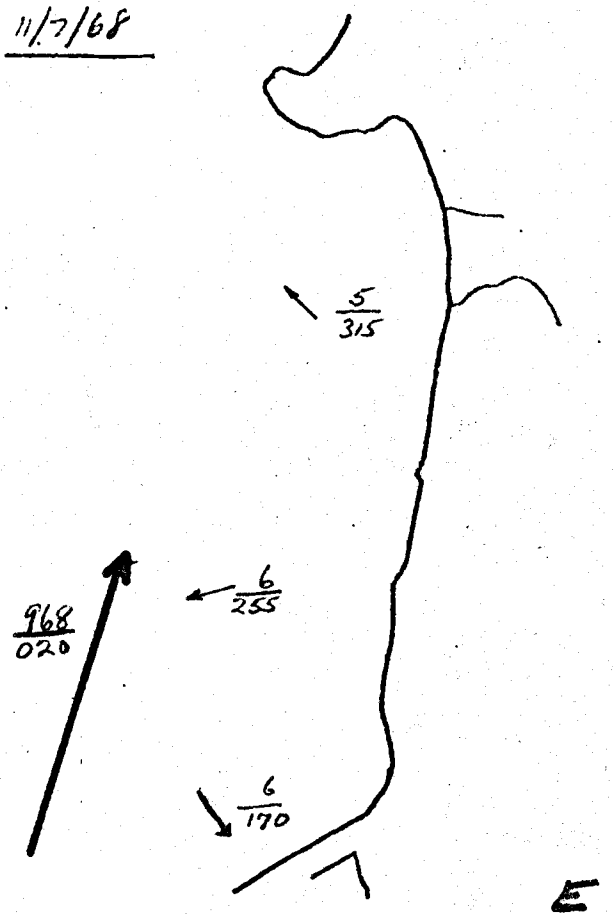

11/14/68

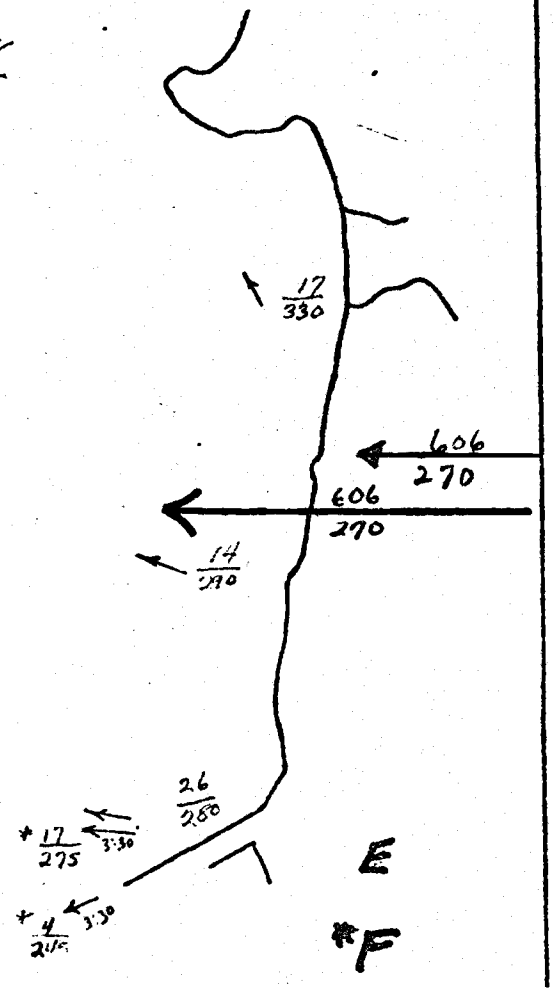

11/19/68

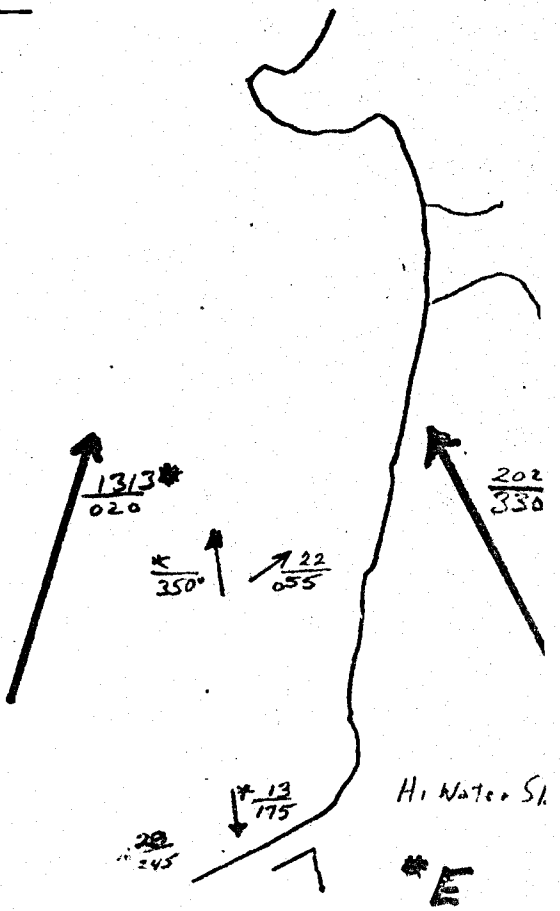

11/26

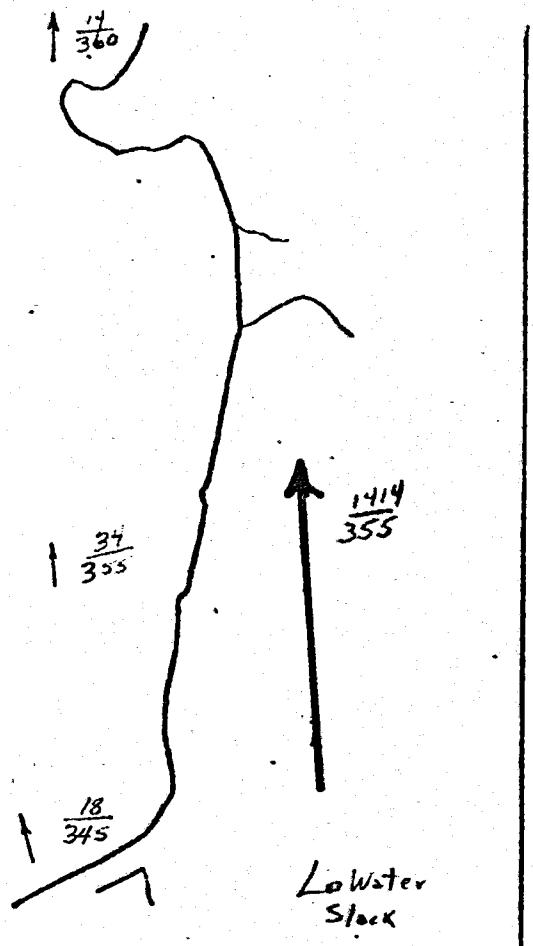
17
360
34
355
1414
355
18
345
Lo Water
Slack

11/29

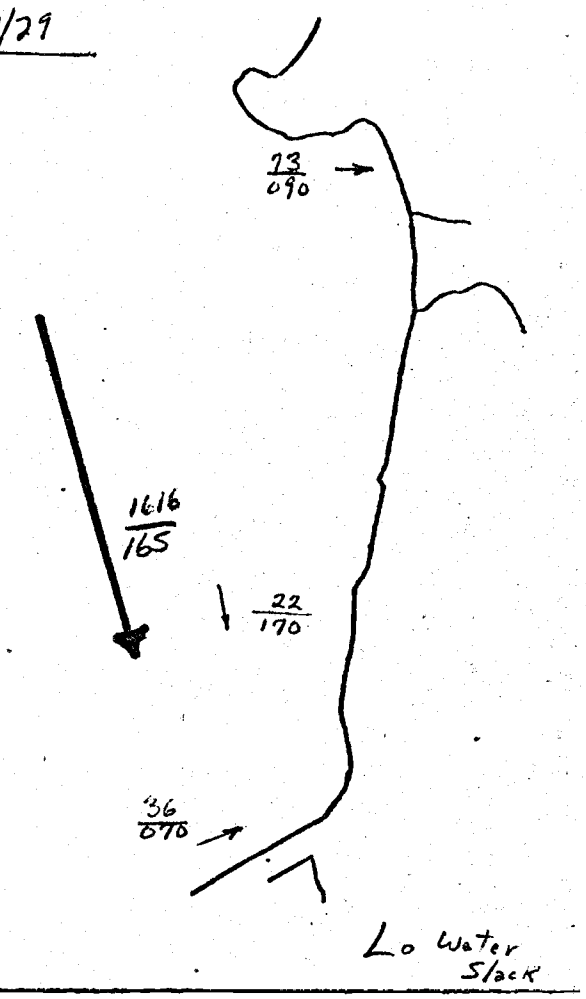
23
090
1616
165
22
170
36
070
Lo Water
Slack

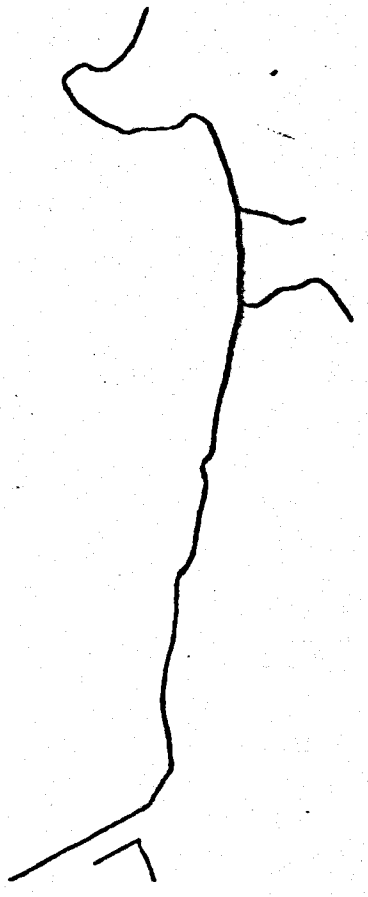

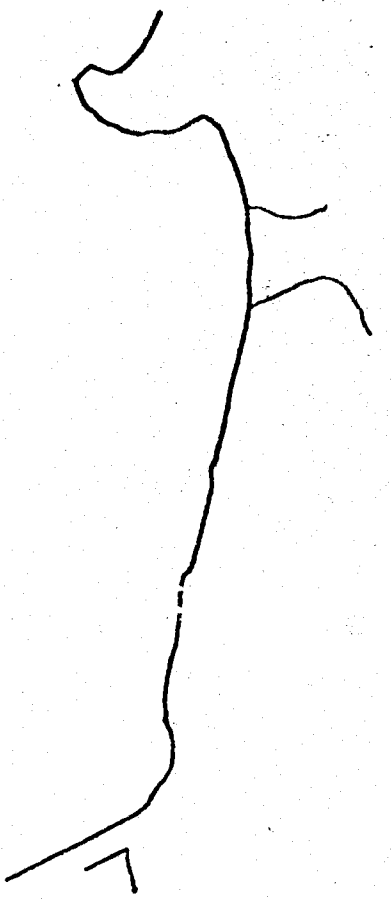

12/5/68

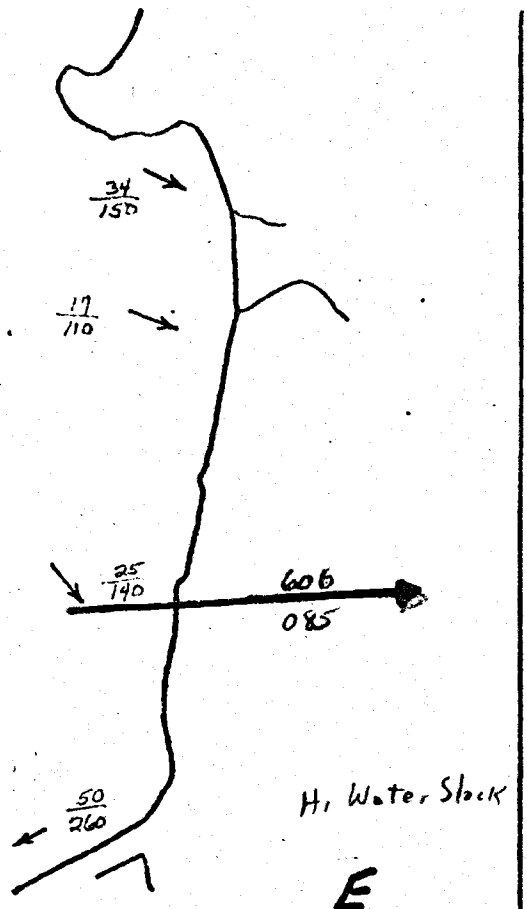

12/11/68

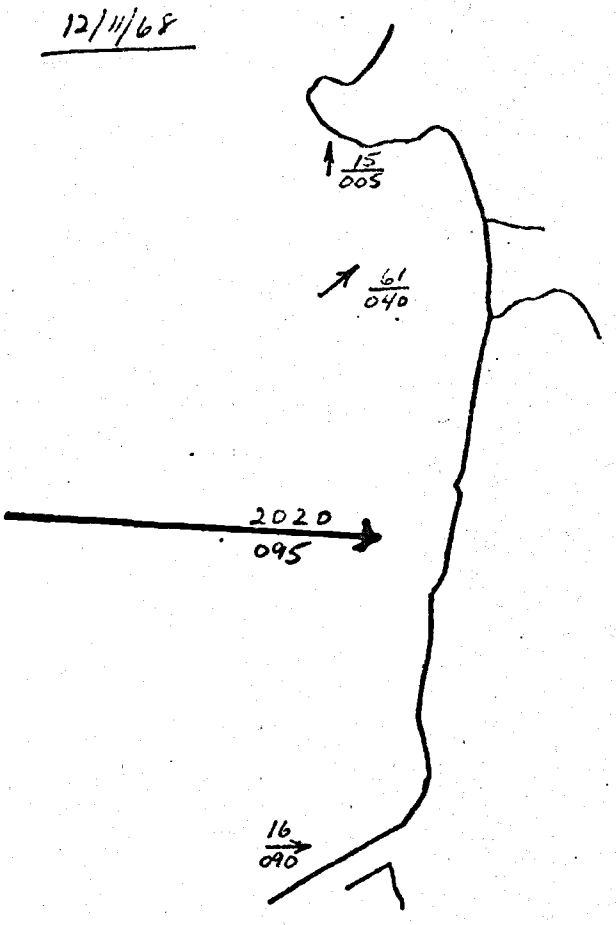

12/17/68

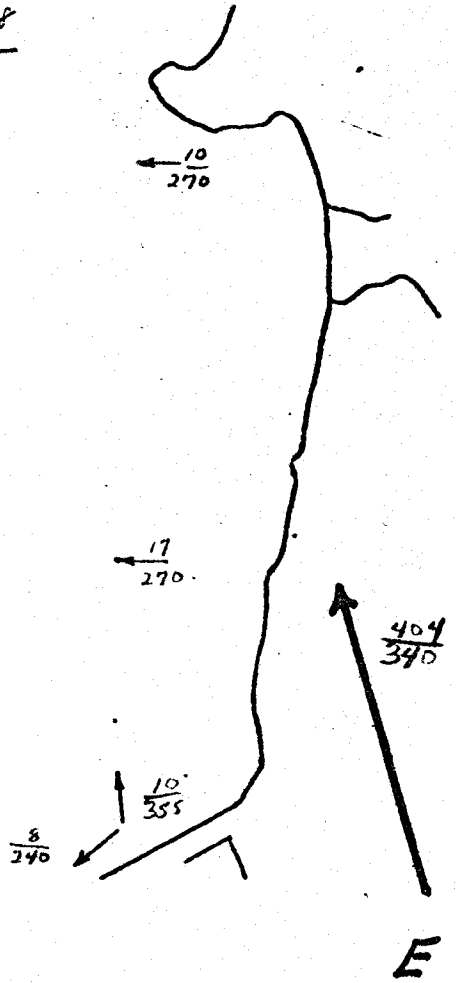

12/20/68

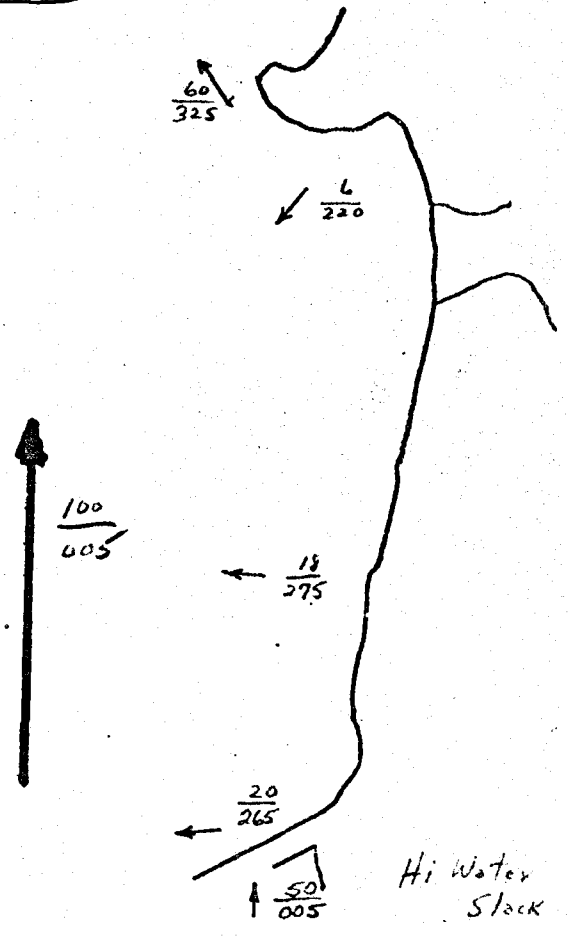

12/24/68

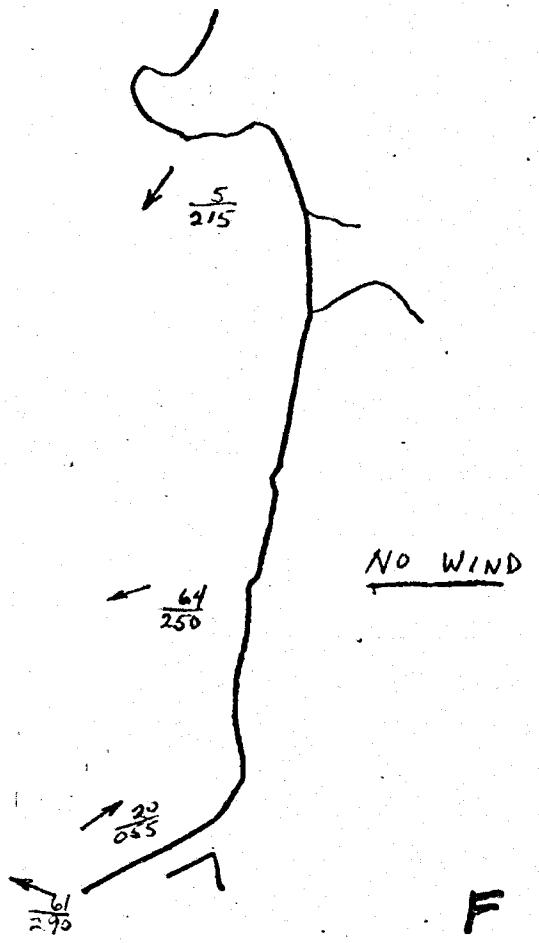

12/26/68

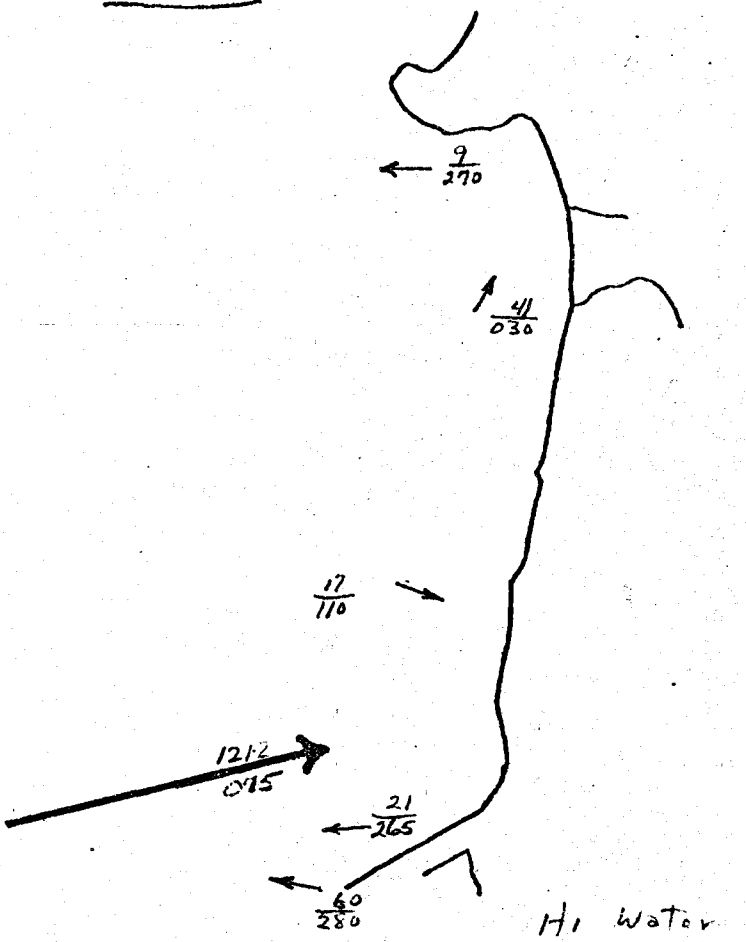

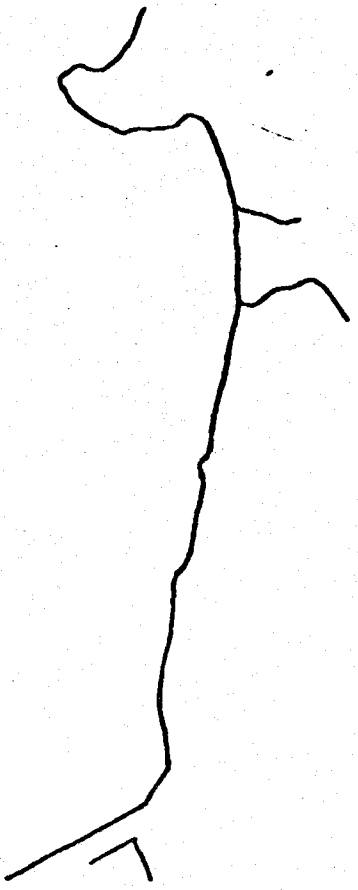

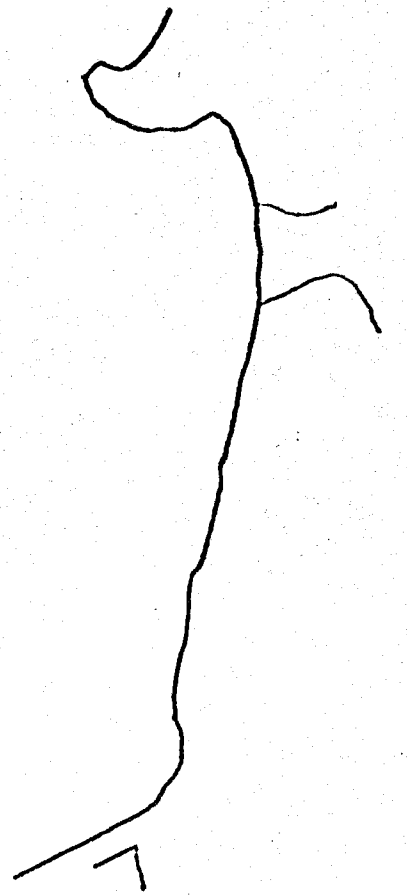

1/3/69

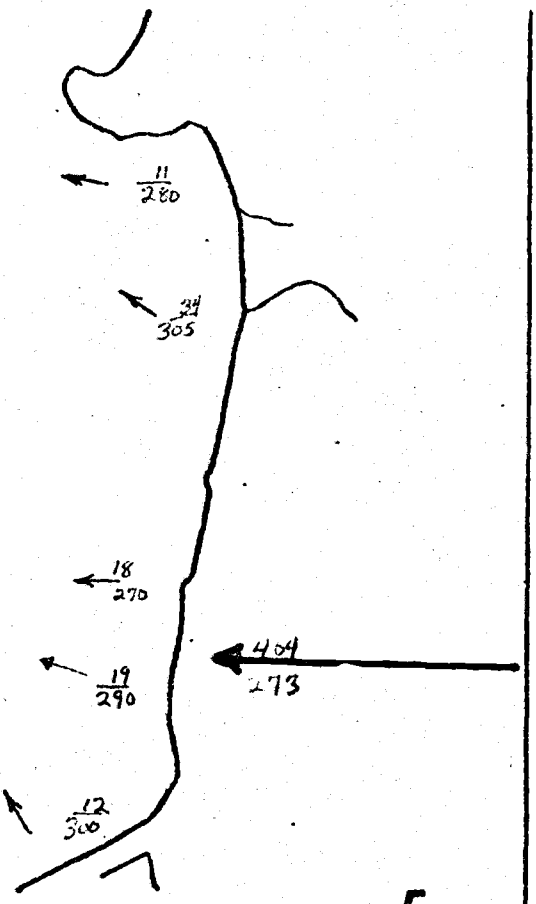

1/7/69

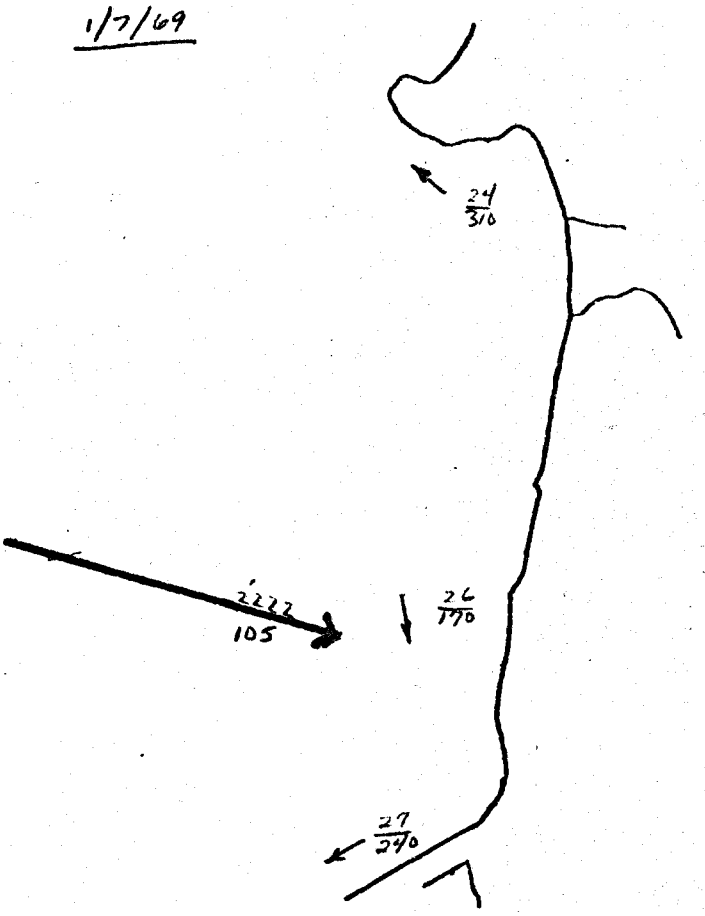

1/9/69

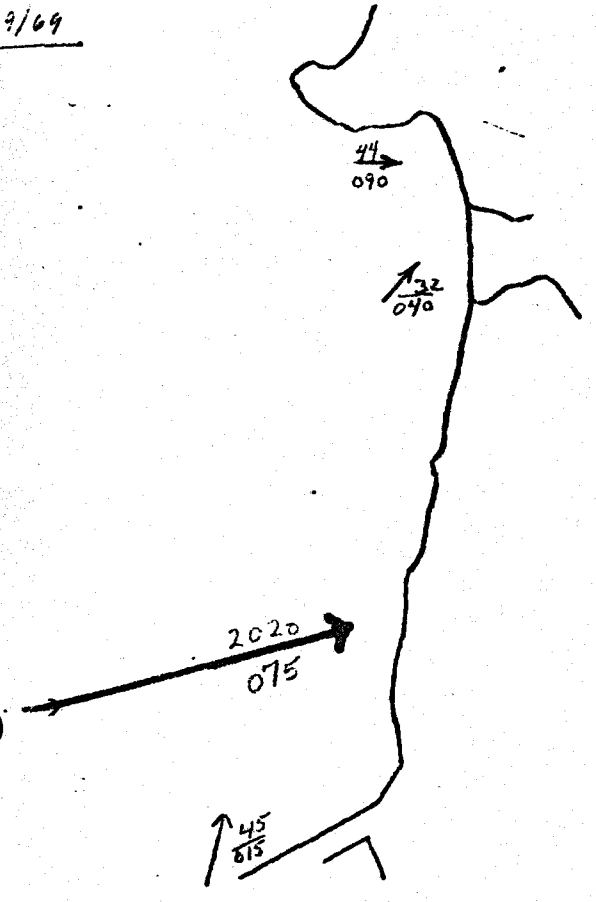

1/14/69

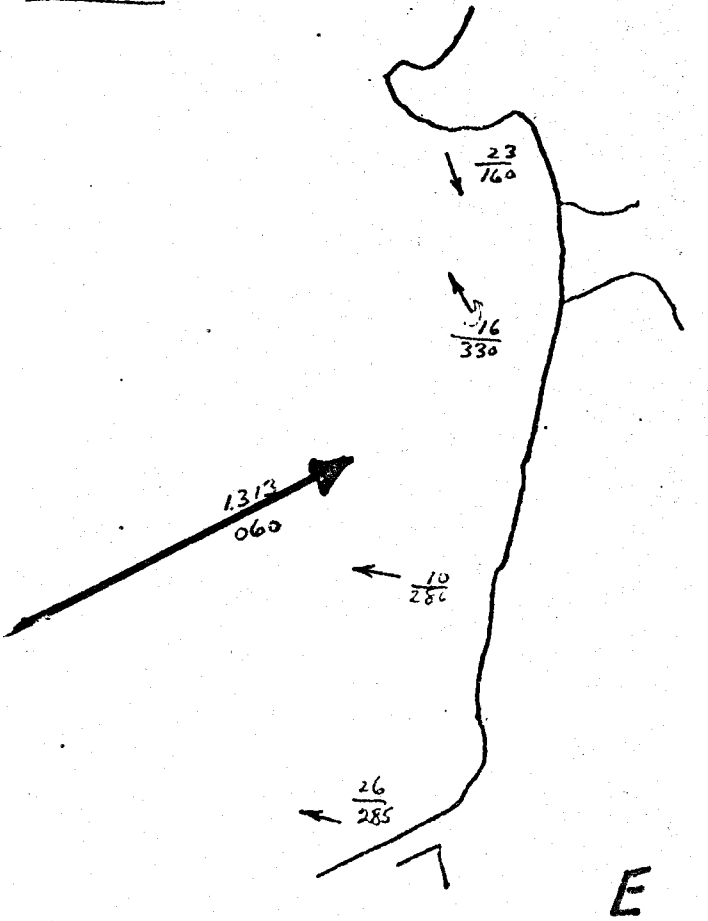

1/16/69

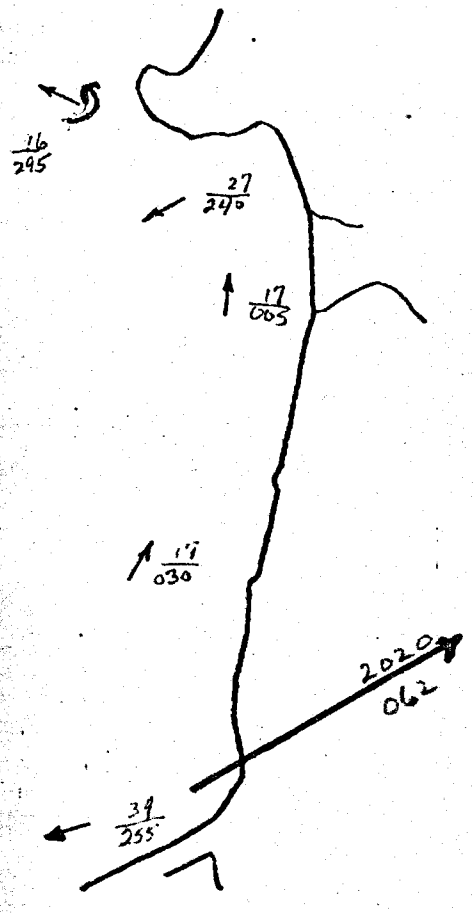

1/21/69

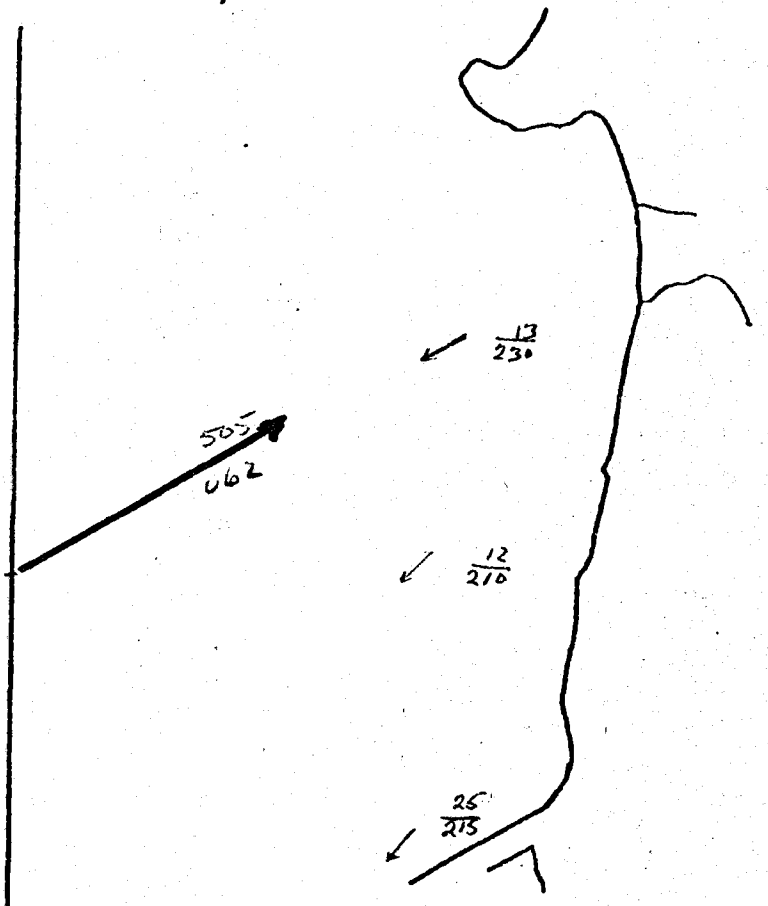

1/23/69

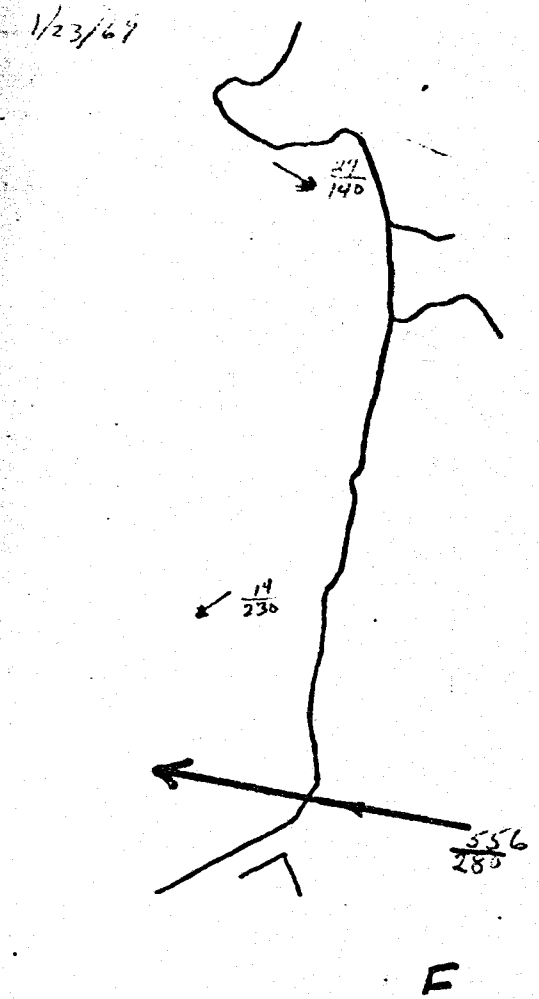

2/4/69

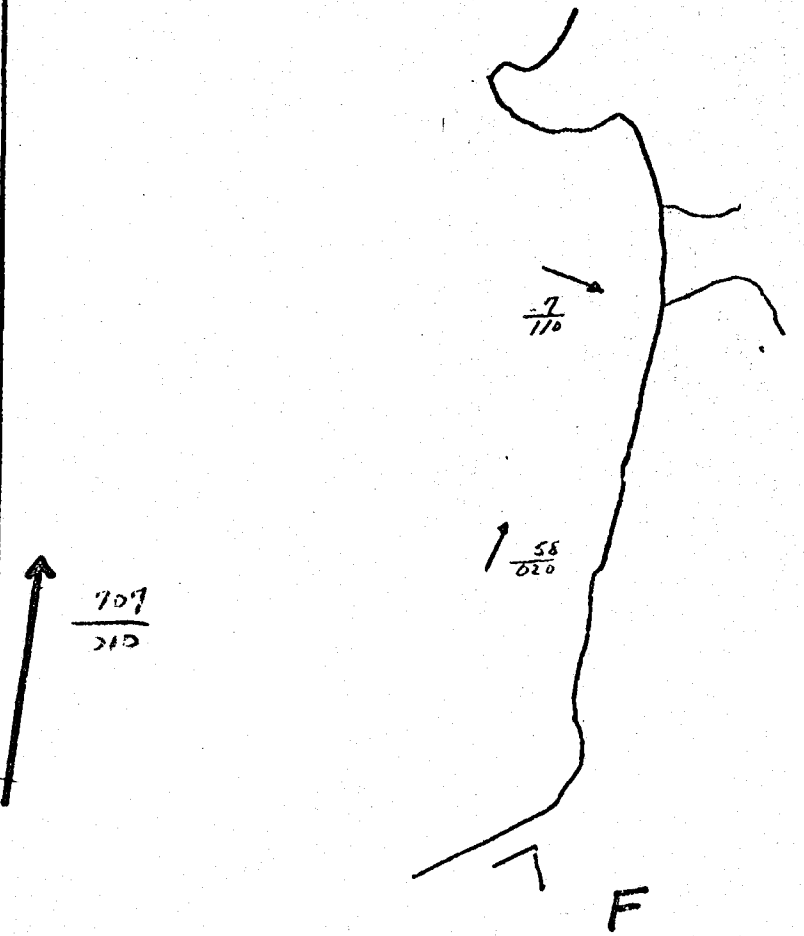

2/6/69

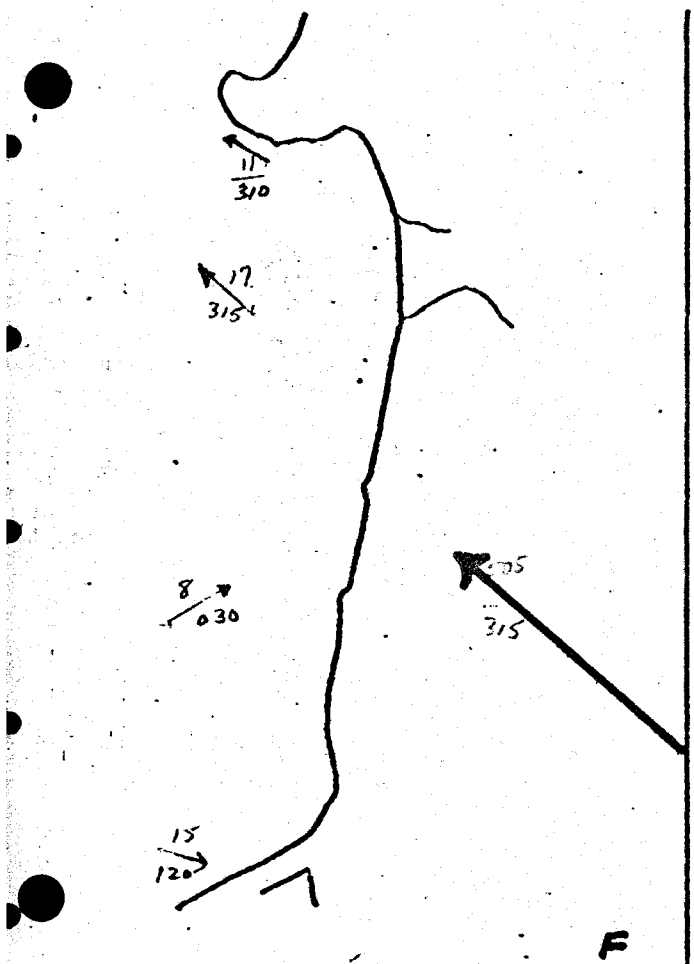

2/11/67

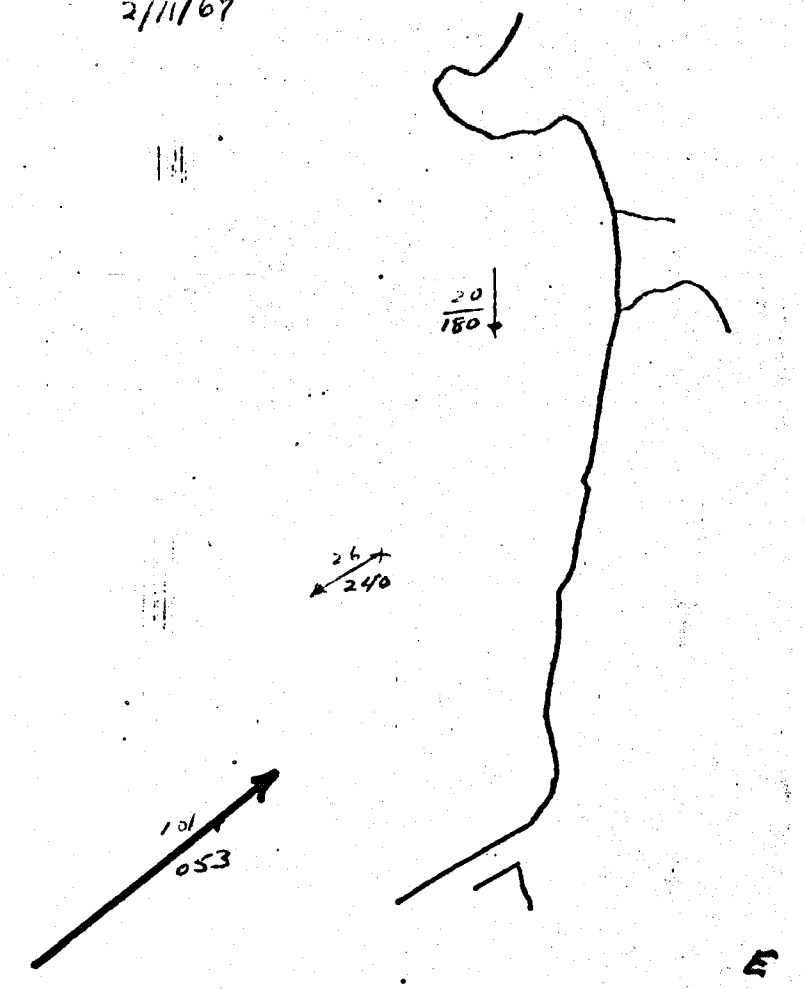

2/13/69

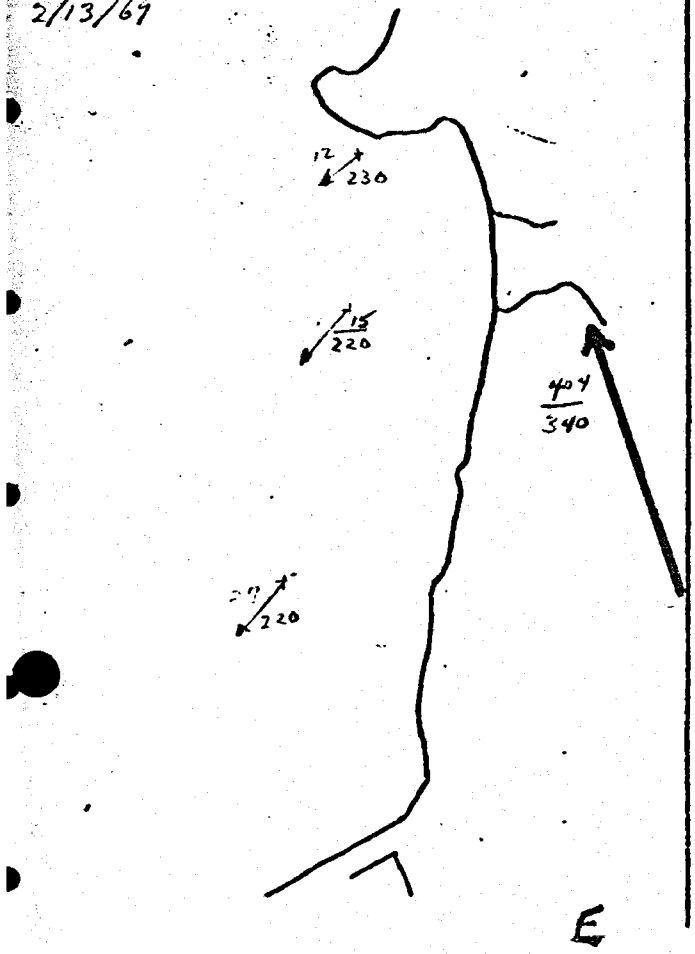

2/18/69

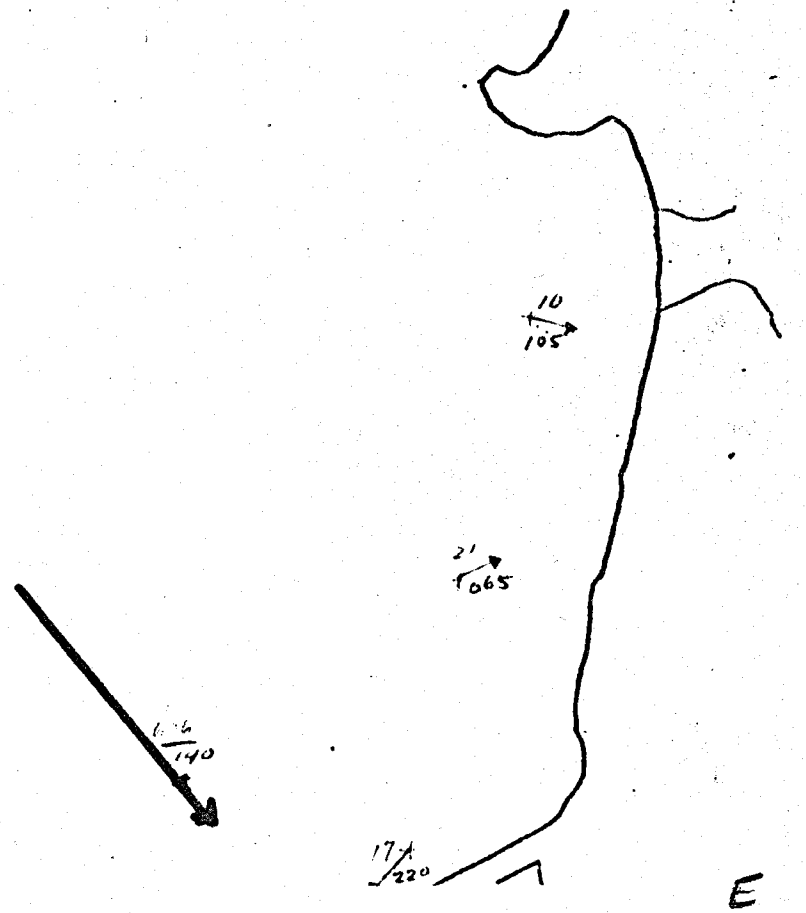

2/20/69

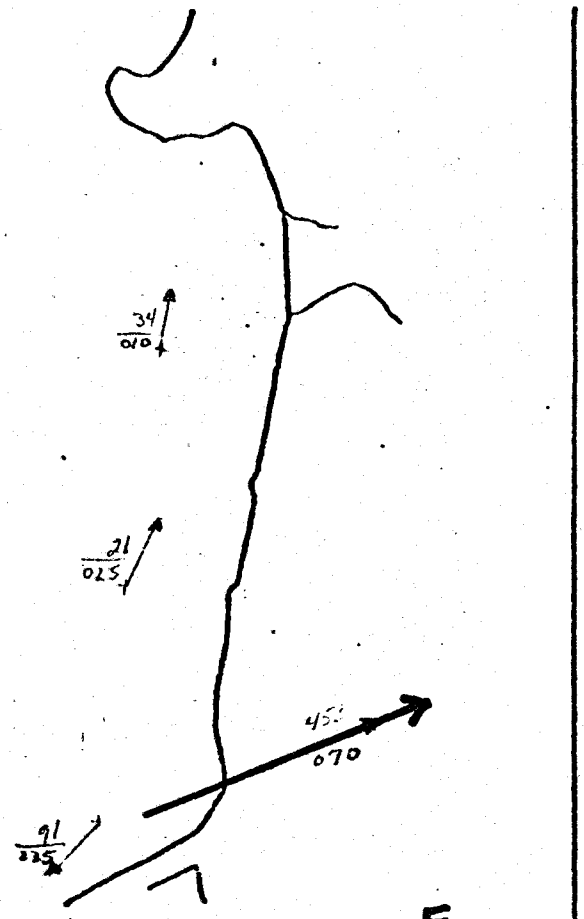

2/25/69

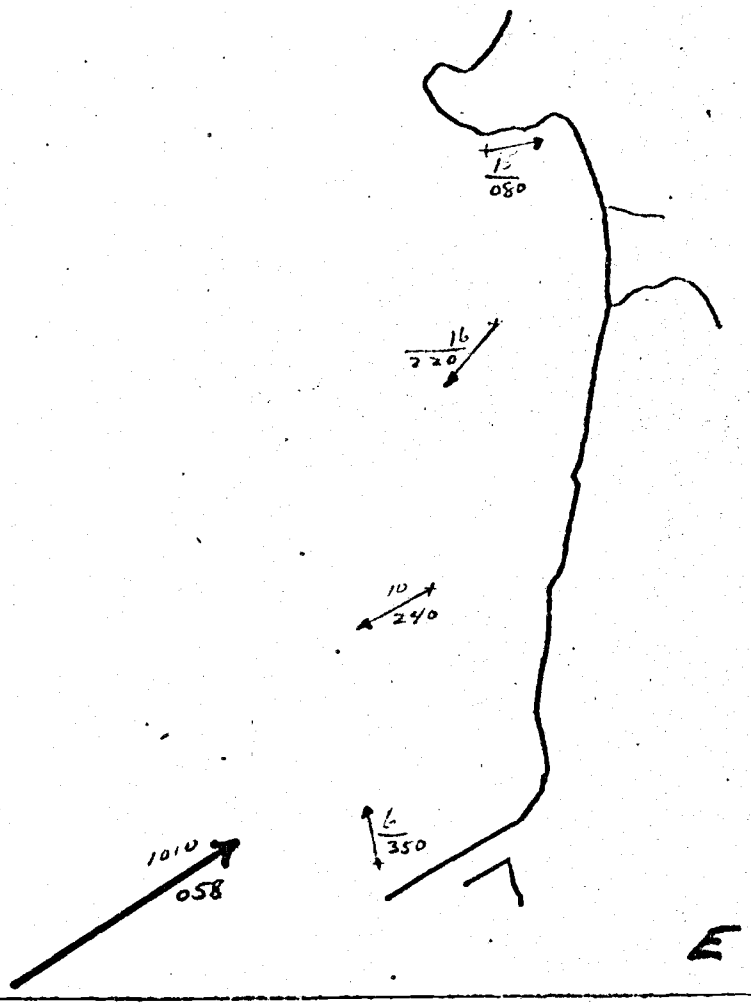

2/27/69

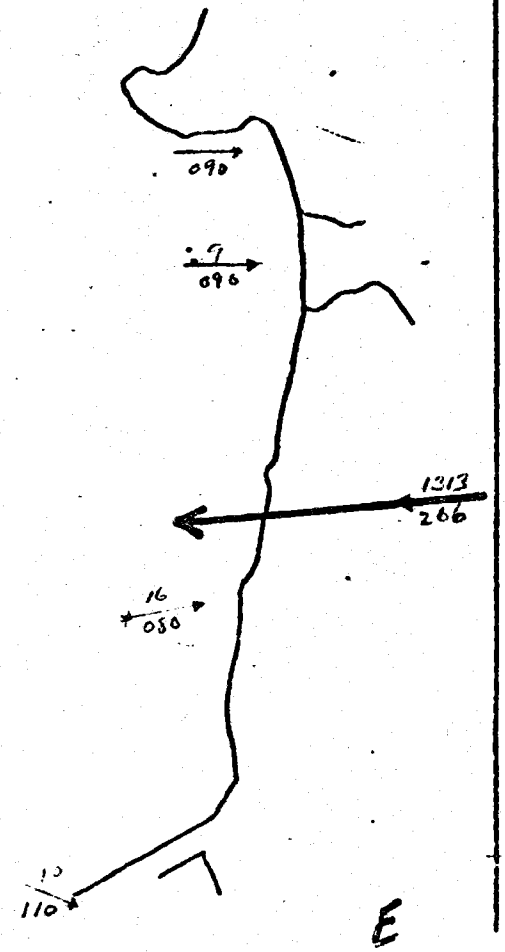

3/4/69

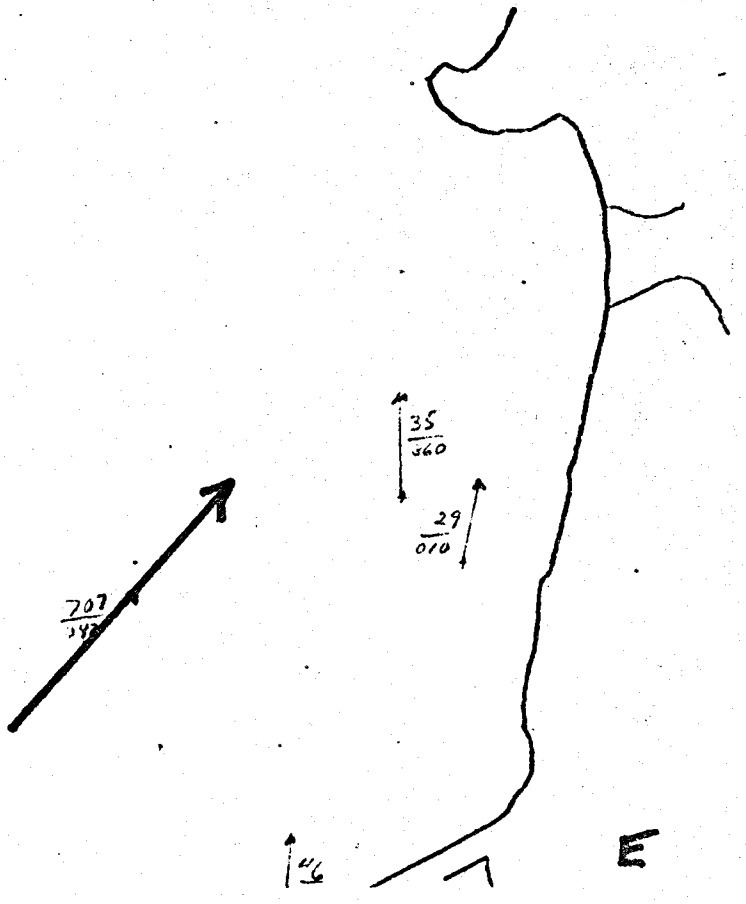

3/6/69

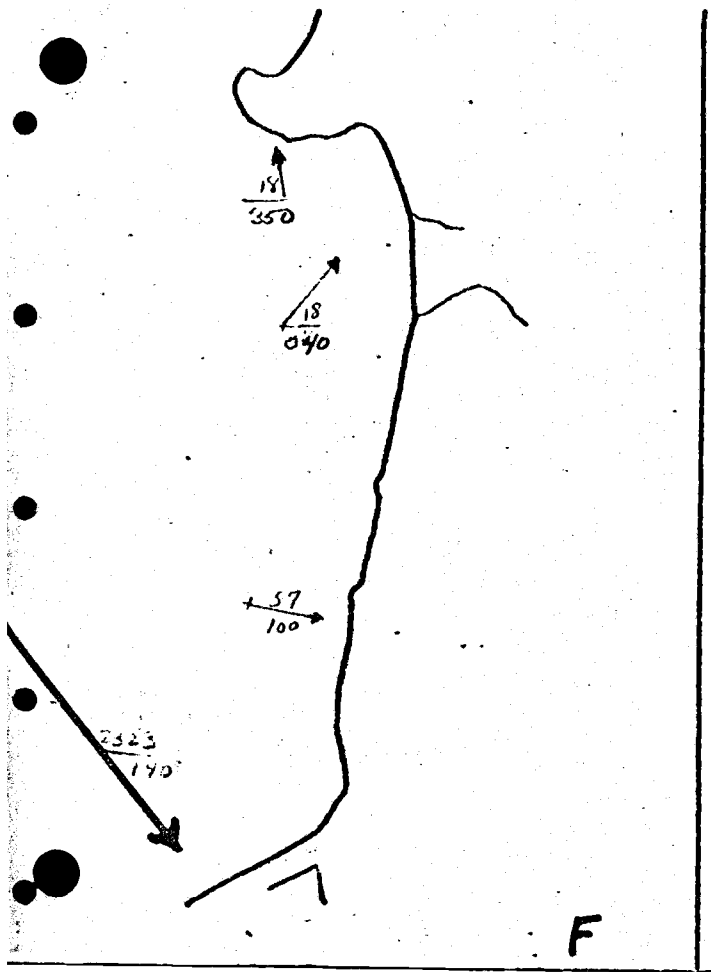

F

3/11/69

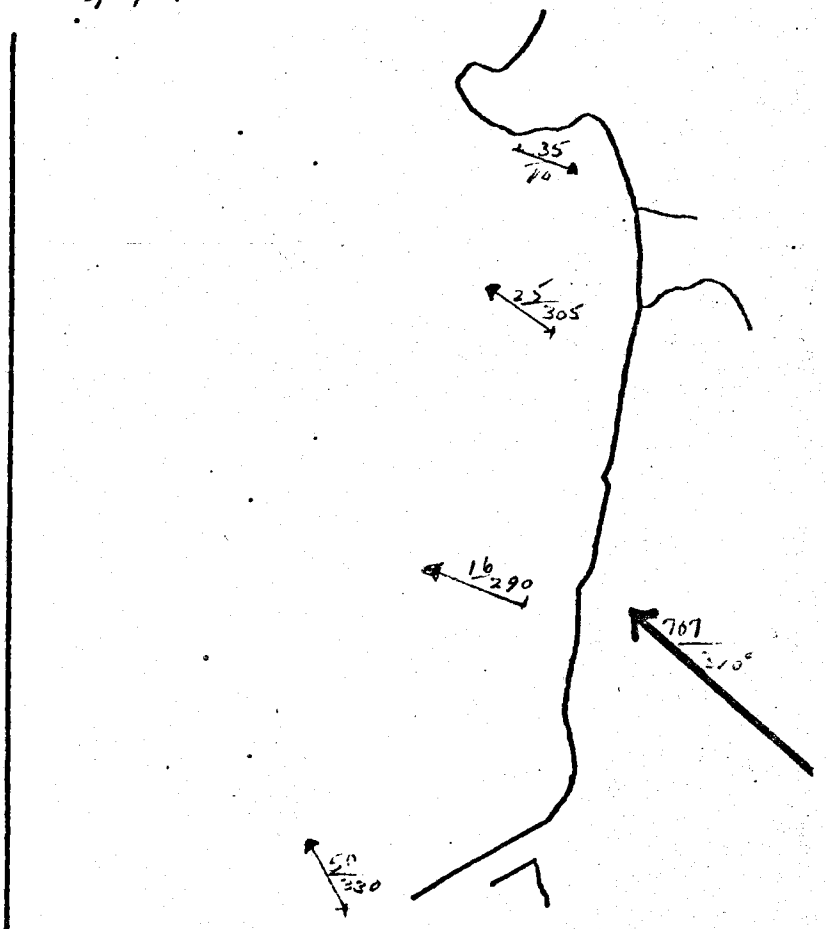

E

3/13/69

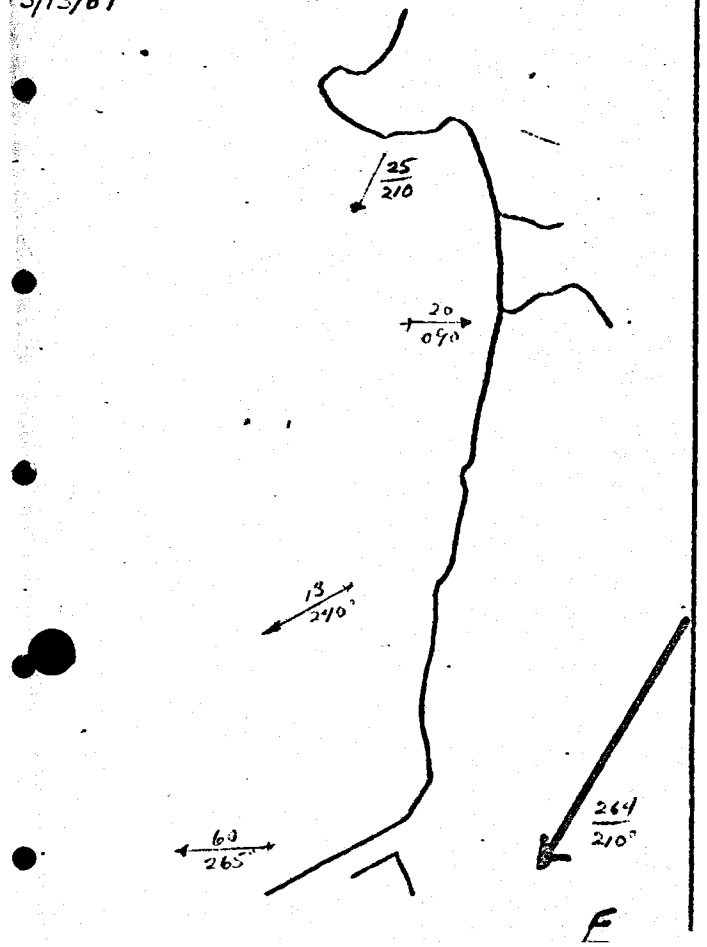

F

3/18/69

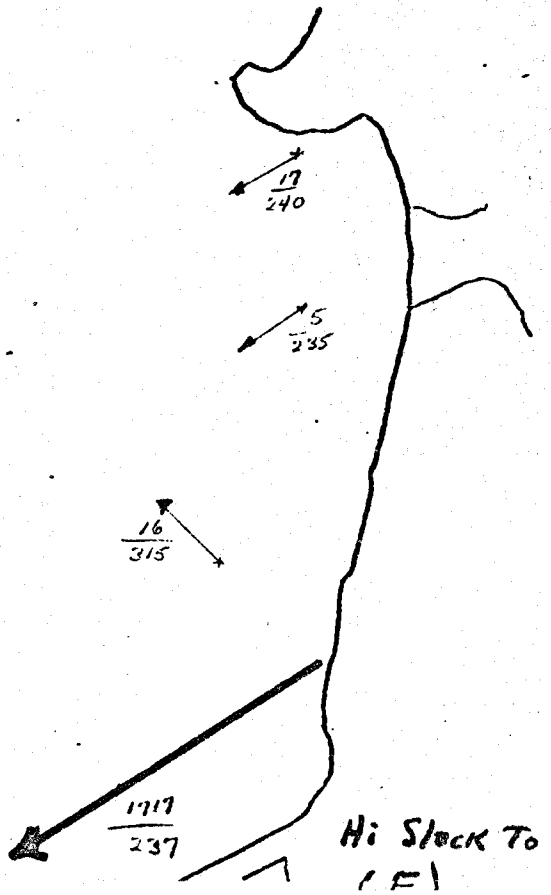

Hi Stock To
(F)

24/69

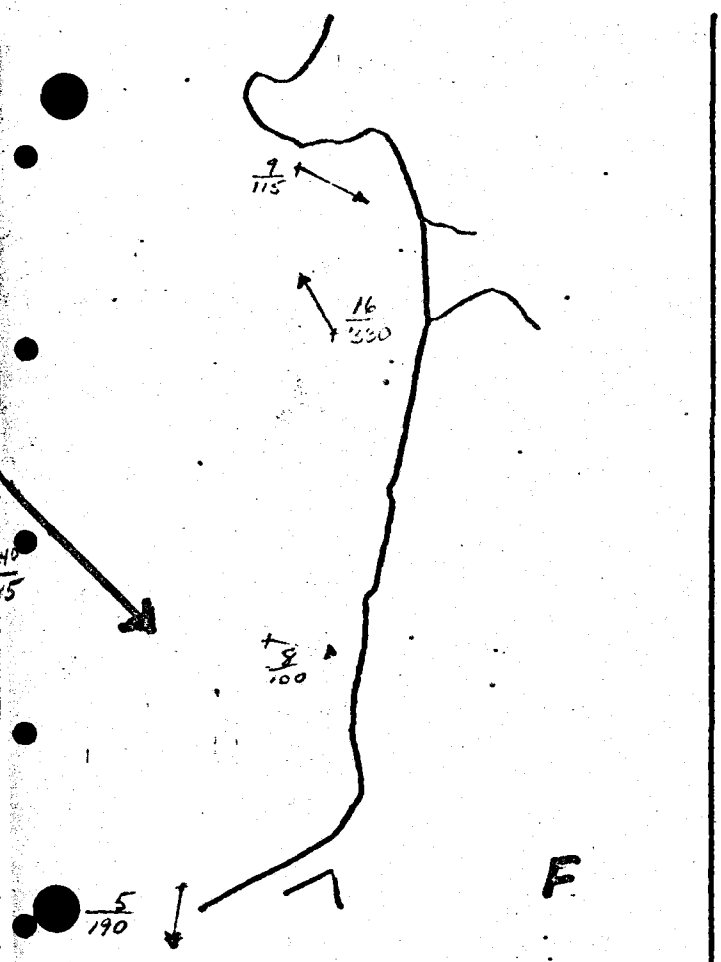

3/24/69 (AM)

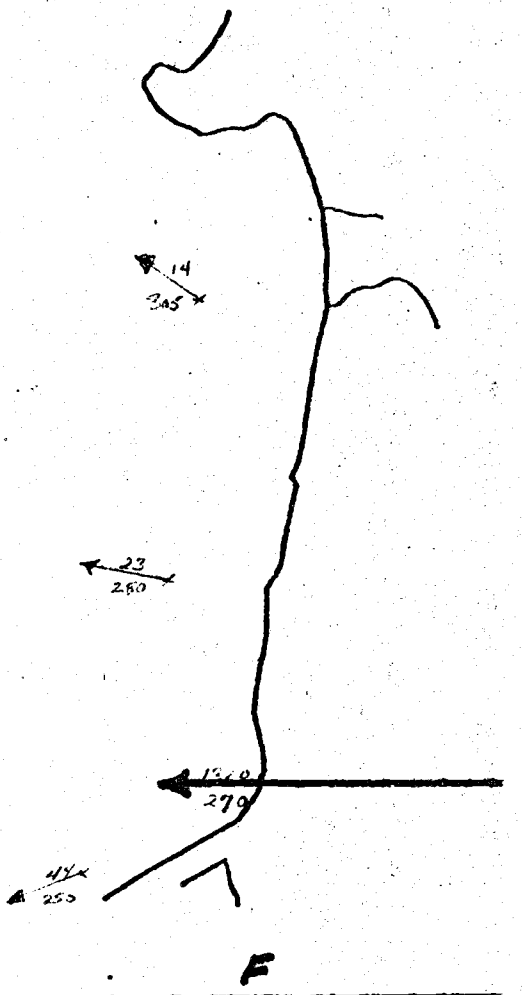

24/69 (PM)

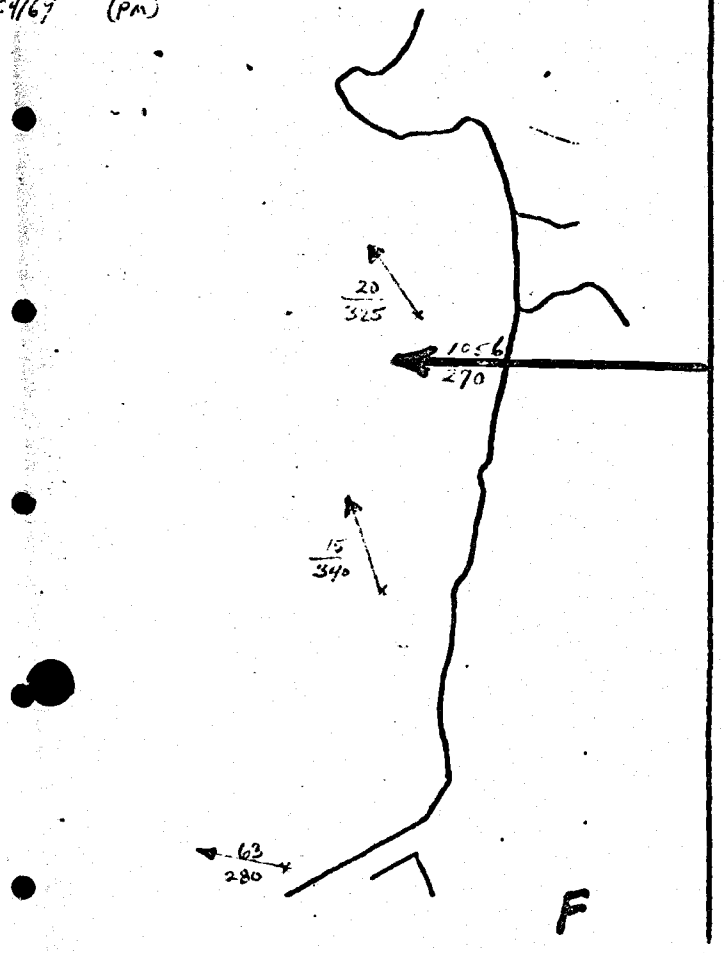

3/25/69

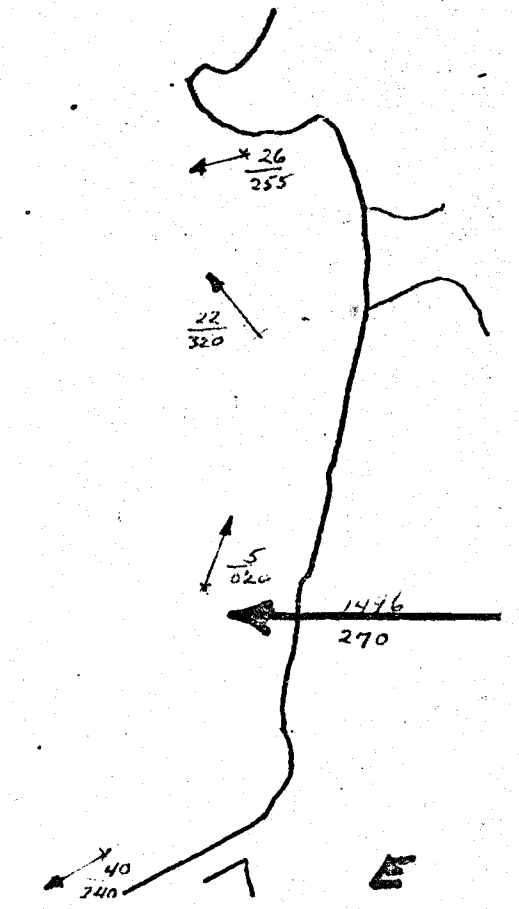

1/69

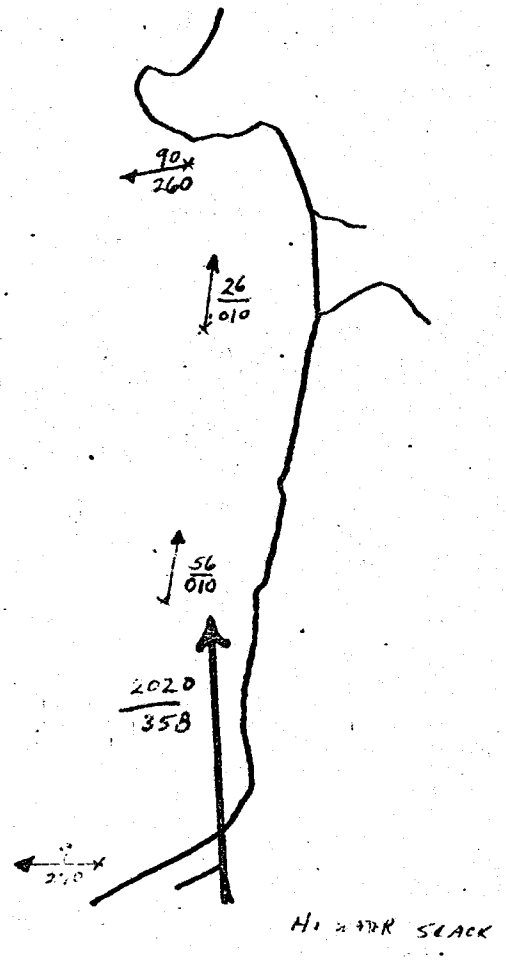

4/3/69

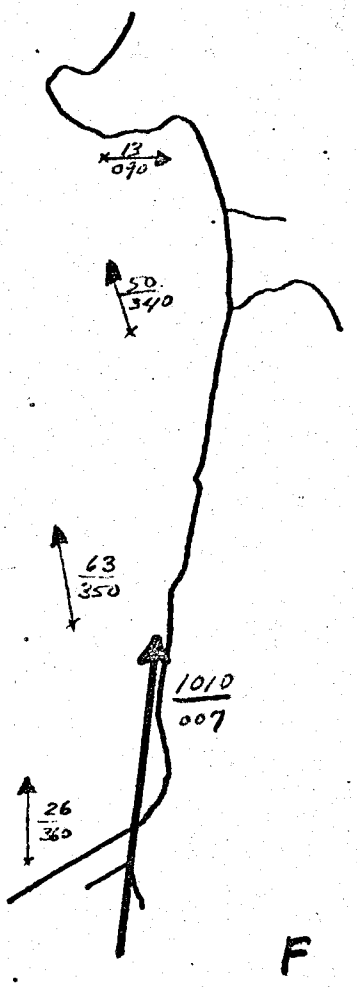

4/7/69

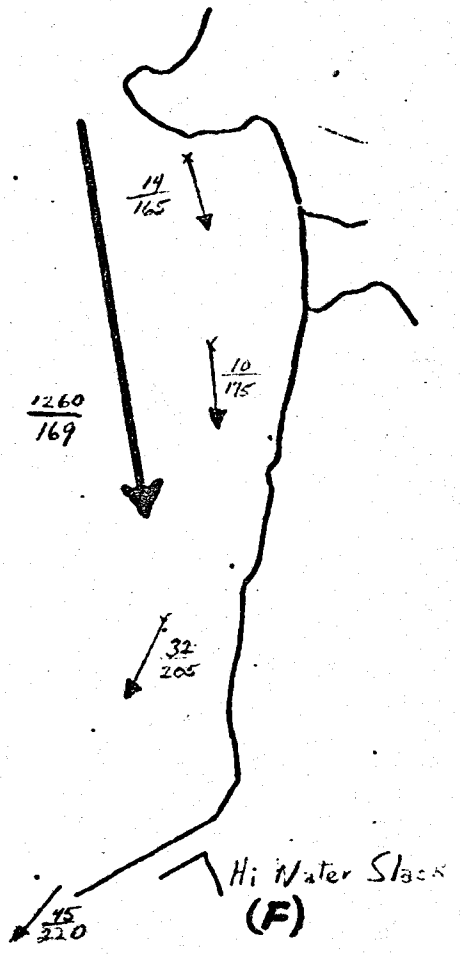

4/8/69

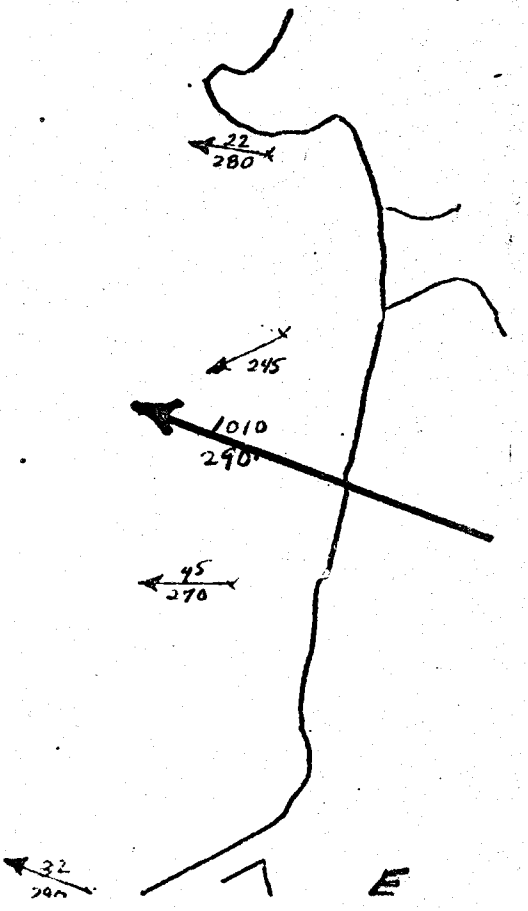

4/10/69

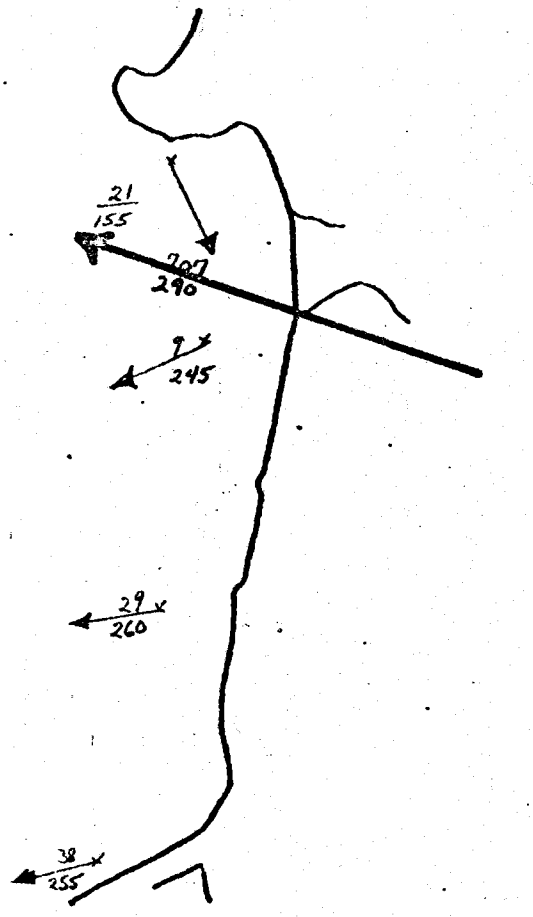

4/17/69

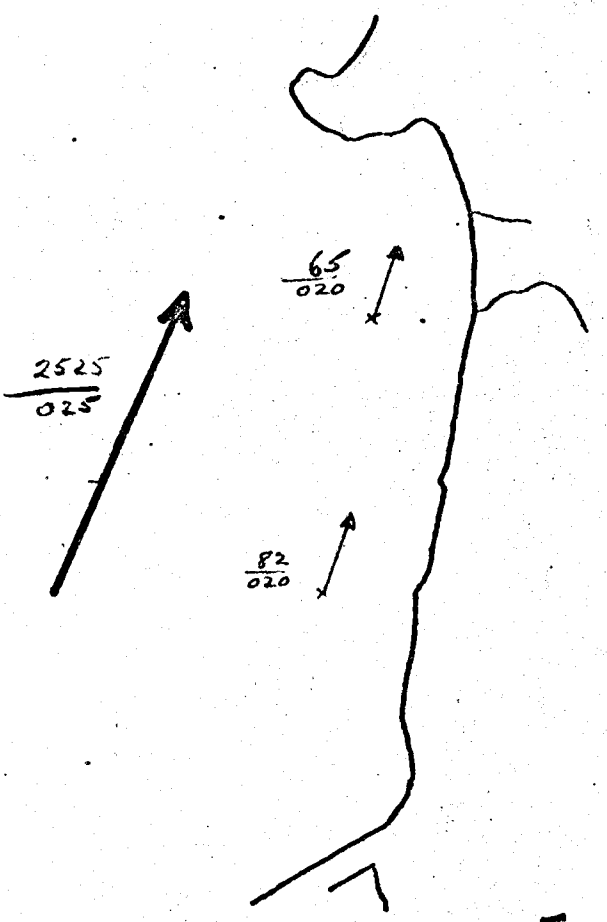

:2/69

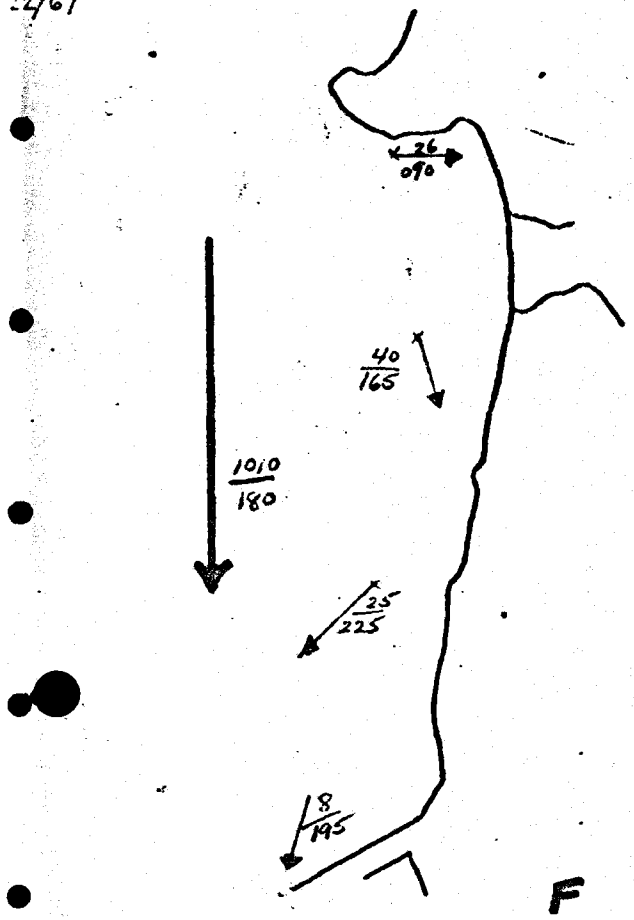

4/24/69

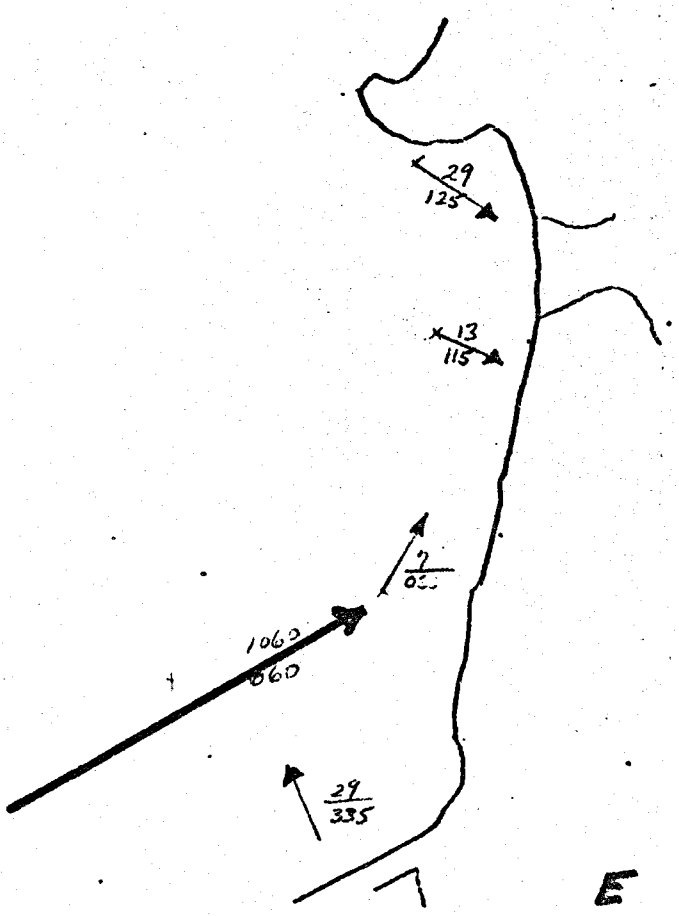

29/69

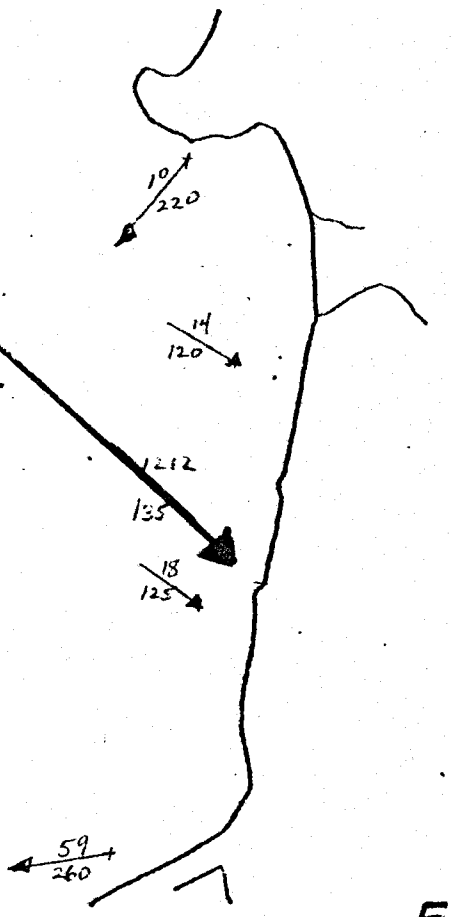

F (H. water)
Slick

5/1/69

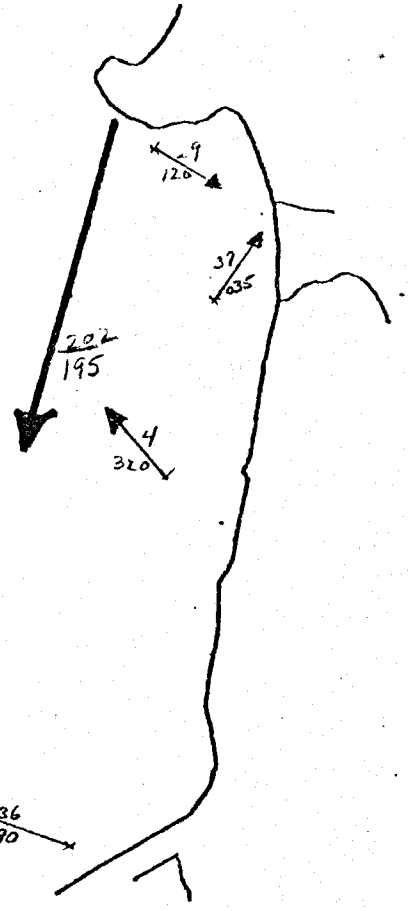

F

5/5/69

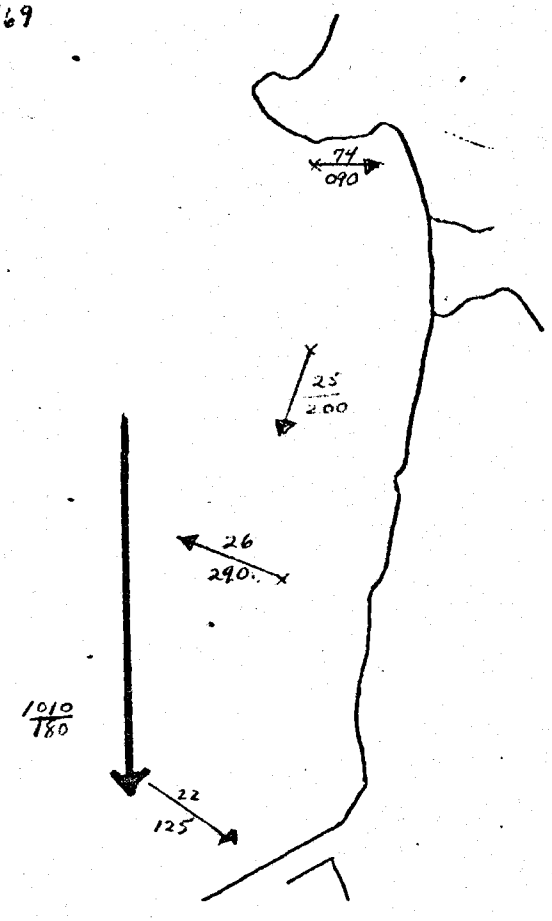

5/8/69

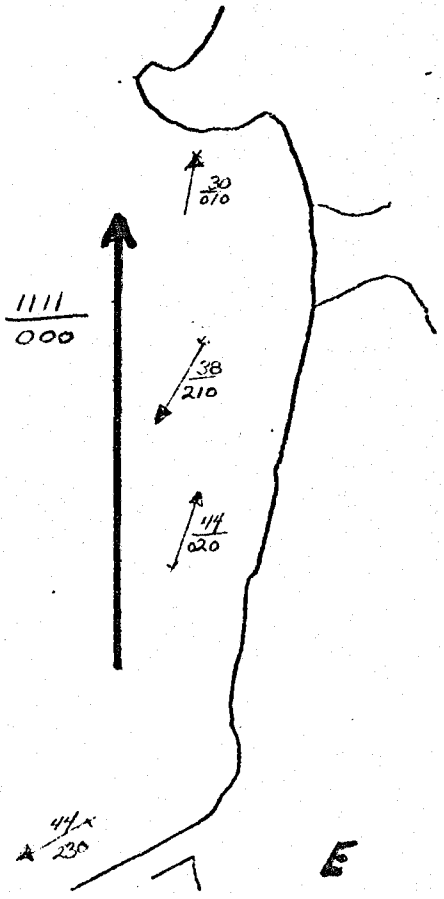

E

5/12/69

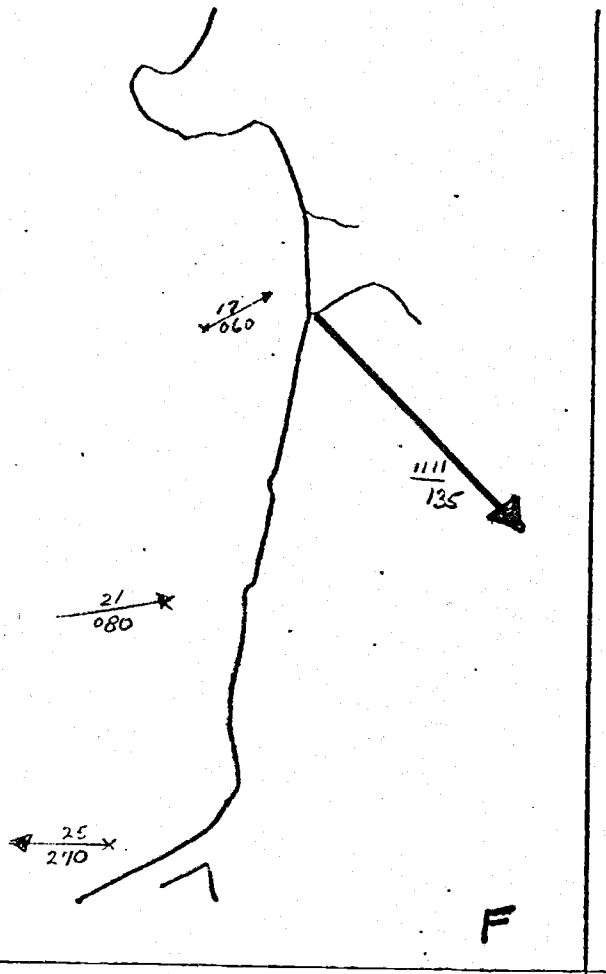

5/13/69

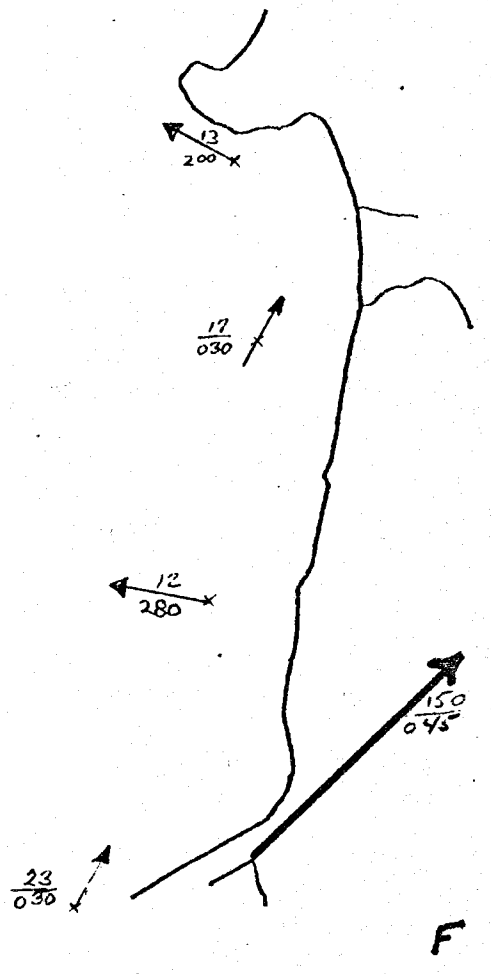

5/16/69

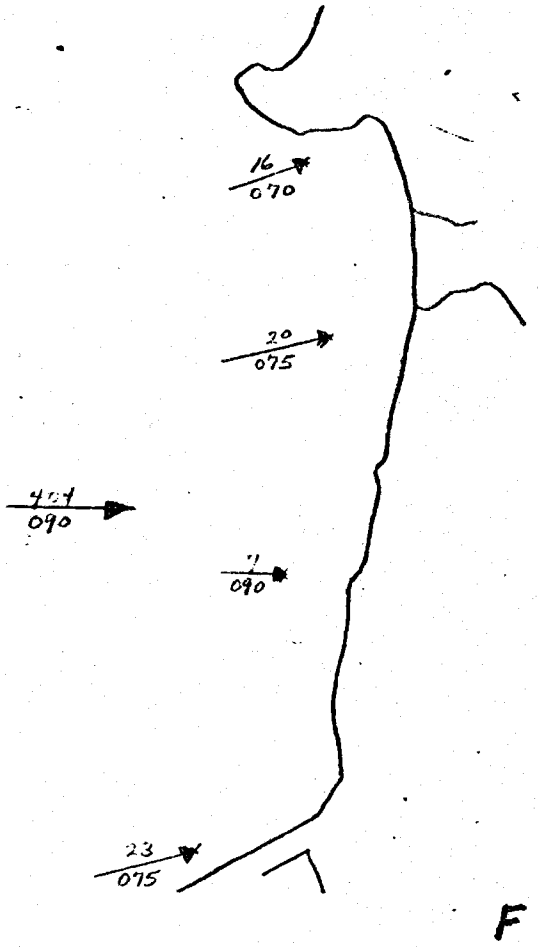

5/24/69

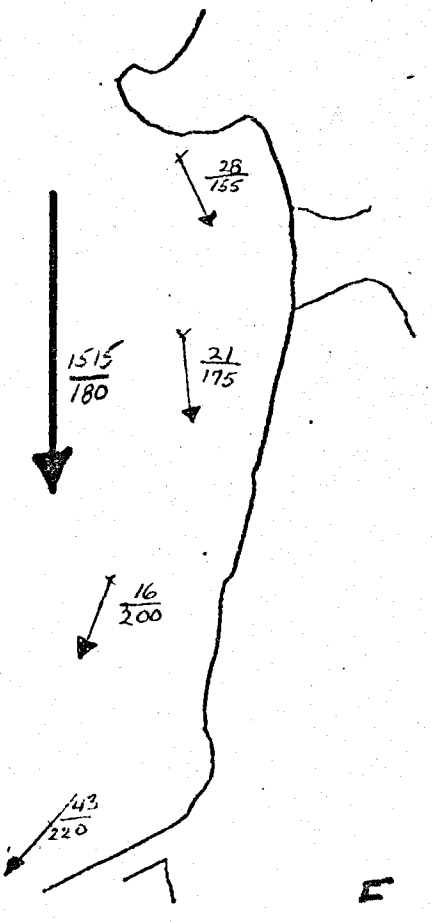

6/3/69

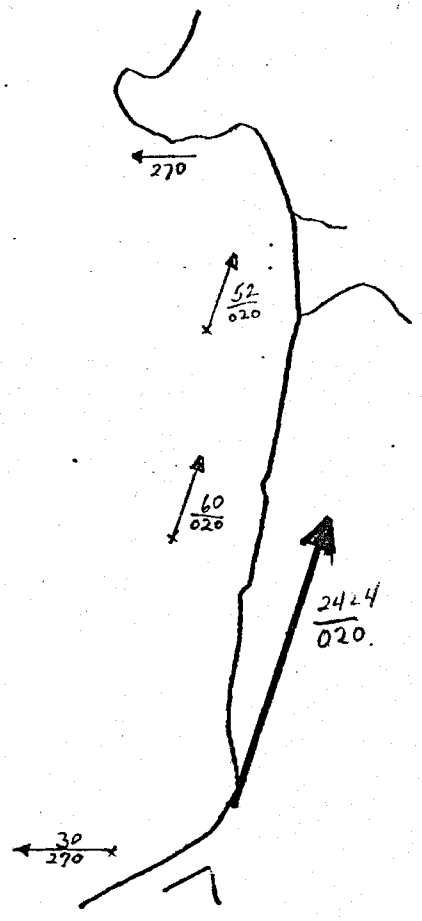

E

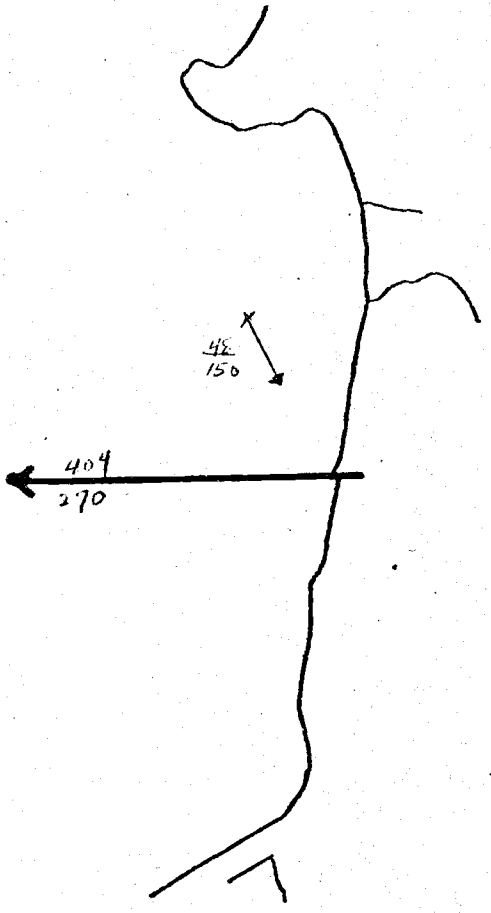

F

7/69 (AM)

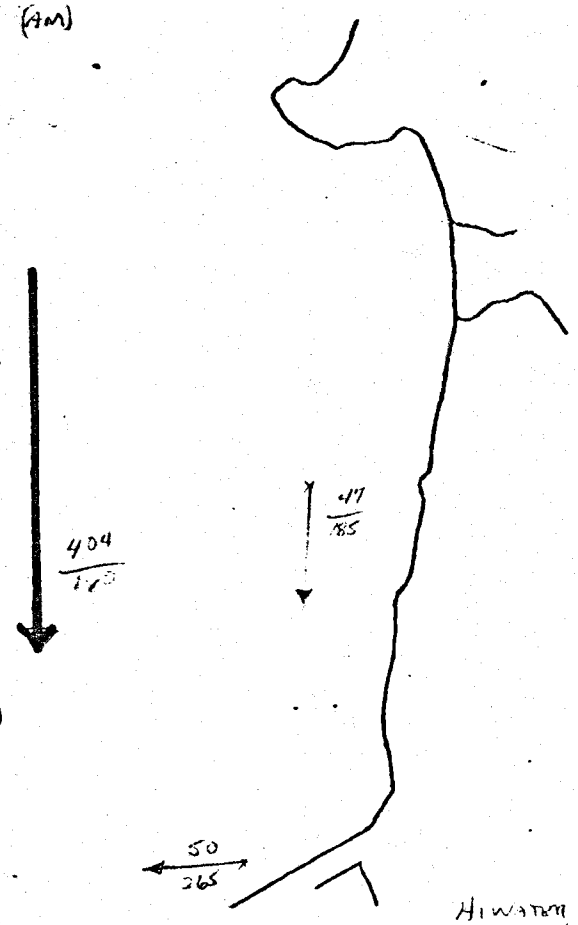

HIWATER SLACK (E)

6/5/69 PM

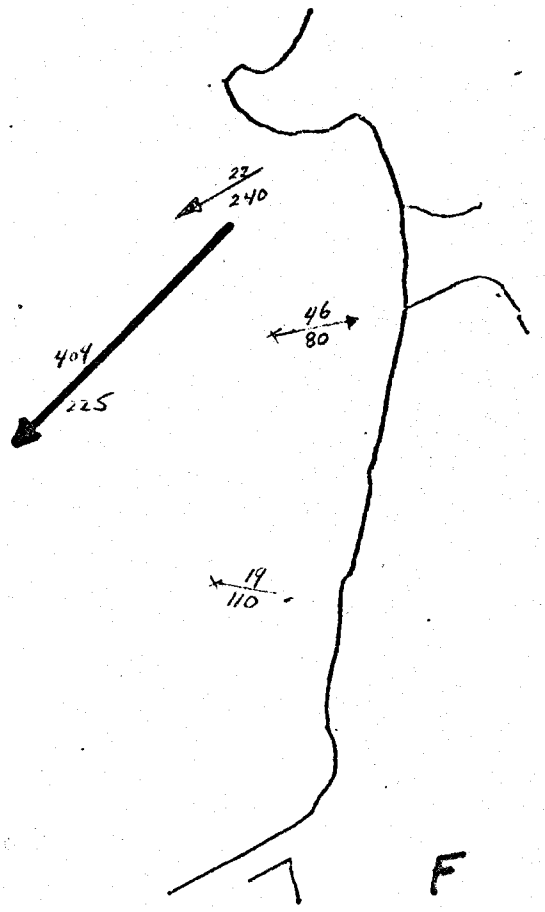

F

1/10/69

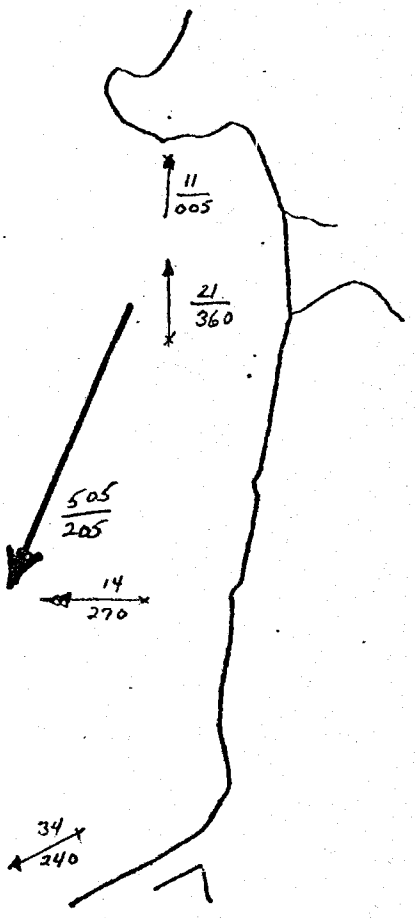

6/13/69 (AM)

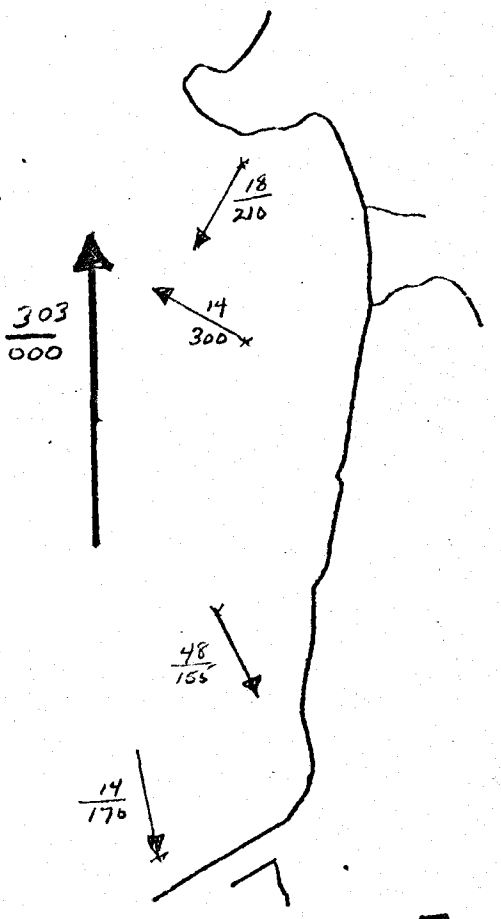

6/13/69 (PM)

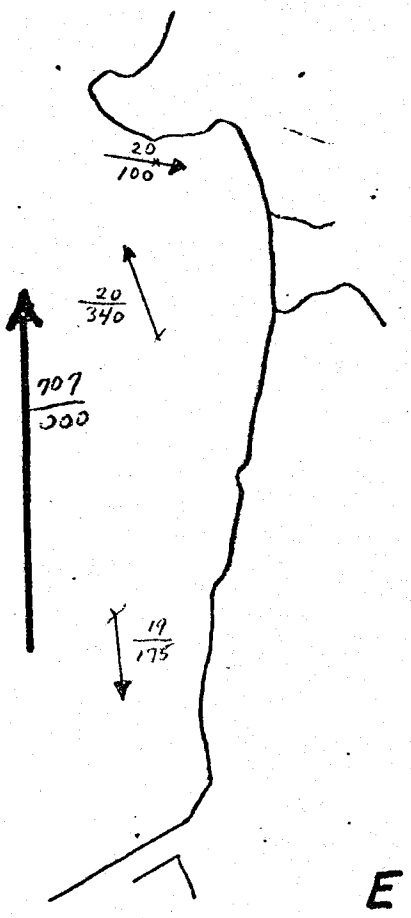

6/14/69

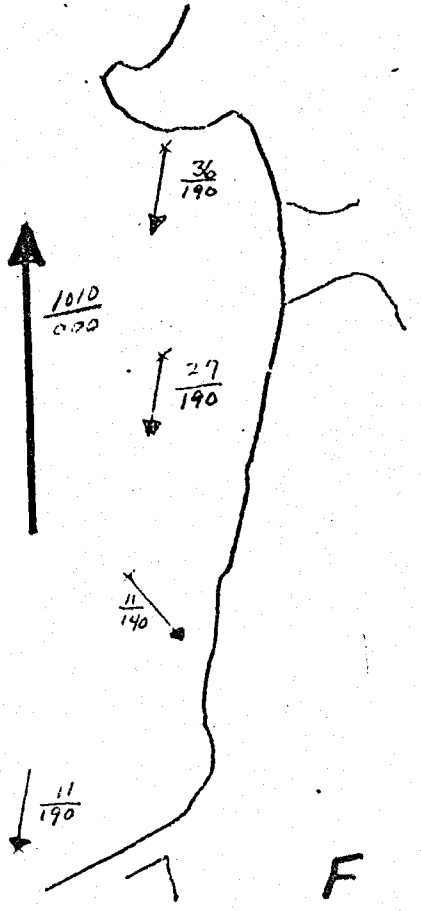

6/18/69

6/19/69.

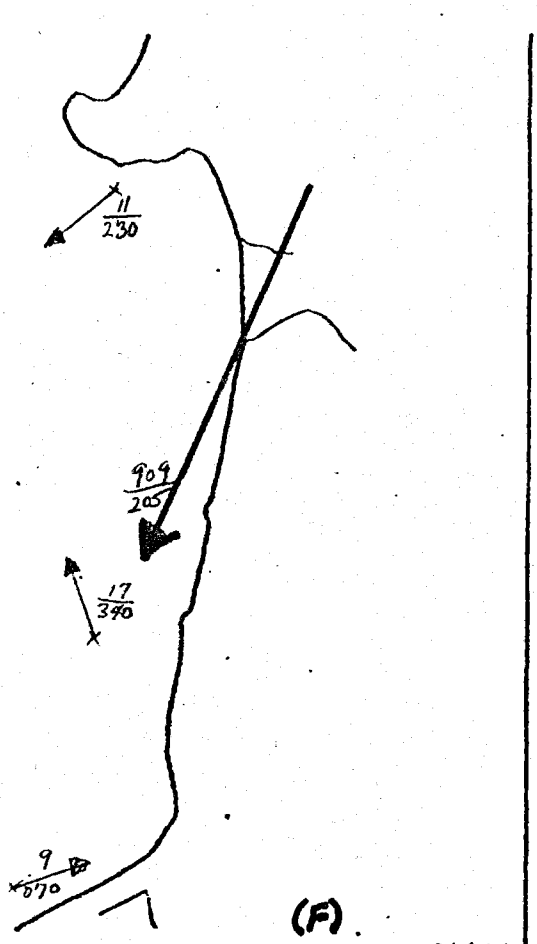

(F)

NEAR HI WATER SLACK

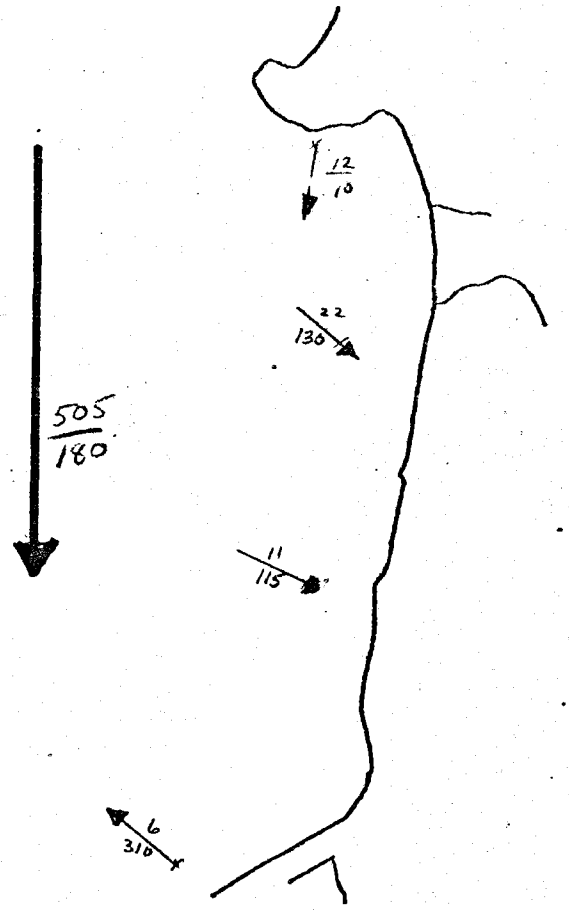

LO WATER SLACK

6/25/69 (AM)

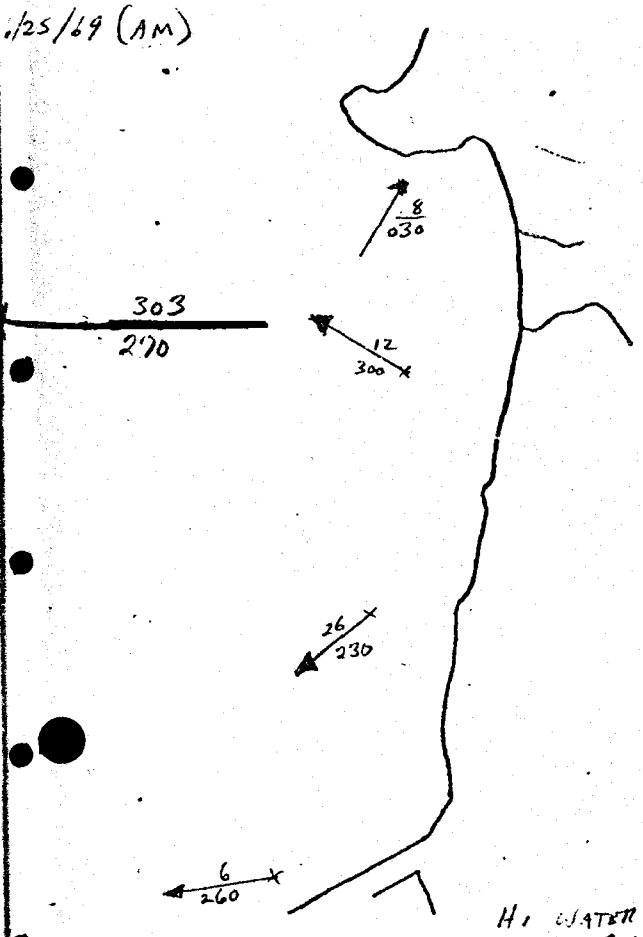

HI WATER SLACK

(E)

6/25/69 (PM)

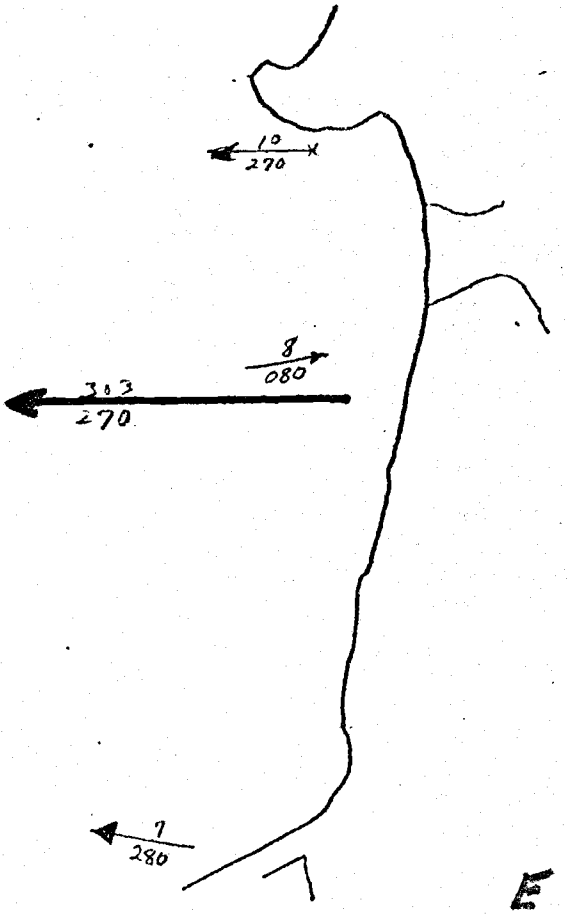

E

6/30/69 (AM)

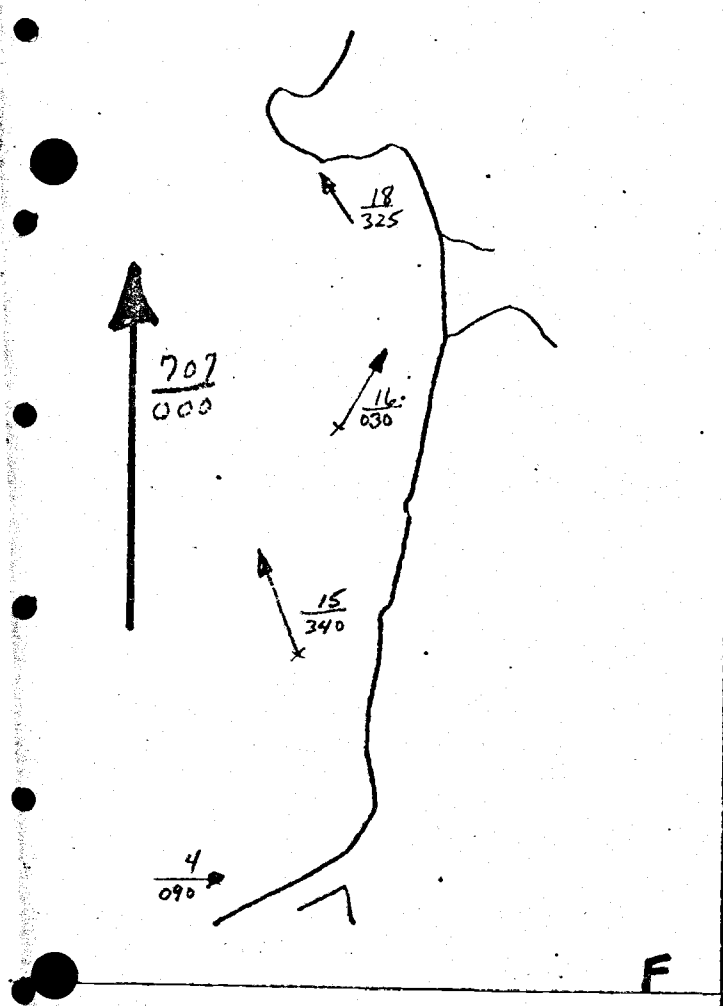

6/30/69 (PM)

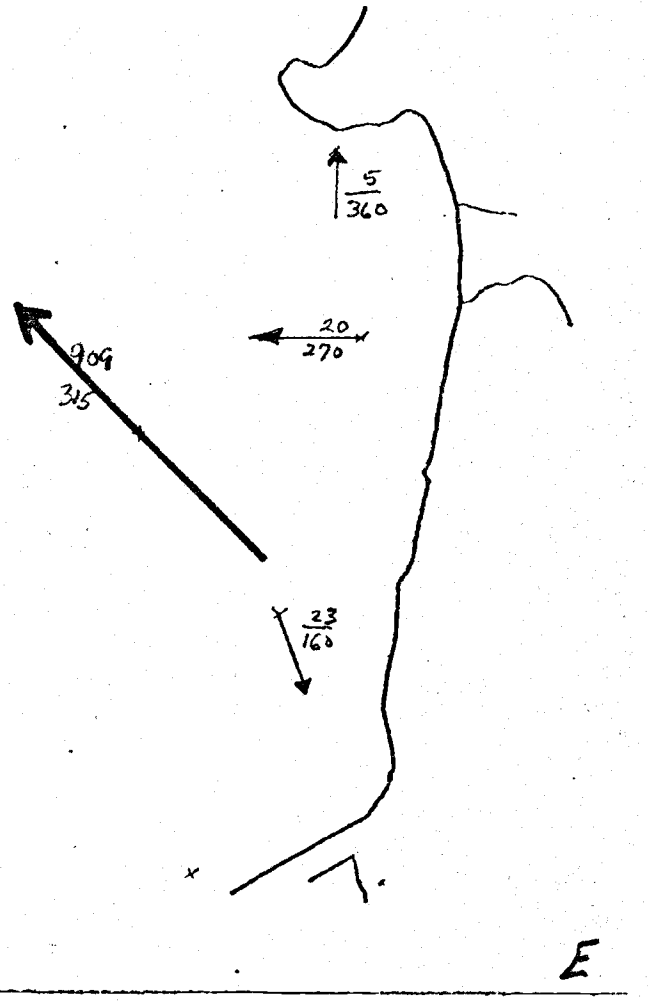

7/1/69 (AM)

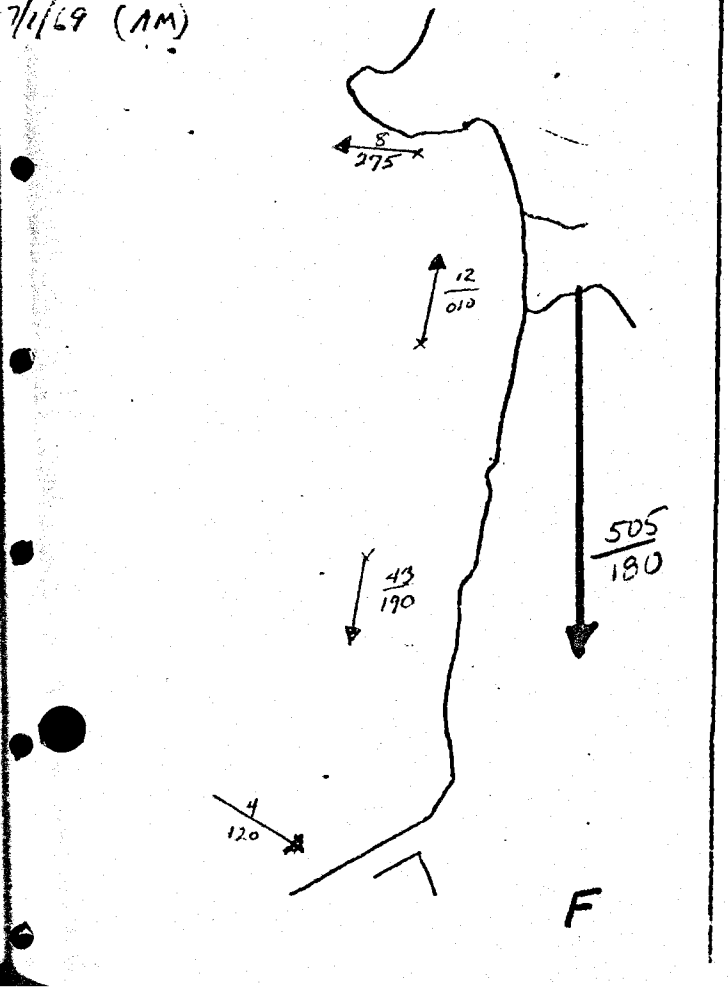

7/1/69 (PM)

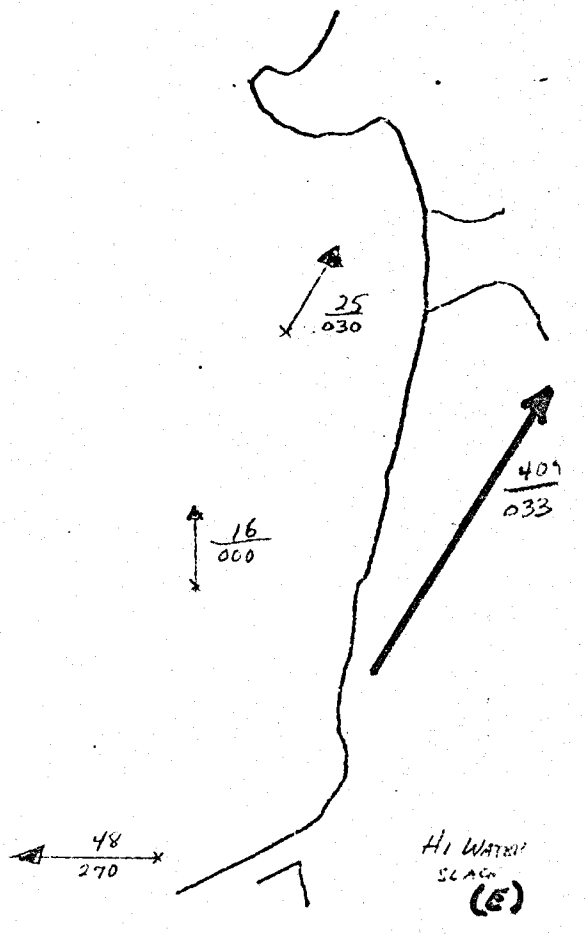

7/7/69 (AM)

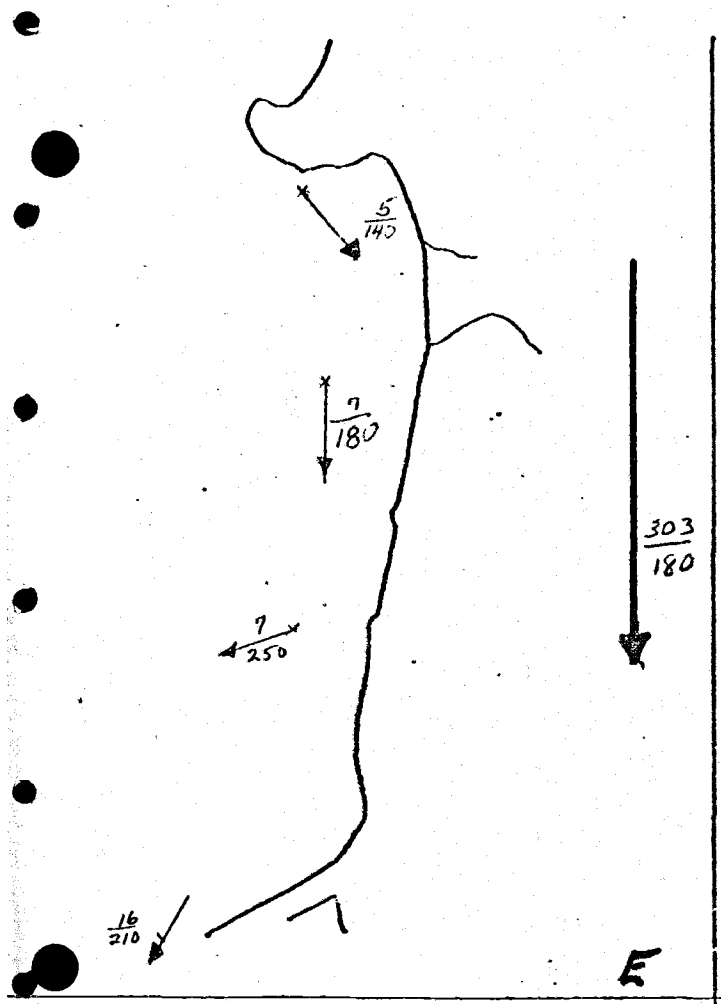

7/7/69 (PM)

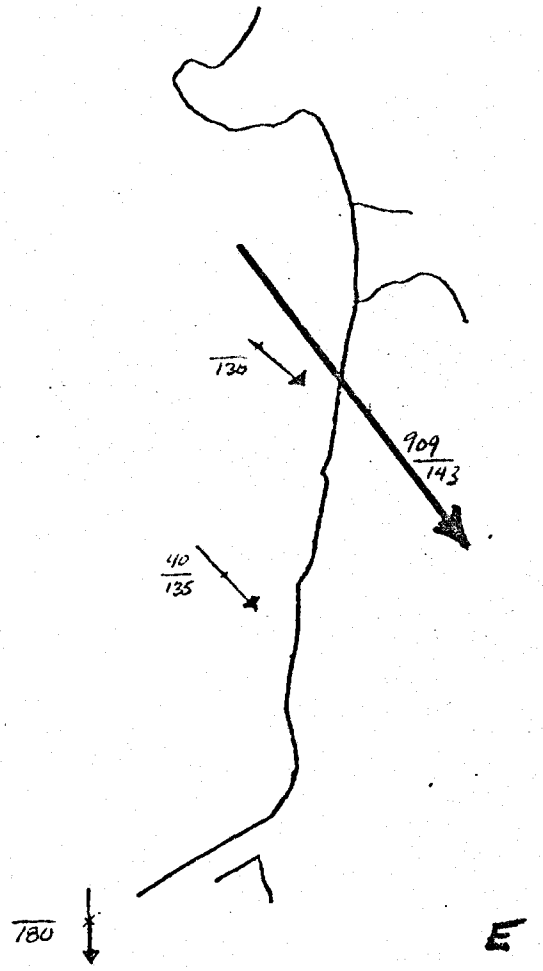

7/8/69 (AM)

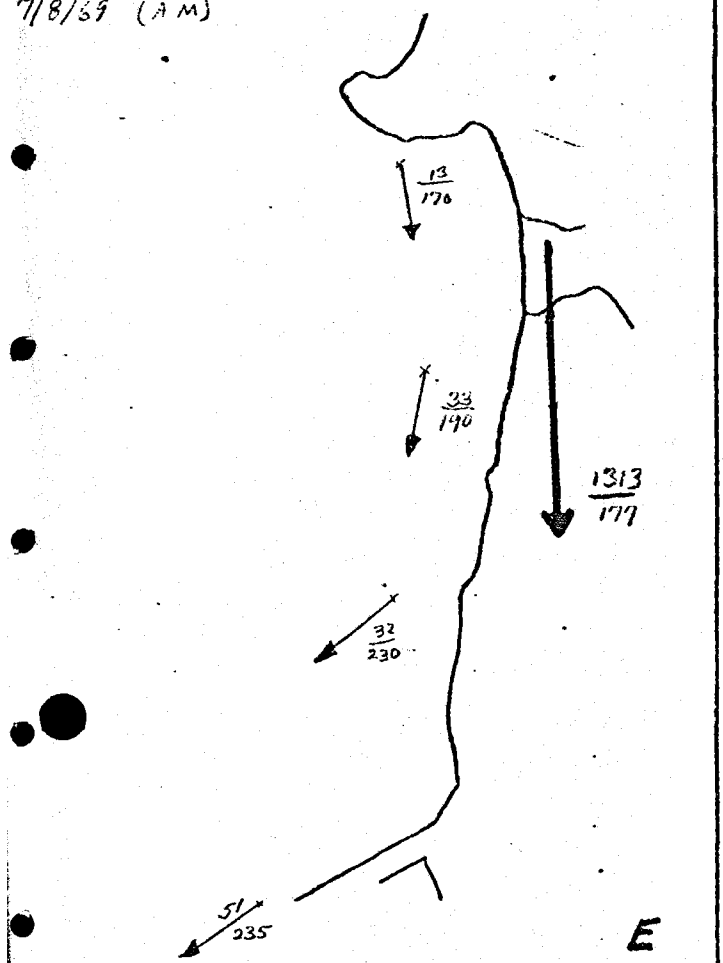

7/8/69 (PM)

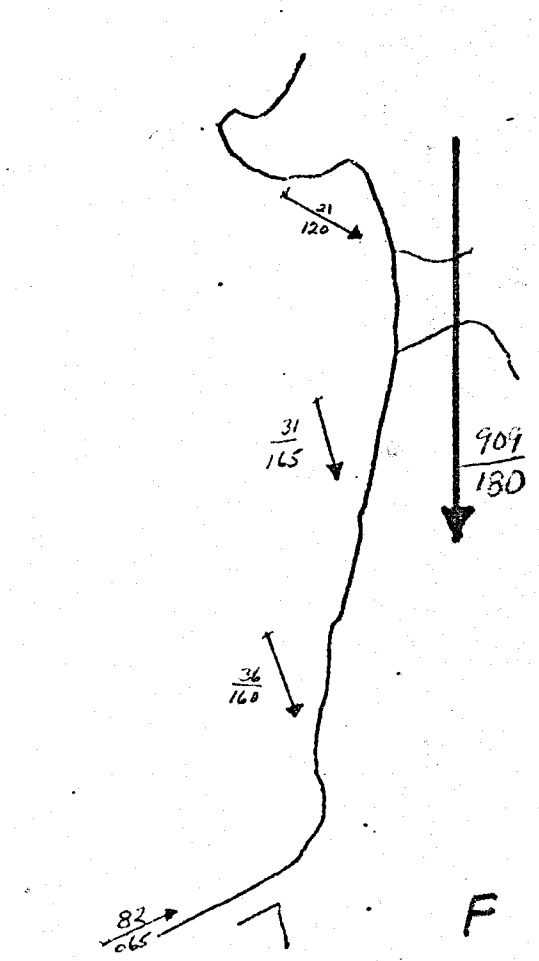

7/14-9 (AM)

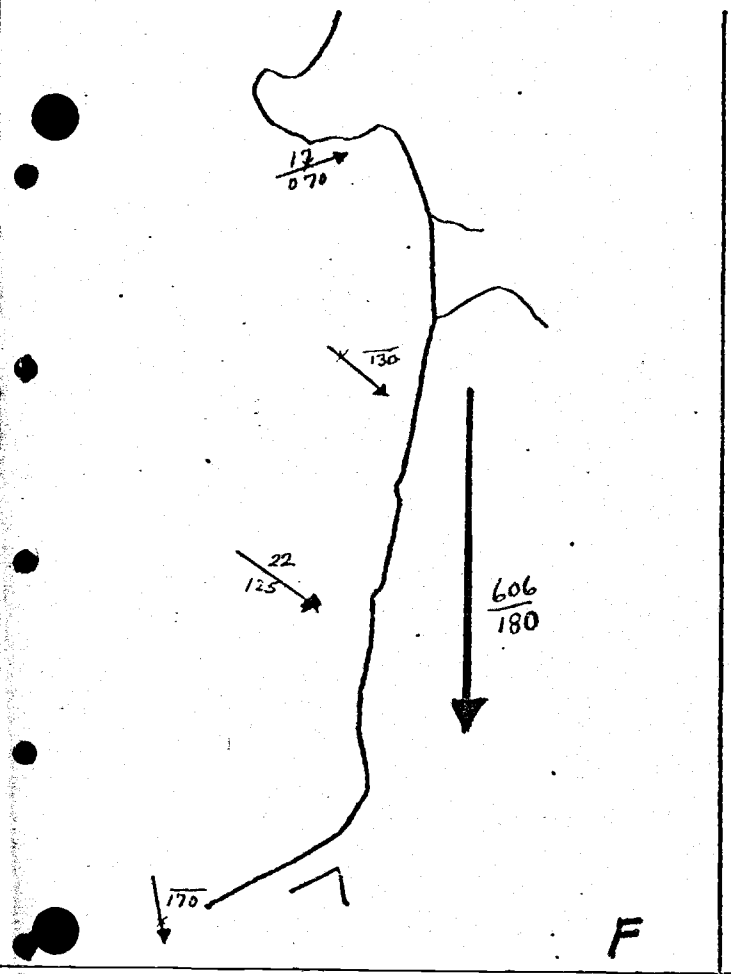

7/14/69 (PM)

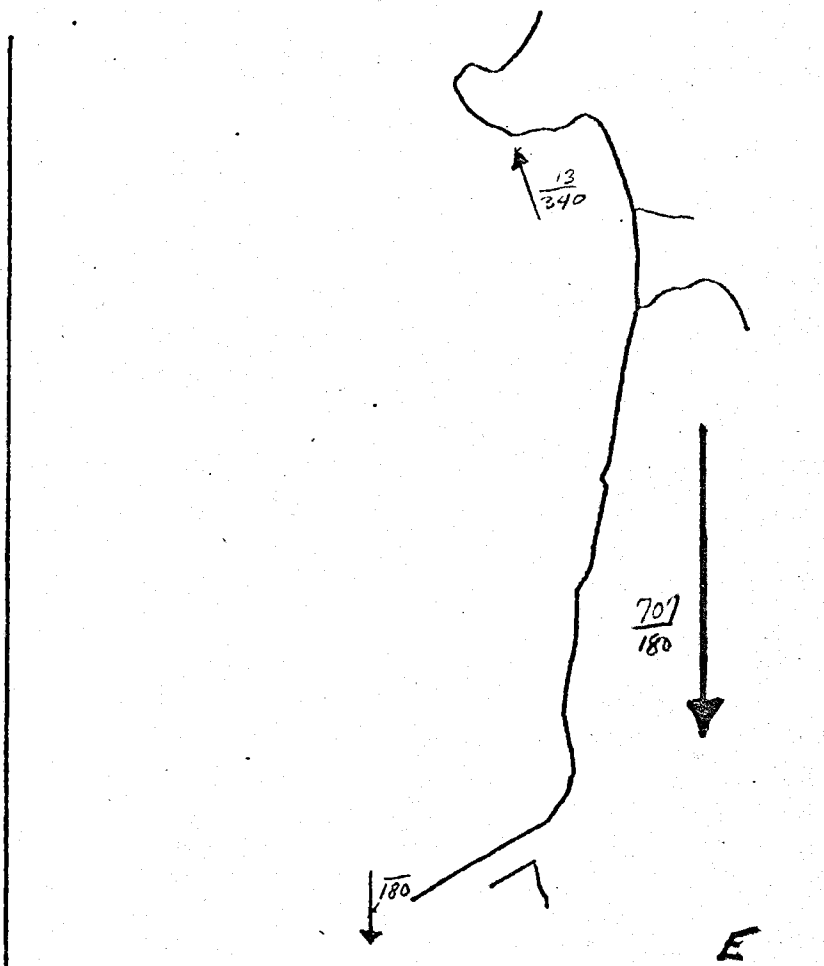

/69

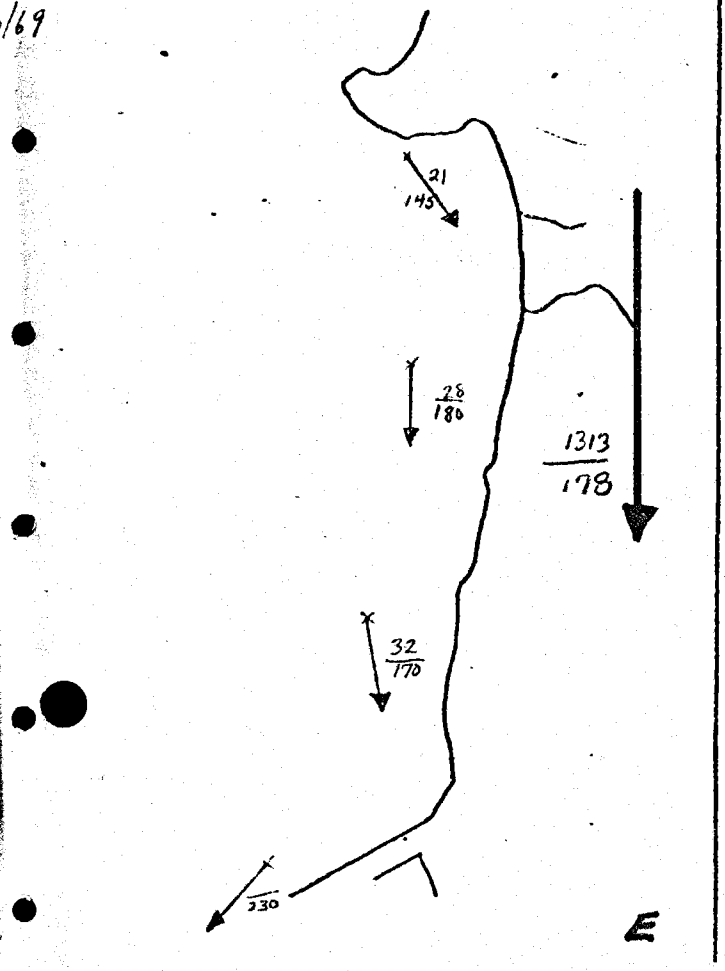

7/18/69

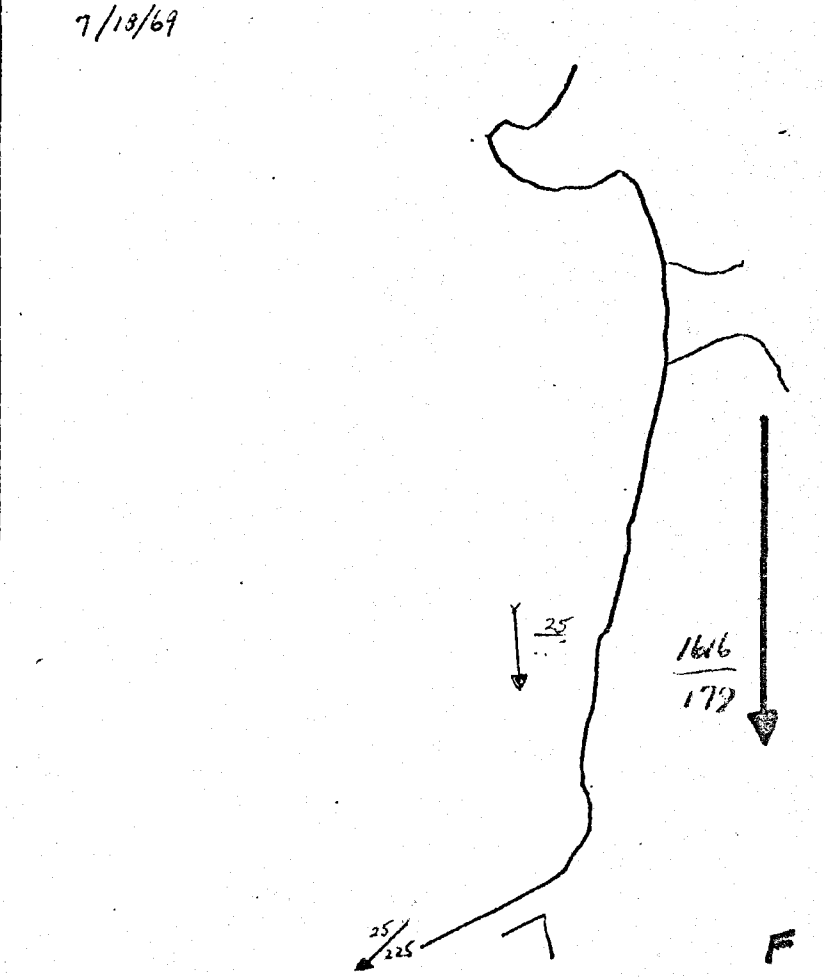

7/21/69

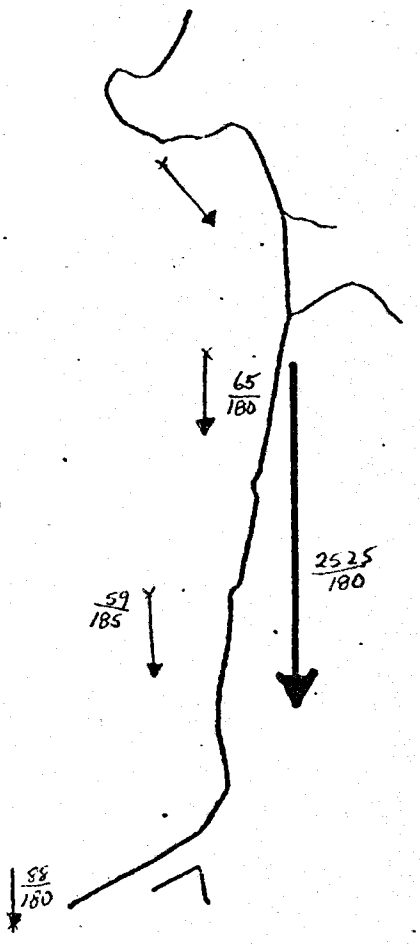

7/22/69

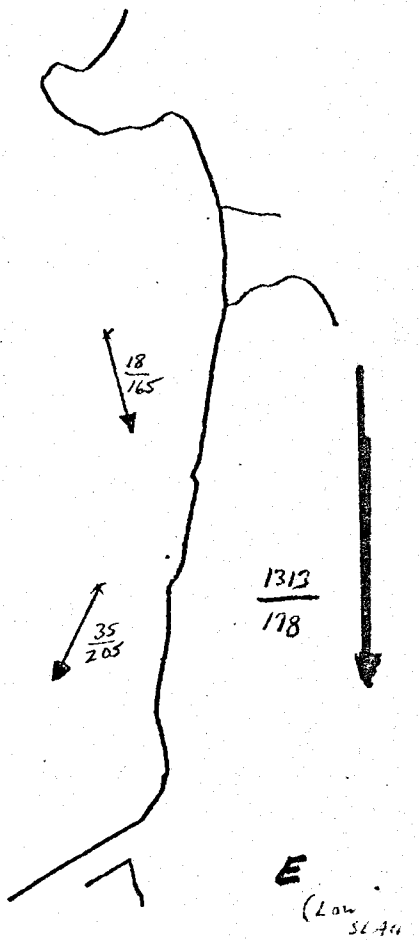

7/23/69

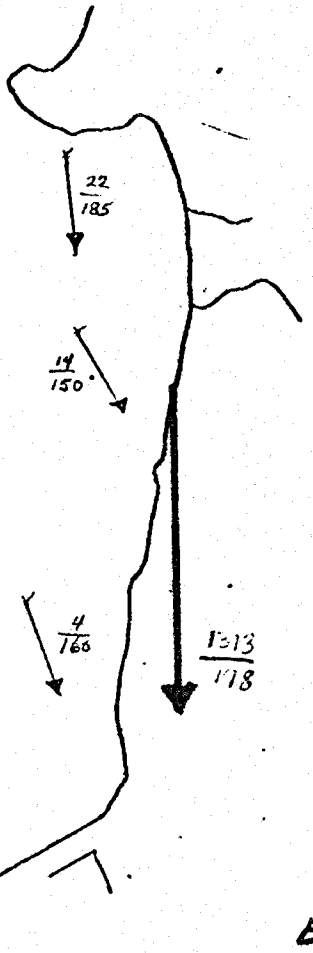

7/28/69 (AM)

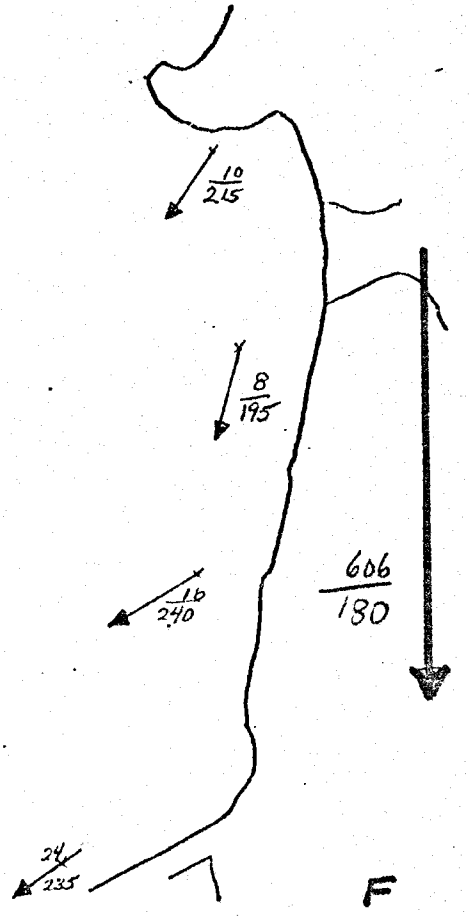

7/28/69 (PM)

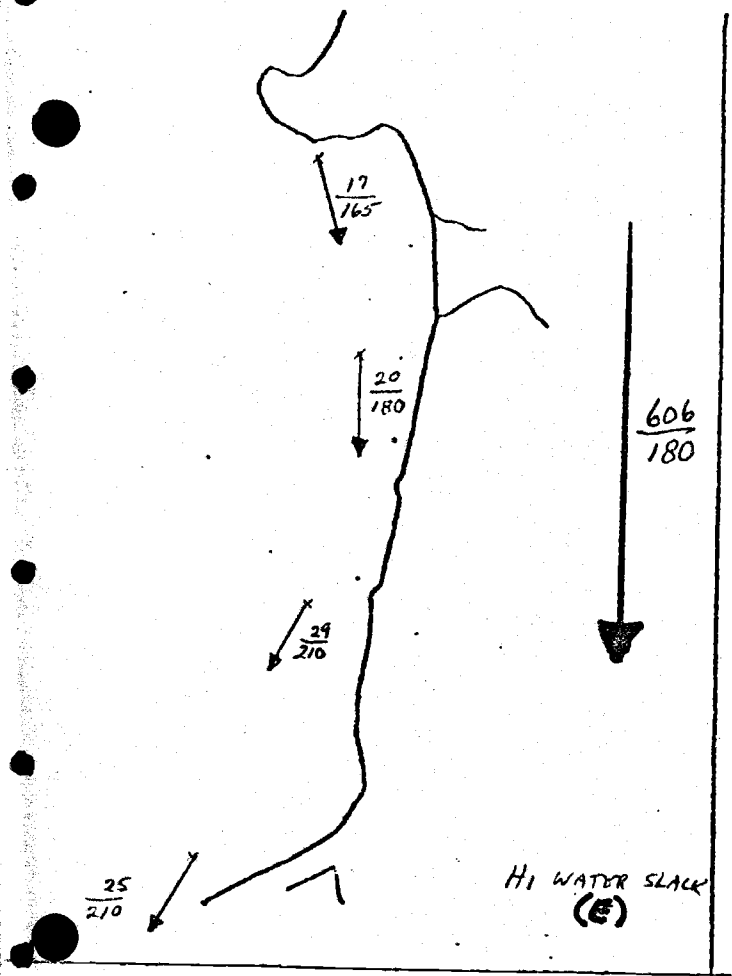

7/29/69

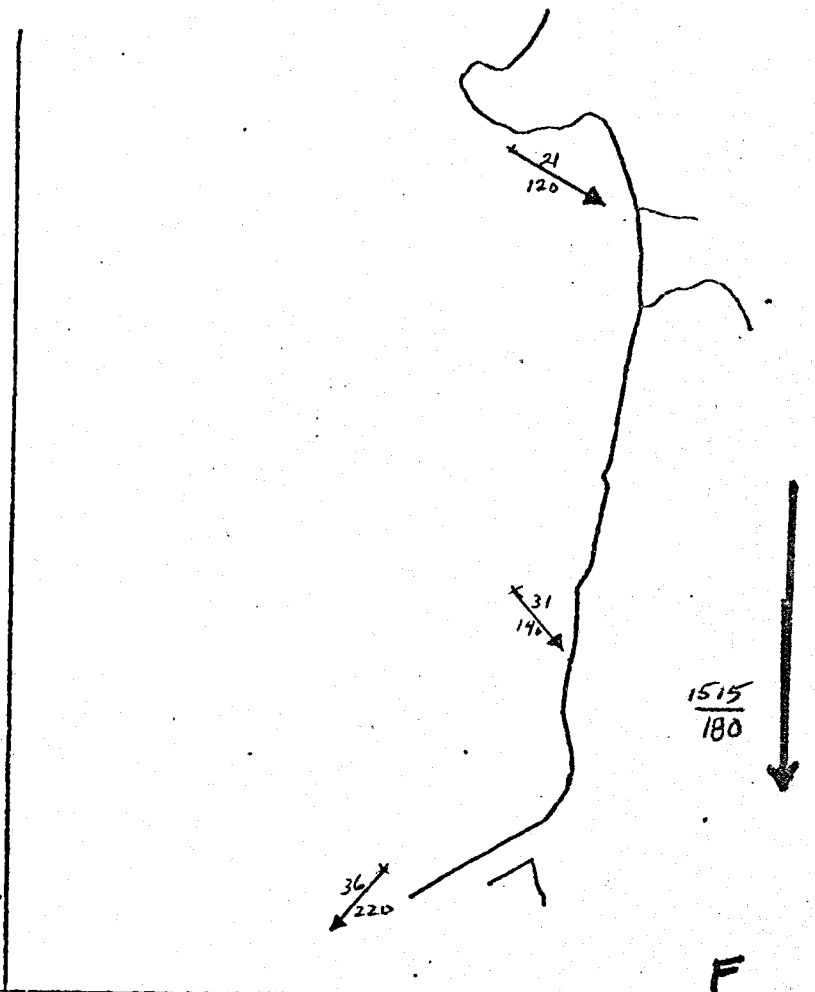

/69

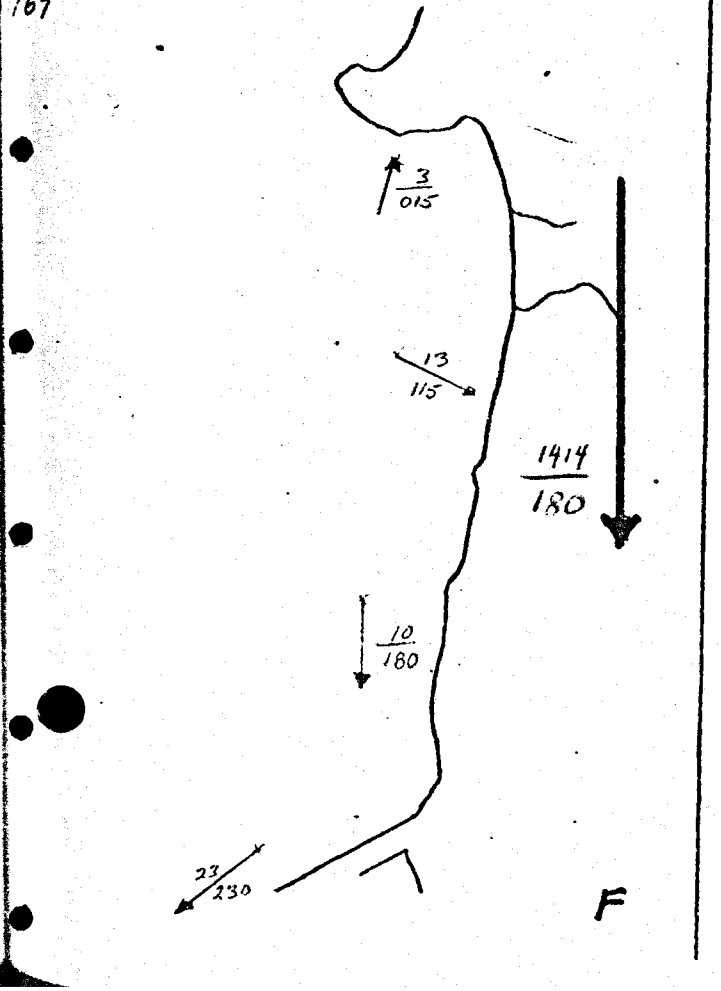

8/4/69

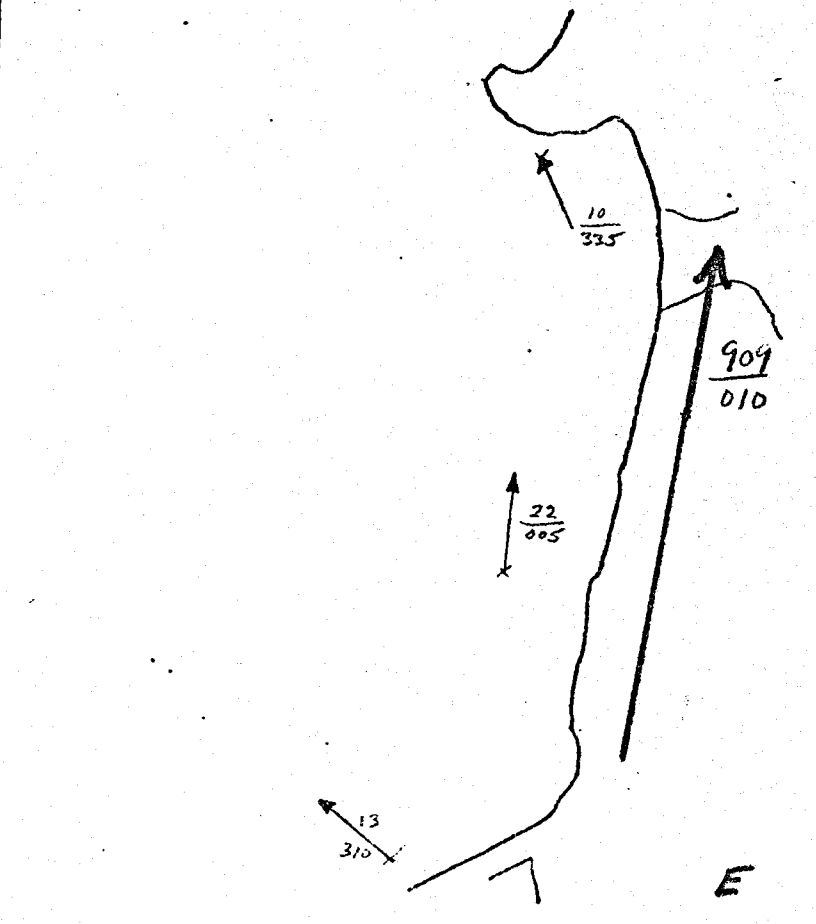

8/5/69

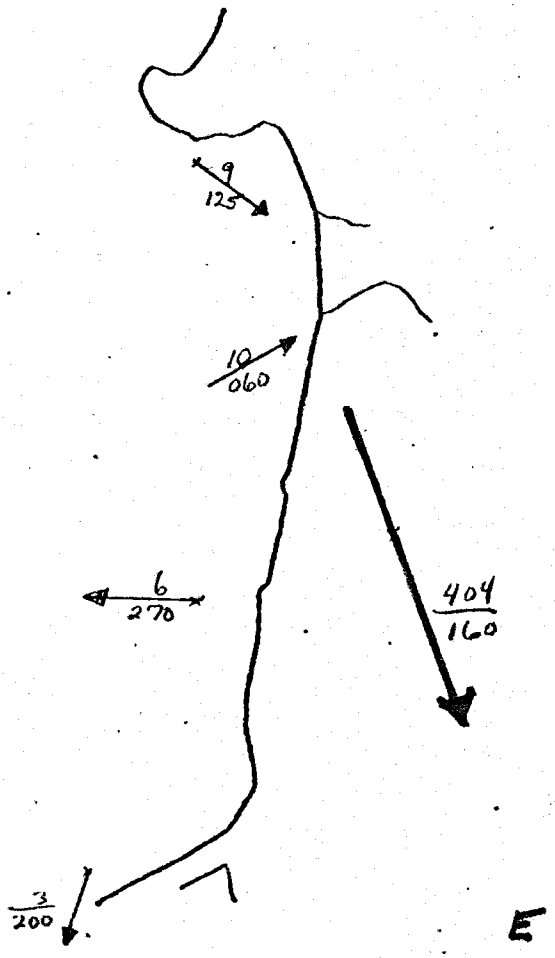

8/11/69 (AM)

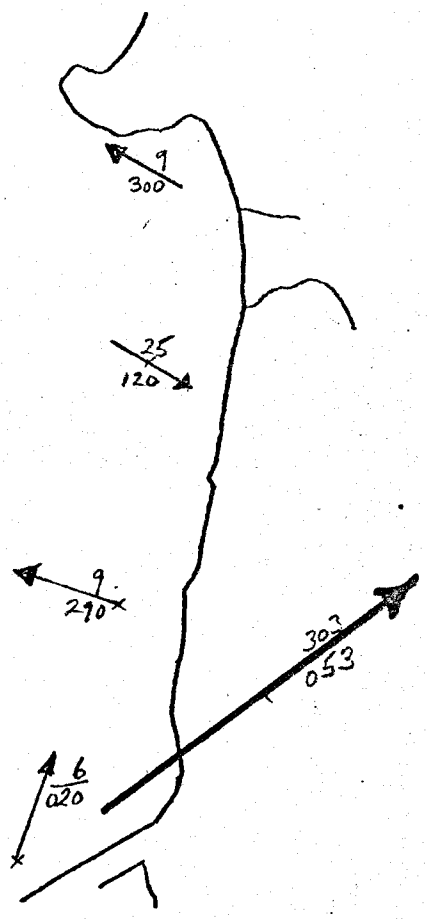

8/11/69 (PM)

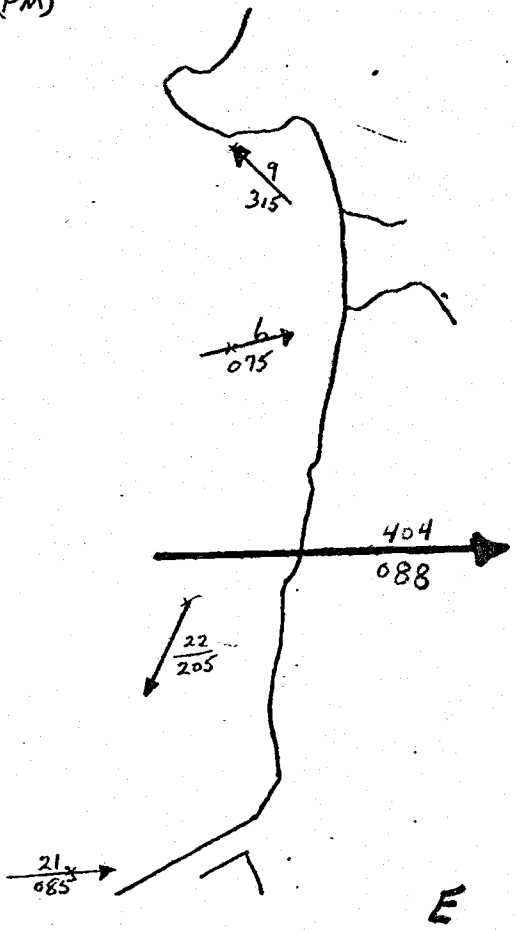

8/12/69 (AM)

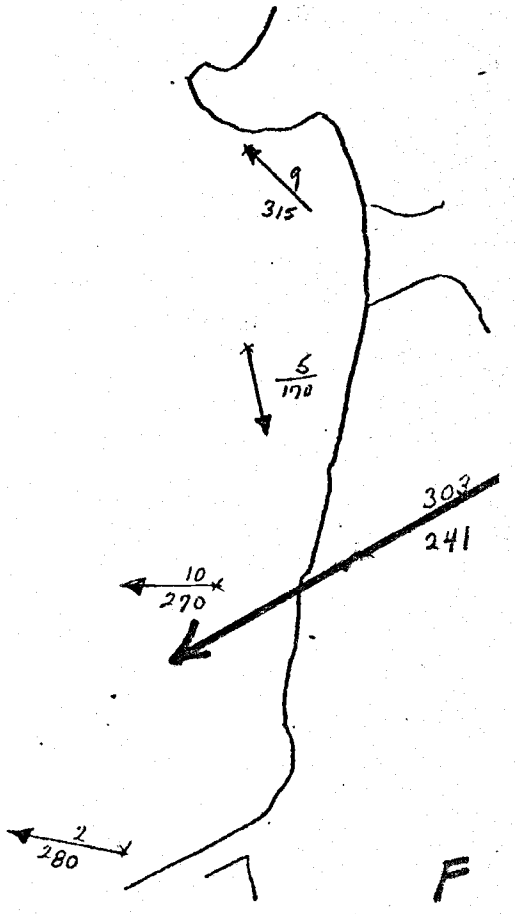

2/69 (PM)

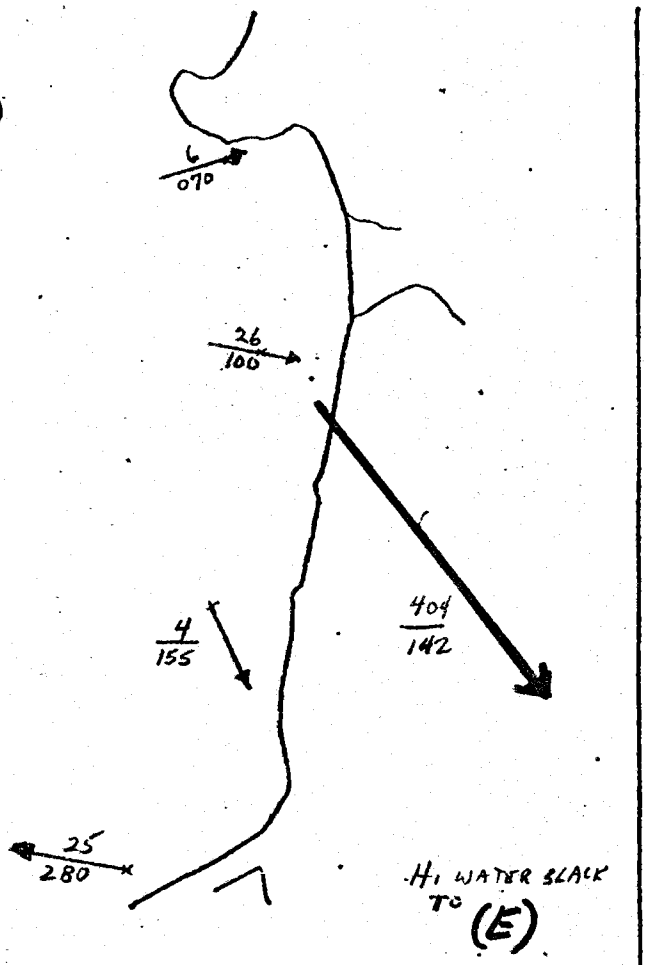

8/18/69 (AM)

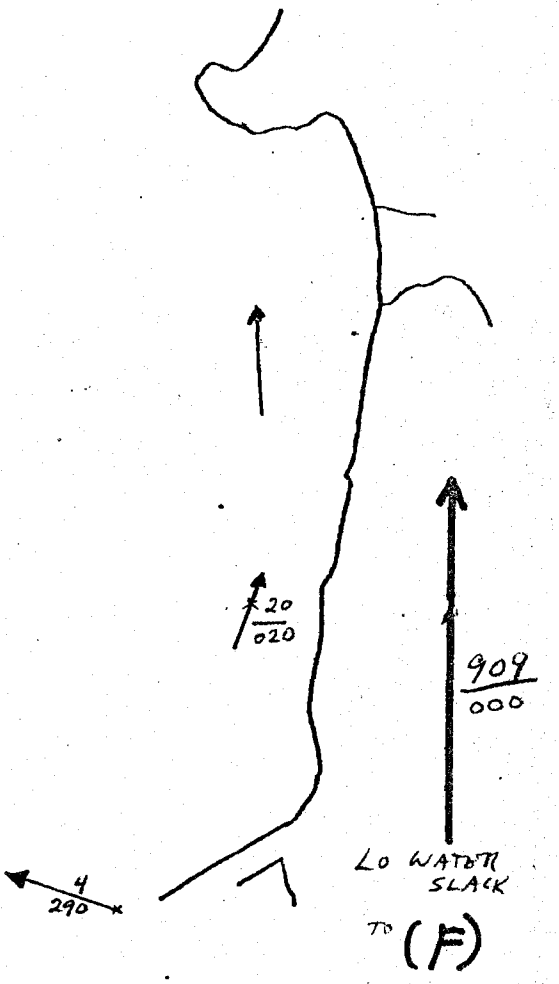

8/69 (PM)

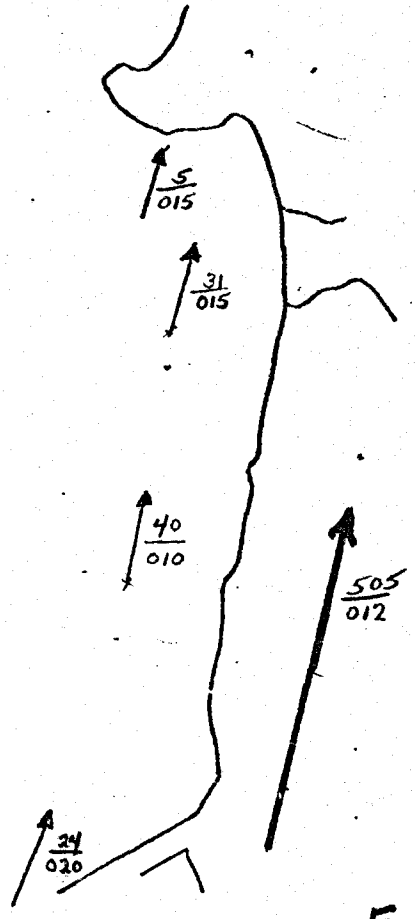

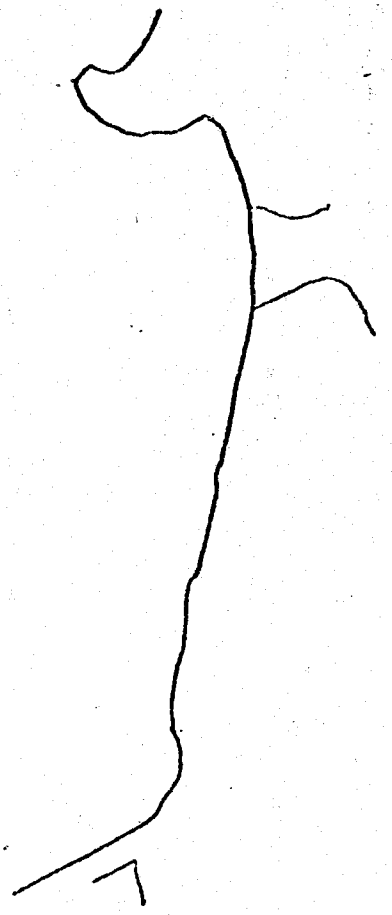

8/19/69 (AM)

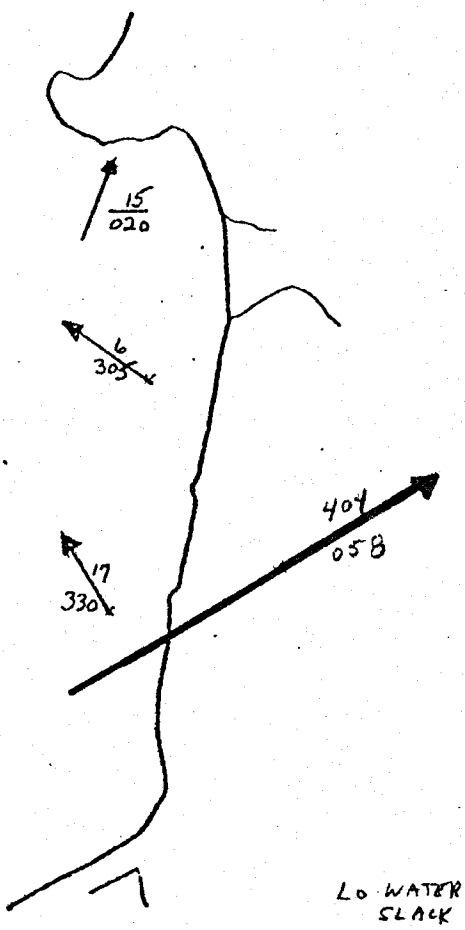

8/19/69 (PM)

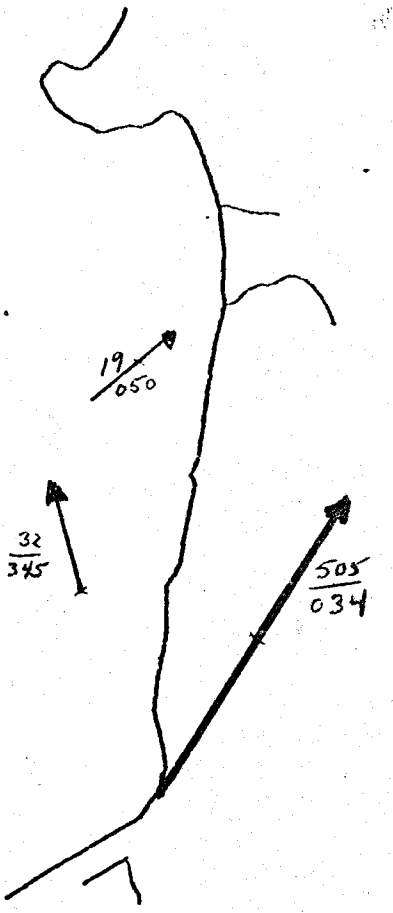

F

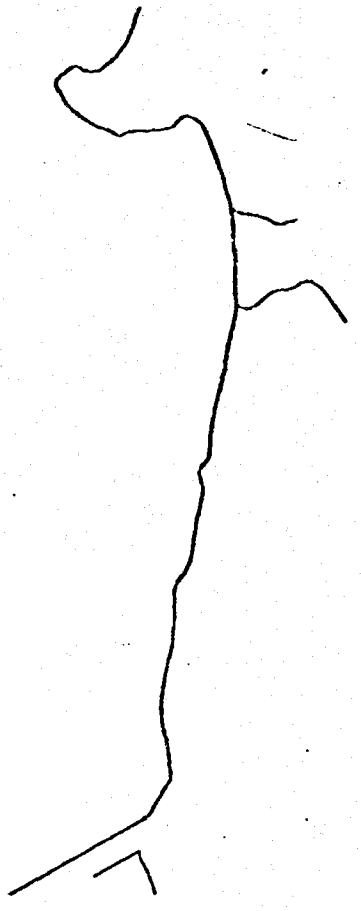

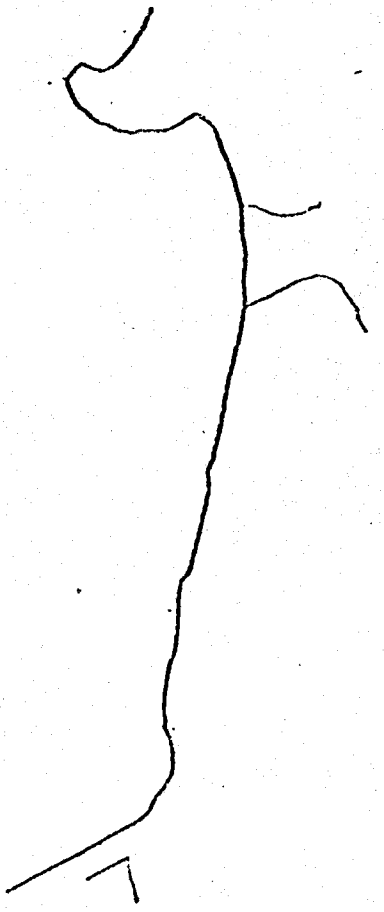

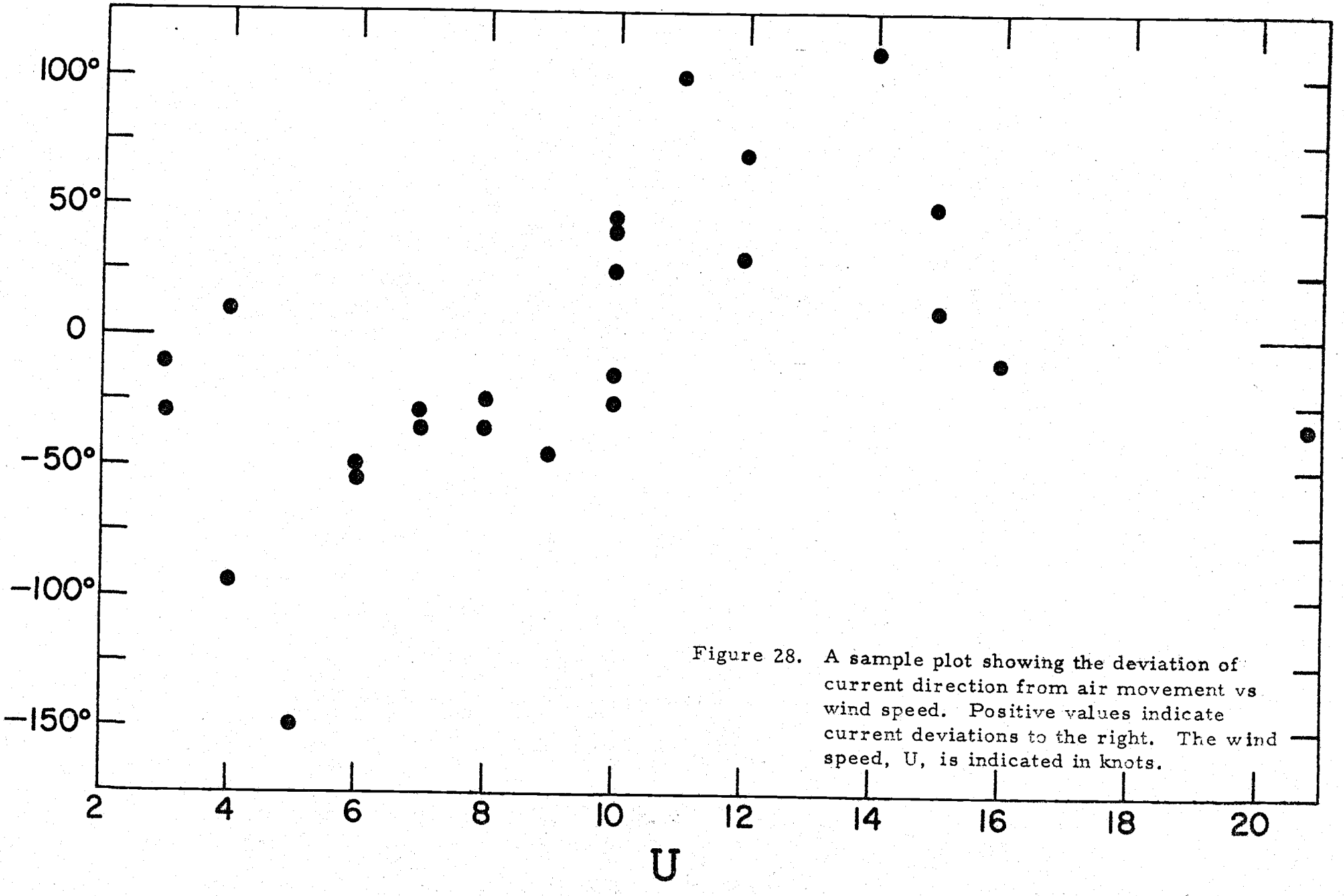

Figure 28. A sample plot showing the deviation of current direction from air movement vs wind speed. Positive values indicate current deviations to the right. The wind speed, U, is indicated in knots.

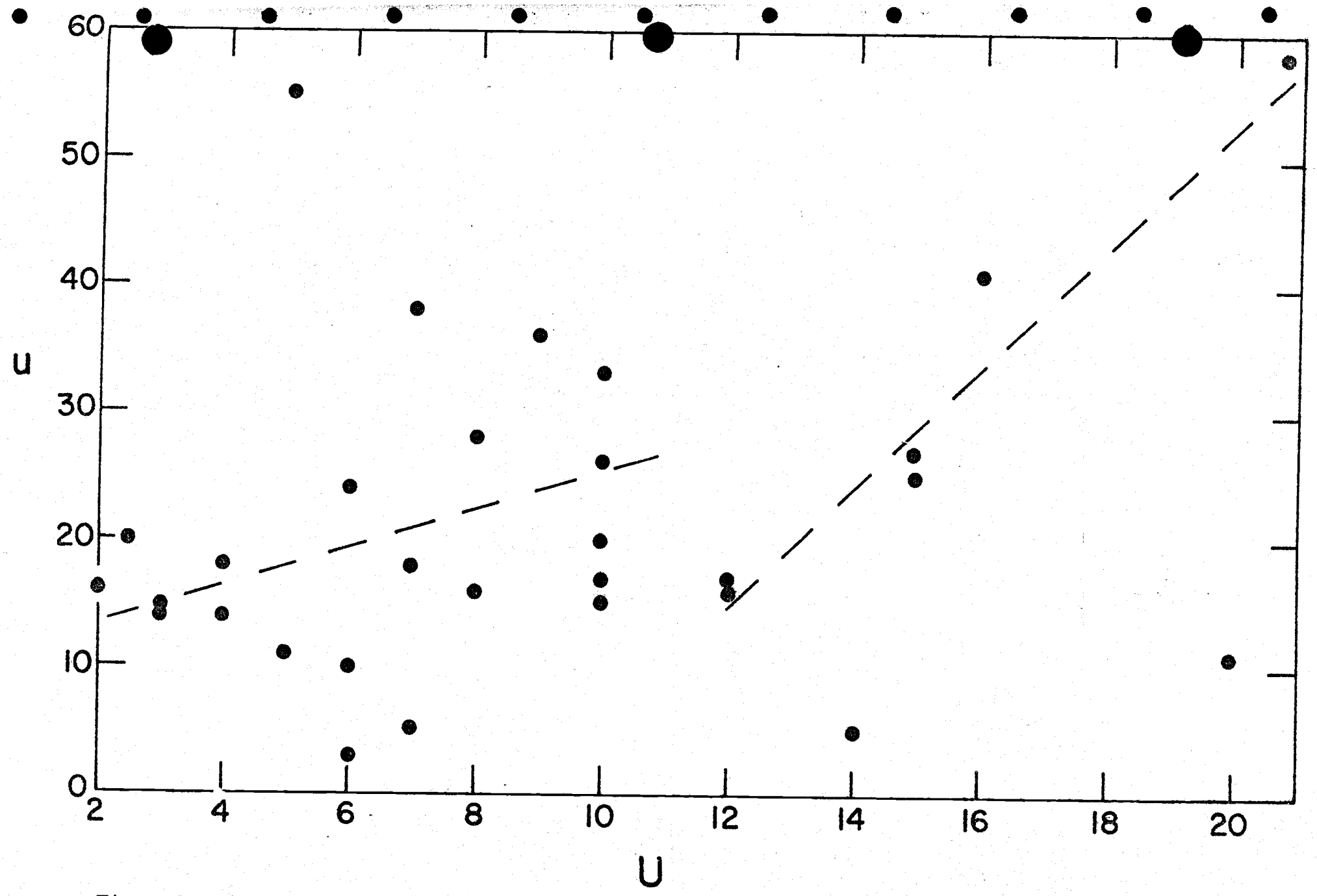

Figure 29. A sample plot of current speeds, u, in ft/min vs. wind speed, U, in knots.

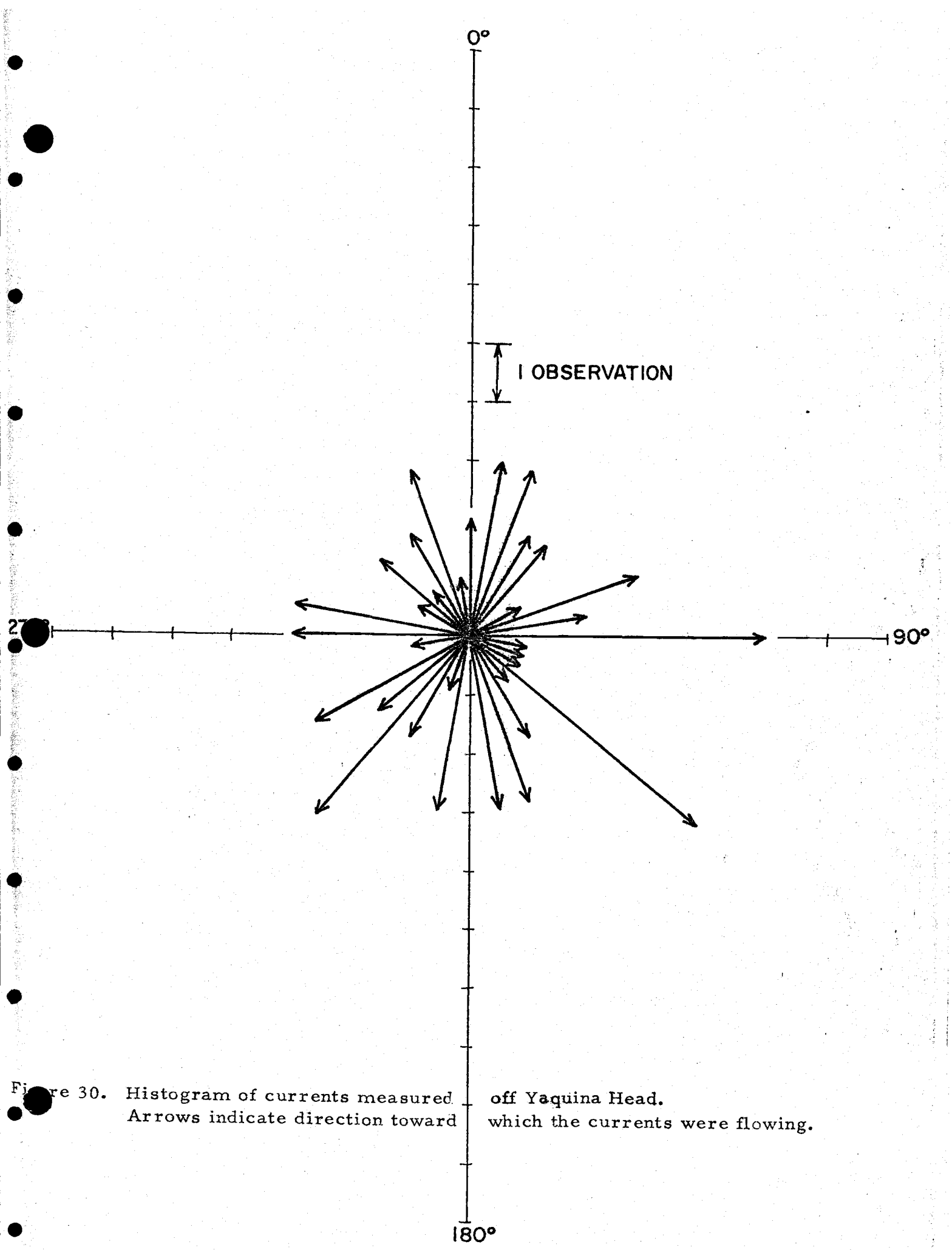

Figure 30. Histogram of currents measured off Yaquina Head. Arrows indicate direction toward which the currents were flowing.

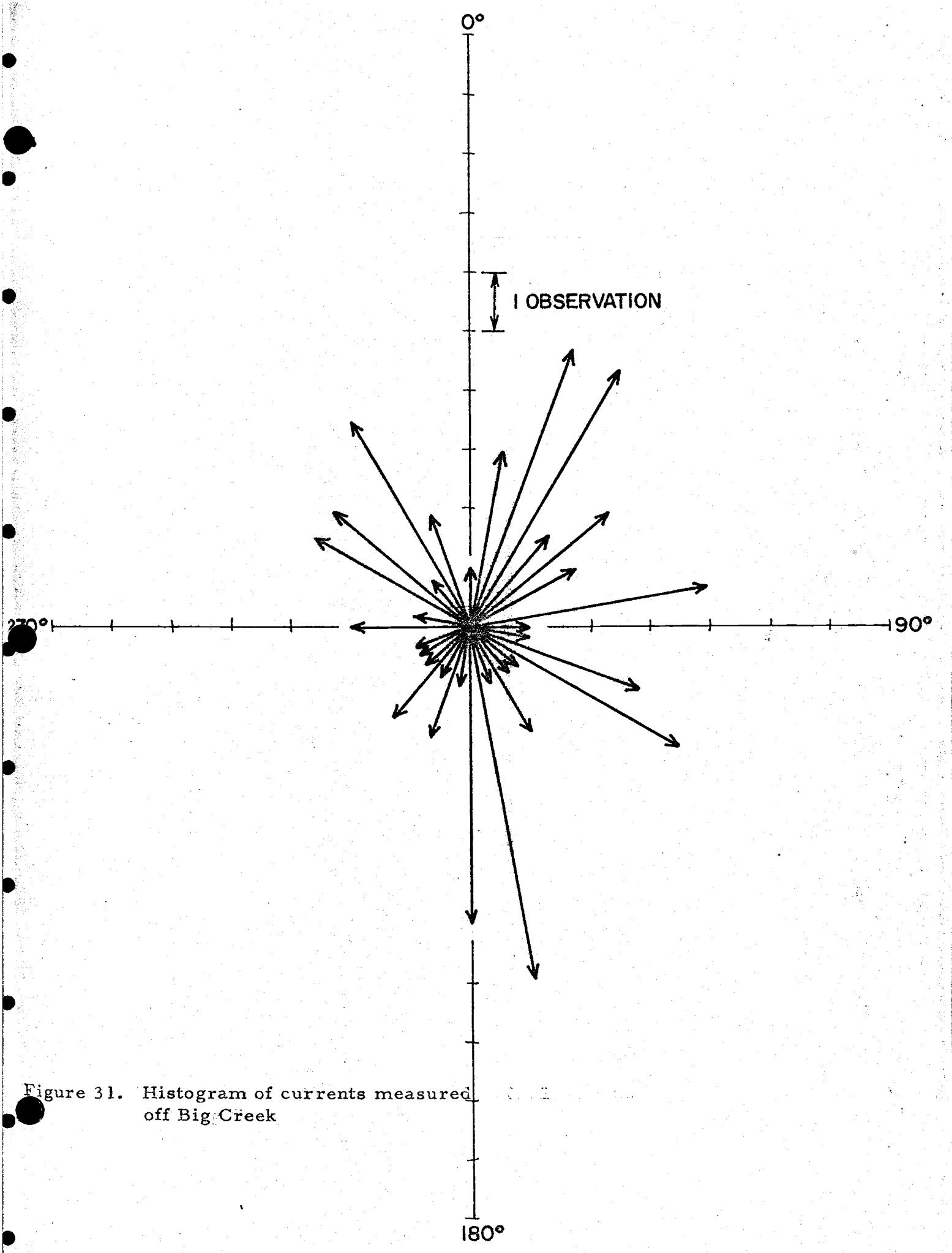

Figure 31. Histogram of currents measured off Big Creek

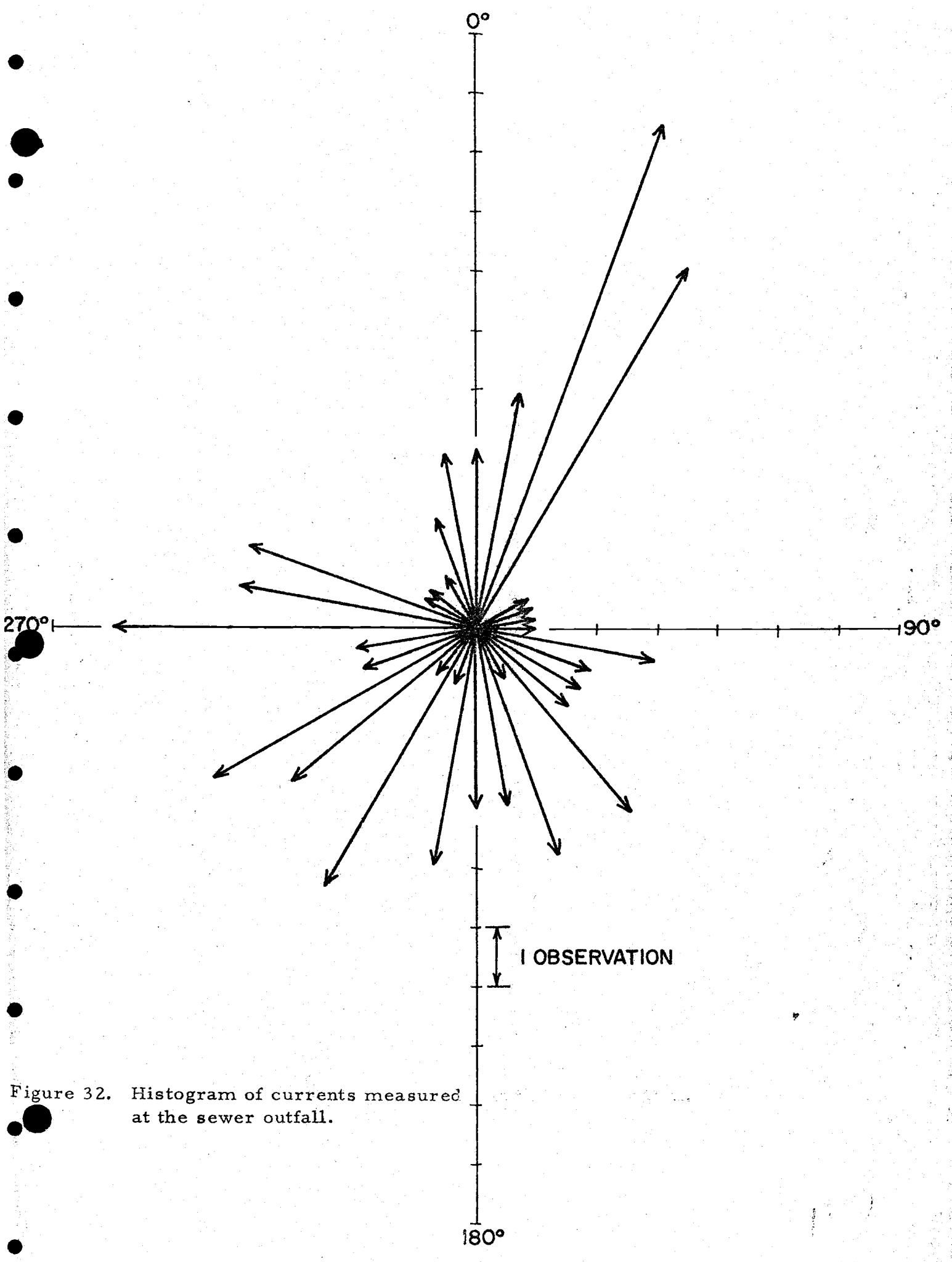

Figure 32. Histogram of currents measured at the sewer outfall.

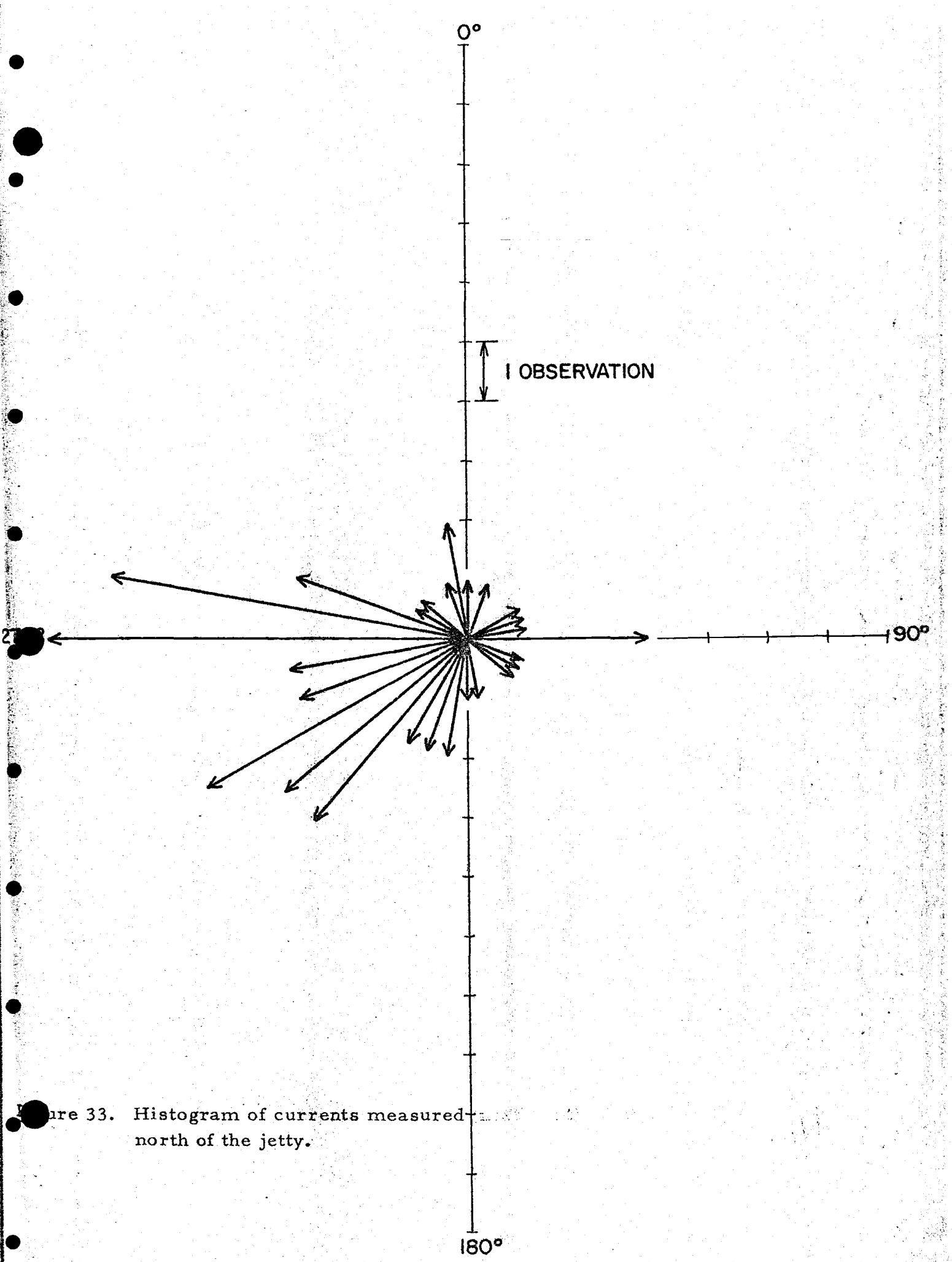

re 33. Histogram of currents measured north of the jetty.

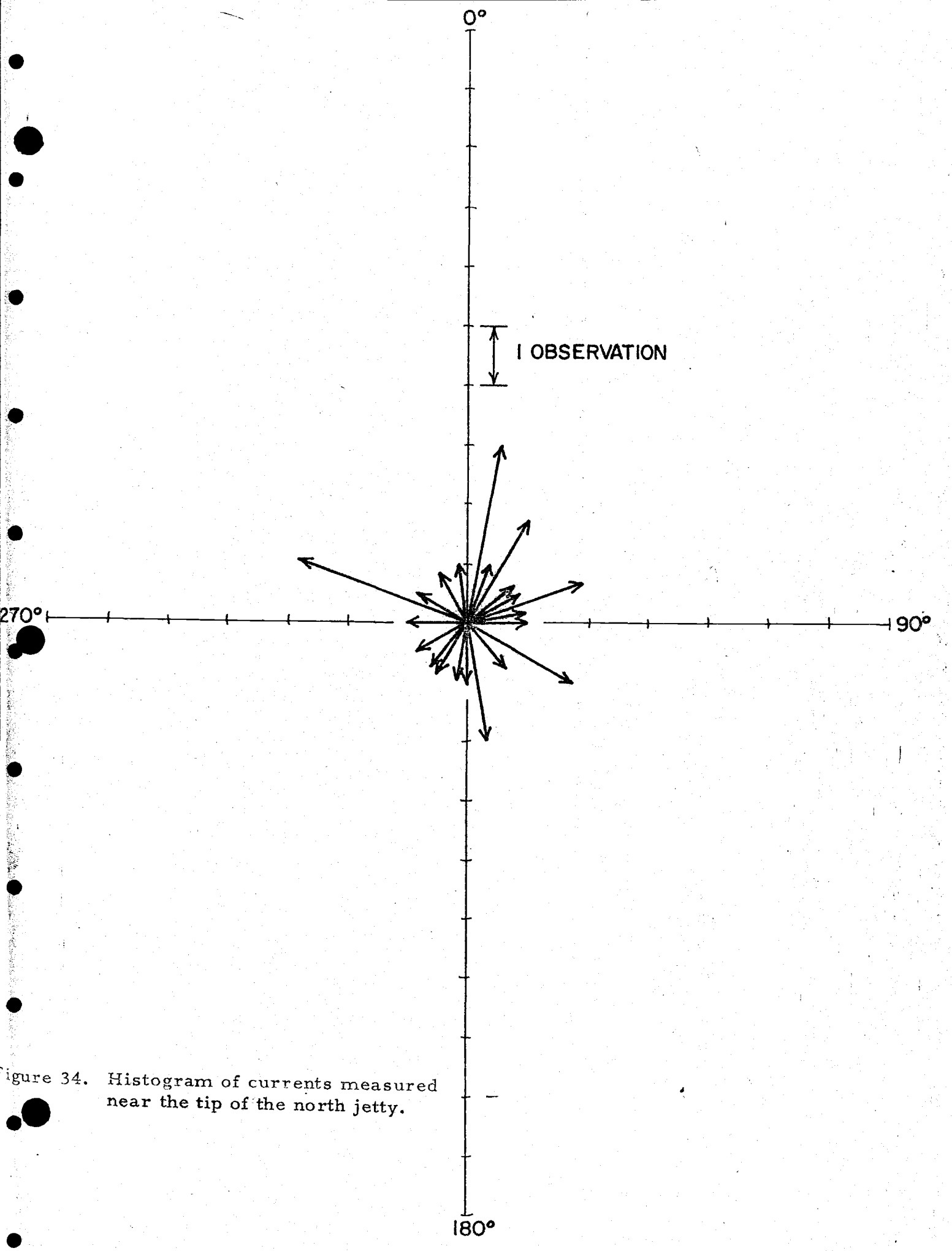

Figure 34. Histogram of currents measured near the tip of the north jetty.

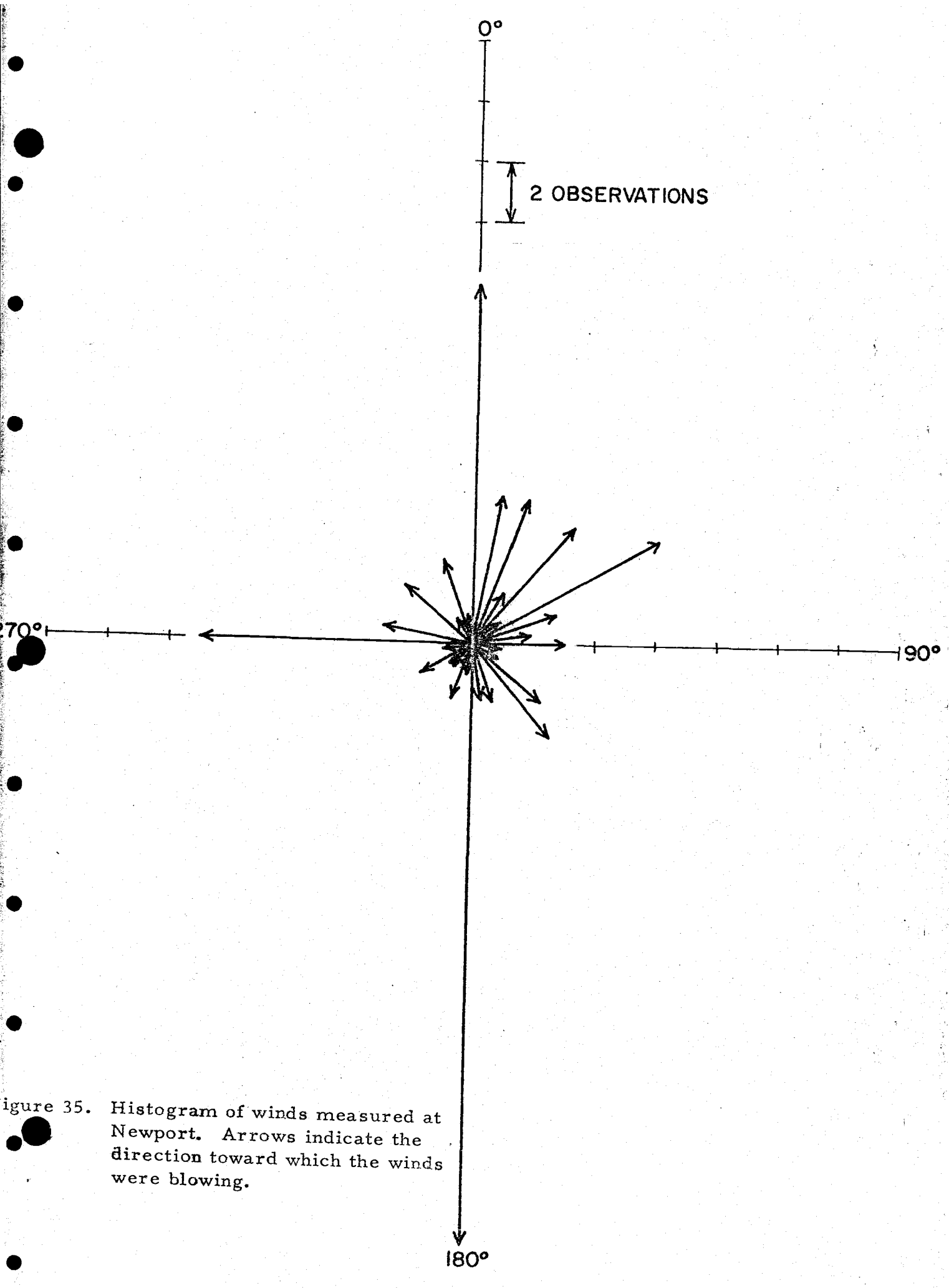

igure 35. Histogram of winds measured at Newport. Arrows indicate the direction toward which the winds were blowing.

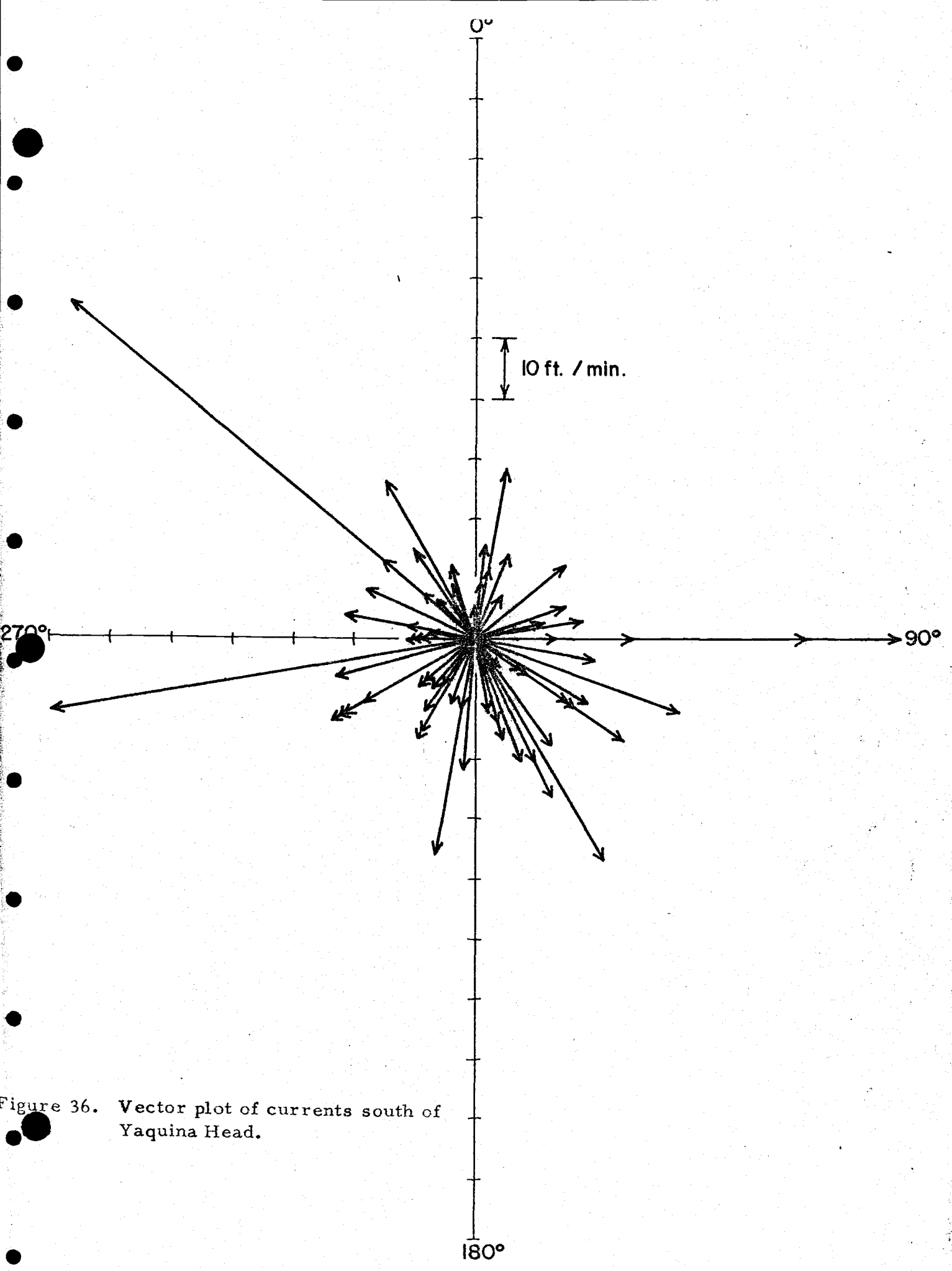

Figure 36. Vector plot of currents south of Yaquina Head.

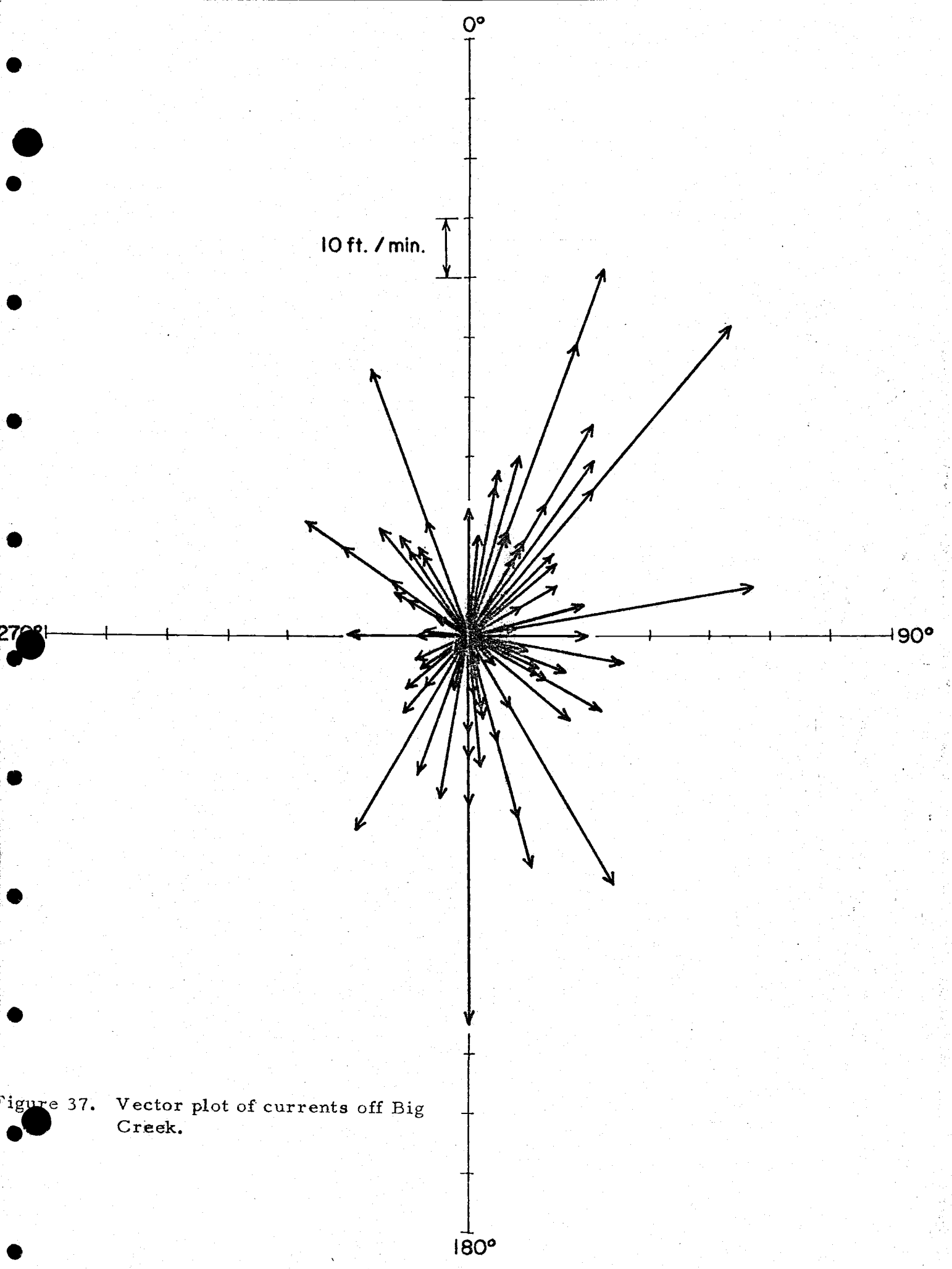

Figure 37. Vector plot of currents off Big Creek.

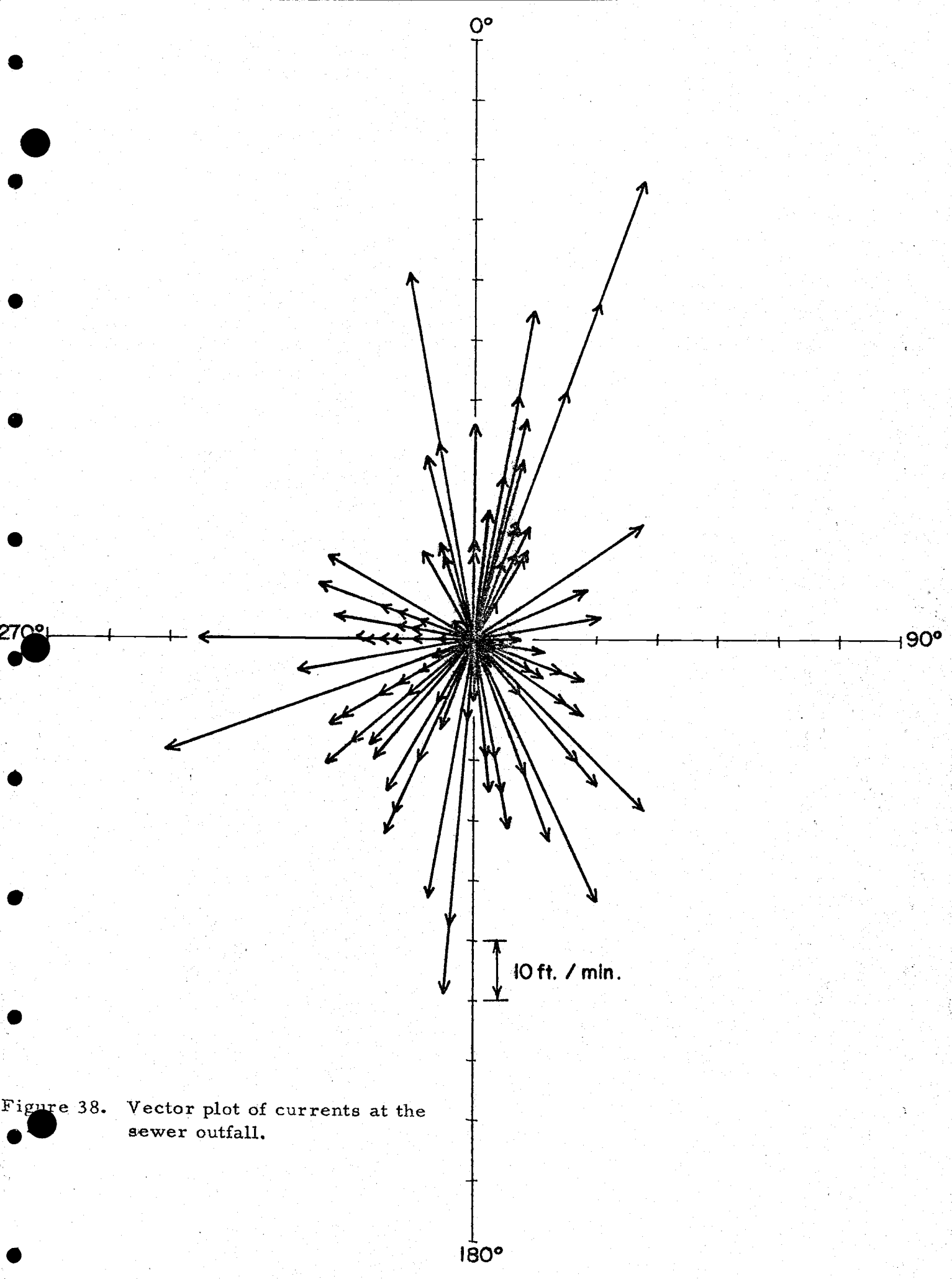

Figure 38. Vector plot of currents at the sewer outfall.

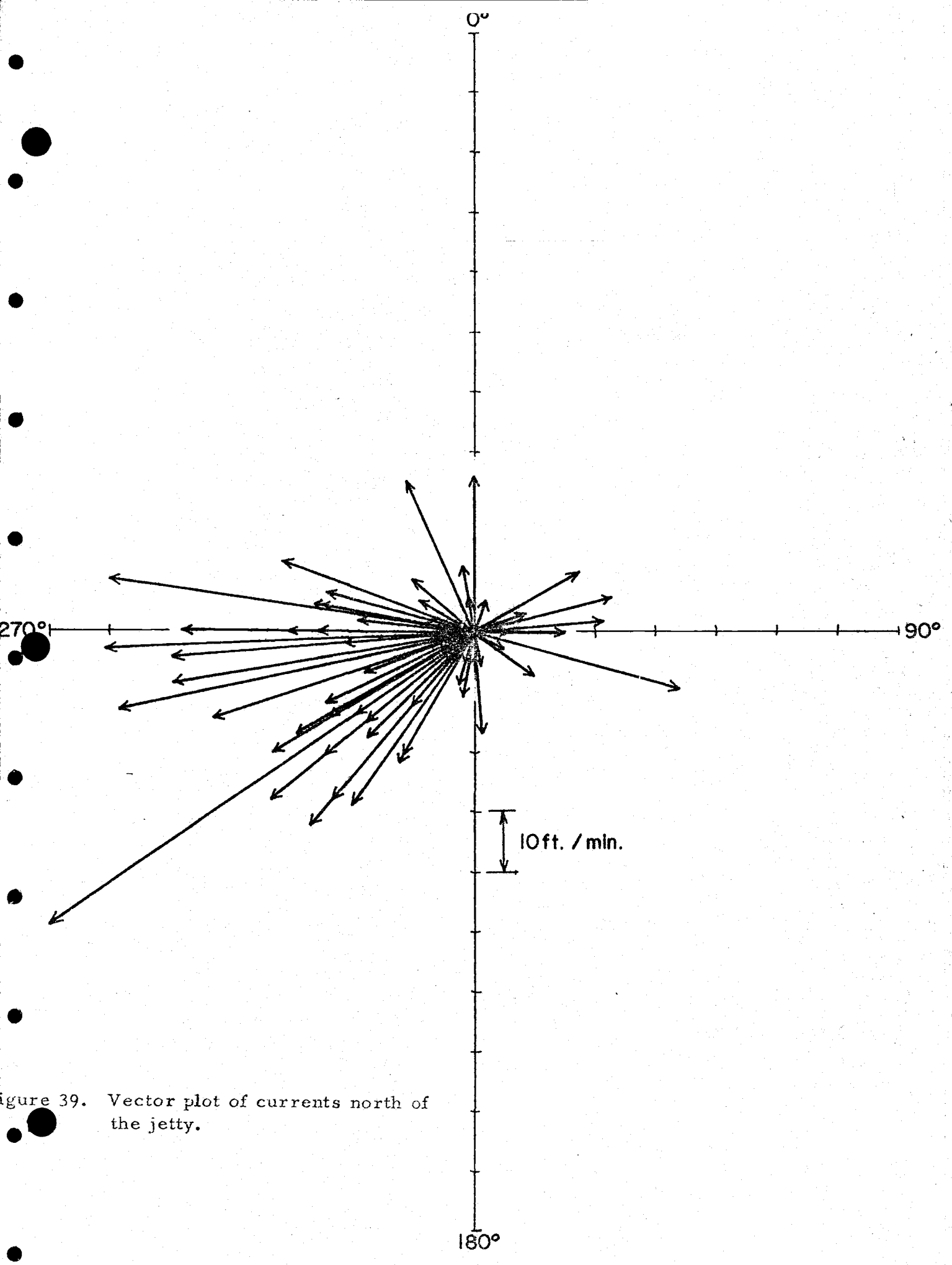

igure 39. Vector plot of currents north of the jetty.

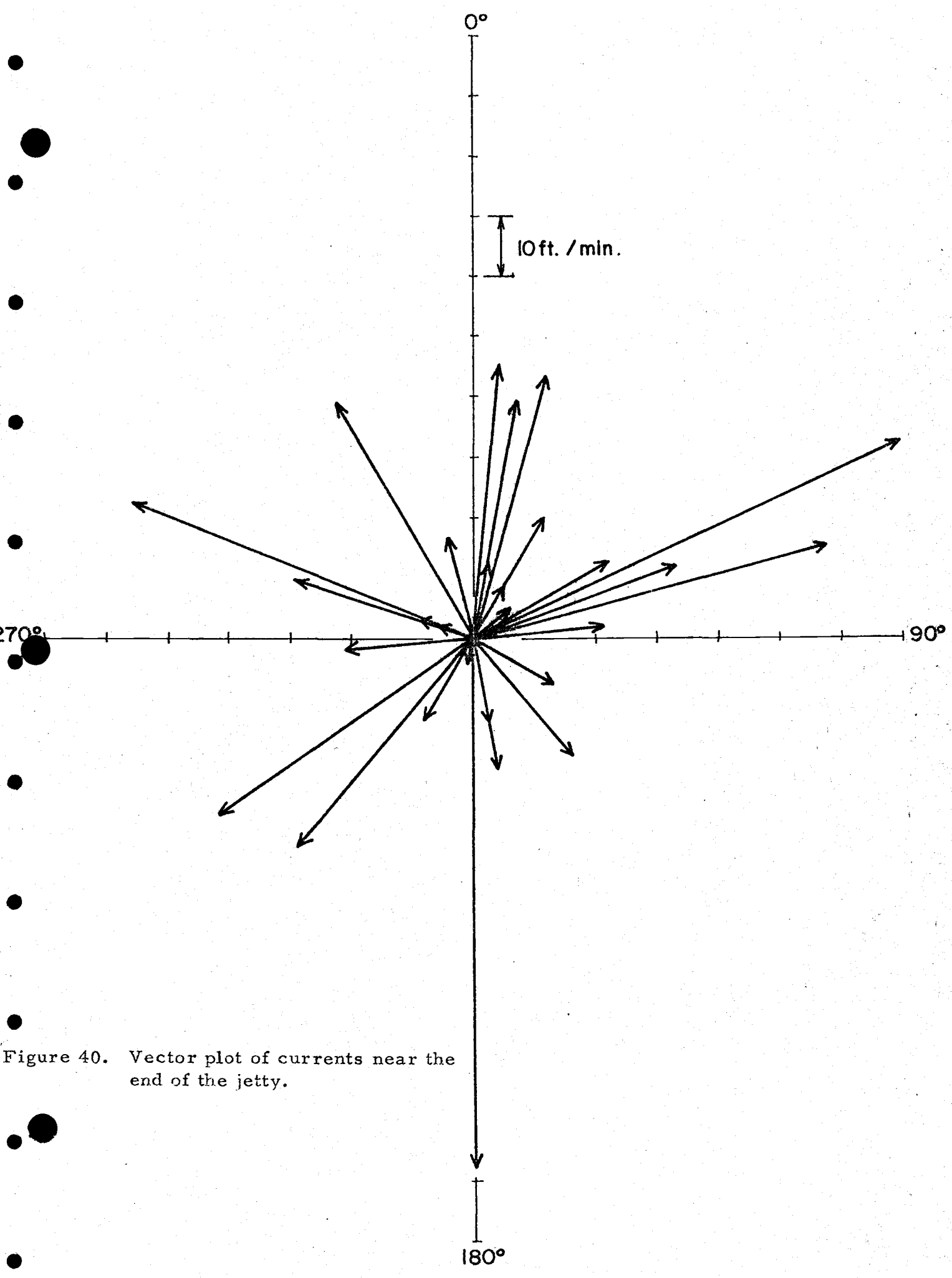

Figure 40. Vector plot of currents near the end of the jetty.

APPENDIX CONTENTS

*Fortran programs for

a) Calculation of current speed by photographs, dividers and data tabulation (basic data)

b) Wind data processing

c) Calculation of regression coefficients

*The STEP program is not included because it is on tape and does not print out.

a) Basic data program.

```
OS3 FORTRAN  VERSION 2.1                10/07/69  1153
      PROGRAM BASIC DATA
      WRITE(61,3)
    3 FORMAT(#  DATE SITE  DEPTH  TIME    CURRENT CURRENT  WIND  WIND
     1 TIDAL TIDAL    TIDAL  WAVE   WAVE   WAVE    PHOTO PHOTO  DELTA
     2PERCENT#/#                          OF OBS  SPEED   DIRECT   SPEED DIREC
     3T  STAGE FRACTION RANGE  HEIGHT PERIOD DIRECT  TIME   SPEED  SPEED
     4  MEAN#//# #)
  100 READ(60,1)IMO,IDA,IYR,ILOC,DEPT,TIH,TIM,TOH,TOM,DIVDIS,ALT, DIR,
     1 WDSP, WDDIR,FTTH,FTTM,STTH,STTM,FTH,STH,WAHT,WAPD, WADIR,PALT,
     2POH,POM,DISMEA
    1 FORMAT(3I2,I1,F2.0,4F2.0,F4.1,F4.0,F3.0,F2.0,F3.0,4F2.0,4F4.1,F3.0
     1,F4.0,2F2.0,F4.1)
      IF(EOF(60))STOP
      TIHF=TIM/60.0
      TOHF=TOM/60.0
      TIHT=TIH+TIHF
      TOHT=TOH+TOHF
      TELA=TOHT-TIHT
      TOBS=TIHT+(TELA/2.0)
      POHF=POM/60.0
      POHT=POH+POHF
      PELA=POHT-TIHT
      POBS=TIHT+(PELA/2.0)
      FTTF=FTTM/60.0
      STTF=STTM/60.0
      FTTT=FTTH+FTTF
      STTT=STTH+STTF
      DURT=STTT-FTTT
      TAT=ABS(TOBS-FTTT)
      PAT=ABS(POBS-FTTT)
      RANGE=ABS(FTH-STH)
      IF(FTH-STH)10,10,20
   10 TIFR=SIN((TAT/DURT)*22.0/14.0)
      NTIST=1
      IF(TOBS.LT.FTTT)NTIST=3
      IF(TOBS.GT.STTT)NTIST=3
      THL=FTH
      PIFR=SIN((PAT/DURT)*22.0/14.0)
      NPIST=1
      IF(POBS.LT.FTTT)NPIST=3
      IF(POBS.GT.STTT)NPIST=3
      GO TO 30
   20 TIFR=SIN(((DURT-TAT)/DURT)*22.0/14.0)
      NTIST=2
      IF(TOBS.LT.FTTT)NTIST=4
      IF(TOBS.GT.STTT)NTIST=4
      THL=STH
      PIFR=SIN(((DURT-PAT)/DURT)*22.0/14.0)
      NPIST=2
      IF(POBS.LT.FTTT)NPIST=4
      IF(POBS.GT.STTT)NPIST=4
   30 CDEP=DEPT+RANGE*TIFR+THL
      BDEP=CDEP
      IF(CDEP.GT.60.0)BDEP=60.0
      A=DIVDIS/52.0
      IF(A-1.0)60,60,70
   60 DITR=2.0*ALT*A/SQRT(1.0-A**2)
      DISC=60.0*(SQRT(1.0-(BDEP/60.0)**2))
      DITR=DITR+DISC
      CURV=DITR/(TELA*60.0)
```

a) Basic data program (continued).

```
OS3 FORTRAN  VERSION 2.1  BASICDAT  10/07/69  1153
      GO TO 80
   70 CURV=999.99
   80 PDEP=DEPT+RANGE*PIFR*THL
      PDEP=PDEP
      IF(PDEP.GT.60.0)PDEP=60.0
      IF(DISMEA.EQ.99.9)GO TO 90
      PDITR=(DISMEA*.705*PALT)/20.0
      PDISC=60.0*(SQRT(1.0-(PDEP/60.0)**2))
      PDITR=PDISC+PDITR
      PCURV=PDITR/(PFLA*60.0)
      GO TO 95
   90 PCURV=999.99
   95 VDIF=ABS(PCURV-CURV)
      PRMFN=(VDIF/((PCURV+CURV)/2.0))*100.0
      CURD=DIR+20.0
      IF(CURD-360.0) 50,50,40
   40 CURD=CURD-360.0
   50 WSDP=WDSP*101.0
      WADIR= WADIR+20.0
      IF( WADIR-360.0) 110,110,120
  120  WADIR= WADIR-360.0
  110  WDDIR= WDDIR+180.0
      IF( WDDIR-360.0) 130,130,140
  140  WDDIR= WDDIR-360.0
  130 WRITE(61,4)IMO,IDA,ILOC,CDEP,TORS,CURV, CURD, WDSP, WDDIR,NTIST,
     1ITTER,RANGE,WAHT,WAPD, WADIR,PORS,PCURV,VDIF,PRMFN
    4 FORMAT(1X,3I3,F8.0,F7.2,F8.2,F6.0,F10.0,F5.0,I8,F9.4,3F7.1,F6.0,
     1F10.2,2F7.2,F7.0)
      GO TO 100
      END

NO ERRORS FOR BASICDAT

01271   C 00000   D 00000
```

b) Wind data program.

```
OS3 FORTRAN  VERSION 2.1                    09/19/69  1639
      PROGRAM WINDCOM
      DIMENSION ANOR(24),EAS (24),SOU(24),WES(24),DIR(24),AMILE(24),AKN
     1T(24)
   80 READ(60,1) IDATE,(ANOR(I),EAS(I),SOU(I),WES(I),AMILE(I),I=1,24)
    1 FORMAT(I6/(40F2.0))
      IF(EOF(60))STOP
      DO70I=1,24
      IF(ANOR(I).EQ.SOU(I).AND.EAS(I).EQ.WES(I))GO TO 40
      VICT=ABS(ANOR(I)-SOU(I))
      UNIF=ABS(EAS(I)-WES(I))
      IF(VICT.EQ.0.0)GO TO 10
      GO TO 20
   10 TDIR=90.0
      GO TO 30
   20 TDIR=ATAN(UNIF/VICT)
      TDIR=TDIR*(180.0/3.1416)
   30 IF(ANOR(I).GT.SOU(I).AND.EAS(I).GE.WES(I))DIR(I)=TDIR
      IF(SOU(I).GT.ANOR(I).AND.EAS(I).GE.WES(I))DIR(I)=180.0-TDIR
      IF(SOU(I).GE.ANOR(I).AND.WES(I).GT.EAS(I))DIR(I)=180.0+TDIR
      IF(ANOR(I).GT.SOU(I).AND.WES(I).GT.EAS(I))DIR(I)=360.0-TDIR
      IF(ANOR(I).EQ.SOU(I).AND.EAS(I).GT.WES(I))DIR(I)=90.0
      GO TO 50
   40 DIR(I)=999.0
   50 IF(AMILE(I).EQ.99.0) GO TO 60
      AKNOT(I)=(0.868)*AMILE(I)
      GO TO 70
   60 AKNOT(I)=99.0
   70 CONTINUE
      WRITE(61,2)IDATE,(DIR(I),AKNOT(I),I=1,24)
    2 FORMAT(1X,I6/3X,≠01-08≠,8(F10.0,F5.0)/3X,≠09-16≠,8(F10.0,F5.0)/3X
     1≠17-24≠,8(F10.0,F5.0))
      WRITE(62,3)IDATE,(DIR(I),AKNOT(I),I=1,12)
    3 FORMAT(I6,2X,≠01-12≠,2X,12(F3.0,F2.0))
      WRITE(62,4)IDATE,(DIR(I),AKNOT(I),I=13,24)
    4 FORMAT(I6,2X,≠13-24≠,2X,12(F3.0,F2.0))
      GO TO 80
      END

NO ERRORS FOR WINDCOM

 01203  C 00000  D 00000
UN
```

c) Regression coefficient program.

```
FORTRAN  VERSION 2.1                10/15/69  1714
    PROGRAM BASIC DATA
100 READ(60,1)IMO,IDA,IYR,ILOC,DEPT,TIH,TIM,TCH,TCM,DIVDIS,ALT, DIR,
   1 WDSP, WDDIR,FTTH,FTTM,STTH,STTM,FTH,STH,WAHT,WAPD, WADIR,PALT,
   2PCH,PCM,DISMEA
  1 FORMAT(3I2,I1,F2.0,4F2.0,F4.1,F4.0,F3.0,F2.0,F3.0,4F2.0,4F4.1,F3.0
   1,F4.0,2F2.0,F4.1)
    IF(EOF(60))STOP
    TIHF=TIM/60.0
    TCHF=TCM/60.0
    TIHT=TIH+TIHF
    TCHT=TCH+TCHF
    TELA=TCHT-TIHT
    TOBS=TIHT+(TELA/2.0)
    PCHF=PCM/60.0
    PCHT=PCH+PCHF
    PELA=PCHT-TIHT
    POBS=TIHT+(PELA/2.0)
    FTTF=FTTM/60.0
    STTF=STTM/60.0
    FTTT=FTTH+FTTF
    STTT=STTH+STTF
    DURT=STTT-FTTT
    TAT=ABS(TOBS-FTTT)
    PAT=ABS(POBS-FTTT)
    RANGE=ABS(FTH-STH)
    IF(FTH-STH)10,10,20
 10 TIFR=SIN((TAT/DURT)*22.0/14.0)
    NTIST=1
    THL=FTH
    PIFR=SIN((PAT/DURT)*22.0/14.0)
    NPIST=1
    GO TO 30
 20 TIFR=SIN(((DURT-TAT)/DURT)*22.0/14.0)
    NTIST=2
    THL=STH
    PIFR=SIN(((DURT-PAT)/DURT)*22.0/14.0)
    NPIST=2
 30 CDEP=DEPT+RANGE*TIFR+THL
    BDEP=CDEP
    IF(CDEP.GT.60.0)BDEP=60.0
    A=DIVDIS/52.0
    IF(A-1.0)60,60,70
 60 DITR=2.0*ALT*A/SQRT(1.0-A**2)
    DISC=60.0*(SQRT(1.0-(BDEP/60.0)**2))
    DITR=DITR+DISC
    CURV=DITR/(TELA*60.0)
    GO TO 80
 70 CURV=999.99
 80 PDEP=DEPT+RANGE*PIFR+THL
    RDEP=PDEP
    IF(PDEP.GT.60.0)RDEP=60.0
    IF(DISMEA.EQ.99.9)GO TO 90
    PDITR=(DISMEA*.705*PALT)/20.0
    PDISC=60.0*(SQRT(1.0-(RDEP/60.0)**2))
    PDITR=PDISC+PDITR
    PCURV=PDITR/(PELA*60.0)
    GO TO 95
 90 PCURV=999.99
 95 VDIF=ABS(PCURV-CURV)
    PRMEN=(VDIF/((PCURV+CURV)/2.0))*100.0
```

c) Regression coefficient program (continued).

```
OS3 FORTRAN  VERSION 2.1  BASICDAT  10/15/69  1714
      CURD=DIR+20.0
      IF(CURD-360.0) 50,50,40
   40 CURD=CURD-360.0
   50 WDSP=WDSP*101.0
      WADIR= WADIR+20.0
      IF( WADIR-360.0) 110,110,120
  120  WADIR= WADIR-360.0
  110  WDDIR= WDDIR+180.0
      IF( WDDIR-360.0) 130,130,140
  140  WDDIR= WDDIR-360.0
  130  WADIR= WADIR+180.0
      IF(WADIR.LT.360.0) GO TO 190
       WADIR= WADIR-360.0
  190 WDDIR=(WDDIR-CURD+360.0)*.01745
      WADIR=(WADIR-CURD+360.0)*.01745
      IF(PCURV.EQ.999.99) GO TO 220
      ACURV=PCURV
      ZDEP=PDEP
      FRT=TIFR
      NZIST=NTIST
      GO TO 230
  220 ACURV=CURV
      ZDEP=CDEP
      FRT=PIFR
      NZIST=NPIST
  230 IF(WDSP.LT.1212.0)WDSP=SQRT(WDSP)
      WINV= WDSP*COS(WDDIR)
      HS=1.731*SQRT(WAHT**3/ZDEP)
      CHAR=60.0*SQRT(32.2*ZDEP+6.95*(HS*WAPD/ZDEP)**2)
      UNIF=9.9*((HS/WAPD)**2/CHAR)*EXP(-75.3/(WAPD*CHAR))
      UNIF=UNIF*COS(WADIR)
      SPAN=60.0*DURT
      TDS=SIN(6.28*FRT/SPAN)*((6.28*RANGE/2.0)*3600.0/(SPAN*ZDEP))
      IF(NZIST.EQ.2) TIDD=3.92*FRT*3.1416*6.28
      IF(NZIST.EQ.1) TIDD=0.785*FRT*3.141*6.28
      CURD=CURD*.01745
      TDS=TDS*COS(TIDD-CURD)
      WRITE(61,4) IMO,IDA,UNIF,WINV,TDS,ACURV
      WRITE(62,4) IMO,IDA,UNIF,WINV,TDS,ACURV
    4 FORMAT(2I2,4E15.5)
      GO TO 100
      END

 NO ERRORS FOR BASICDAT

P 01356    C 00000    D 00000
RUN
```